

ISOSTRUCTURALITY AND POLYMORPHISM IN MODEL COMPOUNDS AND ACTIVE PHARMACEUTICAL INGREDIENTS

**A Thesis Submitted during 2006-2011 to the
University of Hyderabad in partial fulfillment of
the award of a Ph.D. degree in Chemistry**

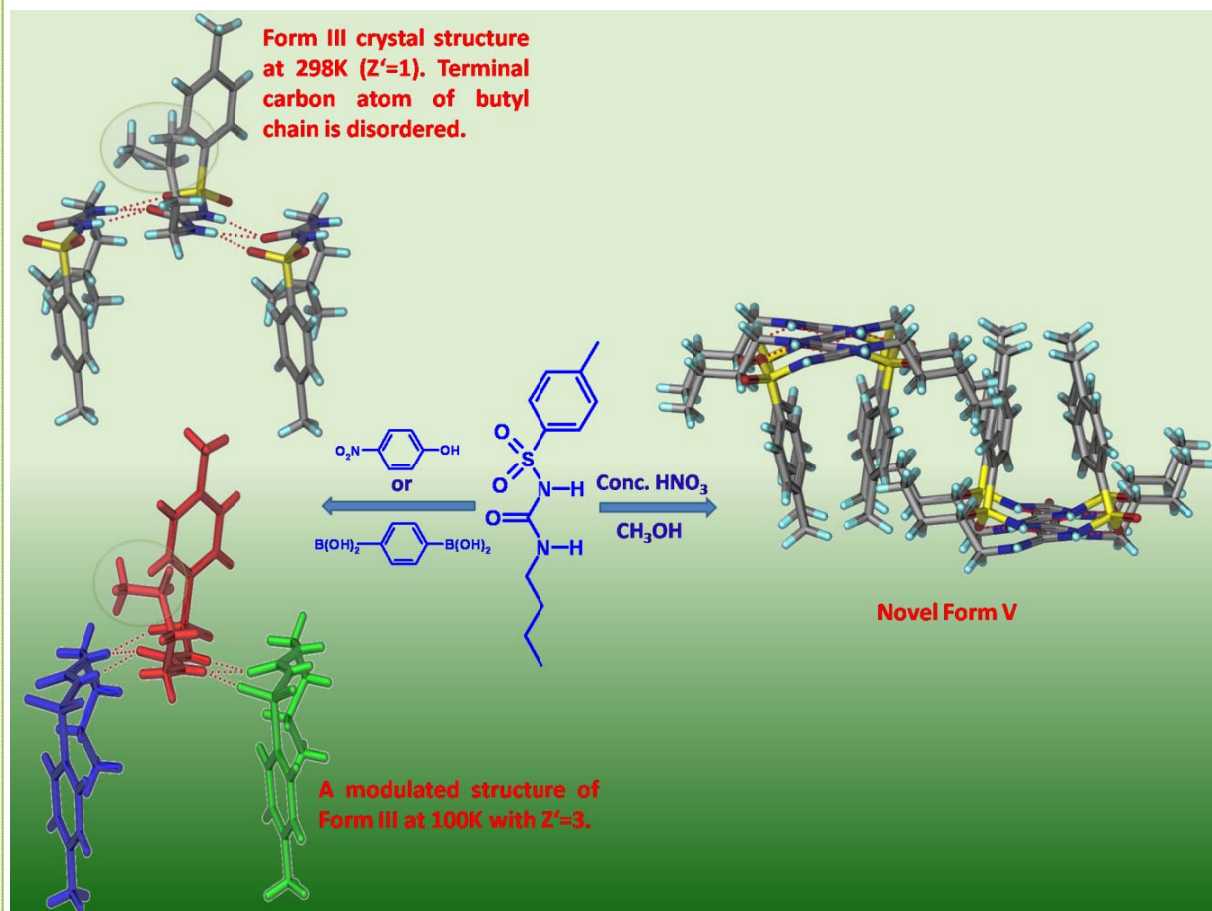
By

Naba Kamal Nath



**School of Chemistry
University of Hyderabad
Central University P. O., Gachibowli
Hyderabad 500 046
Andhra Pradesh
India**

June 2011



A modulated structure of Form III and a novel polymorph Form V of Tolbutamide, an oral hypoglycemic agent, were obtained in presence of coformers/additives.

*N. K. Nath and A. Nangia, CrystEngComm, **2011**, 13, 47–51.*

(Structure of the week in Crystal Growth & Design Network)

ISOSTRUCTURALITY AND POLYMORPHISM IN MODEL COMPOUNDS AND ACTIVE PHARMACEUTICAL INGREDIENTS

**A Thesis Submitted during 2006-2011 to the
University of Hyderabad in partial fulfillment of the award of a
Ph.D. degree in Chemistry**

**By
NABA KAMAL NATH**



**School of Chemistry
University of Hyderabad
Central University P.O., Gachibowli
Hyderabad 500 046
Andhra Pradesh
India**

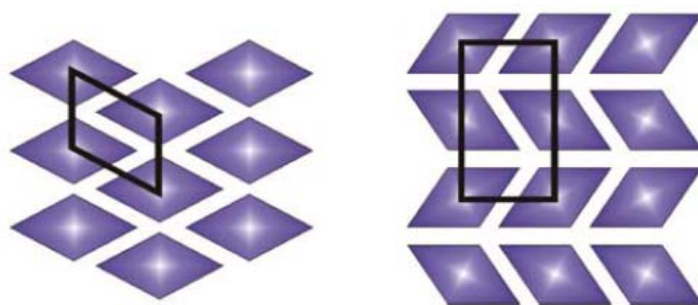
DEDICATION

This Thesis is

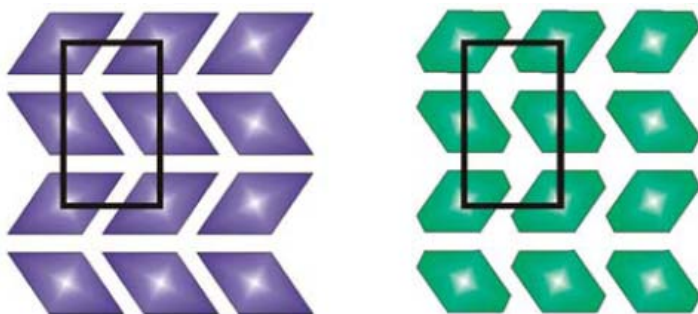
Dedicated To My Parents

Chapter One

Introduction



Two polymorphic structures: Identical molecules packed differently to give distinct crystal structures with different unit cell



Two isostructural structures: Different molecules packed similarly to give similar crystal structures with similar unit cell

“The important thing in science is not so much to obtain new facts as to discover new ways of thinking about them.” Sir William Henry Bragg (1862–1942), Nobel Prize for Physics 1915.

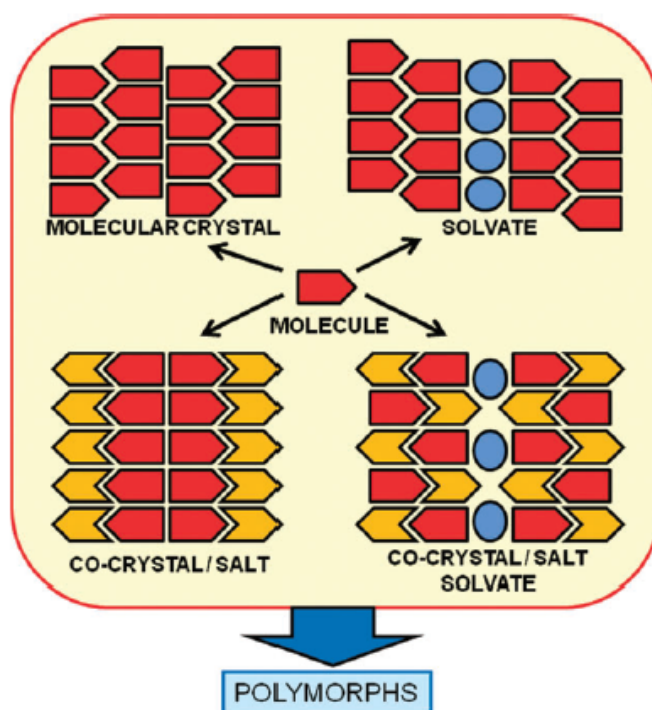
1.1 Chemistry of Solid State and Crystal Forms

There have been major advances in solid state and materials chemistry in the last two decades and the subject is growing rapidly and contributing to the betterment of many processes that are mainly an integral part of modern life.¹ In the present times, solid state chemistry is concerned with the development of new methods of synthesis, new ways of identifying and characterizing materials, and of describing their structure and and above all, with new strategies for tailor-made materials with desired and controllable properties.² The identification and characterization of different crystal forms (polymorphs, solvates) of the same molecule, or of aggregates of the same molecule with other molecules or ions (salts and co-crystals), is one of the most active and challenging research areas of modern solid-state chemistry. The last decade has witnessed many developments in the design and characterization of new crystal forms. The reasons include increased awareness of the possibility of multiple crystal forms of a substance with enhanced properties and the potential intellectual property implications of new crystal forms combined with the development of new technology and attempts to design and control the crystal structure.³

Based on the internal structure and the degree of periodicity, solids can be broadly classified into two categories, crystalline and amorphous. Crystalline forms are characterized by long range order while amorphous forms have short range order.⁴ Each class of solids have their individual properties, advantages and disadvantages, and applications.

A chemical compound can crystallize to give a molecular crystal or can crystallize by including solvent molecules in its crystal lattice to give solvates or pseudopolymorphs⁵ or as hydrates⁶ when the solvent molecule is water. When two or more compounds (solid at ambient temperature) coexist in a crystal lattice through hydrogen bonds or non-covalent interactions then it is called a cocrystal.⁷ However, the

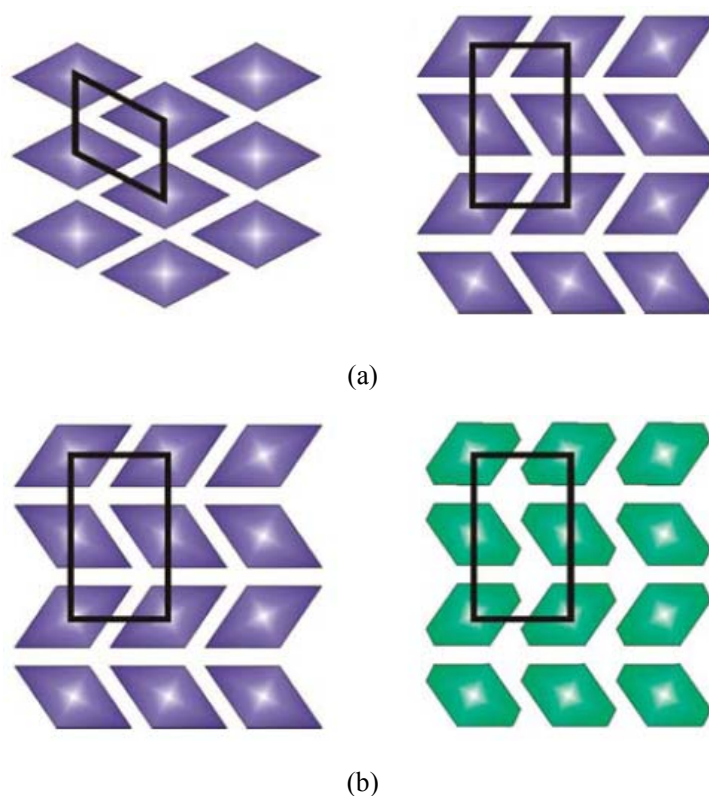
multi-component crystalline system is known as molecular salt/salt⁸ if the proton is transferred from acid to base and the ionic state is formed. Cocrystal and salts can also incorporate solvent molecules in their crystal lattice to form solvates and hydrates. The single molecular entity can crystallize in different packing patterns to give rise to polymorphs. Polymorphism is possible in other classes of crystalline solids such as solvates, hydrates, salts, cocrystals and their solvates and hydrates, resulting in various solid forms as shown in Scheme 1.1. Therefore a single molecular entity can lead to the formation of multiple crystal forms.⁹



Scheme 1.1 Multiple crystal forms from a single molecule. Red and yellow symbols represents single molecule in either neutral (molecular crystal, solvates, cocrystal cocrystal solvate) or in ionic state (salt and salt solvate). Blue circles indicate solvent molecules. This scheme is culled from Ref. 9a.

On the contrary, the above mentioned crystal forms of different chemical compounds can have similar crystal structures to produce isostructural crystals. Isostructurality is another phenomenon, inversely related to polymorphism, which refers to identical or a nearly identical crystal packing arrangement of chemically related

compounds. Both isostructurality and polymorphism have potential applicability in solid state chemistry. While isostructurality is an aid to the crystal engineering, polymorphism is still a challenge. Scheme 1.2 depicts the inverse relationship of these twin phenomena.¹⁰



Scheme 1.2 (a) Two polymorphic structures where the identical building blocks packed differently to produce distinct crystal structures as depicted by different unit cell shapes. (b) Two isostructural structures where different building blocks arranged in an identical manner as depicted by the same shape of the unit cell. This scheme is culled from Ref. 10.

1.2 Polymorphism: Definition and Background

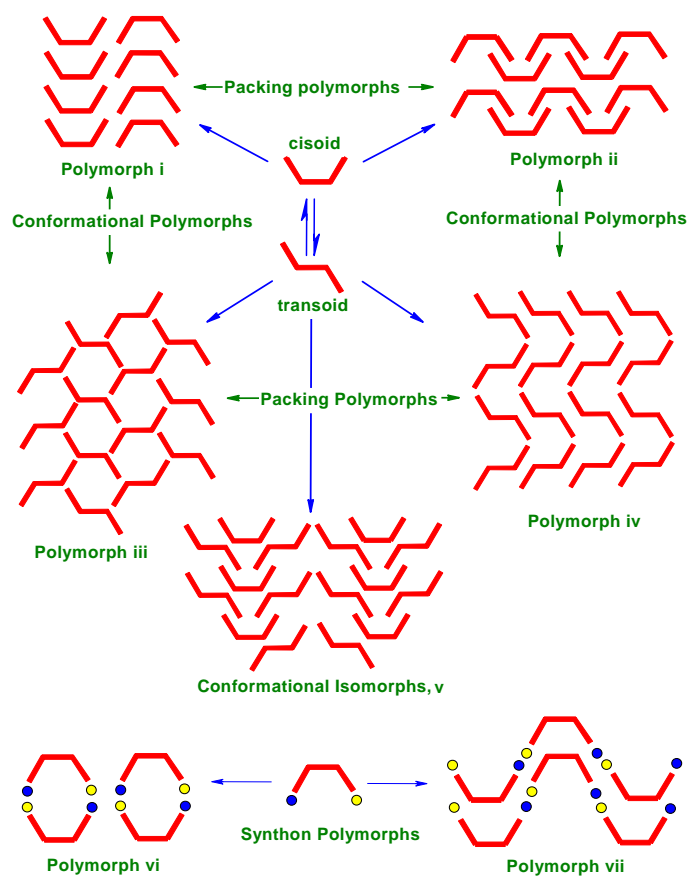
The word ‘*Polymorphism*’ originally comes from the Greek literature (*poly* = many, *morph* = form). Although the concept of existence of different crystal forms was realized as early as the nineteenth century, the widely accepted definition was given by McCrone who stated that “*a polymorph is a solid crystalline phase of a given compound resulting from the possibility of at least two different arrangements of the molecules of*

that compound in the solid state". Burger tried to simplify it as "*if these (solids composed of only one component) can exist in different crystal lattices, then we speak of polymorphism*".¹¹ In modern chemistry, a crystal is described as a 'supermolecule par excellence' by Dunitz.¹² In his view polymorphic modifications are 'superisomers' and polymorphism is a kind of 'superisomerism'.

Mitscherlich, in 1822, was the first to document polymorphism in the context of crystallography.^{13a} He noticed that arsenates and phosphates can exist as different crystal forms. Berzelius first described the existence of different crystal structures for the same element as allotrope.^{13b} Allotropes and polymorphs are closely related. Polymorphism is used in general to refer to structural diversity of molecular compounds whereas allotropy is the structural diversity of elements. In 1844, Amici invented polarizing microscope which is responsible for the development of chemical crystallography and especially polymorphism.^{13c} Mallard in his 1876 paper considered crystals to be built up by different packing arrangements of minute elementary crystallites giving rise to different crystal forms.^{13d} In 1891 Lehman characterized polymorphism depending on their reversible or irreversible phase changes as enantiotropic and monotropic respectively.^{13e} A major development in polymorphism came with the work of Ostwald in 1897, who found that unstable polymorphic forms have a greater solubility than the more stable forms in a particular solvent.^{13f} He developed the famous 'Rule of Steps' on relative stability of polymorphs. During the turn of the twentieth century many experimental techniques and theoretical models were developed such as hot stage microscopy (Lehman, 1891), dilatometry, vapor pressure and solubility measurement, heat capacity and transition point determination, the Gibbs Phase Rule and the Clapeyron equation to determine thermodynamic relations and used to test the earlier observations and experimental findings. With the help of polarizing microscope identification and characterization of materials became easy and many of such observations were compiled by Groth in the last three volumes (1910, 1917 and 1919) of his five volume epic collection.^{13g} Later during 1937 Bloom and Buerger pointed out the fundamental property change and importance of polymorphism.^{13h} During the period of 1956-69 McCrone worked on the pharmaceutical importance of polymorphism.¹³ⁱ

1.3 Classification and Terminologies

Polymorphism can be classified mainly as conformational polymorphism, synthon polymorphism and packing polymorphism depending on the basis of its occurrences. Scheme 1.3 depicts the different types of polymorphism. Although polymorphism is due to packing differences of the molecules in different crystal structures, however if the packing difference is due to differences in the molecular conformation then it is termed as conformational polymorphism.¹⁴ Conformationally flexible molecules have greater scope for polymorphic occurrence because of large number of degrees of freedom as the energy differences between conformational polymorphs generally lies in a small window of 0.5-3 kcal mol⁻¹.^{14c} A metastable conformation may be stabilized by stronger hydrogen bonds in the crystal structure while a stable conformer may not be able to form strong hydrogen bonds. The overall stability of a polymorph is accounted by the conformation energy and lattice energy (total) for a given polymorphic system. The energy compensation towards overall energy minimization in a polymorphic system is referred to as systematic effect. This phenomenon was recently reviewed by Nangia^{14c} with several examples of conformational polymorphs. Polymorphism in several cases discussed in this thesis such as, Fuchsones (Chapter 3 and Chapter 4), 2-(*p*-tolylamino)nicotinic acid (Chapter 5), Tolbutamide (Chapter 6), and Zolpidem•Succinic acid cocrystal (Chapter 6), are examples of conformational polymorphs.



Scheme 1.3 Schematic illustrations of different arrangement of molecules in the crystalline lattice that leads to different kinds of polymorphism. This scheme is culled from Ref. 14c.

A study by Yu and co-workers showed that 5-Methyl-2-[(2-nitrophenyl)amino]-3-thiophenecarbonitrile (**ROY**),^{14c} has a record number of seven polymorphs that result from the rotation of thiophene ring. Recently Nangia et al. reported the conformational polymorphs of Nimesulide^{14f}, a NSAID, and Curcumin^{14g}, a principal curcuminoid in the popular Indian dietary spice turmeric (Figure 1.1).

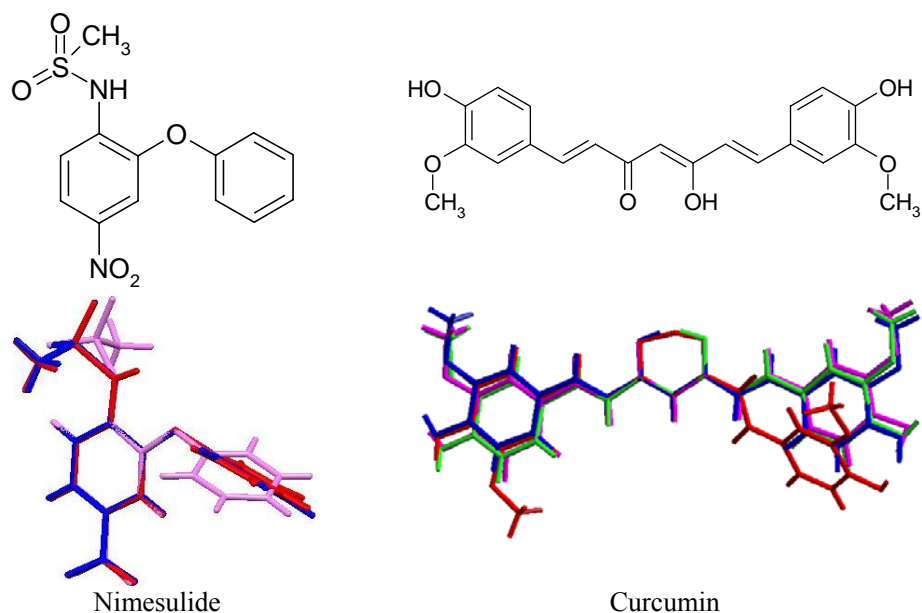


Figure 1.1 Conformational polymorphism in Nimesulide is due to the presence of the flexible phenoxy and sulfonamide groups whereas in Curcumin rotation of the aromatic ring about C–C single bond.

Polymorphs with different kind of hydrogen bonding pattern in different forms is termed as synthon polymorphism.¹⁵ The presence of multiple functional groups capable of forming various hydrogen bonding motifs increases the scope of polymorphism engaging *via* different kinds of hydrogen bond synthons in crystal structures. Polymorphism in isomeric hydroxybenzoic acids^{15d} is an example of synthon polymorphism. When polymorphism arises only because of different packing arrangement of molecules with the presence of same synthon or similar conformation, then it represents the case of packing polymorphism.¹⁶ Polymorphs can be identified using this classification but there are cases where two or more types of polymorphism exist in the same polymorphic system. Polymorphism in Furosemide, a diuretic drug, is due to both synthon and conformational differences (Figure 1.2 and 1.3).¹⁷ Pyrazinamide¹⁸ is also a similar case where both synthon and packing polymorphism was observed.

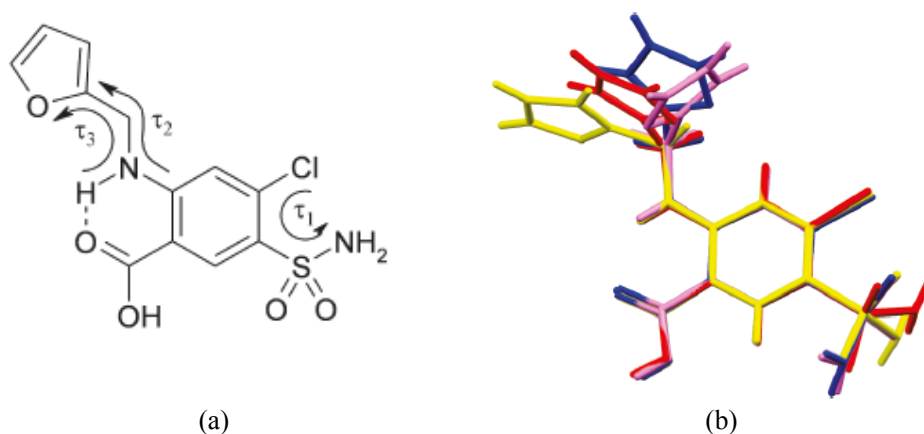


Figure 1.2 (a) The three torsion parameters in Furosemide: τ_1 =C-C-S-N, τ_2 =C-N-C-C, τ_3 =N-C-C-O. The anthranilic acid moiety is locked in an intramolecular hydrogen bond. (b) Overlay of four conformations in Furosemide crystal structures. Form 1 conformers (magenta and blue) have similar τ_1 but different τ_2 and τ_3 values, whereas all three torsion angles are different in form 2 and 3 conformers (yellow and red).

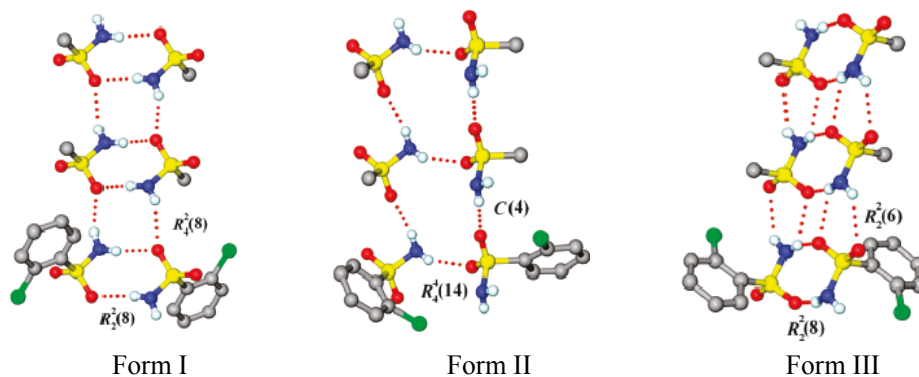


Figure 1.3 Synthon polymorphs of Furosemide: $R_2^2(8)$ N-H \cdots O dimer and $R_4^2(8)$ motif in form 1, $C(4)$ catemer and $R_4^4(8)$ tetramer motif in form 2, $R_2^2(8)$ N-H \cdots O motif and $R_2^2(6)$ rings in skewed dimer form 3. Anthranilic acid moiety is not shown for clarity.

Conformational isomorphism and conformational synmorphism are two phenomena which arise due to conformational differences present in molecules.¹⁹ The existence of different conformers of the same molecule in the same crystal structure represents conformational isomorphism. This situation arises when there is more than one molecule in the asymmetric unit ($Z > 1$). Conformational synmorphism refers to a random distribution of different conformers within the crystal structure.

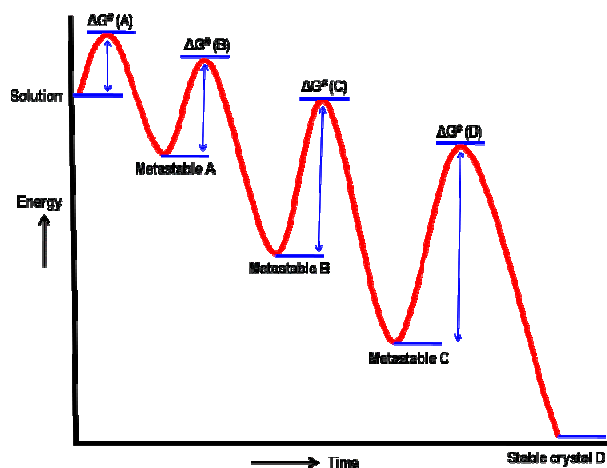
When polymorphs crystallize simultaneously in the same flask under identical crystal growth conditions from the same solvent, they are termed as concomitant polymorphs.²⁰ This phenomenon occurs when there are many metastable forms with almost similar energies that crystallize together. Concomitant polymorphism in benzamide is the first example of a polymorphic organic substance reported by Wöhler and Liebig in 1832.^{20b} Isotopomeric polymorphism is a term recently coined to describe a situation where a change in crystal structure is due to the changing the isotopic identity of one or more of the atoms in a molecule.²¹ Polytypism²² is a special case of polymorphism where the two-dimensional translations within the layers are essentially preserved. An element or compound is polytypic if it occurs in several structural modifications, each of which can be regarded as built up by stacking layers of (nearly) identical structure and composition, and if the modifications differ only in their stacking sequence.

1.4 Basis of Polymorphism – Kinetic Vs Thermodynamic Polymorph

The crystallization process consists of two main events, (i) nucleation and (ii) crystal growth. Although the exact mechanism of nucleation is not clear, a plausible mechanism is supported partly by some experimental evidence.²³ A solution is an entropy-dominated situation and a crystal is largely the enthalpically determined outcome. In solution various clusters involving both solute molecules and solvent molecules are formed using various intermolecular interactions. This brings elements of short range order in solution. These clusters are continuously breaking, forming and rearranging. At supersaturation these clusters become larger in size and more short range order enters in the system. At this stage nucleation occurs either by homogeneous nucleation (no effect of any external factor) or by heterogeneous nucleation (effect due to foreign particle, physical disturbance, scratched surface of vessel etc.) and solvent molecules from solute-solvent clusters exit into the bulk solvent simultaneously forming the crystal, which is characterised by long range order.²⁴

Ostwald^{13f} stated that a system moves to equilibrium from an initial high-energy state through minimal changes in free energy. Therefore the structure that crystallizes first is the one which has the lowest energy barrier (highest energy, kinetically

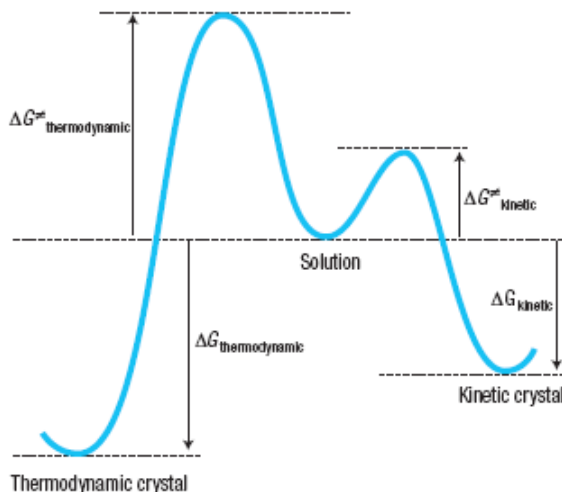
metastable). This form would then transform to the next lower energy polymorph until a thermodynamically stable state is reached, the so-called Ostwald's Law of Stages (Scheme 1.4).



Scheme 1.4 Ostwald's Rule of Stages. Initial high-energy state (metastable A) through minimal changes in free energy crystallizes first and is the one which has the lowest energy barrier. Metastable A form will then transform to the next lower energy polymorph (metastable B) and so on (metastable C) until thermodynamically stable crystal D.

The Curtin–Hammett principle can be applied to the crystallization process in the same way as it is to chemical reactions (Scheme 1.5). Accordingly the route to the kinetically favoured crystal structure would be the fastest, because the activation energy (G) barrier to that state is lower ($\Delta G^{\ddagger}_{\text{kinetic}}$). The thermodynamically favoured crystal would take longer to form because the activation barrier is much higher ($\Delta G^{\ddagger}_{\text{thermodynamic}}$), but it would be more stable because the final energy state is the lowest. If the same crystalline form is both kinetically and thermodynamically favoured, polymorphism is less likely.²⁵ There are two main and often competing factors which govern the crystallization reaction, (1) directional intermolecular interactions like hydrogen bonds and (2) close packing. Generally, the energy contribution from close packing is more than that of the intermolecular interactions. This would tend to favor the thermodynamic crystal. Conversely, solute-solvent clusters present in solution, which in turn give birth to

crystal nucleus, are stabilized by intermolecular interactions. Therefore, intermolecular interactions generally favor kinetic crystals. It is highly unlikely to observe polymorphism in crystal systems where the best interactions are accompanied by the best packing. Examples like benzoic acids, naphthalene and D-glucose belong to this category where polymorphism is not observed so far.²⁵



Scheme 1.5 Kinetic and thermodynamic outcome of crystallization reaction. This scheme is culled from Ref. 25.

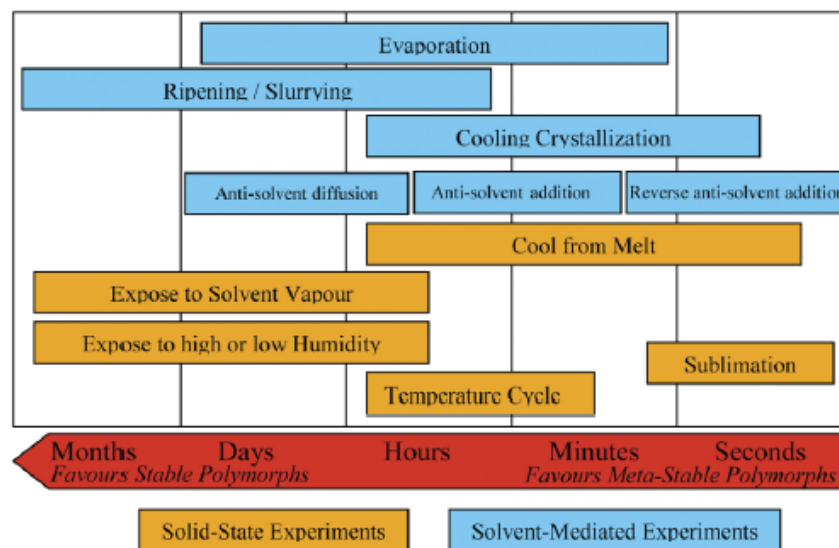
From thermodynamic consideration polymorphic pairs can be divided as monotropic and enantiotropic systems.²⁶ Monotropic systems are defined as systems where a single form is more stable regardless of temperature. Enantiotropic systems are defined as systems where the relative stabilities of the two forms invert at some transition temperature. In other words, if the free energy curves of two forms cross below the melting point of the lower melting polymorph, they are said to be enantiotropically related and if the free energy curves do not cross below the lower melting polymorph, they are said to be monotropically related.

The next step after nucleation is the crystal growth.²⁷ After clusters attain a critical size in the system and the nucleation stage is complete, the growth stage commences. Among the clusters that are formed, those exceeding the critical size do not dissociate and can grow larger. Since the structure is already formed, the solute

component will be incorporated into the crystal at the expense of a much smaller energy than that necessary for nucleation. The crystal growth mechanism will be different depending on the atomic roughness or smoothness of the interface between the solid and liquid phases that appeared as a result of nucleation. The morphology of single crystals is determined by the crystal structure (the internal factors), the crystal growth conditions, and the process of crystal growth (the external factors). Crystals having different crystal structures usually take geometrical external forms following the symmetries involved in their respective structures, but they may also take very different external forms if the growth conditions are dissimilar. Crystals formed under small driving force conditions in dilute ambient phases, such as the vapor phase or solution phase, will generally exhibit polyhedral forms, irrespective of their size. When a crystal is synthesized using a seed crystal or by a controlled growth technique such as one-directional solidification, it takes on a very different morphology from that of a freely grown crystal.

1.5 The Experimental Search for Polymorphs

Among the various methods of polymorph generation, solution crystallization and/or high throughput crystallization technique²⁸ is traditionally used. Conditions for solution crystallization can be varied by changing solvents (or solvent mixtures), temperature, supersaturation, stirring, slurrying, cooling rate, seeding, use of antisolvent etc. Recent approaches for polymorph generation include crystallization with structurally related additives,^{29a,b} epitaxial growth,^{29c} melting, sublimation, laser induced nucleation,^{29d} crystallization in capillaries,^{29e} confinement within porous materials,^{29f} using polymers as heteronuclei,^{29g,h} mechanical grinding,²⁹ⁱ using supercritical liquids,^{29j} using self assembled monolayer with different functional moieties,^{29k} potentiometric cycling,^{29m} crystallization in gel medium^{29n,o} etc. Goodman et al.³⁰ presented the following scheme to illustrate the time scale required for most of the traditional crystallization process (Scheme 1.6).



Scheme 1.6 Time scale required for various solid state (cool from melt, solvent vapor exposure, expose to humid conditions, sublimation etc, in yellow boxes) as well as solvent mediated (evaporation, slurring, cooling crystallization, addition or diffusion of antisolvent etc. in light blue boxes) crystallization techniques. (This scheme is culled from Ref. 30).

Control over crystallization of a particular polymorph is possible by using a particular solvent system if the polymorphic systems have well documented crystal structures and phase relations.³¹ Form I of ranitidine hydrochloride which contains enamine tautomer can be crystallized by using non-polar solvents which leads to the strong hydrogen bonding interactions. In more polar solvent, such as water or methanol, Form II (nitronic acid tautomer) was obtained as ranitidine–ranitidine hydrogen-bonding interactions were disrupted in the polar medium.^{31c} The degree of supersaturation of a solution can also affect the preference for crystallization of different polymorphs. In a supersaturated solution any nucleation point may lead to the formation of metastable polymorph compared to the stable one. Using seed crystal to obtain a desired polymorph is a well established technique but it is not always successful.³² Seeding may be successful provided the seed crystal is added to a saturated solution before the nucleation of other nuclei starts. Addition of the seed crystals to a dilute solution may result in dissolution of the added crystal. On the other hand seeding may result in a different polymorph due to heterogeneous nucleation.³³

Use of hetero-seed is found to be successful in certain cases.³⁴ A crystalline sample formed by molecules having almost same structure as the compound of interest but only difference is due to a substituent or counterion (in case of a salt) is termed as hetero-seeding.

In recent times new polymorphic forms of many drug molecules were obtained serendipitously during attempted cocrystallization.^{14g,35} This subject has now undergone a renaissance. Although in most of the cases the reason of this unpredicted occurrences of novel polymorphs were unknown, but to obtain a particular crystal form or to inhibit the formation of an unwanted polymorph is proved to be successful by using tailor made additives.³⁶ An additive can inhibit the growth of some initially formed nuclei without interfering with the growth of the other phases.

1.6 Statistics on Polymorphs

McCrone's statement¹¹ four decade ago "*the number of polymorphs known for a given compound is proportional to the time and money spent in research on that compound*" is strongly validated in last few years. Many papers³⁷ and reviews³⁸ and theme issues dedicated to polymorphism came up highlighting its importance, scope and challenges. Statistics on polymorphs are not easy as the result may be biased by many factors such as choice of database where many reports on multiple crystal forms in primary literature is not included, intent of survey etc. Different research groups carried out database analyses to estimate the percentage of compounds that are polymorphic. It was found that about 4-5% of organic compounds,³⁹ 5.5% organometallics, and 2.1% of coordination compounds are shown to exhibit polymorphism.⁴⁰ Polymorphism is more widespread in pharmaceutical solids, with estimates of 30-50% in drug-like molecules⁴¹ compared to CSD statistics of 4-5% in organic compounds. However drug polymorphs are often not archived in the CSD for proprietary reasons.

A recent report on statistics on multiple crystal forms⁴² from various sources is shown in Table 1.1.

Table 1.1 Statistics on multiple crystal forms (The entries do not necessarily add to 100% as there are many cases of solvates and/or hydrates and/or polymorphs for a single compound, Ref. 42).

.Database	Total no. of entries	Monomorphic (%)	Polymorphs (%)	Hydrates (%)	Solvates (%)
Merck Index 13 th ed. (2001)	10,250	(10,160)			
CSD (Nov 2008)	456,637	70.4	3.5 (16,035)	26.1 (119,107)	
Beilstein (2009)	11,000,000	99.85			
Agrochemicals	686	78	18.8	42	2.2
Pharmacopoeia Europa 5.8	960 drugs	36	41	34	18

There is a considerable growth in the reported structures and papers on polymorphism. Number of trimorphic and tetramorphic polymorphic clusters identified by Gavezotti and Filipini⁴³ in 1995 were 13 and 3 respectively. There was no report of more than tetramorphic crystal structures. Database search by Yu et. al. in 2005^{14e} and later by Nangia et. al. in 2006^{44a} and by Dr. S. Roy for his PhD thesis in 2007^{44b} shows that there is a tremendous increase of trimorphic crystal structure as well as a reasonable increase of tetramorphic crystal structures too. A CSD (Ver. 1.12, Aug. 2010) search for tetramorphic or more than tetramorphic crystal structures is presented in Chapter 4.

1.7 Importance of Polymorphism

Polymorphism in organic solids is of fundamental importance because of its ability to alter various physical and chemical properties.⁴⁵ Table 1.2 depicts the properties that can vary for polymorphs. From the studies on polymorphism molecular recognition, crystal nucleation, crystallization, and phase relationship between solids can be inferred.⁴⁶ Polymorphism presents special opportunities to analyze structure–property relationships⁴⁷ because the conformation, hydrogen bonding and lattice energy of the

same molecule in different crystalline environments may be compared in polymorphic structures.

Table 1.2 Properties that can be different for polymorphs. This table is culled from Ref. 45d.

Packing properties	Thermodynamic properties
• Molar volume and density	• Melting and sublimation temperatures
• Refractive index, optical properties	• Internal energy
• Conductivity, electrical and thermal	• Enthalpy
• Hygroscopicity	• Heat capacity
Kinetic properties	• Entropy
• Dissolution rate	• Free energy and chemical potential
• Rates of solid state reactions	• Thermodynamic activity
• Stability	• Vapour pressure
Surface properties	• Solubility
• Surface free energy	Spectroscopic properties
• Interfacial tensions	• Electronic transitions, ultraviolet-visible spectra
• Habit	• Vibrational transitions, infrared and Raman spectra
Mechanical properties	• Rotational transitions
• Hardness	• Nuclear magnetic resonance chemical shifts
• Tensile strength	
• Compactibility, tabletability	
• Handling, flow and blending	

1.7.1 Polymorphism in pharmaceutical industry

Polymorphism has received particular attention in the recent literature because of its importance in drug substances and pharmaceutical formulation.^{41,45} As shown in Table 1.2, drug polymorphs can have different physico-chemical properties that can affect drug performance drastically. Dissolution rate and solubility properties are the most crucial for API polymorphs.⁴¹ In the physiological absorption of a drug, the dissolution of the drug is often the rate determining step and it may affect the bioavailability of the drug. The rate and extent of physiological absorption determines the overall efficacy of a drug.

Bioavailability may vary for polymorphic forms and this is an important scientific and regulatory issue.⁴⁸ There are many examples where the bioavailability of polymorphs varies significantly viz. Phenobarbital,⁴⁹ Indomethacin⁵⁰, Mercaptopurine⁵¹ and Mebendazole⁵² are a few examples. Hence a polymorph having higher dissolution rate, solubility and/or bioavailability may be considered for formulation. Sometimes high solubility is not preferred because of adverse effects. One such example is the antihelminthic drug Mebendazole, which is trimorphic and physical properties of the three polymorphs are very different. The solubility of these forms in physiological media is Form B > Form C > Form A. Based on these differences Form C is pharmaceutically preferred since its solubility is sufficient enough to ensure optimal bioavailability without the possible toxicity of the more soluble Form B.⁵³

Generally, metastable states exhibit better solubility properties than stable polymorphs but the former have stability problems.^{41b} These metastable forms might be chemically less stable and/or may have a tendency to convert into a stable polymorph. Such forms should be avoided in the formulation. For example in ritonavir,⁵³ the more soluble polymorph converted to a new, less soluble and more stable polymorph, leading to recall of the product.

Different structures and properties make polymorphs patentable.⁵⁴ If a generic pharmaceutical company discovers a novel crystal form of an already marketed drug, it will gain an early access into the market place; therefore, the innovator companies must find out all possible polymorphs of the drug and patent them in order to extend their monopoly in pharmaceutical industry and to protect their product. A well-known example is the polymorphs of anti-ulcer drug Ranitidine hydrochloride.⁵⁴ Glaxo obtained a patent on the two polymorphs (I followed by II) of Ranitidine hydrochloride. In the mid 1990s, as the patent on the drug (form I) was approaching expiration, other companies began preparing to market a cheaper, generic versions of form I. But the generic manufacturers were not able to crystallize form I exclusively as it was always crystallizing as a mixture of form I and form II. This kept the generic companies products off the market for several years and during that period Glaxo was making \$10 million in sales each day on this simple drug. Ultimately Novopharm could find a method to prepare exclusively form I with non-detectable amounts of form II, and won

the battle and since then generic entry was made into the market. Cefadroxil, terazosin hydrochloride and aspartame are other well known examples of patent issues surrounding polymorphism.^{54a}

1.7.2 Importance of polymorphism in other fields

Apart from pharmaceutical industry polymorphism plays important role in a number of industrial and commercial applications⁵⁵ such as in agrochemicals, photographic industry, food additives industry, fat-based food products (ice cream, chocolate, and margarine), pigment industry, high energy materials etc.

Differences in solubility of polymorphs can pose problems during manufacture, and can lead to impaired performance also observed in photographic industry. Polymorphism is well known with colorants. In pigment industry polymorphism plays important role as the essential properties for a pigment to be useful such as, maximum molar extinction coefficient, particle size distribution, morphology, solubility, lightfastness, weatherfastness, tendency to aggregate, crystallinity, flocculation, wetting capability, dispersibility, dissolution rate, filtration properties, tendency to cake, dispersion properties, and powder flow properties may vary with different polymorphic forms.⁵⁵ Pigment Violet 19, quinacridone^{55b,c,d}, exists in four known polymorphs. Quinacridone was first synthesised in 1935 as the reddish α -form which was not commercialised because of its poor fastness properties. Twenty years later its potential as a pigment was recognised after the discovery of two new polymorphs, β and γ , with remarkably different colour properties. Treatment in high boiling organic solvents at elevated temperature converts, the α -quinacridone to the β - or γ -forms, which are violet and pink, and characterized by a high stability to light, weather, temperature (up to 400 °C) and solvents.

High energy materials polymorphs are well known and their polymorphic behavior can change properties like sensitivity to detonation, the rate of deflagration to detonation transition, the detonation velocity, the detonation pressure, the crystal density, thermal and shock stability and crystal morphology which influence their performance as explosives.⁵⁵ 2,4,6-trinitrotoluene, TNT, exists as two structurally similar dimorphs, with the less stable form converting with time to the more stable one.^{55f} This solid–solid

transformation from one polymorph to the other is associated with risk as its phase transition can cause macroscopic defects in the crystalline material, increasing the detonation sensitivity.

The herbicide metazachlor^{55g} exists as five polymorphic modifications. Since metazachlor is used as an aqueous suspension, the use of metastable forms (at ambient conditions these are forms I and II) is not advisable because of a potential transformation to form III.

1.8 Characterization of Polymorphs

The characterization of polymorphs is the first step after screening all possible forms of a compound. Optical and hot stage microscopy⁵⁶ are widely used to study various properties of polymorphic compounds such as homogeneity or diversity of crystalline samples, variations in size, shape or color, melting point, phase transformation, detection of discontinuous changes in polarization colors during the heating, sublimation behavior, etc. Thermal analysis⁵⁷ has been an extremely important analytical tool in the pharmaceutical industry for more than 40 years. Differential Scanning Calorimetry (DSC) measures the rate of heat flow and is used to measure the heat of transition. As all the transitions in materials involve heat flow (into the sample in endothermic events and out of the sample for exothermic events), DSC became the universal technique for measuring the wide variety of temperature induced transitions in solid materials. Thermogravimetric analysis (TGA) measures physical changes in materials. TGA provides quantitative measurement of mass change in materials associated with transition and thermal degradation.

X-ray crystallography⁵⁸, which reflect differences in crystal structures, is one of the most definitive methods in the identification and characterization of polymorphs. Different solid forms possess different X-ray powder patterns in most cases; therefore it is a primary tool for characterizing them. The X-ray powder diffraction pattern of a solid is a plot of the diffraction intensity as a function of 2θ values and can be considered as a fingerprint of that solid. Single crystal X-ray crystallographic techniques are employed to determine details of the molecular and crystal structure and bonding interactions in the

solid. Single crystal X-ray crystallography is advantageous over X-ray powder diffraction in cases where two genuine polymorphs possess almost similar powder pattern.

Spectroscopic investigations deliver chemical and physical information combined high throughput analysis and the non-invasive measurements with high selectivity and sensitivity. Various spectroscopic techniques such as FT-IR⁵⁹, FT-Raman⁶⁰, near IR⁶¹ and more recently solid state NMR⁶² are used regularly to characterize various polymorphic forms. Scanning electron microscopy (SEM) provides greater magnification than optical microscopy. Resolution in atomic force microscopy (AFM) and scanning tunneling microscopy (STM) are even higher and these techniques provide useful information about morphology and surface properties of polymorphs.⁶³

1.9 Utility of Hirshfeld Surface Analysis in Polymorphism

In polymorphic crystals, understanding the differences between the chemical environments of identical molecules is a key to understand the structure as a whole. Spackman et al.⁶⁴ developed a very powerful technique, to determine how different is the chemical surrounding of the molecule in two (or more) comparing crystal structures or if two (or more) structures are true polymorph, which utilizes the Hirshfeld surfaces, originally conceptualized in the 1970s by Hirshfeld.⁶⁵ The Hirshfeld surface of a molecule in a crystal is constructed by partitioning space in the crystal into regions where the electron distribution of a sum of spherical atoms for the molecule (the promolecule) dominates the corresponding sum over the crystal (the procrystal). The Hirshfeld surface is then defined in a crystal as that region around a molecule where $w(r) \geq 0.5$. These representations have been incorporated into a software package *Crystal Explorer*. The two-dimensional “molecular fingerprint” associated with Hirshfeld surfaces, allows one to analyze in detail the intermolecular interactions and is very useful in comparing crystal structure and identifying polymorphs. The fingerprint is a standard graphical two-dimensional map that indicates the distribution of the interactions for a single molecule in the structure and is perhaps one of the most useful tools for comparing polymorphic crystal structures.

Differentiation of polymorphic crystal structures using 2D fingerprint plot as Hirshfeld surface are explained in Chapters 5 and 6. The example below demonstrates how 2D fingerprint plots are useful in determining whether two crystal structures are true polymorphs or not. Three crystal structures of methyl paraben were archived (CEBGOF, CEBGOF01, and CEBGOF02) in the CSD.⁶⁶ The crystal structures with $Z'=3$, corresponding to these three refcodes represent the same polymorphs, Form I, although earlier claimed to be different. The 2D fingerprint plot as Hirshfeld surface applied on the crystal structures corresponding to CEBGOF01, and CEBGOF02 shows clearly the similarity of the fingerprints as shown in Figure 1.4. From visual observation of the finger print plot it is clear that CEBGOF01 molecule 1= CEBGOF02 molecule 2; CEBGOF01 molecule 2= CEBGOF02 molecule 1 and CEBGOF01 molecule 3= CEBGOF02 molecule 2. Therefore, chemical environment of the 3 symmetry independent molecule of the crystal structure corresponding to refcode CEBGOF01 is same as that of the three molecules of the crystal structure corresponding to refcode CEBGOF02. Therefore both the structures are one and the same not true polymorphs.

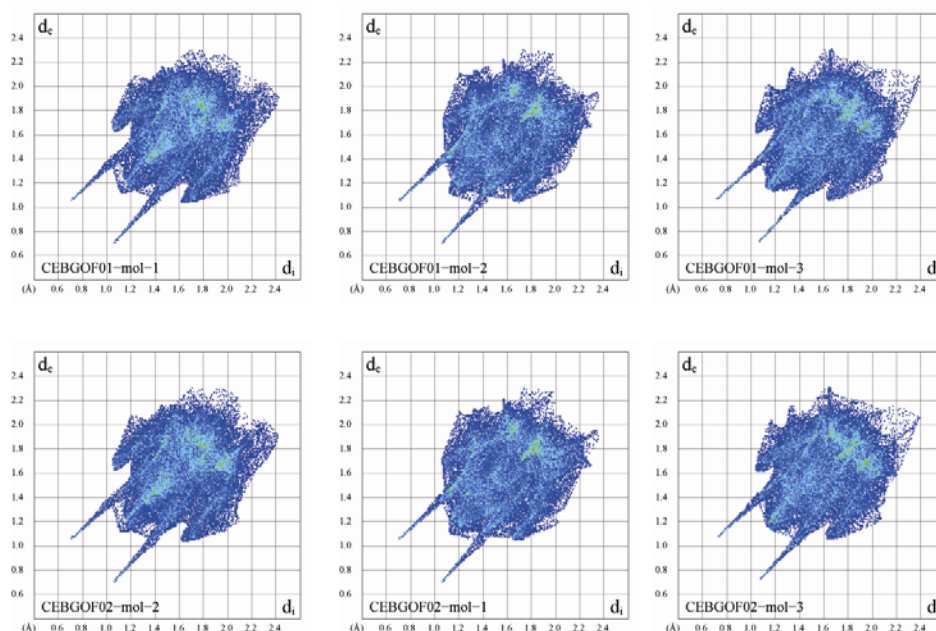


Figure 1.4 Comparison of the 2D Hirschfeld finger print plot of two of three reported crystal structures (CEBGOF01 and CEBGOF02) of methyl paraben.

1.10 Isomorphism and Isostructurality: Definitions and Background

According to IUCr online dictionary⁶⁷, two crystals are said to be Isomorphous (isometric) if (a) both have the same space group and unit-cell dimensions and (b) the types and the positions of atoms in both are the same except for a replacement of one or more atoms in one structure with different types of atoms in the other (isomorphous replacement), such as heavy atoms, or the presence of one or more additional atoms in one of them (isomorphous addition). Isomorphism here does not mean molecular isomorphism, i.e. similar morphology of crystalline substances, but it means crystallographic isomorphism where isomorphous crystals form solid solutions. Two crystals are said to be Isostructural if they have the same structure, but not necessarily the same unit cell dimensions nor the same chemical composition, and with a 'comparable' variability in the atomic coordinates to that of the cell dimensions and chemical composition.

The history of isostructurality⁶⁸ started when Romédel'Isle (in 1772) for the first time observed growing crystals of potassium alum, with a coat ammonium alum layer over them, when placed in a saturated solution of ammonium alum. In the year 1809, Wollaston recognized that calcite (CaCO_3), magnesite (MgCO_3) and siderite (FeCO_3) crystallize as rhombohedra with slightly different faces. Mitscherlich (1819) observed pairs of phosphate and arsenate salts (e. g. KH_2PO_4 , KH_2AsO_4 , $\text{NH}_4\text{H}_2\text{PO}_4$ and $\text{NH}_4\text{H}_2\text{AsO}_4$) acquired the same crystalline form and these salts have similar chemical formulae, i.e., one kind of atom in one compound being replaced by another kind in the related salts. These pairs of salts were then called isomorphous. At the same time the term polymorphism also came up after observing different crystals for same compounds. Berzelius used the isomorphous nature of Na_2SO_4 , Ag_2SO_4 , Na_2SeO_4 and Ag_2SeO_4 to establish the atomic weight of selenium in 1828. Von Groth (1874), Náray-Szabó (1969) and others developed the phenomena and concluded that the basic conditions for isomorphism of compounds is that the crystals are closely similar in shape and one of the crystals continue growing in the solution of the others. Wells, Bloss and other authors introduced the term isostructural and isostructurality (or isotypism).^{68c} Zoltai and Stout^{68c} gave the definitions as, solid solution series in which the crystal structures remain same

throughout the series is isomorphism whereas isostructurality is the relationship among minerals of different chemical composition and identical crystal structures.

Kitaigorodskii⁶⁹ was the first to review isostructurality in organic molecular crystals by using the term isomorphism. Kálmán et al.⁷⁰ studied crystal structures of various steroids such as digitoxigenin, digirezigenin, 3-epidigitoxigenin, uzarigenin, bufalin, cinobufagin etc. and used the term ‘isostructural’ to define identical or quasi-identical packing motifs of organic crystals. They have divided isostructurality into two categories—isostructural crystals or main-part isostructuralism of related molecules and homeostructural crystals.

(1) Isostructural crystal: Isomorphous (isometric) molecules form identical packing motifs. This phenomenon was previously termed as main-part isostructuralism of related molecules. They may differ by the substituents present, chirality of one atom, or multivalent shielded core atoms having similar atomic radii of the interchangeable atoms. In general isomorphous crystals which differ by only one substituent have high degree of structural similarity. Isostructural crystal pairs formed by molecules differing only in the chirality of one atom are termed as configurationally isostructural.

(2) Homeostructural crystals: When the related molecules differing by substitutions on more than one atomic site have similar packing, it is called homeostructural crystals.

1.11 When Isostructurality Occurs?

Geometrical properties like shape, size and chemical properties such as electronegativity, polarizability of functional group influence crystal packing. Kitaigorodskii has given importance to the volume and shape of functional groups in crystal packing,⁶⁹ however, the electronic properties of functional groups cannot be ignored.⁷¹ As the size of the molecule increases the significance of geometric effects becomes important. A given packing motif may be able to tolerate small changes in the molecular structure without a considerable change in the close-packed crystal structure. These changes are minor alterations in substitution and/or epimerization. The tolerance may be ascribed to the presence of ~30% free space in close-packed structures because the packing coefficients of organic crystals are generally about 70%.

There are certain substituents when present in a molecule can be replaced with other substituents without altering the crystal packing. This is known as functional group exchange in terms of isostructurality. It is important to have some knowledge about which groups are interchangeable and under which circumstances to see the isostructural behavior between two structures. Kitaigorodskii⁶⁹ has ranked them as, (i) the halogens Cl, Br, I; (ii) O and S; (iii) C, quadrivalent Si, Ge, Sn and Pb.

The most well studied substituents are halogen atoms.⁷² Cl→methyl and Br→methyl exchange to result isostructural crystal is observed in many cases.⁷³ The other examples which shows isostructural behavior to a certain extent include⁷⁴ OH→=O^{74a}, CH₃→C₂H₅^{74b}, H→O-H^{74a}, H→CH₃^{74c,d}, H₂→=O^{74e}, N→C-H^{74f,g}, P=O→P (l. p.)^{74h}, C-H→*t*-Bu⁷⁴ⁱ etc.

The almost similar van der Waals radii of Cl and methyl allow them to form isostructural crystals. Kitaigorodskii and others^{69,75} have used the principle of close packing by interchanging substituents in such a way that each group occupies approximately the same volume. Kitaigorodskii's "close-packing model" proposed⁶⁹ that the packing of molecules in a crystal structure can be predicted in such a way that the 'voids' in one are locked into the 'protrusions' of the other, volume and shape considerations hold sway rather than electronic factors. Since chloro (19 Å³) and methyl (24 Å³) groups have nearly the same volume, they may be interchanged in a molecule without altering the crystal structure, the so-called 'chloro-methyl exchange rule'. Thus each non-polar substituent group of a certain volume can be exchanged for another non-polar group of a similar volume without any change in the crystal structure. Such isostructural behavior is found when crystal stabilization is mainly through dispersive and repulsive interactions. A recent study by Fernandes showed^{73j} the chloro-methyl exchange between a series of 2,6-disubstituted-N-phenylformamides. Violations of this rule are observed when directional forces or weak bonds are involved and the failure of complete chloro-methyl exchange in a substance like hexachlorobenzene points to the importance of weakly attractive Cl⋯Cl interactions.

Isostructurality was observed in the crystal structures of various steroids with an exchange of functional groups such as H→OH in cinobufagin↔cinobufotalin,

digitoxigenin bisdigitoxoside \leftrightarrow gitoxigenin bisdigitoxoside, H \rightarrow CH₃ in digitoxigenin \leftrightarrow (21*R*)- and (21*S*)-methyldigitoxigenins, CH₂ \rightarrow C=O in gamabufotalin \leftrightarrow arenobufagin, H₂ \rightarrow =O in gamabufotalin \leftrightarrow arenobufagin etc.

There is reported bromide and nitrate exchange in isostructural crystals in spite of their different shapes where both of the anions make strong H-bonds with the cation counter part.⁷⁶ Above all these groups, the halogen exchange, specially Cl, Br and I to produce isostructurality, are more frequent. Propargylammonium halides (Cl⁻, Br⁻, I⁻) are isostructural where halide ions accept three H-bonds from ammonium group and one from terminal alkyne group. Another interesting isostructurality has been reported by Bar et al.^{72e} in *para* substituted X-C₆H₄-CH=N-C₆H₄-X' molecules. When X = X' = Cl or Br, the molecules are not isostructural, but the molecule with X = Cl and X' = Br is isostructural to the dichloro compound. On the other hand, X = Br and X' = Cl substituted molecule is isostructural to dibromo derivative. It indicates the importance of halogens as well as the position of substitution in the molecules.

The size of the molecules also plays an important role in producing isostructural crystals. Small molecules such as urea (CH₄N₂O) and thiourea (CH₄N₂S) cannot form isostructural crystal structures since the difference in volume of S and O is significant with respect to the volumes of the individual molecules.⁷⁷ As the molecular volume increases, possibility of functional group exchangeability also increases and the possibility of an isostructural relationship becomes higher. For example, the 5-halo-substituted indol-3-ylacetic acid^{70a} contains 14 non-H and eight H atoms. The 5-F and 5-Cl derivatives are isostructural with F \rightarrow Cl exchange but corresponding 5-Br derivative is not isostructural as volume of Br is much higher volume of Cl and F. In contrast, 17-halo-3-methoxy-16,17-secoestra-1,3,5-triene-16-nitrile^{72b} which contains 22 non-H atoms and 24 H atoms, Cl \rightarrow Br \rightarrow I exchange occurs to produce isostructurality. In an extreme case, the biosides of digitoxigenin and gitoxigenin⁷⁸ (16-OH-digitoxigenin) which possesses 52 non-H atoms with 62 H atoms are isostructural.

The isostructurality due to exchange is equally applicable for host guest complexes. (Triphenylisocyanurate).(trinitrobenzene).(benzene) solvate is isostructural to the corresponding 1:1:1 thiophene solvate. This is a case of the benzene-thiophene

exchange rule.^{79a} Chlorobenzene/toluene solvates of tetraphenyl-anthridine,^{79b} substituted *gem*-alkynols^{79c} are some of the notable examples that show solvent/substituent exchange without altering the overall packing arrangements.

In organometallic compounds isomorphous replacement of core atoms may also take place.^{79d,e} Crystal structures of the series of organometallic compounds $\text{Ph}_3\text{X}-\text{X}'\text{Me}_3$ (X, X' = metal atom) when X, X' are Si, Si; Ge, Si; Si, Ge and Ge, Si are isostructural.

Molecules differing only in the chirality of one atom can form isostructural crystal. (21*R*)- and (21*S*)-methyldigitoxigenins form isostructural crystals despite having inverted molecular structure due to the chiral carbon atom.^{80d,79f,g} Isostructurality may also be seen in certain compounds due to orientational, positional and substitutional disorders.^{73c,79h}

1.12 Isostructurality Among Polymorphs

Isostructurality in three dimensions means the similarity of complete crystal packing. One and two dimensional isostructurality⁸⁰ is documented. If two crystal structures contain similar rows of molecules such as an infinite hydrogen bonded chain, then they are called one dimensional isostructural. Similarly, if two molecules contain similar infinite two dimensional arrangements of molecules, such as sheets of hydrogen bonded molecules extending in one plane, they are called two dimensional isostructural. For one and two dimensional isostructural crystal structures, similar unit cell parameters and space group is not a requirement and this phenomenon is not rare in literature. Fábíán and Kálmán documented 1D, 2D and 3D isostructurality among polymorphs.^{80a} The four polymorphs of glycine^{80h,i,j,k} (α , β , γ and δ) shows similarity in their crystal structures (Figure 1.5).

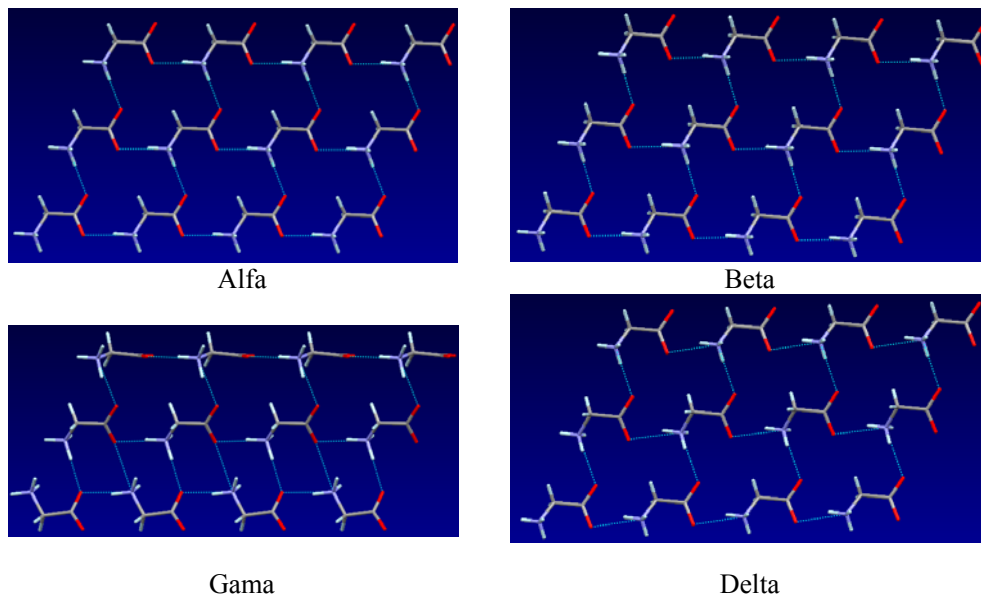


Figure 1.5 α , β and δ polymorphs of Glycine contain similar two dimensional layers of molecules whereas γ polymorph contains 1D infinite molecular chain similar to the α , β and δ polymorphs. Therefore α , β and δ are two dimensional isostructural whereas γ polymorph is 1D isostructural with α , β and δ polymorphs.

1.13 Descriptors of Isostructurality

Kálmán et al. proposed two descriptors to quantify isostructurality^{68a,70a}, viz. unit cell similarity index ‘ Π ’ and isostructurality index ‘ $I_i(n)$ ’ and can be defined as the following equations.

$$\Pi = \left| \frac{a + b + c}{a' + b' + c'} \right| - 1 \cong 0$$

where a , b , c and a' , b' , c' are orthogonalized lattice parameters of the related structures. For a pair of completely isostructural crystals Π should be close to zero. Value of Π can be calculated using *cell.cmp* software.

$$I_i(n) = \left[1 - \left(\frac{\sum_i \Delta R_i^2}{n} \right)^{1/2} \right] \times 100$$

The isostructurality index, $[I_i(n)]$ is a measure of the degree of internal isostructurality where n is the number of distance differences (ΔR_i) between the absolute coordinates of identical non-hydrogen atoms within the same section of asymmetric units of related structures. $I_i(n)$ should be close to 100% for isomorphous crystals. *Isov* or *isov2* softwares were developed to calculate $[I_i(n)]$.^{15j}

A recent approach to identify similar packing motifs is the XPac method.⁸¹ Xpac is a computer program written by Dr. T. Gelbrich and Prof. Michael B. Hursthouse at the University of Southampton Highfield, UK. In this method similarities and differences between two crystal structures are expressed in terms of ‘*supramolecular construct*’. Analysis of crystal structures using the XPac technique is presented in Chapter 3.

1.14 Solid Solution

Solid solution or mixed crystal⁸² is a solid state solution of two or more components where addition of the solute does not change the crystal structure of the solvent but the ratio of solute to solvent will vary in a non-stoichiometric proportion throughout the structure. Solid solutions are frequently encountered in the field of metallurgy but are less probable with organic molecules. The necessary condition for solid solution formation is that the compounds should be isomorphous. Some compounds with different crystal structures can also form solid solution where the minor component adopts the structure of the major component. This phenomenon is termed as structural mimicry.^{82c,d,e} For example, the crystal structures of chlorinated (**1**) and methylated (**2**) derivatives of the fragment 2-benzyl-5-bromobenzylidene-cyclopentanone (Figure 1.6) are not isostructural and **1** has a bent conformation whereas **2** is planar. These two compounds can form solid solution where **1** adopts a planar conformation.^{82d}

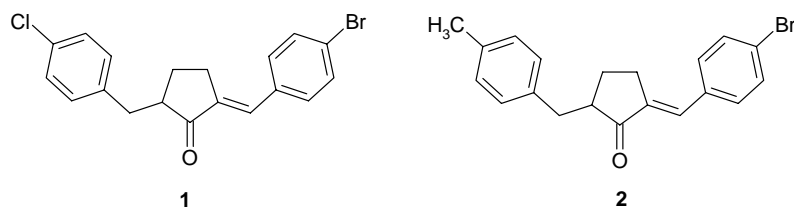


Figure 1.6 Non-isostructural chloro (**1**) and methyl (**2**) derivatives of 2-benzyl-5-bromobenzylidene-cyclopentanone forms solid solution where the minor component **1** adopts the conformation of the major component **2** showing structural mimicry.

1.15 Importance of Isostructurality

The main importance of isostructurality lies in the fact that, it is possible to design isostructural crystals to some extent. In isostructural compounds the structural parameter is kept nearly fixed and therefore chemical perturbation can be evaluated. Predicting crystal structures is a challenge in crystallography. The concept of isostructurality is helpful in crystal structure prediction.⁸³ Isostructurality helps in a logical expectation of polymorphism. For two isostructural compounds if one of them is polymorphic, one can expect the other molecule could be polymorphic too.⁸⁴ Such an example is explained in Chapter 2, where crystallization of triiodoresorcinol in $P2_1/n$ space group finds logic to be polymorphic as the terminal members of the series, triiodophenol and triiodophloroglucinol are isomorphous in orthorhombic space group $P2_12_12_1$. Isostructurality can also be used in inorganic-organic hybrid materials. Isostructural series of metal organic frameworks (MOFs) with controllable H_2 gas storage properties are documented. Isostructural MOFs with same crystal structure and different metal atoms may serve as the ideal system to study the H_2 binding capacity of metals.⁸⁵ Structural equivalence of functional group can be utilized to design and synthesize material with controllable desired properties. Formation of solid solution is an aid of isostructurality. Multi-component systems whether cocrystal or solid solution, can show enhanced properties compared to the individual components. Jones et al.⁸⁶ used the structural equivalence of halogen-bonded iodine and bromine functionalities to construct pairs of solids that exhibit different melting point, stability, and crystal morphology. The physical properties of solid solutions can be finely tuned by changing the nature and relative ratios of the different components as solid solutions share the properties of the

individual components.⁸⁷ This approach may find application in pharmaceuticals where tuning of properties of an API is still a challenge.

1.16 References

1. (a) M. Jansen, *Angew Chem Int Ed.*, 41, **2002**, 3746. (b) F. J. Disalvo, *Pure Appl Chem.*, 72, **2000**, 1799. (c) J.-M. Lehn, *Supramolecular Chemistry: Concepts and Perspectives*, VCH: Weinheim, **1995**. (d) R. Bishop, F. Toda and D. D. MacNicol, *Solid-State Supramolecular Chemistry: Crystal Engineering* Vol.6, in *Comprehensive Supramolecular Chemistry*, Pergamon, Chichester (UK), **1996**. (e) A. Nangia and G. R. Desiraju, *Acta Cryst.*, A54, **1998**, 934. (f) C. B. Aakeröy, N. R. Champness and C. Janiak, *CrystEngComm*, 12, **2010**, 22. (g) P. W. Caine, *Chemistry Today*, 25, **2007**, 10.
2. (a) M. G. Kanatzidis and K. R. Poeppelmeier (Organizers), *Prog. in Solid State Chem.*, 36, **2007**, 1.
3. (a) S. L. Morissette, S. Soukasenem, D. Levinson, M. J. Cima and Ö. Almarsson, *Proc. Natl. Acad. Sci. U. S. A.*, 100, **2003**, 2180. (b) G. R. Desiraju, *Crystal Design: Structure and Function*, ed. Wiley, Chichester, **2003**. (b) D. Braga and F. Grepioni, *Angew. Chem., Int. Ed.*, 43, **2004**, 4002.
4. L. R. Hilden and K. R. Morris, *J. Pharm. Sci.*, 93, **2004**, 3.
5. (a) A. Nangia and G. R. Desiraju, *Chem. Commun.* **1998**, 605. (b) A. L. Bingham, D. S. Hughes, M. B. Hursthouse, R. W. Lancaster, S. Tavener and T. L. Threlfall, *Chem. Commun.* **2001**, 603. (c) A. Nangia, *Cryst. Growth Des.* 6, **2006**, 2. (d) A. Nangia, *Cryst. Growth Des.*, 8, **2008**, 1079. (d) G. R. Desiraju, *CrystEngComm.*, 5, **2003**, 466. (e) J. D. Dunitz, *CrystEngComm.*, 5, **2003**, 506.
6. (a) L. Infantes, J. Chisholm and S. Motherwell, *CrystEngComm*, 5, **2003**, 480. (b) A. Gillon, N. Feeder, R. J. Davey, R. Storey, *Cryst. Growth Des.*, 3, **2003**, 663. (c) G. R. Desiraju, *J. Chem. Soc.*, 6, **1991**, 426.
7. (a) G. R. Desiraju, *CrystEngComm*, 5, **2003**, 466. (b) J. D. Dunitz, *CrystEngComm*, 5, **2003**, 506. (c) A. D. Bond, *CrystEngComm*, 9, **2007**, 833. (d) J. Z. Schpector and E. R. T. Tiekink, *Z. Kristallogr.*, 223, **2008**, 233.

8. (a) S. L. Childs and K. I. Hardcastle, *Cryst. Growth Des.*, **7**, **2007**, 1291. (b) S. L. Childs, G. P. Stahly and A. Park, *Mol. Pharmaceutics*, **4**, **2007**, 323.
9. (a) D. Braga, F. Grepioni and L. Maini, *Chem. Commun.*, **2010**, 6232. (b) Dario Braga, Fabrizia Grepioni, Lucia Maini, and Marco Polito *Struct Bond*, **132**, **2009**, 25.
10. D. Cinčić, T. Friščić and W. Jones, *New J. Chem.*, **32**, **2008**, 1776.
11. W. C. McCrone, in *Physics and Chemistry of the Organic Solid State*, Vol. 2, eds. D. Fox, M. M. Labes and A. Weissberger, Wiley Interscience, New York, **1965**, pp. 725-767.
12. J. D. Dunitz, in *The crystal as a supramolecular entity*. Perspective in supramolecular chemistry, Vol. 2, ed. G. R. Desiraju, Wiley, Chichester, **1996**, pp 1-30.
13. (a) E. Mitscherlich, *Abhl. Akad. Berlin*, **1822–1823**, 43. (b) J. Berzelius, *Jahresbericht*, **23**, **1844**, 44. (c) G. B. Amici, *Ann. Chim. Phys., Ser. 12*, **1844**, 114. (d) E. Mallard, *Annales Mines*, **10**, **1876**, 60. (e) O. Lehmann, *Die Krystallanalyse oder die chemische Analyse durch Beobachtung der Krystallbildung mit Hülfe des Mikroskops*, Wilhelm Engelmann, Leipzig, **1891**. (f) W. F. Ostwald, *Z. Phys. Chem.*, **22**, **1897**, 289. (g) P. H. R. Groth, *volume 1-5*, W. Engelmann, Leipzig, **1906-1919**. (h) M. J. Buerger and M. C. Bloom, *Z. Kristallogr.*, **96**, **1937**, 182. (i) J. Halebian and W. C McCrone, *J. Pharma. Sci.*, **58**, **1969**, 911. (j) J. Bernstein, *Polymorphism in Molecular Crystals*, Clarendon, Oxford, **2002**, pp.19-26.
14. (a) V. S. S. Kumar, A. Anthony, A. Nangia, W. T. Robinson, C. K. Broder, R. Mondal, I. R. Evans, J. A. K. Howard and F. H. Allen, *Angew. Chem. Int. Ed.*, **41**, **2002**, 3848. (b) N. J. Babu, L. S. Reddy, S. Aitipamula, A. Nangia, *Chem Asian J.* **3**, **2008**, 1122. (c) A. Nangia, *Acc. Chem. Res.*, **41**, **2008**, 595. (d) B. Sarma, S. Roy and A. Nangia, *Chem. Commun.* **2006**, 4918. (e) S. Roy and A. Nangia, *Cryst. Growth Des.*, **7**, **2007**, 2047. (f) S. Chen, I. A. Guzei and L. Yu, *J. Am. Chem. Soc.*, **127**, **2005**, 9881. (g) P. Sanphui, B. Sarma and A. Nangia, *J Pharm Sci.*, **100**, **2011**, 2287. (g) P. Sanphui, N. R. Goud, U. B. R. Khandavilli, S. Bhanoth and A. Nangia, *Chem. Commun.*, **47**, **2011**, 5013.

15. (a) R. K. R. Jetti, R. Boese, J. A. R. P. Sarma, L. S. Reddy, P. Vishweshwar and G. R. Desiraju, *Angew. Chem., Int. Ed.*, **42**, **2003**, 1963. (b) B. R. Sreekanth, P. Vishweshwar and K. Vyas, *Chem. Commun.* **2007**, 2375. (c) P. Sanphui, B. Sarma, and A. Nangia, *Cryst. Growth Des.*, **10**, **2010**, 4550. (d) B. Sarma, P. Sanphui and A. Nangia, *Cryst. Growth Des.*, **10**, **2010**, 2388.
16. S. R. Vippagunta, H. G. Brittain and D. J. W. Grant, *Adv. Drug Deliv. Rev.*, **48**, **2001**, 3.
17. N. J. Babu, S. Cherukuvada, R. Thakuria and A. Nangia, *Cryst. Growth Des.*, **10**, **2010**, 1979.
18. S. Cherukuvada, R. Thakuria and A. Nangia, *Cryst. Growth Des.*, **10**, **2010**, 3931.
19. J. Bernstein, *Polymorphism in Molecular Crystals*, Clarendon, Oxford, **2002**, pp. 155-156.
20. (a) J. Bernstein, R. J. Davey and J. -O. Henck, *Angew. Chem. Int. Ed.*, **38**, **1999**, 3440. (b) F. Wöhler and J. Liebig, *Annal. Pharm.*, **3**, **1832**, 249. (c) S. Aitipamula and A. Nangia, *Chem. Commun.*, **2005**, 3159.
21. J. Zhou, Y.-S. Kye and G. S. Harbison, *J. Am. Chem. Soc.*, **126**, **2004**, 8392.
22. <http://reference.iucr.org/dictionary/Polytypism>
23. (a) A. S. Myerson and P. Y. Lo, *J. Cryst. Growth*, **99**, **1990**, 1048. (b) A. S. Myerson and P. Y. Lo, *J. Cryst. Growth*, **110**, **1991**, 26. (c) R. M. Ginde and A. S. Myerson, *J. Cryst. Growth*, **116**, **1992**, 41. (d) A. S. Myerson and R. M. Ginde, *Handbook of Industrial Crystallization*, A. S. Myerson, Ed.; Butterworth-Heinemann: Stoneham, MA, **1992**. (e) L. G. M. Beekmans, R. Vallee and G. J. Vancso, *Macromolecules*, **35**, **2002**, 9383. (f) S. Devarakonda, J. M. B. Evans and A. S. Myerson, *Cryst. Growth Des.*, **3**, **2003**, 741. (g) S. Ueno, R. I. Ristic, K. Higaki and K. Sato, *J. Phys. Chem. B.*, **107**, **2003**, 4927. (h) I. Weissbuch, V. Y. Torbeev, L. Leiserowitz and M. Lahav, *Angew. Chem. Int. Ed.*, **44**, **2005**, 3226.
24. (a) M. Volmer, *Kinetik der Phasenbildung*, Steinkopf: Leipzig, **1939**. (c) A. C. Zettlemoyer, *Nucleation*, Dekker: New York, **1969**. (b) B. Lewis, *Nucleation and Growth Theory: Crystal Growth*, Ed.; B. R., Pamplin, Pergamon: Oxford, **1980**. (c) R. J. Davey and J. Garside, *From Molecules to Crystallizers*, Oxford

- University Press: Oxford, U.K., **2000**. (d) R. J. Davey, N. Blagden, S. Righini, H. Alison, M. J. Quayle and S. Fuller, *Cryst. Growth Des.*, **1**, **2001**, 59. (e) R. J. Davey, W. Liu, M. J. Quayle, and G. J. T. Tiddy, *Cryst. Growth Des.*, **4**, **2002**, 269. (f) R. Banerjee, P. M. Bhatt, M. T. Kirchner and G. R. Desiraju, *Angew. Chem. Int. Ed.*, **44**, **2005**, 2515. (g) G. R. Desiraju, *Angew. Chem. Int. Ed.*, **46**, **2007**, 8342.
25. G. R. Desiraju, *Nature Materials*, **1**, **2002**, 77.
26. J. Bernstein, *Polymorphism in Molecular Crystals*, Clarendon, Oxford, **2002**, pp.29-41.
27. I. Sunagawa, *Crystals Growth, Morphology, and Perfection*, Cambridge University Press, **2005**.
28. (a) S. L. Morissette, Ö. Almarsson, M. L. Peterson, J. F. Remenar, M. J. Read, A. V. Lemmo, S. Ellis, M. J. Cima and C. R. Gardner, *Adv. Drug. Del. Rev.*, **56**, **2004**, 275. (b) A. Linás and J. M. Goodman, *Drug. Disc. Today*, **13**, **2008**, 198.
29. (a) P. K. Thallapally, R. K. R. Jetty, A. K. Katz, H. L. Carrell, K. Singh, K. Lahiri, S. Kotha, R. Boese and G. R. Desiraju, *Angew. Chem. Int. Ed.*, **43**, **2004**, 1149. (b) C. -H. Gu, K. Chatterjee, V. Young Jr and D. J. W. Grant, *J. Cryst. Growth*, **235**, **2002**, 471. (c) C. A. Mitchell, L. Yu and M. D. Ward, *J. Am. Chem. Soc.*, **123**, **2001**, 10830. (d) X. Sun, B. A. Garetz and A. S. Myerson, *Cryst. Growth Des.*, **6**, **2006**, 684. (e) J. L. Hilden, C. E. Reyes, M. J. Kelm, J. S. Tan, J. G. Stowell and K. R. Morris, *Cryst. Growth Des.*, **3**, **2003**, 921. (f) G. Di Profio, S. Tucci, E. Curcio and E. Drioli, *Cryst. Growth Des.*, **7**, **2007**, 526. (g) M. D. Lang, A. L. Grzesiak and A. J. Matzger, *J. Am. Chem. Soc.*, **124**, **2002**, 14834. (h) C. P. Price, A. L. Grzesiak and A. J. Matzger, *J. Am. Chem. Soc.*, **127**, **2005**, 5512. (i) A. V. Trask, N. Shan, W. D. S. Motherwell, W. Jones, S. Feng, R. B. H. Tan and K. J. Carpenter, *Chem. Commun.* **2005**, 880. (j) A. Bouchard, N. Jovanović, G. W. Hofland, E. Mendes, D. J. A. Crommelin, W. Jiskoot and G. Witkamp, *Cryst. Growth Des.*, **7**, **2007**, 1432. (k) R. Hiremath, J. A. Basile, S. W. Varney and J. A. Swift, *J. Am. Chem. Soc.*, **127**, **2005**, 18321; (m) A. Llinás, K. J. Box, J. C. Burley, R. C. Glen and J. M. Goodman, *J. Appl. Crystallogr.*, **40**, **2007**, 379. (n) J. A. Foster, M.-O. M. Piepenbrock, G. O. Lloyd, N. Clarke, J. A. K. Howard and J. W. Steed, *Nature Chem.*, **2**, **2010**,

1037. (o) R. I. Petrova, R. Patel and J. A. Swift, *Cryst. Growth Des.*, 6, **2006**, 2709.
30. A. Llinàs and J. M. Goodman, *Drug Discovery Today*, 13, **2008**, 198.
31. (a) I. Weissbuch, V. Y. Torbeev, L. Leiserowitz and M. Lahav, *Angew. Chem. Int. Ed.*, 44, **2005**, 3226. (b) M. Kitamura, T. Hara and M. Takimoto-Kamimura, *Cryst. Growth Des.*, 6, **2006**, 1945. (c) M. Trifkovic, S. Rohani and M. Mirmehrabi, *Org. Proc. Res. Dev.*, 11, **2007**, 138.
32. J. D. Dunitz, *CrystEngComm*, 5, **2003**, 506.
33. L. Yu, *J. Am. Chem. Soc.*, 125, **2003**, 6380.
34. (a) D. Braga, F. Grepioni, L. Maini, M. Polito, K. Rubini, M. R. Chierotti and R. Gobetto, *Chem. Eur. J.*, 15, **2009**, 1508. (b) D. Braga, G. Cojazzi, D. Paolucci, and F. Grepioni, *CrystEngComm*, 3, **2001**, 159. (c) H. Miura, T. Ushio, K. Nagai, D. Fujimoto, Z. Lepp, H. Takahashi and R. Tamura, *Cryst. Growth Des.*, 3, **2003**, 959.
35. (a) M. Rafilovich and J. Bernstein, *J. Am. Chem. Soc.*, 128, **2006**, 12185. (b) P. Vishweshwar, J. A. McMahon, M. Oliveira, M. L. Peterson, and M. J. Zaworotko, *J. Am. Chem. Soc.*, 127, **2005**, 16802. (c) A. D. Bond, K. A. Solanko, S. Parsons, S. Redder and R. Boese, *CrystEngComm*, 13, **2011**, 399. (d) M. Wenger and J. Bernstein, *Mol. Pharm.*, 4, **2007**, 355. (e) B. Lou, D. Boström and S. P. Velaga, *Cryst. Growth Des.*, 9, **2009**, 1254. (f) X. Mei and C. Wolf, *Cryst. Growth Des.*, 4, **2004**, 1099.
36. (a) T. Li, K. R. Morris and K. Park, *Pharm. Res.*, 18, **2001**, 398. (b) J. M. Rubin-Preminger and J. Bernstein, *Cryst. Growth Des.*, 5, **2005**, 1343. (c) O-P. Kwon, S.-J. Kwon, M. Jazbinsek, A. Choubey, P. A. Losio, V. Gramlich and P. Günter, *Cryst. Growth Des.*, 6, **2006**, 2327.
37. (a) C. Bilton, J. A. K. Howard, N. N. L. Madhavi, A. Nangia, G. R. Desiraju, F. H. Allen and C. C. Wilson, *Chem. Commun.*, **1999**, 1675. (b) V. S. S. Kumar, A. Anthony, A. Nangia, W. T. Robinson, C. K. Broder, R. Mondal, I. R. Evans, J. A. K. Howard and F. H. Allen, *Angew. Chem. Int. Ed.*, 41, **2002**, 3848. (c) S. Chen, I. A. Guzei and L. Yu, *J. Am. Chem. Soc.*, 127, **2005**, 9881. (d) Z.-Q. Zhang, J. M. Njus, D. J. Sandman, C. Guo, B. M. Foxman, P. Erk and R. V. Gelder, *Chem. Commun.*, **2004**, 886.

38. (a) N. Blagden and R. J. Davey, *Cryst. Growth Des.*, **3**, **2003**, 873. (b) P. Erk, H. Hengelsberg, M. F. Haddow and R. van Gelder, *CrystEngComm*, **6**, **2004**, 474.
39. (a) J. Van de Streek and S. Motherwell, *Acta Cryst.*, B61, **2005**, 504. (b) J. A. R. P. Sarma and G. R. Desiraju, *Crystal Engineering: The Design and Application of Functional Solids*; eds. M. J. Zaworotko and K. R. Seddon, Kluwer: Dordrecht, **1999**, 325.
40. D. Braga and F. Grepioni, *Chem. Soc. Rev.*, **29**, **2000**, 229.
41. (a) R. Hilfiker, F. Blatter and M. von Raumer, in *Polymorphism in the Pharmaceutical Industry*, ed. R. Hilfiker, Wiley-VCH, Weinheim, **2006**, pp. 1-19. (b) S. R. Byrn, R. R. Pfeiffer and J. G. Stowell, *Solid-State Chemistry of Drugs*; SSCI: West Lafayette, IN, **1999**.
42. J. Bernstein, *Cryst. Growth Des.*, **11**, **2011**, 632.
43. A. Gavezzotti and G. Filippini, *J. Am. Chem. Soc.*, **117**, **1995**, 12299.
44. (a) S. Roy, R. Banerjee, A. Nangia and G. J. Kruger, *Chem. Eur. J.*, **12**, **2006**, 3777. (b) Ph D thesis by S. Roy entitled *X-ray Crystal Structures, Thermal Analysis and Computations of Conformational Polymorphs*, **2007**.
45. (a) S. L. Morissette, Ö. Almarsson, M. L. Peterson, J. F. Remenar, M. J. Read, A. V. Lemmo, S. Ellis, M. J. Cima and C. R. Gardner, *Adv. Drug Delivery Rev.*, **56**, **2004**, 275. (b) Ö. Almarsson and M. J. Zaworotko, *Chem. Commun.*, **2004**, 1889. (c) C. R. Gardner, C. T. Walsh and Ö. Almarsson, *Nat. Rev.*, **3**, **2004**, 926. (d) S. Datta and D. J. W. Grant, *Nat. Rev. Drug Discovery*, **3**, **2004**, 42.
46. (a) J. D. Dunitz and J. Bernstein, *Acc. Chem. Res.*, **28**, **1995**, 193. (b) D. Braga and F. Grepioni, *Chem. Soc. Rev.*, **4**, **2000**, 229. (c) N. Blagden and R. J. Davey, *Cryst. Growth Des.*, **3**, **2003**, 873. (d) R. J. Davey, K. Allen, N. Blagden, W. I. Cross, F. H. Lieberman, M.J. Quayle, S. Righini, L. Seton and G. J.T. Tiddy, *CrystEngComm*, **4**, **2002**, 257.
47. (a) C. P. Brock, W. B. Schweizer and J. D. Dunitz, *J. Am. Chem. Soc.*, **113**, **1991**, 9811. (b) J. D. Dunitz, *Acta Cryst.*, B51, **1995**, 619.
48. (a) P. N. Zannikos, W. I. Li, J. K. Drennen and R. A. Lodder, *Pharm. Res.*, **8**, **1991**, 974. (b) G. Ahr, B. Voith and J. Kuhlmann, *Eur. J. Drug. Metab. Pharmacokinet.*, **25**, **2000**, 25.

49. M. Draguet-Brughmans, R. Bouche, J. P. Flandre and A. van den Bulcke, *Pharm. Acta helv.*, **54**, **1979**, 140.
50. T. Yokoyama, T. Umeda, K. Kuroda, T. Nagafuku, T. Yamamoto and S. Asada, *J. Pharm. Soc. Jpn.*, **99**, **1979**, 837.
51. T. Yokoyama, T. Umeda, K. Kuroda, T. Kuroda and S. Asada, *Chem. Pharm. Bull.*, **29**, **1980**, 194.
52. (a) E. Swanepoela, W. Liebenberga and M. M. de Villiers, *Eur. J. Pharm. Biopharma.*, **55**, **2003**, 345. (b) K. Kachrimanis, M. Rontogianni and S. Malamataris, *J. Pharm. Biomed. Anal.*, **51**, **2010**, 512. (c) S. Agatonovic-Kustrin, B.D. Glass, M. Mangan and J. Smithson, *Inter. J. Pharm.*, **361**, **2008**, 245. (d) M. M. de Villiers, R. J. Terblanche, W. Liebenberg, E. Swanepoel, T. G. Dekker and M. Songa, *J. Pharm. Biomed. Anal.*, **38**, **2005**, 435.
53. J. Bauer, S. Spanton, R. Henry, J. Quick, W. Dziki, W. Porter and J. Morris, *Pharm. Res.*, **18**, **2001**, 859.
54. (a) J. Bernstein, *Polymorphism in Molecular Crystals*, Clarendon, Oxford, **2002**, pp.297-307.
(b) http://findarticles.com/p/articles/mi_m1200/is_8_166/ai_n7069007/
55. (a) J. Bernstein, *Polymorphism in Molecular Crystals*, Clarendon, Oxford, **2002**, pp.27-28, 257-274, 275-296. (b) E. F. Paulus, F. J. J. Leusen and M. U. Schmidt, *CrystEngComm*, **9**, 2007, 131. (c) H. Liebermann and J. Liebigs *Ann. Chem.*, **518**, **1935**, 245. (d) W. S. Sturve, US Pat., 2,844,485, 1958. (e) A. D. Reidinger and W. S. Sturve, US Pat., 2,844,484, 1958. (f) R. M. Vrcelj, J. N. Sherwood, A. R. Kennedy, H. G. Gallagher and T. Gelbrich, *Cryst. Growth Des.*, **3**, **2003**, 1027. (g) U. J. Griesser, D. Weigand, J. M. Rollinger, M. Haddow and E. Gstrein, *J. Therm. Anal. Calorim.*, **77**, **2004**, 511.
56. (a) F. W. McLafferty, *Acc. Chem.Res.*, **23**, **1990**, 63. (b) W. H. Streng, *Drug Disc. Today*, **2**, **1997**, 415. (c) J. Bernstein, and J. -O. Henck, *Cryst. Eng.*, **1**, **1998**, 119.
57. (a) T. Threlfall, *The Analyst*, **120**, **1995**, 2435. (b) S. R. Vippagunta, H. G. Brittain and D. J. W. Grant, *Advanced Drug Deliv. Sys.*, **48**, 2001, 3.
58. (a) L. V. Azaroff and M. J. Burger, *The powder method in x-ray crystallography*. McGraw-Hill Book Company, New York, U. S. A., **1958**. (b)

- R. Jenkins and R. L. Snyder, Introduction to X-ray powder diffractometry. In *Chemical Analysis: A Series of monographs on analytical chemistry and its applications*, Vol. 138 (ed. J. D. Winefordner), pp. 324–35. Wiley-Interscience, New York., **1996**. (c) C. Giacovazzo, (ed.), *Fundamentals of crystallography*. International Union of Crystallography, Oxford, **1992**.
59. (a) E. Suzuki, K. –I. Shirotani, Y. Tsuda and K. Sekiguchi, *Chem. Pharm. Bull.*, **33**, **1985**, 5028. (b) T. Norris, P. K. Aldridge and S. S. Sekulic, *Analyst*, **122**, **1997**, 549.
60. X. J. Gu and W. Jiang, *J. Pharm. Sci.*, **84**, **1995**, 1438.
61. A. M. Tudor, M. C. Davies, C. D. Melia, D. C. Lee, R. C. Mitchell, P. J. Hendra and S. J. Church, *Spectrochim. Acta Part A*, **47**, **1991**, 1389.
62. (a) D. C. Apperley, R. A. Fletton, R. K. Harris, R. W. Lancaster, S. Tavener and T. L. Threlfall, *J. Pharm. Sci.*, **88**, **1999**, 1275. (b) J. A. Ripmeester, *Chem. Phys. Lett.*, **74**, **1980**, 536.
63. (a) G. Nichols and C. S. Frampton, *J. Pharm. Sci.*, **87**, **1998**, 684. (b) G. T. R. Palmore, T. J. Luo, T. L. Martin, M. T. McBride-Wieser and N. T. Voong, *Trans. Am. Crystallogr. Assoc.*, **33**, **1998**, 45.
64. (a) M. A. Spackman and D. Jayatilaka, *CrystEngComm*, **11**, **2009**, 19. (b) J. J. McKinnon, D. Jayatilaka and M. A. Spackman, *Chem. Commun.*, **2007**, 3814.
65. F. L. Hirshfeld, *Theor. Chim. Acta*, **44**, **1977**, 129.
66. (a) L. Xianti, *Chin. J. Struct. Chem.*, **2**, **1983**, 213. (b) D. Vujovic, L. R. Nassimbeni, *Cryst. Growth Des.*, **6**, **2006**, 1595. (c) H.-K. Fun, S. R. Jebas, *Acta Cryst.*, **E64**, **2008**, o1255.
67. (a) http://reference.iucr.org/dictionary/Isomorphous_crystals.
(b) http://reference.iucr.org/dictionary/Isostructural_crystals.
68. (a) A. Kálmán and L. Párkányi, *Advances in Molecular Structure Research*, **3**, **1997**, 189. (b) I. Náray-Szabó, *Inorganic Crystal Chemistry*, Akadémiai Kiadó: Budapest, **1969**. (c) A. F. Wells, *Structural Inorganic Chemistry*, Clarendon Press: Oxford, **1962**, pp 182-186. (d) F. D. Bloss, *Crystallography and Crystal Chemistry*, Holt, Rinehart and Winston: New York, **1971**. (e) T. Zoltai, J. H. Stout, *Mineralogy: Concepts and Principles*, Burgess Publishing: Minneapolis, **1985**, pp 490.

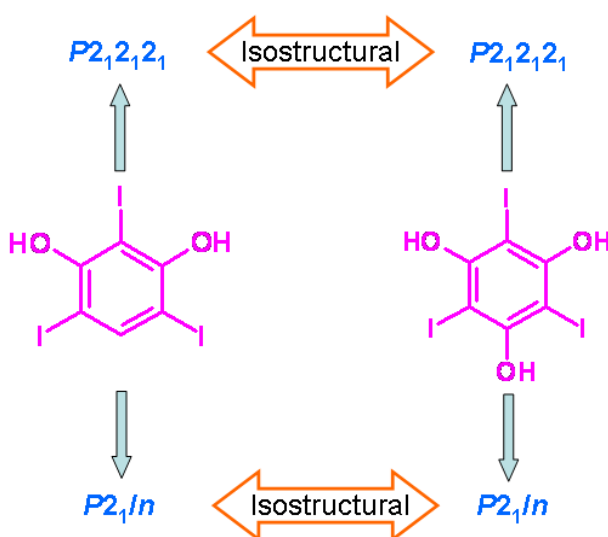
69. A. I. Kitaigorodskii, *Molecular Crystals and Molecules*, Academic Press, New York, 1973.
70. (a) A. Kálmán, L. Párkányi and G. Argay, *Acta. Cryst.*, B49, **1993**, 1039. (b) G. Argay and A. Kálmán, *Acta. Cryst.*, C43, **1987**, 922. (c) L. Fábián, G. Argay, A. Kálmán and M. Báthori, *Acta. Cryst.*, B58, **2002**, 710.
71. (a) A. Kálmán, L. Fábián and G. Argay, *Chem. Commun.* **2000**, 2255; (b) A. Nangia and G. R. Desiraju, *Acta Cryst.* A54, **1998**, 934.
72. (a) S. Ianelli, M. Nardelli, C. Giordano, L. Coppi, and A. Restelli, C48, **1992**, 1722. (b) J. Petrović, D. Miljković, V. Pejanović, R. Kovacević, A. Stefanović and M. Bruvo, , *Acta Cryst.*, C48, **1992**, 1248. (c) B. K. Saha and A. Nangia, *Heteroatom Chemistry*, 18, **2007**, 185. (d) T. Steiner, *J. Mol. Struct.*, 443, **1998**, 149. (e) I. Bar and J. Bernstein, *Tetrahedron*, 43, **1987**, 1299.
73. (a) J. A. R. P. Sarma and G. R. Desiraju, *Acc. Chem. Res.*, 19, **1986**, 222. (b) M. R. Edwards, W. Jones and W. D. S. Motherwell, *CrystEngComm*, 8, **2006**, 545. (c) J. van de Streek and S. Motherwell, *J. Appl. Cryst.*, 38, **2005**, 694. (d) N. N. L. Madhavi, A. K. Katz, H. L. Carrell, A. Nangia and G. R. Desiraju, *Chem. Commun.*, **1997**, 1953. (e) R. Banerjee, R. Mondal, J. A. K. Howard and G. R. Desiraju, *Cryst. Growth & Des.*, 6, **2006**, 999. (f) M. R. Edwards, W. Jones, W. D. S. Motherwell and G. P. Shields, *Mol. Cryst. And Liq. Cryst.*, 356, **2001**, 337. (g) G. R. Desiraju and J. A. R. P. Sarma, *Proc. Indian Acad. Sci. (Chem. Sci.)*, 96, **1986**, 599. (h) M. Polito, E. D'Oria, L. Maini, P. G. Karamertzanis, F. Grepioni, D. Braga and S. L. Price, *CrystEngComm*, 10, **2008**, 1848. (i) L. Fábián and A. Kálmán, *Acta Cryst.*, B55, **1999**, 1099. (j) B. Omondi, M. A. Fernandes, M. Layh, D. C. Levendis, J. L. Look and T. S. P. Mkwizu, *CrystEngComm*, 7, **2005**, 690.
74. (a) A. Kálmán, V. Folop, G. Argay, B. Ribár, D. Lazar, D. Zivanov-Stakic and S. Vladimirov, *Acta. Cryst.* C44, **1988**, 1634. (b) S. S. C. Chu, V. Napoleone, A. I. Jr. Ternay and S. Chang, *Acta Cryst.*, B38, **1982**, 2508. (c) L. Prasad and E. J. Gabe, *Acta Cryst.*, C39, **1983**, 273. (d) A. Kálmán, G. Argay, D. Scharfenberg-Pfeiffer, E. Hohne and B. Ribar, *Acta Cryst.*, B47, **1991**, 68. (e) G. Argay, A. Kálmán, B. Ribár, S. Vladimirov and D. Zivanov-Stakic, *Acta. Cryst.*, C43, **1987**, 922. (f) T. Smolka, R. Boese and R. Sustmann, *Struct.*

- Chem.*, 10, **1999**, 429. (g) N. J. Babu and A. Nangia, *Cryst. Growth Des.*, 6, **2006**, 1753. (h) M. Chakarvarty, P. Kommana and K. C. K. Swamy, *Chem. Commun.*, **2005**, 5396. (i) A. Kálmán, L. Fábián and G. Argay, *Chem. Commun.*, **2000**, 2255.
75. L. Addadi and M. Lahav, *Pure Appl. Chem.*, 51, **1979**, 1269.
76. L. -P. Zhang and T. C. W. Mak, *J. Mol. Struct.* 693, **2004**, 1.
77. A. I. Kitaigorodskii, *Organic Chemical Crystallography*, New York: Consultants Bureau., pp 222-231.
78. K. Go and K. K. Bhandary, *Acta Cryst.* B45, **1989**, 306.
79. (a) P. K. Thallapally, K. Chakraborty, H. L. Carrell, S. Kotha and G. R. Desiraju, *Tetrahedron*, 56, **2000**, , 6721. (b) N. N. Laxmi Madhavi, A. K. Katz, H. L. Carrell, A. Nangia, G. R. Desiraju, *Chem. Commun.* **1997**, 1953. (c) R. Banerjee, R. Mondal, J. A. K. Howard and G. R. Desiraju, *Cryst. Growth Des.*, 6, **2006**, 6999. (d) L. Párkányi and E. Hengge, *J. Organomet. Chem.*, 235, **1982**, 273. (e) L. Párkányi, C. Herbadez and K. H. Pannell, *J. Organomet. Chem.*, 301, **1986**, 145. (f) A. Kálmán, G. Argay, D. Zivanov-Stakić, S. Vladimirov and B. Ribár, *Acta Cryst.*, B48, **1992**, 812. (g) D. F. Mullica, C. M. Garner, M. E. Prince, B. C. Mossman and E. L. Sappenfield, *J. Crystallogr. Spectrosc. Res.*, 22, **1922**, 515. (h) I. Bar and J. Bernstein, *Acta. Cryst.* B39, **1983**, 266.
80. (a) L. Fábián and A. Kálmán, *Acta Cryst.*, B60, **2004**, 547. (b) A. Budzianowski and A. Katrusiak, *Acta Cryst.* B58, **2002**, 125. (c) A. Xia, J. P. Selegue, A. Carrillo, B. O. Patrick, S. Parkin and C. P. Brock, *Acta Cryst.*, B57, **2001**, 507. (d) D. Britton, *Acta Cryst.*, B58, **2002**, 553. (e) S. Matsumoto and J. Mizuguchi, *Acta Cryst.*, B57, **2001**, 82. (f) M. Kaftory, M. Botoshansky, M. Kapon and V. Shteiman, *Acta Cryst.*, B57, **2001**, 791. (g) M. Pink and D. Britton, *Acta Cryst.*, B58, **2002**, 116. (h) D. Britton, *Acta Cryst.*, B58, **2002**, 553. (i) P. Langan, S. A. Mason, D. Myles and B. P. Schoenborn, *Acta Cryst.*, B58, **2002**, 728. (j) Y. Iitaka, *Acta Cryst.*, 13, **1960**, 35. (k) A. Kvik, W. M. Canning, T. F. Koetzle and G. J. B. Williams, *Acta Cryst.*, B36, **1980**, 115. (l) A. Dawson, D. R. Allan, S. A. Belmonte, S. J. Clark, W. I. F. David, P. A. McGregor, S. Parsons, C. R. Pulham and L. Sawyer, *Cryst. Growth Des.*, 5, **2005**, 1415.

81. (a) T. Gelbrich and M. B. Hursthouse, *CrystEngComm*, 7, **2005**, 324. (b) T. Gelbrich and M. B. Hursthouse, *CrystEngComm*, 8, **2006**, 448. (c) T. Gelbrich, D. S. Hughes, M. B. Hursthouse and T. L. Threlfall, *CrystEngComm*, 10, **2008**, 1328. (d) F. P. A., Fabbiani, B. Dittrich, A. J. Florence, T. Gelbrich, M. B. Hursthouse, W. F. Kuhs, N. Shankland and H. Sowa, *CrystEngComm*, 11, **2009**, 1396.
82. (a) A. I. Kitaigorodski, *Mixed Crystals*, Springer: Berlin, **1984**, 275. (b) A. Anthony, M. Jaskólski, A. Nangia and G. R. Desiraju, *Chem. Comm.*, **1998**, 2537. (c) G. R. Desiraju, *Crystal Engineering - The Design of Organic Solids*, Elsevier. Amsterdam, **1989**, pp. (d) M. R. Edwards, W. Jones, W. D. S. Motherwell and G. P. Shields, *Mol. Cryst. And Liq. Cryst*, 356, 2001, 337. (e) G. R. Desiraju, J. A. R. P. Sarma, *Proc. Indian Acad. Sci. (Chem. Sci.)*, 96, **1986**, 599.
83. (a) A. Asmadi, J. Kendrick and F. J. J. Leu, *Chem. Eur. J.*, 16, **2010**, 12701. (b) A. Asmadi, J. Kendrick and F. J. J. Leusen, *Phys. Chem. Chem. Phys.*, 12, **2010**, 8571.
84. N. K. Nath, B. K. Saha and A. Nangia, *New J. Chem.*, 32, **2008**, 1693.
85. W. Zhou, H. Wu and T. Yildirim, *J. Am. Chem. Soc.*, 130, **2008**, 15268.
86. D. Cinčič, T. Frisčič and W. Jones, *Chem. Mater.*, 20, **2008**, 6623.
87. M. Dabros, P. R. Emery and V. R. Thalladi, *Angew. Chem. Int. Ed.*, 119, **2007**, 4132.

Chapter Two

Isostructural Polymorphs of Triiodoresorcinol and Triiodophloroglucinol



The orthorhombic and monoclinic forms of triiodoresorcinol and triiodophloroglucinol establish a structural link in the crystal structure series from triiodobenzene ($P2_12_12_1$) to trifluorotriiodobenzene ($P2_1/n$).

2.1 Introduction

The two important phenomena of isostructutrality and polymorphism typify almost opposite molecule to crystal structure behavior in the organic solid-state. When different molecules, usually within a family of compounds, adopt the same (similar) crystal structure they are isostructural and the phenomenon is termed isostructutrality.¹ Polymorphism² is the existence of the same chemical substance in more than one crystalline modification. Both phenomena are well known, well studied and are important in crystal engineering as well as in materials science and pharmaceutical chemistry.³ There are reports of polymorphs of single compounds which are isostructural in one dimension (similar rows of molecules) or in two dimensions (similar infinite two dimensional molecular arrangements).⁴ Examples are available in the literature which display both polymorphism and isostructutrality.⁵ Polymorphism and isostructutrality of 2-amino-4-chloro-6-morpholinepyrimidine and 2-amino-4-chloro-6-piperidinopyrimidine is such an example.^{5a} The morpholine derivative yields two polymorphs, both in space group $P2_1/c$, with two and one molecules in the asymmetric unit respectively ($Z' = 2$ and 1, Figure 2.1). Its piperidine derivative (O acceptor is replaced by CH_2), has only one crystal structure with two molecules in the asymmetric unit of $P2_1/c$ space group ($Z' = 2$, Figure 2.1). Interestingly it is found to be isomorphous with one of the polymorphs of morpholine derivative which also has $Z' = 2$. A second form with $Z' = 1$ was not observed for piperidine derivative. Another interesting example which depicts both isostructutrality and polymorphism is 1,3,5-triarylbenzenes (TAB).^{5b} 4-chloroTAB crystallized as dimorph, in $Pca2_1$ and in $P\bar{1}$ space group. The $P\bar{1}$ polymorph is isostructural with the 4-bromo TAB which does not have a second form (Figure 2.1). In both the cases the second isostructural molecule is not showing polymorphic behaviour.

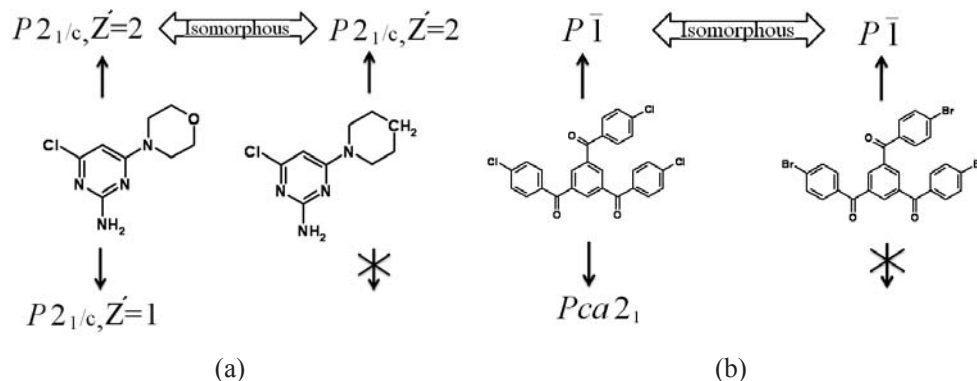


Figure 2.1 (a) Piperidine derivative is a dimorphic substance with $Z' = 2$ and 1 in $P2_1/c$ space group, while the morpholine derivative has only one crystal structure with $Z' = 2$. It is isomorphous with piperidine $Z' = 2$ polymorph showing $O \leftrightarrow C-H$ replacement. (b) 4-chloroTAB is dimorphic and triclinic form is isomorphous with 4-bromoTAB but the latter does not have an orthorhombic polymorph ($Pca2_1$) isomorphous with that of the former.

Examples of polymorphic compound where each polymorph is isostructural with the corresponding polymorph of other compound/compounds are rare. Triiodoresorcinol and triiodophloroglucinol have two polymorphs each and these forms are in turn isomorphous and isostructural.⁶

Halogenated phloroglucinol were studied in our laboratory because of their ability to crystallize as hydrates.⁷ In dibromophloroglucinol channel structure a T6(2) tape of hydrogen bonded water molecules resides in boat cyclohexane conformation. Water helices of opposite handedness were found in the channel structures of tribromophloroglucinol and trichlorophloroglucinol. But their guest free structures could not be crystallized. Triiodophloroglucinol crystallized as guest free structure. This compound and its derivatives have importance in the design of MRI contrasting agent.⁸ 2,4,6 triiodoresorcinol is used in medicine for treating mycoses, viral disease of the eye and acute respiratory disease.⁹ Triiodophenol was originally described as a nonsteroid antiinflammatory molecule and its selected derivatives show cytotoxic activity accompanied by DNA synthesis inhibition.¹⁰

2.1.1 Hetero-seeding

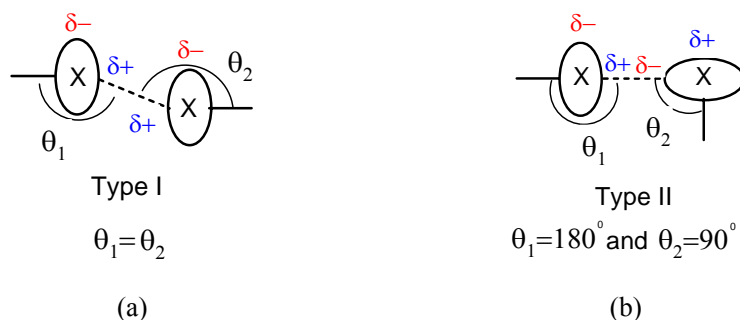
Systematic (manual or automatic) solvent and thermal screenings of solid forms is the main method to examine crystal polymorphism.¹¹ Methodologies proposed in the recent literature to obtain polymorphs were described in Chapter 1. Among these techniques the use of hetero-seed is found to be successful in some cases.¹² A crystalline sample formed by molecules having almost same structure as the compound of interest but only difference is due to a substituent or counterion (in case of a salt) is termed as hetero-seeding. The two compounds *p*-methyl benzyl alcohol and *p*-chloro benzyl alcohol are not isomorphous. A polymorph of the former which is isomorphous with the later can be obtained by using crystals of the later as hetero-seed.^{12a}

2.2 Interactions Involving Halogens

Halogens engage in halogen bonding¹³ ($D\cdots X-Y$) with weak to very strong interaction energy where the halogen (X) bonded to another atom (Y) is electron acceptor and the other atom (D) donates electrons are inter halogen interactions and weak bonds.

2.2.1 Inter-halogen interactions

Halogens can make short contact with respect to their spherical van der Waals radii sum, as it has been seen in several crystal structures. The Cl_2 , Br_2 and I_2 molecules make side on contact in their orthorhombic crystal structures (*Cmca*).¹⁴ Bondi, observed that the effective shapes of some atoms might not be truly spherical but rather ellipsoid or ‘pear-shaped’ especially for heavier elements.¹⁵ The atomic radii of the non-spherical halogen atoms along C–X bond vector are found to be shorter than the distance perpendicular to it.¹⁶ Halogen \cdots halogen contacts have two preferred geometries, type I ($\theta_1 \cong \theta_2$) and type II ($\theta_1 \cong 180^\circ$ and $\theta_2 \cong 90^\circ$) as shown in Scheme 2.1. It was shown by theoretical calculations that $Cl\cdots Cl$ interactions are quite normal, with the repulsion, dispersion and electrostatic contributions being the most important, but the non-sphericity of the chlorine charge distribution has a significant effect on these contributions.¹⁷



Scheme 2.1 (a) Type I geometry of halogen···halogen interaction. (b) Type II geometry of halogen···halogen interaction.

It is believed that the halogens are polarized positively in the polar region and negatively in the equatorial region (Scheme 2.1). The size and polarization increases in the order $\text{Cl} < \text{Br} < \text{I}$, whereas electronegativity change is in the reverse direction. Thus in the cases of unsymmetrical inter halogen interactions the negative equatorial part of the lighter-halogen approaches the positive axial region of a heavier halogen.¹⁸ F behaves quite differently than the other three halogens due to its hardness, small size and very high electronegativity. Thus various researches described the short inter halogen contacts as a result of close packing due to elliptical shape of the halogen atoms or electrophile···nucleophile interaction type due to polarization. It appears that inter-halogen type I is van der Waals interaction and type II is induced by the mutual polarization. Type II geometry is believed to be a result of specific inter-halogen interactions and hence favored for iodine because of stabilization from the dual polarization in $\text{C}-\text{I}^{(\delta+)}\cdots\text{I}^{(\delta-)}-\text{C}$. On the other hand, electronegative chlorine atom is more often present in type I geometry, a result largely of close packing consideration. The nature of interhalogen interactions is described in several papers.¹⁹

2.2.2 Halogen bonding

The term “halogen bonding” was introduced by Dumas et al. for describing the attractive donor–acceptor interactions that involve halogen atoms functioning as Lewis acids and another atom containing lone pair of electrons functioning as Lewis base.²⁰ In halogen bond with $\text{D}\cdots\text{X}-\text{Y}$ geometry the angle around X (halogen) tends to be linear. The halogen atoms that are involved in halogen bonding can be bound to other halogen or to carbon or to nitrogen atoms and the electron pair donor can be neutral or anionic

(N, O, S, Se, I⁻, Br⁻, Cl⁻, F⁻, etc.). The interaction energy of halogen bonding spans over a very wide range, from 10 to 200 kJ/mol.²¹ Theoretical and experimental data prove that all four halogens can act as halogen bond donor and the bond strength order is F < Cl < Br < I. Though F is a strong acceptor but organic F hardly participate in halogen bond as acceptor.²² The halogen bond accepting strength of halide ions increases as F⁻ < Cl⁻ < Br⁻ < I⁻ and aromatic nitrogen is better acceptor than oxygen and sulfur.²³ Halogen bonding can play a crucial role in some biological systems. Short I...O interactions play important roles in the recognition of some hormones by their cognate proteins. A very large number of short I...O contacts from thyroxine and its derivatives to their associated proteins were identified.²⁴

2.2.3 Halogens in hydrogen bonding

Organic halogens can participate in hydrogen bond but energetically very weak because of the weak acceptor property. C-F is most surprising because F has high electronegativity and yet weak accepting capacity. It is interesting that strong donors/acceptors O and N are also electronegative atoms and in H-bonding electronegativity of donor and acceptors play an active role. The H-bonding capability is not very different for other three halogens Cl, Br and I.

2.3 Results and Discussion

Triiodoresorcinol (TIR, 2,4,6-triiodoresorcinol) and triiodophloroglucinol (TIG, 2,4,6-triiodophloroglucinol) crystallized as orthorhombic (TIR-O and TIG-O in $P2_12_12_1$) and monoclinic (TIR-M and TIG-M in $P2_1/n$) polymorphs. The orthorhombic polymorphs are isostructural and in turn similar to the crystal structure of 1,3,5-triiodobenzene (TIB). The isostructural monoclinic polymorphs are similar to the structure of 1,3,5-trifluoro-2,4,6-triiodobenzene (TIF). Triiodophenol (TIP) crystallized in a single orthorhombic form only. Figure 2.2 shows the triiodo compounds studied in this chapter.

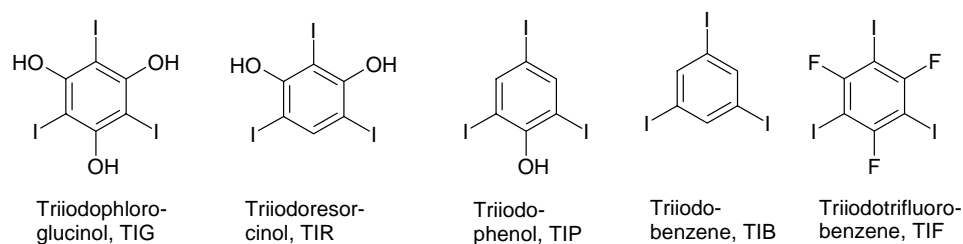


Figure 2.2 Triiodo-hydroxy-benzene compounds studied.

TIR and TIG were synthesized²⁵ by the iodination of resorcinol and phloroglucinol. TIP was purchased (Aldrich) and used as such for crystallization. Synthesis, crystallization and X-ray diffraction are detailed in the Experimental Section.

2.3.1 Polymorphism

Crystallization from EtOAc, CHCl₃ or mesitylene afforded good quality single crystals. Crystals obtained from CHCl₃ were solved and refined in the non-centrosymmetric orthorhombic space group $P2_12_12_1$ are designated as TIG-O. A second form was obtained when a hot solution of TIG in mesitylene was poured over the filter paper. Quick precipitation gave single crystals for X-ray diffraction in the centrosymmetric space group $P2_1/n$, or TIG-M form. The H atom of OH groups could not be located in difference electron density maps of X-ray radiation because of the flanking heavy iodine atoms. The molecular packing is discussed via inter-halogen interactions listed in Table 2.1. Details of unit cell parameters are summarized in Appendix.

In the crystal structure of TIG-O, the three OH groups are flanked by iodine atoms and do not engage in significant hydrogen bonding for steric reasons. The structure is directed by type-II iodo...iodo interactions. The molecules form 1D zigzag tapes via I3...I2 interaction (3.77 Å, 164.0°, 103.7°) along the [010] direction. These tapes extend into the third dimension via I1...I3 interaction (3.89 Å, 145.9°, 82.2°) forming left-handed helix in the [100] direction. The molecules form corrugated sheet-like structure parallel to (100) plane (Figure 2.3).

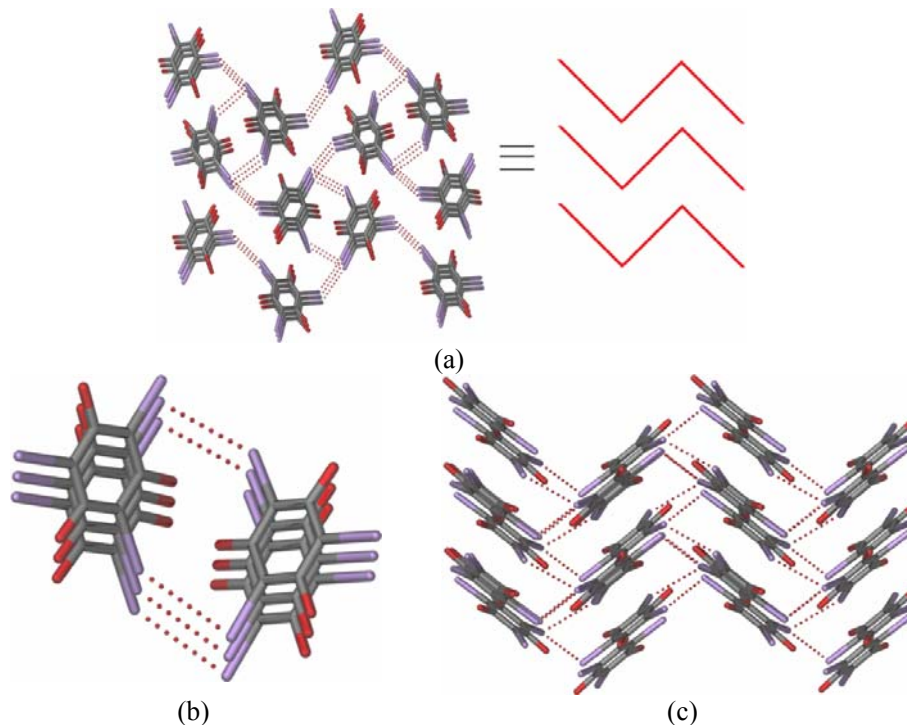
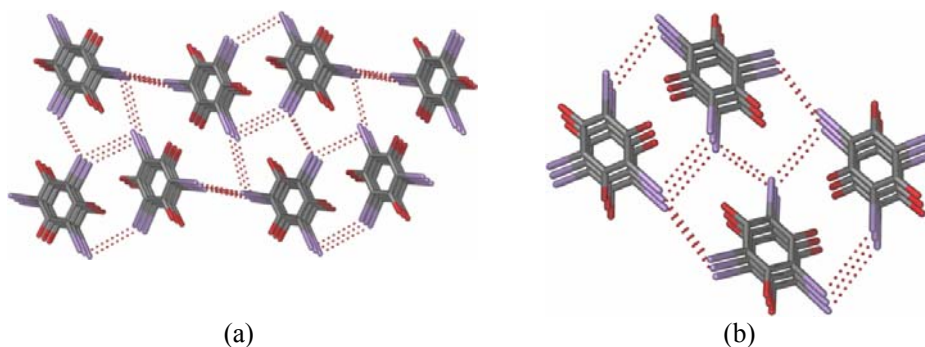


Figure 2.3 Molecular packing in TIG-O. (a) Zigzag tapes mediated by type-II I...I interaction are shown as line diagram, (b) a left-handed helix down [100], and (c) corrugated sheet parallel to (100) plane.

In TIG-M form, molecules extend along [100] via I1...I1 (3.70 Å, 175.7°, 107.2°) and I2...I3 (4.00 Å, 145.5°, 82.8°) type-II interaction to form tapes which extend in the third dimension via I2...I3 (4.02 Å, 159.6°, 109.9°) and type-I I2...I2 interaction (3.99 Å, 131.1°). I2...I3 interactions makes left- and right-handed helices in the [010] direction. Zigzag chains of I1...I1 interaction along [010] and corrugated sheet-like structure in (010) are present (Figure 2.4).



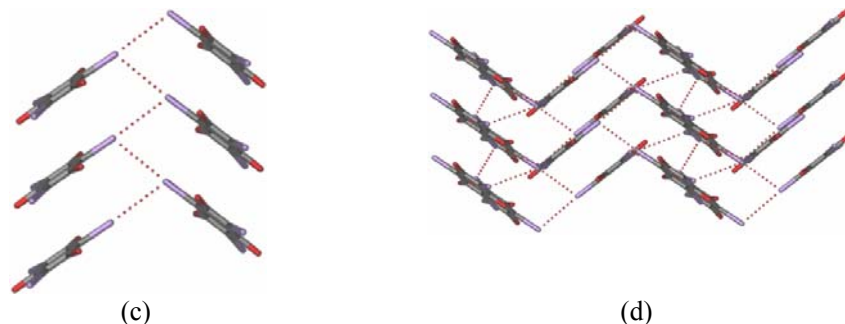


Figure 2.4 TIG-M. (a) Tapes along [100] complete the 3D packing via formation of and I...I zigzag chains, (b) right- and left-handed helices are connected by type-I I...I interaction, (c) type II I...I zigzag chain along [010], and (d) corrugated sheet parallel to (010) plane.

When TIR was crystallized from solvents such as CHCl_3 , mesitylene and CCl_4 reflections (crystal from CHCl_3 was used for X-ray diffraction) were solved in the monoclinic space group $P2_1/n$ (TIR-M). A second orthorhombic form was obtained by the hetero-seeding technique.¹² When 20 mg of TIR in $\text{CHCl}_3/\text{MeOH}$ was seeded with 2-3 crystals (~10% by weight) of TIP and kept for slow evaporation, X-ray diffraction showed that it crystallized in orthorhombic space group $P2_12_12_1$ (TIR-O). The oxygen atoms are disordered so as to mimic a 1,3,5-trihydroxybenzene molecule in both crystal structures. The partial site occupancy factor (s.o.f.) of resorcinol O atoms are O1, O2, O3 are 0.88, 0.86, 0.27 in TIR-M and 0.62, 0.70, 0.68 in TIR-O structure.

In TIR-M form, molecules form a tape along [100] via $\text{I1}\cdots\text{I1}$ (3.736 Å, 175.5°, 112.5°) and $\text{I2}\cdots\text{I3}$ (3.91 Å 152.5°, 79.9°). The tapes extend via $\text{I3}\cdots\text{I1}$ (3.92 Å, 160.5°, 110.0°) interaction. $\text{I2}\cdots\text{I3}$ interactions makes left- and right-handed helices in the [010] direction. The $\text{I1}\cdots\text{I1}$ type-II interaction forms zigzag chain along [010]. The molecule forms corrugated sheet-like structure in the (010) plane (Figure 2.5).

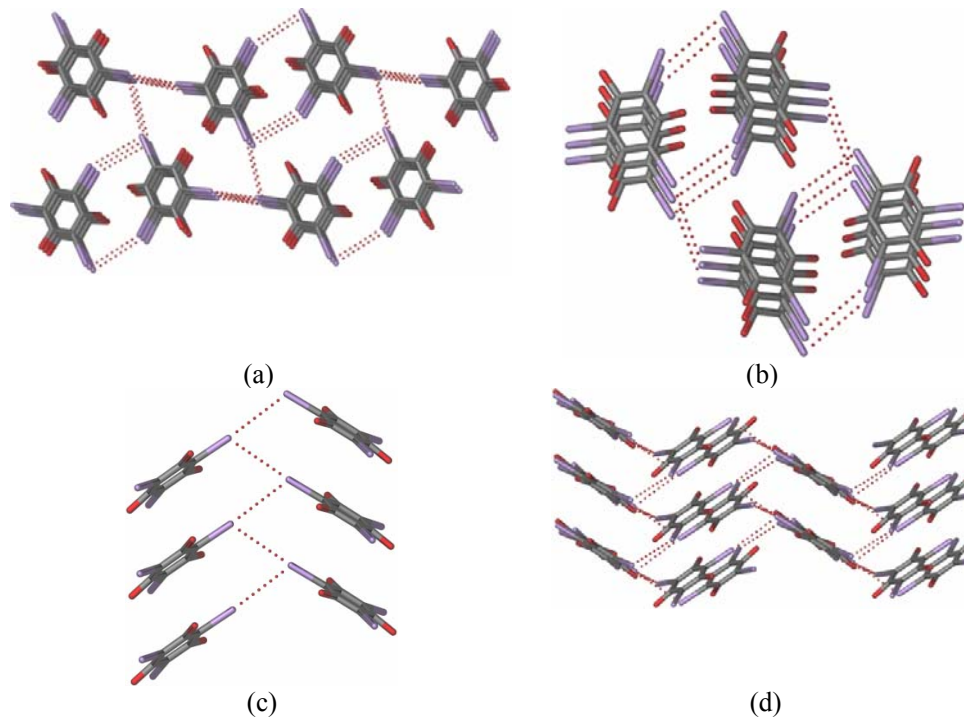
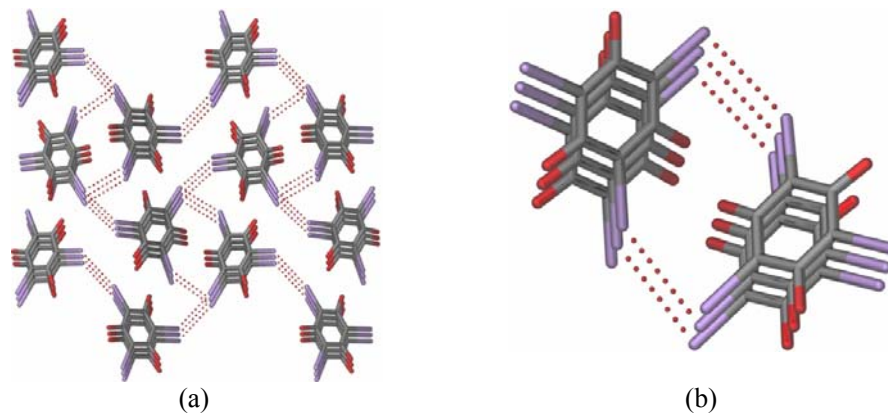


Figure 2.5 TIR-M. (a) Tapes along [100] complete the packing dimension via formation of helix and zigzag chain, (b) right- and left-handed helix, and (c) iodo interaction-mediated zigzag chain, (d) corrugated sheet parallel to (010).

In TIR-O, molecules form zigzag tape along [010] via I3...I2 (3.81 Å, 162.0°, 106.6°) type-II interaction. These tapes extend in the third dimensions via I1...I3 type-II interaction (3.92 Å, 147.2°, 81.7°) forming a left-handed helix along [100]. Molecules forms corrugated sheet in the (100) plane (Figure 2.6). Iodo...iodo interactions direct the crystal packing and OH groups are mostly like bystanders.



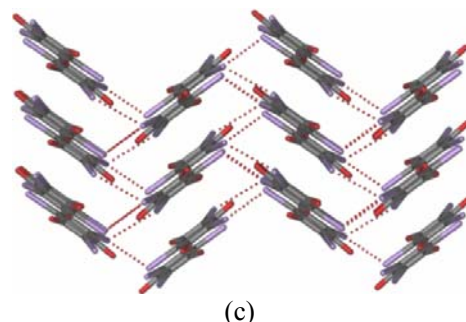


Figure 2.6 TIR-O. (a) Zigzag tapes along [010], (b) right handed helix along [100], and (c) corrugated sheet in (100) plane.

The structure of TIP (crystallized from CHCl_3 , space group $P2_12_12_1$) extends in [010] direction through a zigzag tape of type-II $\text{I3}\cdots\text{I2}$ interaction (4.02 Å, 157.1°, 112.1°). The packing is completed via $\text{I2}\cdots\text{I2}$ (3.99 Å, 153.1°, 108.1°) and $\text{I1}\cdots\text{I3}$ (4.03 Å, 143.4°, 84.7°) type-II interactions. A zigzag chain of $\text{I2}\cdots\text{I2}$ interaction and left-handed helix of $\text{I1}\cdots\text{I3}$ runs along the [100] direction. The molecules form a corrugated sheet in (100) plane (Figure 2.7). A monoclinic form of this compound or another polymorph could not be obtained.

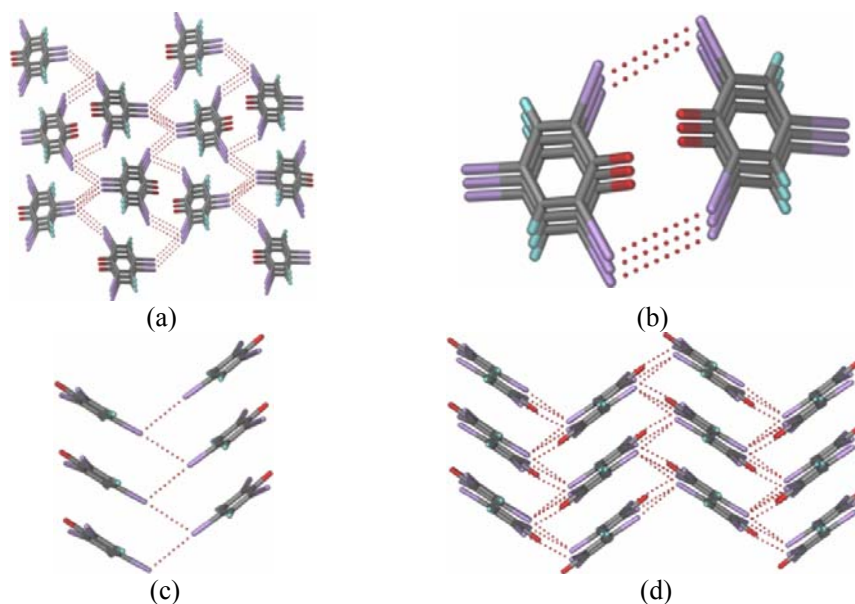


Figure 2.7 Molecular packing and intermolecular interactions in the structure of TIP. (a) Zigzag tapes along [010] extend the packing via zigzag chains and helices, (b) left-handed helix along [100], (c) zigzag chain along [100], (d) corrugated sheet parallel to (100).

Table 2.1 Inter-halogen interactions (D/Å, and $\theta/^\circ$) in crystal structures.

Compound	Interaction	D (I...I)	C-I...I-C		Symmetry code
			θ_1	θ_2	
TIB	I 2...I1	3.985(1)	153.4(1)	112.0(1)	$3/2-x, 1-y, -1/2+z$
	I1...I1	3.944(1)	153.1(1)	108.6(1)	$-1/2+x, 1/2-y, 1-z$
	I 2...I1	4.052(1)	147.8(1)	93.5(1)	$1-x, 1/2+y, 1/2-z$
	I 3...I2	4.048(1)	150.1(1)	77.9(1)	$1/2+x, 1/2-y, -z$
TIP	I 2...I2	3.996(1)	153.1(2)	108.0(2)	$-1/2+x, -1/2-y, -z$
	I1... I3	4.035(1)	143.3(2)	84.7(1)	$-1/2+x, 1/2-y, -z$
	I3... I2	4.022(1)	157.1(2)	112.1(2)	$1-x, 1/2+y, 1/2-z$
TIR-M	I 1... I1	3.736(1)	175.5(2)	112.4(2)	$1/2-x, -1/2+y, 1/2-z$
	I 2... I3	3.907(1)	152.5(2)	79.9(1)	$3/2-x, 1/2+y, 1/2-z$
	I3... I1	3.921(1)	160.5(2)	110.0(2)	$1/2+x, 3/2-y, 1/2+z$
TIR-O	I3 ... I2	3.812(2)	162.1(5)	106.6(1)	$1-x, 1/2+y, 1/2-z$
	I1... I3	3.919(2)	147.2(5)	81.8(2)	$-1/2+x, 1/2-y, -z$
TIG-O	I3... I2	3.771(1)	164.2(2)	103.7(2)	$1-x, 1/2+y, 1/2-z$
	I1... I3	3.888(1)	146.0(2)	82.2(1)	$-1/2+x, 1/2-y, -z$
TIG-M	I1...I1	3.699(2)	175.7(3)	107.2(3)	$1/2-x, -1/2+y, 1/2-z$
	I3...I1	4.021(2)	159.6(3)	109.9(3)	$1/2+x, 3/2-y, 1/2+z$
	I2...I3	4.003(2)	145.4(3)	82.8(1)	$3/2-x, 1/2+y, 1/2-z$
	I2... I2 ^b	3.990(2)	131.1(3)	131.1(3)	$1-x, 3-y, -z$
TIF	F1...F1 ^b	2.766(4)	157.7(2)	157.7(2)	$-x, -y, 1-z$
	I3...I2	3.912(1)	147.1(1)	79.7(1)	$x, -1/2+y, 3/2-z$
	I2...I1	3.994(1)	157.7(1)	105.9(1)	$-1/2+x, -1/2-y, -1/2+z$
	I1...I1	3.736(1)	171.3(1)	100.4(1)	$-x, 1/2+y, 3/2-z$
	I3...I3 ^a	4.048(1)	136.7(1)	136.7(1)	$-x, -2-y, 2-z$
	F2...I3	3.455(3)	164.9(2)	73.0(2)	$-1/2-x, -1/2+y, 3/2-z$
TIP+TIR-O	I3...I2	3.935(1)	159.1(2)	109.4(2)	$1-x, 1/2+y, 1/2-z$
	I1...I3	3.959(1)	146.3(2)	82.1(1)	$-1/2+x, 1/2-y, -z$
TIR+ TIG-O	I1...I3	3.896(1)	146.9(2)	82.1(1)	$-1/2+x, 1/2-y, -z$
	I3...I2	3.768(1)	164.5(2)	104.9(2)	$1-x, 1/2+y, 1/2-z$

^a = Intramolecular interaction.^b = Inter-halogen type-I interaction. All other inter-halogen interactions are type-II.

2.3.2 Isostructurality and solid solution

Solid solution or mixed crystal²⁶ is a solid state solution of two or more components where addition of the solute does not change the crystal structure of the solvent but the ratio of solute to solvent will vary in non-stoichiometric proportion throughout the structure. The necessary condition for the formation of solid solution is

that both the components must be isomorphous. Solid solution formation may enhance properties of the resulting material compared to the starting ones.²⁷

The unit cell similarity index (Π)^{1b} of two crystal structures being compared is calculated using the equation

$$\Pi = \left| \frac{a+b+c}{a'+b'+c'} \right| - 1$$

where a, b, c and a', b', c' are the orthogonalized lattice parameters of related crystals. Π is close to zero for isostructural crystals. Π values calculated for nine crystal pairs (Table 2.2) show that the monoclinic and orthorhombic structures are very similar in each crystal system.

Table 2.2 Unit cell similarity index (Π)

Crystal pair	Π
TIB, TIP	0.0054
TIB, TIR-O	0.0127
TIB, TIG-O	0.0134
TIP, TIR-O	0.0073
TIR-O, TIG-O	0.0007
TIP, TIG-O	0.0079
TIF, TIR-M	0.0227
TIR-M, TIG-M	0.0048
TIF, TIG-M	0.0178

Given the excellent isomorphous and isostructural nature among TIR and TIG polymorphs, we attempted mixed crystal or solid-solution formation with TIP in isomorphous space group $P2_12_12_1$. Dissolution of equimolar amounts of TIP and TIR in CHCl_3 gave single crystals that solved in the orthorhombic space group $P2_12_12_1$. The s.o.f. of O atoms are $\text{O1} = 0.65$, $\text{O2} = 0.47$ and $\text{O3} = 0.41$ which gives a 1:1 stoichiometry of the binary solid-solution. The molecular packing in TIP+TIR-O is similar to TIG-O. Similarly, a 1:1 molar mixture of TIR and TIG in CHCl_3 gave binary 1:1 solid-solution crystal, TIR+TIG-O, in space group $P2_12_12_1$ based on s.o.f. $\text{O1} = 0.76$, $\text{O2} = 0.92$ and $\text{O3} = 0.84$.

2.3.3 Crystal structure of solid solutions

Both the solid solutions are isostructural with the orthorhombic forms in the family. They have the same kind of helix and 3D corrugated sheet structures. Inter-halogen interactions for solid solution are summarized in Table 2.1 and their crystal structures are described in Figure 2.8 and 2.9.

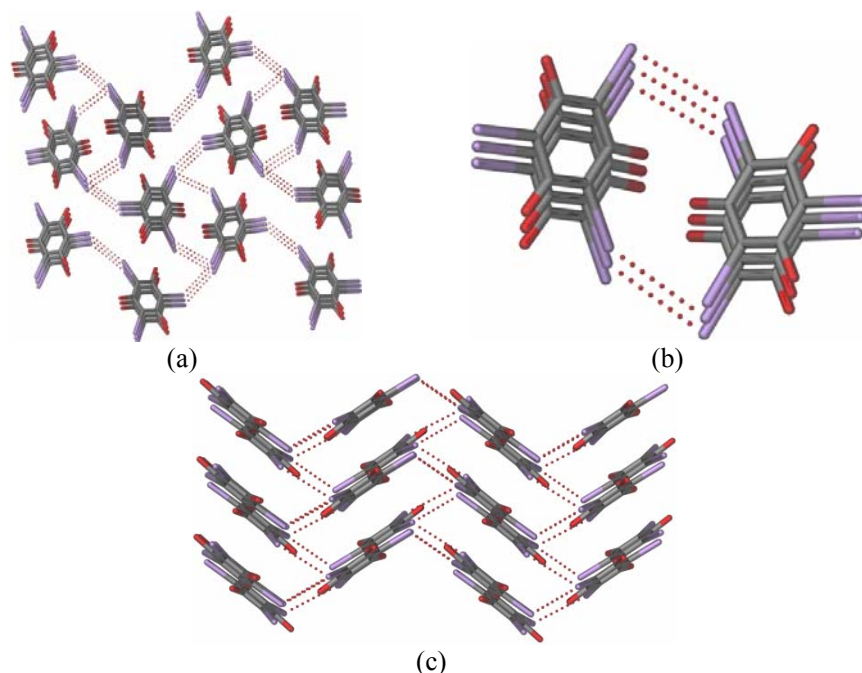
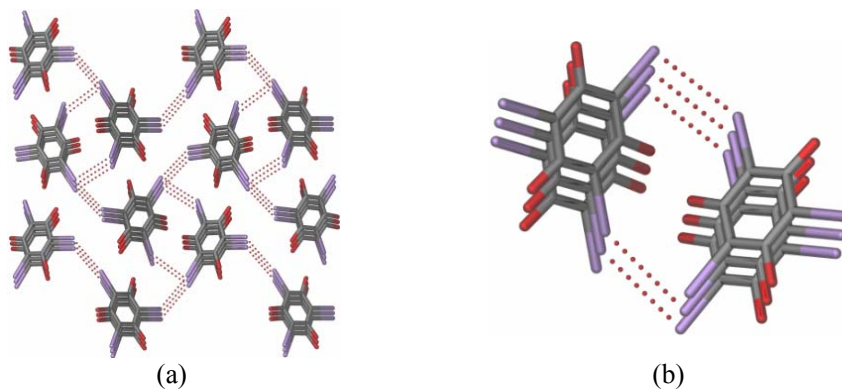


Figure 2.8 Crystal structures of solid-solution TIP+TIR-O. (a) Zigzag tapes mediated by I3...I2 (3.94 Å, 159.1°, 109.4°) type-II interaction along [010], (b) left-handed helix along [100] formed by I1...I3 type-II interaction (3.96 Å, 146.3°, 82.0°), and (c) molecule make a corrugated sheet structure in (100) plane.



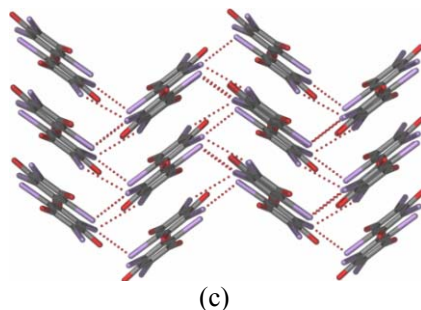


Figure 2.9 Packing diagram in solid-solution TIR+TIG-O. (a) Zigzag tapes mediated by I3⋯I2 type-II interaction (3.77 Å, 164.4°, 104.9°) along [010], (b) right-handed helix formed by I1⋯I3 (3.89 Å, 146.9°, 82.1°) along [100], and (c) corrugated sheet formed parallel to (100) plane.

2.4 Discussion

To our knowledge, triiodoresorcinol and triiodophloroglucinol represent a rare case wherein two polymorphic crystal structures of two different molecules also make an isostructural pair (Figure 2.10). Secondly, the orthorhombic form is similar to the crystal structure of triiodobenzene (in turn TIB is similar to tribromo- and trichloro-benzene) whereas the monoclinic form resembles the crystal structure of trifluorotriiodobenzene (TIF)²⁸ in terms of unit cell parameters and molecular arrangement in the crystal lattice. Thus, the dimorphic crystal structures of TIR and TIG serve as bridges between the monomorphic orthorhombic crystal structure of TIB and TIP and the monoclinic cell of TIF. TIB and TIP crystallized in orthorhombic space group $P2_12_12_1$ (Table 2.3) and the molecules are ordered in both crystal structures. TIG crystallized in $P2_12_12_1$ space group (TIG-O) and the structure is fully ordered. However, the middle member, TIR, crystallized in $P2_1/n$ space group (TIR-M) but the molecules are disordered so as to resemble TIG. As the terminal members (TIP and TIG) crystallized in $P2_12_12_1$ space group, it was expected that the middle member TIR too should be able to adopt the same space group. Similarly as TIR has a crystal structure in $P2_1/n$ space group (TIR-M), TIG should also have a crystal structure in this space group. Indeed a monoclinic polymorph of TIG in the space group $P2_1/n$ (TIG-M) was obtained from mesitylene.

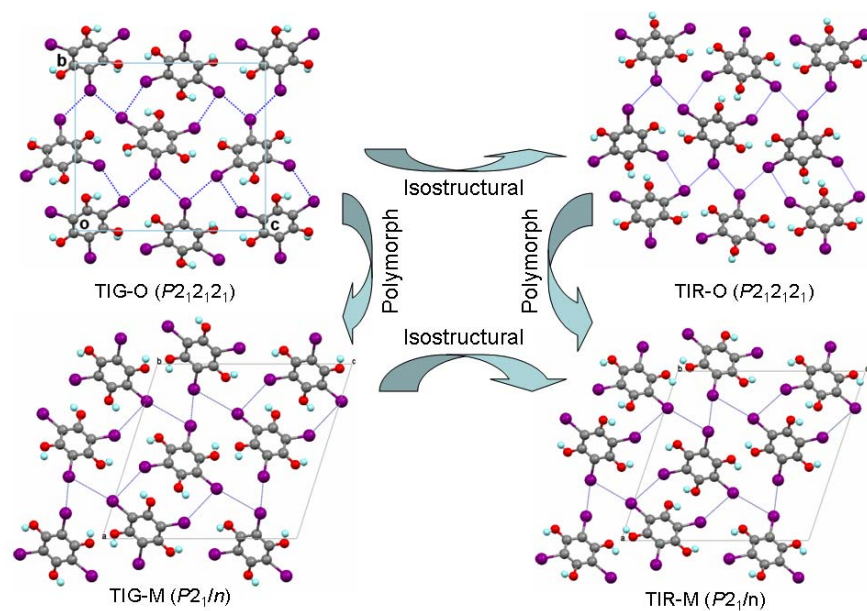
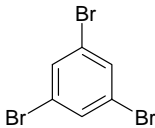
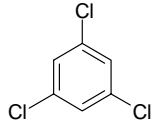
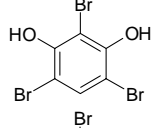
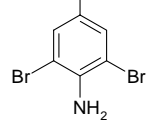
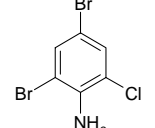
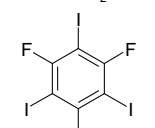


Figure 2.10 Isostructural orthorhombic and monoclinic pairs of TIG and TIR polymorphs.

Table 2.3 Crystal systems of some trihalobenzenes

Compound	Structure	$P2_12_12_1$	$P2_1/n$
TIP		\sqrt{a}	--
TIR		\sqrt{a}	\sqrt{a}
TIG		\sqrt{a}	\sqrt{a}
TIB		\sqrt{b}	--

TBB		$\sqrt{^b}$	--
TCB		$\sqrt{^b}$	--
TBR		$\sqrt{^b}$	--
TBA		$\sqrt{^b}$	--
BCA		$\sqrt{^b}$	--
TIF		--	$\sqrt{^b}$

^a This study; ^b Cambridge Structural Database

Thus the concept of isostructurality in the series of compounds studied led to the discovery of new forms of TIR and TIG taking a cue from TIG-O and TIR-M respectively. The degree of isostructurality in the family of crystals was confirmed by the formation of solid-solution. A solid solution TIP+ TIR and TIR+TIG crystallized in the orthorhombic space group although the monoclinic setting is a possibility. The solid-solution crystal structures resemble the structures of the pure components in $P2_12_12_1$ space group. A reason for dimorphism in TIR and TIG may be found in the less significant OH groups in this family of compounds. The OH groups are buried between the flanking iodine atoms and the structures do not make conventional O–H \cdots O hydrogen bonds despite having one, two and three phenol groups. We note that the OH groups are silent in the orthorhombic crystal structure whereas they participate in tandem hydrogen bonding²⁹ in the monoclinic structures (O–H \cdots O: TIG-M 2.46 Å, 2.80 Å, 104.2°; TIR-M 2.71 Å, 2.73 Å, 82.8°). The energy of tandem hydrogen bonds is estimated as –4.62 kcal

mol^{-1} , weaker than linear ($-5.19 \text{ kcal mol}^{-1}$) but stronger than bifurcated H bonds ($-2.87 \text{ kcal mol}^{-1}$).³⁰ O–H \cdots O hydrogen bonds are much longer in the orthorhombic polymorphs, TIG-O and TIR-O (O \cdots O 3.20, 3.16 Å). The role of tandem H bonding in the monoclinic crystal structures explains why trihalobenzenes and triiodophenol adopt orthorhombic form only (Table 2.3) because O–H \cdots O interactions are not possible to minimal in these structures. The OH disorder in TIR mimics the TIG structure via tandem H bonds. Incidentally, the tandem OH arrangement in TIR-M and TIG-M is replaced by F \cdots F contacts in the monoclinic structure of TIF. TIF has a corrugated layer structure^{28b} sustained by type-II I \cdots I and other inter-halogen contacts (Table 2.1). The complete difference between the crystal structures of TIB (orthorhombic) and TIF (monoclinic) by H \rightarrow F replacement is not surprising but now a link is established in the series through TIR and TIG dimorphs (Figure 2.11). A full list of closely related crystal structures from our results and extracted from the literature³¹ is given in Table 2.4.

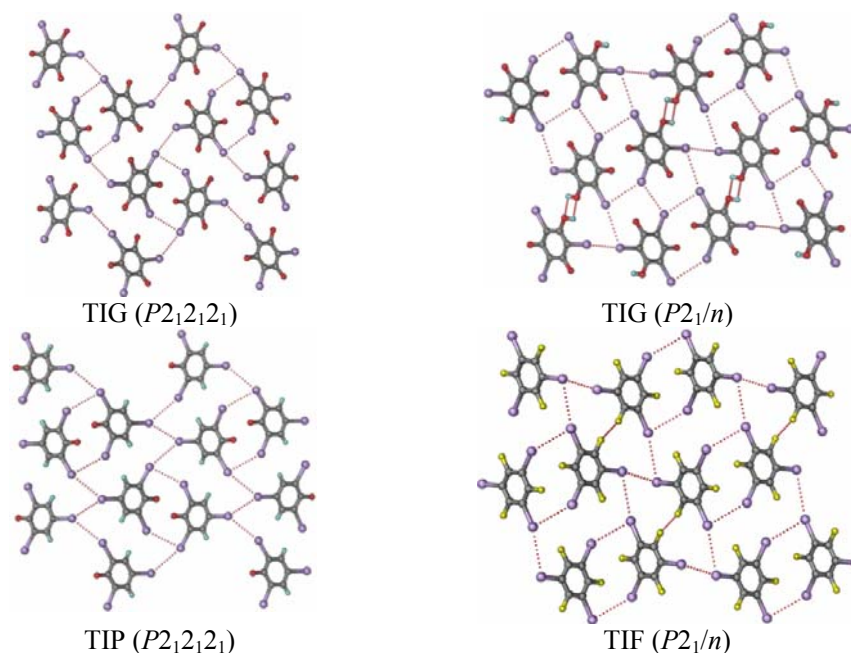
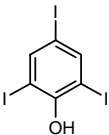
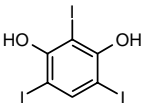
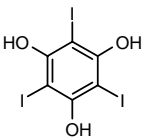
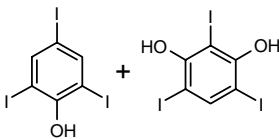
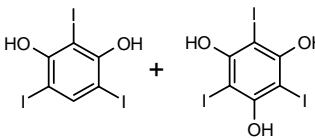
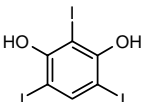


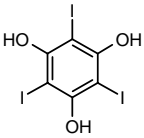
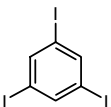
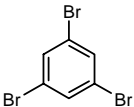
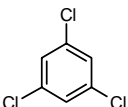
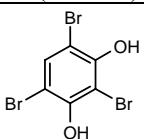
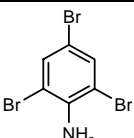
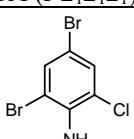
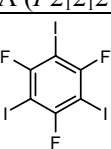
Figure 2.11 Tandem hydrogen bonds in the monoclinic crystal structure of TIG are replaced by F \cdots F interaction in TIF. There are no significant O–H \cdots O hydrogen bonds in the orthorhombic structure of TIG and TIP.

The *ortho*-proximal placement of OH and I groups in these structures means that there are several I \cdots O contacts within the van der Waals sum. However, I \cdots I or O–H \cdots O

contacts from/to the same atoms are shorter in each case and these are taken to be the genuine interactions. Secondly, in no case does the electronegative O approach the electropositive polar region of I–C in a type-II L-geometry. Examples of polymorph and solid-solution crystals based on Br⋯O and Br⋯Br interactions are discussed in recent papers.^{5b, 32}

Table 2.4 Space group and unit cell parameters of some halogen and hydroxyl substituted benzenes. Crystal data are taken from this paper and the Cambridge Structural Database (ConQuest 1.12, November 2009 release, August 2010 update).

Compound/ Space group	<i>a</i> (Å)	<i>b</i> (Å)	<i>c</i> (Å)	β (°)	<i>T</i> (K)	<i>V</i> (Å ³)
Our Result						
 TIP (<i>P</i> ₂ ₁ ₂ ₁ ₂ ₁)	4.370	14.694	14.184	90	100	910.7
 TIR-O (<i>P</i> ₂ ₁ ₂ ₁ ₂ ₁)	4.495	13.958	15.036	90	100	943.3
 TIG-O (<i>P</i> ₂ ₁ ₂ ₁ ₂ ₁)	4.638	13.529	15.345	90	100	962.8
 TIP+TIR (<i>P</i> ₂ ₁ ₂ ₁ ₂ ₁)	4.442	14.368	14.573	90	100	930.1
 TIR+TIG (<i>P</i> ₂ ₁ ₂ ₁ ₂ ₁)	4.561	13.648	15.349	90	100	955.4
 TIR-M (<i>P</i> ₂ ₁ / <i>n</i>)	14.882	4.332	15.585	108.5	100	952.8

	14.582	4.500	15.507	107.6	100	970.2
TIG-M ($P2_1/n$)						
Crystal data from CSD						
	4.329	14.224	14.515	90	161	893.7
TIB ($P2_12_12_1$) ^{31a}						
	14.23	13.55	4.08	90	298	786.7
TBB($P2_12_12_1$) ^{31b}						
	13.93	13.19	3.91	90	298	718.4
TCB ($P2_12_12_1$) ^{31b}						
	4.107	12.855	15.296	90	120	807.6
TBR ($P2_12_12_1$) ^{31c}						
	13.44	14.62	4.26	90	298	837.9
TBA ($P2_12_12_1$) ^{31d}						
	4.178	13.24	14.86	90	298	822.2
BCA ($P2_12_12_1$) ^{31e}						
	13.818	4.758	15.385	107.1	120	966.9
TIF ($P2_1/n$) ^{28b}						

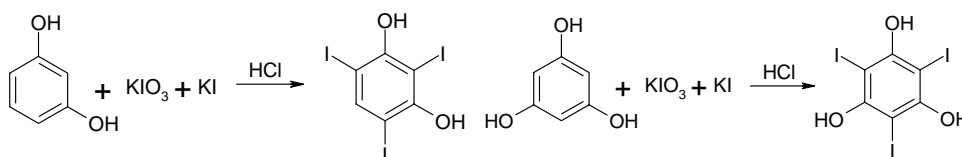
2.5 Conclusions and Future Studies

Triiodoresorcinol and triiodophloroglucinol exhibit dimorphism in contrast to several other members which are monomorphic. Whereas crystal structures of trihalobenzenes in the orthorhombic crystal setting are traditionally well known, a monoclinic structure of TIF was reported recently.²⁸ The present study shows alternative crystal packing arrangements for trihalobenzenes in the monoclinic family of crystal structures. The empty slots in Table 2.3 suggest that there is scope to discover new crystalline forms in these compounds.

2.6 Experimental Section

Synthesis: TIR and TIG were synthesized and characterized by IR and ¹H NMR. NMR spectra (CDCl₃ solution, δ scale) were recorded on Bruker Avance at 400 MHz. FT-IR spectra (KBr pellet, ν cm⁻¹) were recorded on Jasco 5300 spectrophotometer. Melting points were recorded on Fisher-Johns apparatus. All compounds were purified and characterized by ¹H NMR and IR, and finally, the structure was secured by single crystal X-ray diffraction.

Both the compounds were synthesized by poly-iodination of the starting phenol (Scheme 2.2).²⁵



Scheme 2.2 Syntheses of TIR and TIG.

TIR was synthesized by the drop-wise addition of a solution of KI (3.22 g, 20 mmol) and KIO₃ (2.14 g, 10 mmol) in 50 mL water to a solution of resorcinol (1.10 g, 10 mmol) in 10 mL water with 5-6 drops of 50% HCl added. The solution was stirred at room temperature for 6 h to get the desired product as precipitate which was purified by crystallization from CHCl₃.

M.p.: 152 °C (154-157 °C).²⁵

¹H NMR: 5.89 (2H, s), 7.96 (1H, s).

IR: 588, 627, 3430 cm⁻¹.

TIG was synthesized by the same procedure starting from phloroglucinol and the product was crystallized from CHCl₃.

M.p. (dec.) 170 °C (171-172 °C).²⁵

¹H NMR: 5.98 (3H, s).

IR: 534, 638, 3443 cm⁻¹.

X-ray diffraction: Reflections were collected on a Bruker Smart Apex CCD diffractometer at 100 K using Mo-K α incident X-radiation (λ = 0.71073 Å). SAINT software³³ was used for data reduction. Structures were solved using the direct methods in SHELX-97.³⁴ Semi-empirical and multi-scan absorption corrections SADABS³⁵ were applied. All non-hydrogen atoms were refined anisotropically and C–H hydrogens in case of TIP were fixed. O–H hydrogen atoms could not be located in difference electron density maps and were not included. The O atoms in TIR-M, TIR-O, TIP+TIR-O and TIR+TIG-O have disordered oxygen atoms with partial s.o.f. given in table 2.5.

Table 2.5 Partial s.o.f. at the oxygen atoms for the disordered structures.

	O1	O2	O3
TIR-M	0.88	0.86	0.27
TIR-O	0.62	0.70	0.68
TIP+TIR-O	0.65	0.47	0.41
TIR+TIG-O	0.76	0.92	0.84

2.7 References

1. (a) A. Kálmán, L. Párkányi and G. Argay, *Acta Cryst.*, B49, **1993**, 1039. (b) L. Fábián and A. Kálmán, *Acta Cryst.*, B55, **1999**, 1099. (c) A. Kálmán and L. Párkányi, *Adv. Mol. Struct. Res.*, 3, **1997**, 189.

2. (a) W. C. McCrone, in *Physics and Chemistry of the Organic Solid State*, ed. D. Fox, M. M. Labes and A. Weissberger, Wiley-Interscience, New York, vol. 2, **1965**, pp. 725–767. (b) J. Bernstein, *Polymorphism in Molecular Crystals*, Clarendon, Oxford, **2002**.
3. (a) R. Hilfiker (Ed.), *Polymorphism in the Pharmaceutical Industry*, Wiley-VCH: Weinheim, **2006**. (b) J. Galcera and E. Molins, *Crystal Growth & Design*, **9**, **2009**, 327.
4. (a) H. Karfunkel, H. Wilts, Z. Hao, A. Iqbal, J. Mizuguchi and Z. Wu, *Acta Cryst.*, B55, **1999**, 1075. (b) N. J. Babu and A. Nangia, *Cryst. Growth Des.*, **6**, **2006**, 1753.
5. (a) K. F. Bowes, C. Glidewell, J. N. Low, M. Melguizoc and A. Quesadad, *Acta Cryst.*, C59, **2003**, o4. (b) F. C. Pigge, V. R. Vangala and D. C. Swenson, *Chem. Comm.* **2006**, 2123. (c) B. Omondi, M. A. Fernandes, M. Layh, D. C. Leventis, J. L. Look and T. S. P. Mkwizu, *CrystEng Comm.*, **7**, **2005**, 690.
6. (a) N. K. Nath, B. K. Saha and A. Nangia, *New J. Chem.*, **32**, **2008**, 1693.
(b) For definition see http://reference.iucr.org/dictionary/Isomorphous_crystals and http://reference.iucr.org/dictionary/Isostructural_crystals.
7. (a) B. K. Saha and A. Nangia, *Chem. Comm.*, **2006**, 1825. (b) B. K. Saha and A. Nangia, *Chem. Comm.*, **2005**, 3024.
8. (a) F. L. Weitzl, M. Sovak, T. M. Williams and J. H. Lang, *Journal of Medicinal Chemistry*, **19**, **1976**, 1359. (b) M. Sovak, A. L. Seligson and J. G. Dauglass, US patent, No.6072069, **2000**.
9. J. C. Roquet-Jalmar, US patent, No. 4677124, **1987**.
10. M. Parreño, J. P. Vaqué, I. Casanova, P. Frade, M. V. Céspedes, M. A. Pavón, A. Molins, M. Camacho, L. Vila, J. F. Nomdedeu, R. Mangués and J. León, *Mol. Cancer Ther.*, **5**, **2006**, 1166.
11. S. L. Morissette, O. Almarsson, M. L. Peterson, J. F. Remenar, M. J. Read, A. V. Lemmo, S. Ellis, M. J. Cima and C. R. Gardner, *Adv. Drug Delivery Rev.*, **56**, **2004**, 275.
12. (a) D. Braga, F. Grepioni, L. Maini, M. Polito, K. Rubini, M. R. Chierotti and R. Gobetto, *Chem. Eur. J.*, **15**, **2009**, 1508. (b) D. Braga, G. Cojazzi, D. Paolucci, and F. Grepioni, *CrystEngComm*, **3**, **2001**, 159. (c) H. Miura, T. Ushio, K.

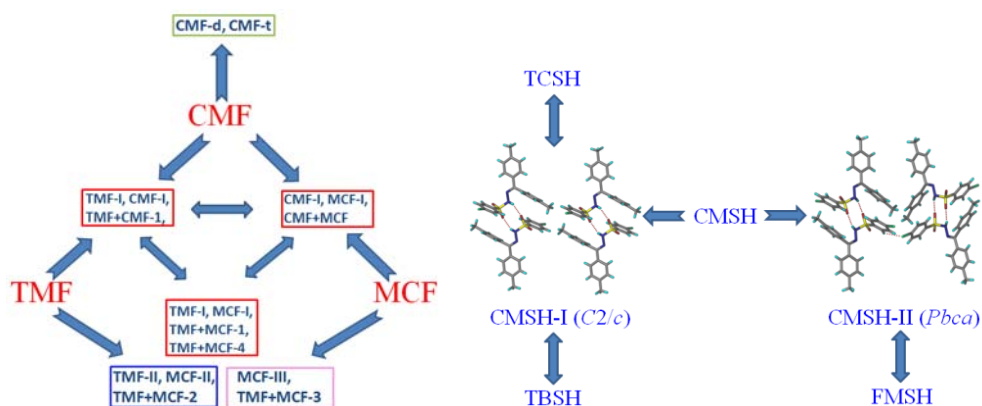
- Nagai, D. Fujimoto, Z. Lepp, H. Takahashi and R. Tamura, *Cryst. Growth Des.*, **3**, **2003**, 959.
13. (a) P. Metrangolo and G. Resnati, *Chem. Eur. J.*, **7**, **2001**, 2511. (b) J. P. M. Lommerse, A. J. Stone, R. Taylor and F. H. Allen, *J. Am. Chem. Soc.*, **118**, **1996**, 3108. (c) P. Metrangolo and G. Resnati, in *Halogen Bonding*; Encyclopedia of Supramolecular Chemistry, **2004**.
14. G. R. Desiraju, in *Crystal Engineering: The Design of Organic Solids*; Elsevier: Amsterdam, **1989**.
15. A. Bondi, *J. Phys. Chem.*, **68**, **1964**, 441.
16. S. C. Nyburg and C. H. Faerman, *Acta Cryst.*, **B43**, **1987**, 106.
17. (a) S. L. Price, A. J. Stone, J. Lucas, R. S. Rowland and A. E. Thornley, *J. Am. Chem. Soc.*, **116**, **1994**, 4910. (b) J. B. O. Mitchell and S. L. Price, *J. Phys. Chem.*, **A105**, **2001**, 9961. (c) G. M. Day and S. L. Price, *J. Am. Chem. Soc.*, **125**, **2003**, 16434.
18. V. R. Pedireddi, D. S. Reddy, B. S. Goud, D. C. Craig, A. D. Rae and G. R. Desiraju, *J. Chem. Soc. Perkin Trans. 2*, **1994**, 2353.
19. (a) B. K. Saha, R. K. R. Jetty, L. S. Reddy, S. Aitipamula and A. Nangia, *Cryst. Growth Des.*, **5**, **2005**, 887. (b) B. K. Saha, A. Nangia and J.-F. Nicoud, *Cryst. Growth Des.*, **6**, **2006**, 1278. (c) R. Paulini, K. Müller and F. Diederich, *Angew. Chem., Int. Ed.*, **44**, **2005**, 1788. (d) F. Zordan, L. Brammer and P. Sherwood, *J. Am. Chem. Soc.*, **127**, **2005**, 5979. (e) C. B. Aakeroy, M. Fasulo, N. Schultheiss, J. Desper and C. Moore, *J. Am. Chem. Soc.*, **129**, **2007**, 13772. (f) J. N. Moorthy, P. Venkatakrishnan, P. Mal, S. Dixit and P. Venugopalan, *Cryst. Growth Des.*, **3**, **2003**, 581. (g) R. G. Gonnade, M. M. Bhadbhade, M. S. Shashidhar and A. K. Sanki, *Chem. Commun.*, **2005**, 5870. (h) D. Chopra, V. Thiruvenkatam, S. G. Manjunath and T. N. Guru Row, *Cryst. Growth Des.*, **7**, **2007**, 868. (i) E. Bosch and C. L. Barnes, *Cryst. Growth Des.*, **2**, **2002**, 299. (j) V. R. Pedireddi, D. S. Reddy, B. S. Goud, D. C. Craig, A. D. Rae and G. R. Desiraju, *J. Chem. Soc., Perkin Trans. 2*, **1994**, 2353.
20. J. M. Dumas, L. Gornel and M. Guerin, in *The Chemistry of functional group, Supplement D*; Eds. S. Patai and Z. Rappoport, Wiley: New York, **1983**, pp- 985.

21. G. A. Landrum, N. Goldberg and R. Hoffmann, *J. Chem. Soc., Dalton Trans.*, **19**, **1997**, 3605.
22. (a) A. C. Legon, *Angew. Chem. Int. Ed.*, **38**, **1999**, 2686. (b) I. Alkorta, I. Rozas and J. Elguero, *J. Phys. Chem.*, **A102**, **1998**, 9278.
23. P. Metrangolo, H. Neukirchi, T. Pilati and G. Resnati, *Acc. Chem. Res.*, **38**, **2005**, 386.
24. P. Auffinger, F. A. Hays, E. Westhof and P. S. Ho, *Proc. Natl. Acad. Sci. USA*, **101**, **2004**, 16789.
25. F. L. Weitz, *J. Org. Chem.*, **41**, **1976**, 2044.
26. (a) A. I. Kitaigorodski, *Mixed Crystals*, Springer: Berlin, **1984**, 275. (b) A. Anthony, M. Jaskólski, A. Nangia and G. R. Desiraju, *Chem. Comm.*, **1998**, 2537.
27. (a) H.-T. Li, Q. Wanga, J.-C. Hea, J.-T. Guob and H.-Q. Yeb, *Materials Characterization*, **59**, **2008**, 1395. (b) A. Nordmann and Y.-B. Cheng, *J. Am. Ceram. Soc.*, **80**, **1997**, 3045. (c) F. Tajarobi, S. Abrahamsén-Alami and A. Larsson, *J. Pharm. Sci.*, **100**, **2011**, 275.
28. (a) A. C. B. Lucassen, A. Karton, G. Leitun, L. J. W. Shimon, J. M. L. Martin and M. E. van der Boom, *Cryst. Growth Des.*, **7**, **2007**, 386. (b) C. M. Reddy, M. T. Kirchner, R. C. Gundakaram, K. A. Padmanabhan and G. R. Desiraju, *Chem. Eur. J.*, **12**, **2006**, 2222.
29. G. A. Jeffrey and W. Saenger, *Hydrogen bonding in Biological Structures*, Springer-Verlag: Berlin, **1991**, pp-24.
30. U. C. Singh and P. A. Kollman, *J. Chem. Phys.*, **83**, **1985**, 4033.
31. (a) D. Margraf and J. W. Batsb, *Acta Cryst.*, **E62**, **2006**, o502. (b) H. J. Milledge and L. M. Pant, *Acta Cryst.*, **13**, **1960**, 285. (c) P. Kirsop, J. M. D. Storey and W. T. A. Harrison, *Acta Cryst.*, **E60**, **2004**, o222. (d) A. T. Christensen and K. O. Strømme, *Acta Cryst.*, **B25**, **1969**, 657. (e) G. Ferguson, J. N. Low, G. H. Penner and J. L. Wardell, *Acta Cryst.*, **C54**, **1998**, 1974.
32. (a) R. G. Gonade, M. M. Bhadbhade, M. S. Shashidhar and A. K. Sanki, *Chem. Commun.*, **2005**, 5870. (b) F. C. Pigge, V. R. Vangala and D. C. Swenson, *Chem. Commun.*, **2006**, 2123.

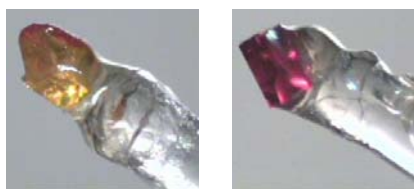
33. *SAINT-Plus*, version 6.45, Bruker AXS Inc., Madison, WI, 2003. G. M. Sheldrick, *SHELX-97: Program for the Solution and Refinement of Crystal Structures*, University of Göttingen, Germany, **1997**.
34. (a) G. M. Sheldrick, *SADABS: Program for Empirical Absorption of Area Detector Data*, University of Göttingen, Germany, **1996**. (b) G. M. Sheldrick, *Program for Multi-scan Absorption Correction of Area Detector Data*, version 2.10, University of Göttingen, Germany, **2003**.

Chapter Three

Isostructurality and Polymorphism in Fuchsones and Sulfonylhydrazones



Interrelation of Isostructurality and Polymorphism among the crystal structures of Fuchsones and Sulfonylhydrazones



Color polymorphism in CMF

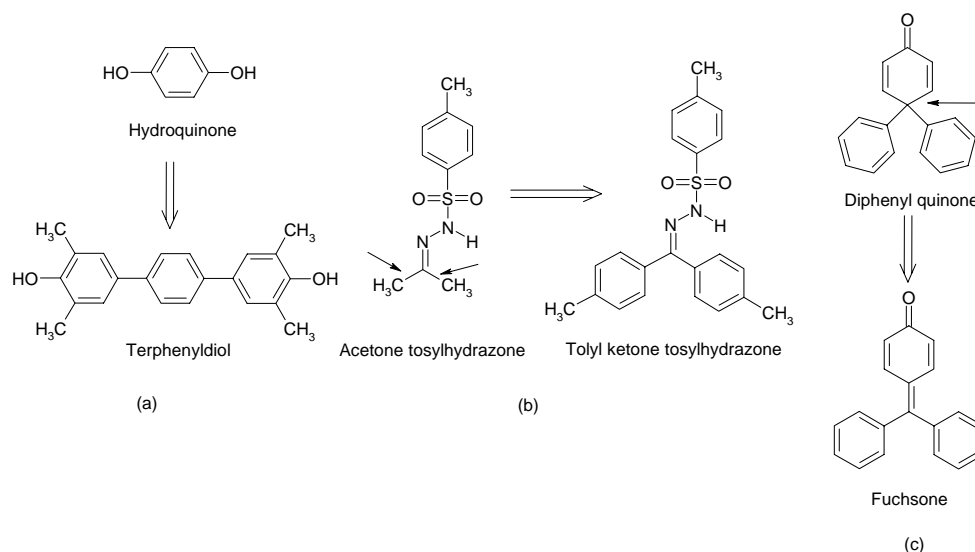
Halogen-methyl and interhalogen exchanged isostructurality among polymorphs of two series of conformationally flexible molecules is presented.

3.1 Introduction

Controlling the solid-state assembly of molecules into crystalline solids is of considerable interest¹ in order to design and synthesize functional materials.² The immense applications of polymorphism (different crystal structure for the same molecular species) in pharmaceutical industry inspires the material chemists to carry out extensive studies on this particular phenomena.³ In contrast, the opposite phenomena, i. e. isostructurality⁴ (occurrence of same or very similar crystal structure for different molecular species) is relatively less studied in recent times. The reason may be due to its rare occurrences⁵, moreover, sets of isostructural compounds rarely include more than two members.⁶ The rare occurrence of isostructural solids may be attributed to the sensitivity of crystal packing to the molecular structure as slight changes can result in entirely different crystal packing arrangement.⁷ Isostructurality and polymorphism were discussed in the Chapter 1.

Functional groups which have the ability to adopt the same structural role in crystal structures may lead to the formation of isostructural crystals. Chloro-methyl and halogen groups are often viewed as the structurally equivalent functional groups. According to Kitaigorodskii's principle of close packing⁸, chlorine (Cl, 21 Å³) and methyl (Me, 19 Å³) substituents have similar size and shape, and so it is possible that Cl/Me interchanged molecules have the same crystal structure, known as chloro-methyl exchange rule.⁹ But, it was found that isostructural Cl-Me interchange occurs relatively infrequent, in about 26% cases (one fourth) and different crystal structures are observed for the majority 74% (three fourth) in a small sample of 118 structures^{9b} which shows Cl-Me exchange is not always predictable. The halogen exchange, especially Cl, Br and I to give isostructurality, is more frequent.¹⁰ Construction of an isostructural organic solid with conformationally flexible molecule is not straightforward as they may lead to different packing arrangement, i. e. polymorph, due to flexibility associated with the molecules.

The study of polymorphism in closely related molecules gives an understanding of molecular structure/crystal structure relationships. For example hydroquinone and 4,4'-terphenyl diol¹¹ make a phenylogue-extended series of polymorphs (Scheme 3.1).

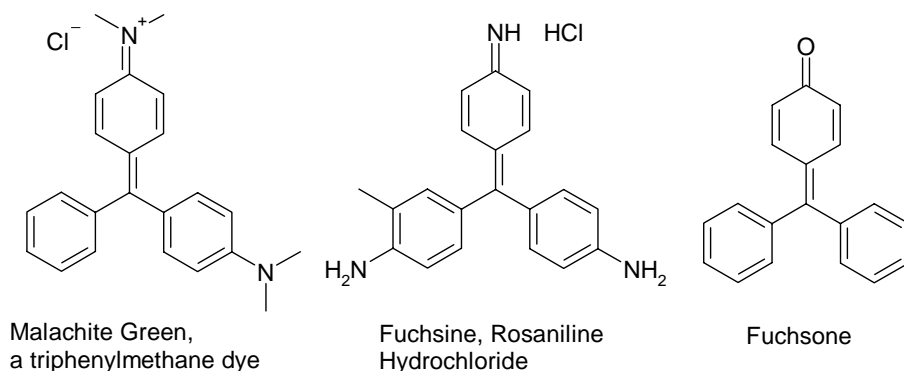


Scheme 3.1 (a) Phenyllogue series approach to polymorph clusters illustrated for hydroquinone (b) From dimorphs of acetone tosylhydrazone \rightarrow trimorphs of tolyl tosylhydrazone (c) Vinylogue extended tetramorphic diphenyl quinone give rise to highly polymorphic Fuchsones.

The fascinating rhombohedral structure of β -hydroquinone was reproduced in another diphenolic compound through applying molecular engineering approach. To discover new conformational polymorphic systems, similar molecular engineering approach was applied to dimorphic acetone tosyl hydrazone (termed as Sulfonylhydrazone), to produce conformational trimorphs of bis(tolyl)ketonetosylhydrazone.¹² 4,4-Diphenyl-2,5-cyclohexadienone¹³ is tetramorphic but its 4-phenyl substituted derivatives do not exhibit polymorphism. Fuchsones may be viewed as a vinylogue extension of diphenyl benzoquinone and it came up as highly polymorphic series of compounds in our recent work.¹⁴

The triphenylmethane derivatives are among the oldest man made dyes.¹⁵ Several other members of the class were discovered before their chemical constitutions were fully understood. Any member of this group of dyes is intensely colored having molecular structures based upon that of the hydrocarbon triphenylmethane. For example Malachite green is well known triphenylmethane dye used for materials such as silk, leather, and paper. Fuchsones, α,α -diphenyl-1,4-benzoquinone methides, is a class of quinone methides which are of particular interest because of their early application as

triphenylmethane dyes. The parent compound has been known for many years and numerous substituted Fuchsones have been described in the literature.¹⁶ Scheme 3.2 depicts the molecular structure of some closely related dyes.



Scheme 3.2 Molecular structures of three closely related molecules triphenylmethane dye malachite green, Fuchsine and the Fuchsones.

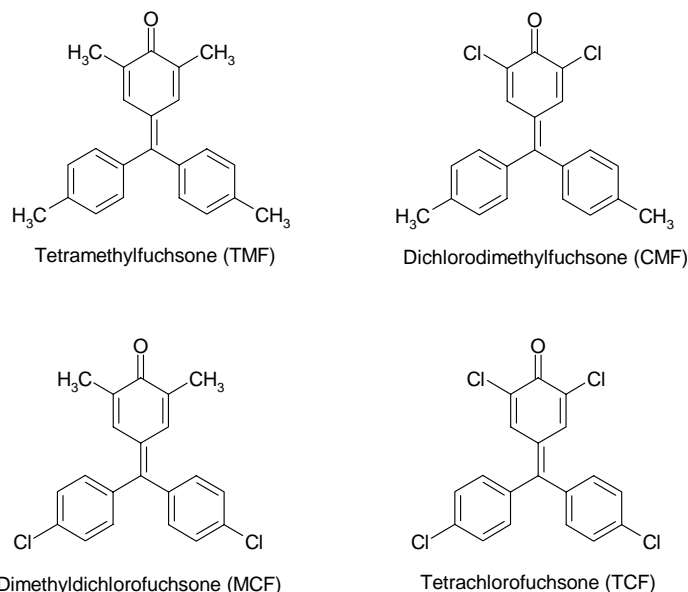
A large number of pigments are known to be polymorphic.¹⁷ Quinacridones, Perylenes, and Phthalocyanines are well known class of pigments which exhibit polymorphic behavior. Utilization of pigments can be greatly influenced by the occurrence of polymorphs as different polymorphs of a pigment can have different spectroscopic properties.

Four derivatives of Fuchsones were synthesized where Me groups were periodically substituted by Cl at four different positions (Section 3.2). Similarly, five new derivatives of Sulfonylhydrazone were synthesized with Me, F, Cl, Br and I substituents at the *para* positions of the three phenyl rings (Section 3.4). Although halogen-methyl exchange and halogen-halogen exchange can direct the formation of isostructural crystals, achieving isostructural crystals in both the series of compounds is challenging. This is because of the fact that the probability of Fuchsones and Sulfonylhydrazones to be polymorphic is high. The reasons are conformational flexibility in both the compounds, presence of multiple numbers of donors compared to one acceptor in Fuchsones and probable sulfonamide dimer/catemer synthon variance¹⁸ in Sulfonylhydrazones.

3.2 Chloro-Methyl Exchange and Polymorphism in Fuchsones

Four derivatives of Fuchsones (Scheme 3.3) were selected: Tetramethylfuchsones (TMF), Dichlorodimethylfuchsones (CMF), Dimethyldichlorofuchsones (MCF), and Tetrachlorofuchsones (TCF).

Fuchsones¹⁶ can either be synthesized by elimination of water from 4-hydroxytriphenylcarbinol or by the oxidation of substituted 4-hydroxytriphenylmethanes. The former can be obtained from the reaction of phenylmagnesium bromide with substituted methyl or ethyl-4-hydroxybenzoates whereas the later can be obtained by acid catalyzed condensation of phenol with aromatic aldehyde or benzhydrol. TMF and CMF were synthesized by dehydration of substituted 4-hydroxytriphenylcarbinol and MCF and TCF were synthesized by oxidizing substituted 4-hydroxytriphenylmethane. TMF can also be synthesized using the second procedure. For TCF, both the reactions were attempted under normal conditions but did not give the desired product. 4-chlorobenzylmagnesium bromide is less reactive compared to the corresponding methyl derivative because of electron withdrawing Cl group. Again, esters are comparatively less reactive towards Grignard reagent compared to aldehydes. A test reaction of 4-chlorobenzylmagnesium bromide with benzaldehyde led to the corresponding benzhydrol but when the reaction was carried out with methylbenzoate the corresponding triphenylcarbinol was not obtained. A modified procedure was successful in synthesizing TCF, where a homogeneous mixture of 2,6-dichlorophenol and 4,4'-dichlorobenzhydrol was dissolved in acetic acid and conc. H_2SO_4 (few drops) and reaction was carried out at 80/90 °C instead of room temperature. Synthetic procedure for their preparation is detailed in the Experimental Section.



Scheme 3.3 Fuchsones selected for studying chloro-methyl exchange and polymorphism.

3.2.1 Crystallization and polymorphism

The four compounds were crystallized from various solvents in search of polymorphs. TMF crystallized as trimorph, form I (TMF-I), form II (TMF-II) and form III (TMF-III), CMF crystallized as dimorph, form I (CMF-I), form II (CMF-II) along with two solvated crystal structures dioxane (CMF-d) and toluene (CMF-t), MCF as trimorphs, form I (MCF-I), form II (MCF-II) and form III (MCF-III). TCF moreover crystallized in one structure only. Various solvents used for crystallization are summarized in Table 3.1. In most of the cases concomitant crystallization of the polymorphs was observed. Comparison of cell parameters, space group in which they crystallized and preliminary crystal structure analysis revealed that TMF-I, CMF-I and MCF-I form an isomorphous crystal structures triplet and TMF-II and MCF-II are isomorphous crystal pair, whereas, TCF has an entirely different crystal structure. The two solvated crystal structures CMF-d and CMF-t also forms an isomorphous crystal pair. A comparison of cell parameters of these isomorphous crystal structures are presented in Table 3.2 (detail cell parameters are summarized in the Appendix). TMF-I, CMF-I and MCF-I crystallized in monoclinic space group $P2_1/c$ and TMF-II and MCF-II crystallized in triclinic space group $P\bar{1}$ with one molecule in the asymmetric unit in each

case. TMF-III, CMF-II and MCF-III crystallized in monoclinic space groups $P2_1/c$, $P2_1/c$ and $C2/c$ with $Z'=1$, 1 and 0.5 respectively. Toluene and dioxane were incorporated in the crystal lattice of CMF when crystallization was carried out from the respective solvent and crystals on X-ray diffraction solved and refined in triclinic space group $P\bar{1}$. TCF crystallized in monoclinic space group $P2_1/n$ with entirely different cell parameters compared to rest of the crystal structures in the series.

Table 3.1 List of solvents used for crystallizing polymorphs of Fuchsones.

Compounds	Form I	Form II	Form III	Solvate
TMF	Hexane, EtOAc, MeOH, CH ₃ NO ₂ , CH ₃ CN, DCM mesitylene	Hexane, benzene, EtOAc, cyclohexane, diethyl ether, mesitylene	MeOH and diethyl ether	-----
CMF	Toluene, dioxane, hexane, benzene, THF, CH ₃ CN, diethylether	CH ₃ NO ₂ , mesitylene CH ₃ CN, dioxane diethylether	-----	Dioxane, toluene
MCF	benzene, diethyl ether, MeOH	DCM, CH ₃ NO ₂	diethyl ether, diisoprpyl ether	-----
TCF	Hexane, benzene, diethyl ether, mesitylene, DCM	-----	-----	-----

Table 3.2 Comparison of the unit cell parameters of the isomorphous crystal structures of Fuchsones.

	TMF-I	CMF-I	MCF-I	TMF-II	MCF-II
Crystal system	Monoclinic	Monoclinic	Monoclinic	Triclinic	Triclinic
Space group	$P2_1/c$	$P2_1/c$	$P2_1/c$	$P\bar{1}$	$P\bar{1}$
T/K	100	100	100	100	100
$a/\text{\AA}$	7.6297(5)	7.5479(5)	7.5638(16)	7.4822(6)	7.5140(7)
$b/\text{\AA}$	12.5889(8)	12.4908(9)	12.612(3)	8.1328(6)	8.1314(7)
$c/\text{\AA}$	18.2064(11)	18.3342(13)	18.207(4)	15.3014(11)	15.2380(14)
α°	90	90	90	97.5620(10)	97.0260(10)
β°	95.4670(10)	95.9850(10)	96.092(3)	101.0460(10)	101.4830(10)
γ°	90	90	90	102.9920(10)	104.0540(10)
Z'/Z	1/4	1/4	1/4	1/2	1/2
$V/\text{\AA}^3$	1740.76(19)	1719.1(2)	1727.0(6)	875.49(11)	870.71(14)
$R_1[I > 2\sigma(I)]$	0.0498	0.0324	0.0328	0.0430	0.0365

CMF-d	CMF-t
Triclinic	Triclinic
$P\bar{1}$	$P\bar{1}$
298	100
7.222(2)	7.2779(7)
12.034(4)	11.8390(11)
12.859(4)	12.4604(11)
102.963(5)	101.2630(10)
102.420(5)	103.8560(10)
92.363(5)	91.1900(10)
1/2	1/2
1058.9(6)	1019.73(16)
0.0540	0.0396

3.2.2 Crystal structure analysis

TMF-I: In the crystal structure C–H···O hydrogen bonded (C16–H16···O1, 2.39 Å, 138.3°) molecules form zig-zag chains along the *c*-axis which are connected to another antiparallel chain by C–H···O hydrogen bond (C9–H9···O1, 2.29 Å, 147.0°) as centrosymmetric dimers (Figure 3.1).

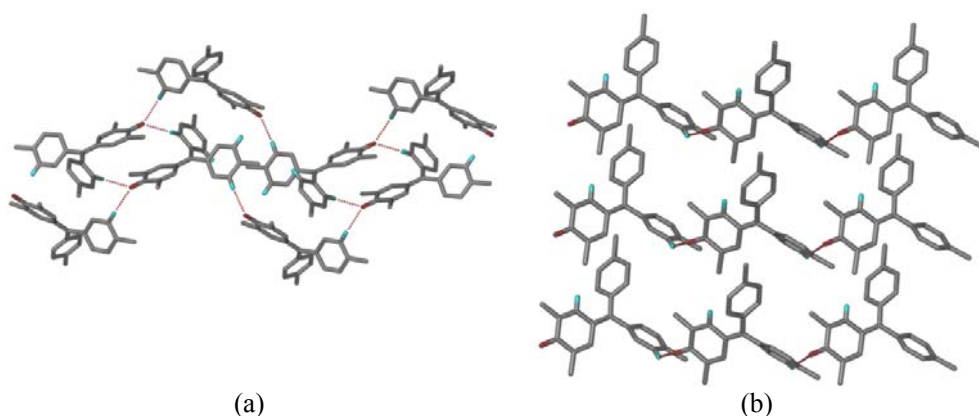


Figure 3.1 Molecular packing in TMF-I. (a) Antiparallel chains of C–H···O hydrogen bonded molecules are connected by another C–H···O hydrogen bond to form 2D sheets. (b) Close packed zig zag chains. Hydrogen atoms are deleted for clarity.

TMF-II: Bifurcated C–H···O hydrogen bonds (C15–H15···O1, 2.26 Å, 136.3°, C9–H9···O1, 2.23 Å, 170.1°) form centrosymmetric dimers which stack along the *a*-axis. The structure is completed by close packing of these centrosymmetric dimers (Figure 3.2).

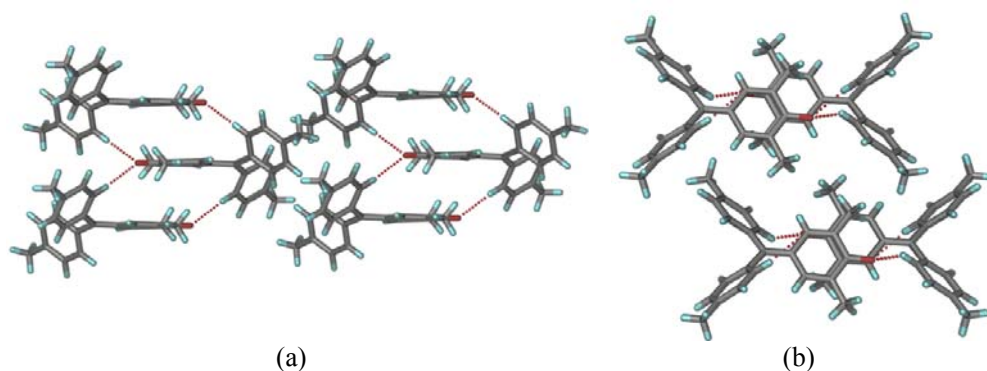


Figure 3.2 Molecular packing in TMF-II. (a) Stacks of centrosymmetric dimers formed by C-H...O hydrogen bond. (b) 3D packing is completed by close packing of these dimers.

TMF-III: The carbonyl oxygen is involved in trifurcated C-H...O hydrogen bonding, two of which make zig zag chains along the *b*-axis (C10-H10...O1, 2.25 Å, 158.1°, C22-H22B...O1, 2.55 Å, 151.5°) to form 2D layer in the *ab*-plane. Two such layers are connected by another C-H...O hydrogen bond (C23-H23C...O1, 2.46 Å, 142.0°) along with auxiliary C-H... π interactions (2.86 Å, 137.0°; 2.62 Å, 151.3°; 2.61 Å, 144.8°) (Figure 3.3).

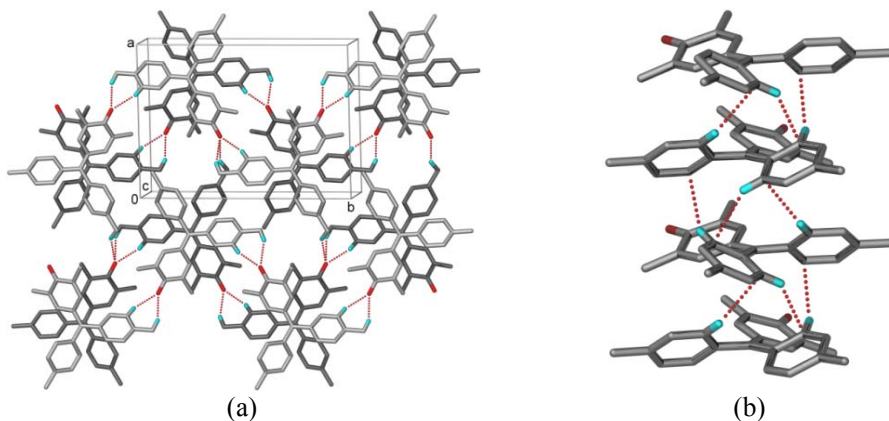


Figure 3.3 Molecular packing in TMF-III. (a) C-H...O hydrogen bond forms 2D layers in the *ab*-plane (two layers are shown with different shadings). (b) C-H... π interactions connecting 2D layers.

CMF-I: In the crystal structure, similar to form I of TMF, C-H...O hydrogen bonded (C16-H16...O1, 2.40 Å, 140.8°) molecules form chains along the *c*-axis, which are in turn connected to another antiparallel chain by C-H...O hydrogen bond (C9-H9...O1, 2.28 Å, 145.2°) and C-H...Cl interactions (C18-H18...Cl1, 2.80 Å, 169.0°) to form 2D

sheet in the *bc*-plane. A C–H \cdots Cl (C3–H3 \cdots Cl2, 2.82 Å, 122.3°) interaction between the sheets completes the 3D packing (Figure 3.4).

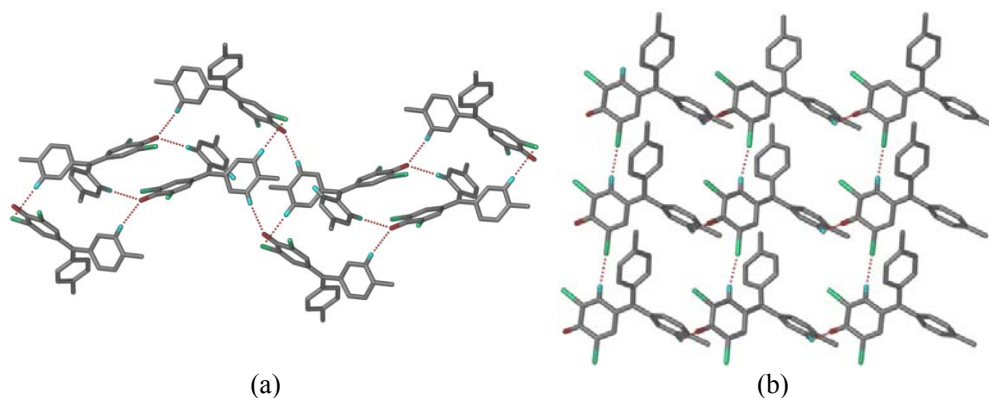


Figure 3.4 CMF-I. (a) Chains of C–H \cdots O hydrogen bonded molecules are connected to another antiparallel chain by C–H \cdots O hydrogen bond and C–H \cdots Cl interactions to form 2D sheets in the *bc* plane. (b) Such sheets are connected to each other by C–H \cdots Cl interactions. Hydrogens are deleted for clarity.

CMF-II: At first sight the crystal structure appears as similar to form I, but structural differences exist between them and is due to the significant variation in the distance of the quinoid ring in the centrosymmetric dimer. In form I, centroid to centroid distance of the overlapping quinoid rings is 4.65 Å whereas this distance in form II is 3.99 Å. Therefore the centrosymmetric dimer of CMF molecules is connected to the nearest neighbor via two C–H \cdots Cl interactions in form II (C3–H3 \cdots Cl1, 2.81 Å, 148.3° and C10–H10 \cdots Cl2, 2.79 Å, 128.1°) compared to single interaction in form I. Figure 3.5 shows the difference in the crystal structure of CMF-I and CMF-II.

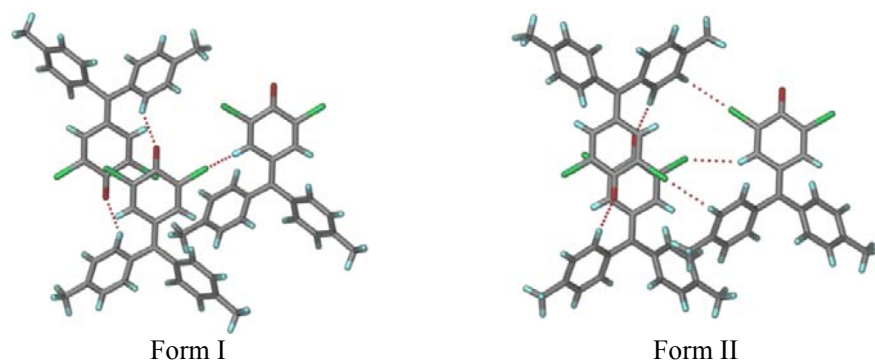


Figure 3.5 Differences of form I and form II CMF. In form I the two quinoid rings are offset whereas they are nearly overlapping in form II.

The crystal structure of CMF-II is explained as shown in Figure 3.6.

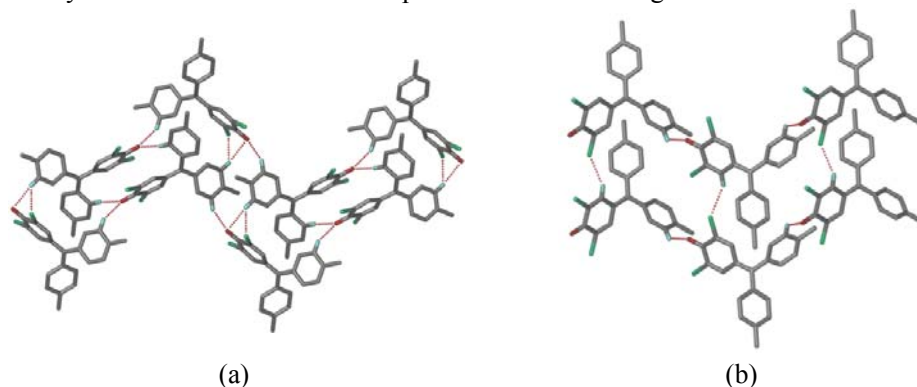


Figure 3.6 Intermolecular interactions and molecular packing in CMF-II. (a) Antiparallel C–H...O hydrogen bonded chains (C16–H16...O1, 2.50 Å, 128.2°) are connected to each other by C–H...O (C9–H9...O1, 2.19 Å, 169.8°) and C–H...Cl hydrogen bond (C21–H21C...Cl2, 2.92 Å, 143.7°). (b) C–H...Cl interactions complete the 3D packing.

CMF-d and CMF-t: CMF crystallized as dioxane (CMF-d) and toluene (CMF-t) solvates on crystallization from the respective solvents. The solvates are isomorphous, having centrosymmetric dimers of bifurcated C–H...O hydrogen bonds which stack along the *a*-axis. A cavity accommodates solvent molecules by space filling (Figure 3.7).

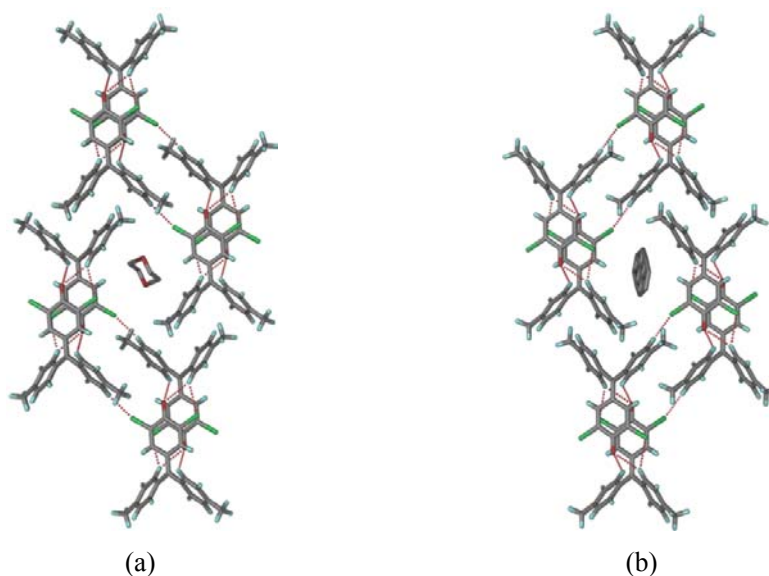


Figure 3.7 Solvated crystal structures of CMF, (a) dioxane solvate CMF-d where C–H...O hydrogen bonded (C9–H9...O1, 2.37 Å, 133.0°; C15–H15...O1, 2.39 Å, 152.6°) dimers extends in 3D forming cavity where solvent molecules are sitting. (b) Toluene

solvate CMF-t has a similar crystal structure as CMF-d (C9–H9···O1, 2.47 Å, 127.9°; C15–H15···O1, 2.49 Å, 150.9°).

MCF-I: The crystal structure is similar to form I of TMF and CMF. Zig-zag chains of C–H···O hydrogen bonded molecules (C18–H18···O1, 2.35 Å, 139.9°) are connected to an oppositely running chain by C–H···O (C9–H9···O1, 2.24 Å, 143.9°) and C–H···Cl (C13–H13···Cl2, 2.66 Å, 140.1°) interactions forming 2D sheet in the *bc* plane (Figure 3.8).

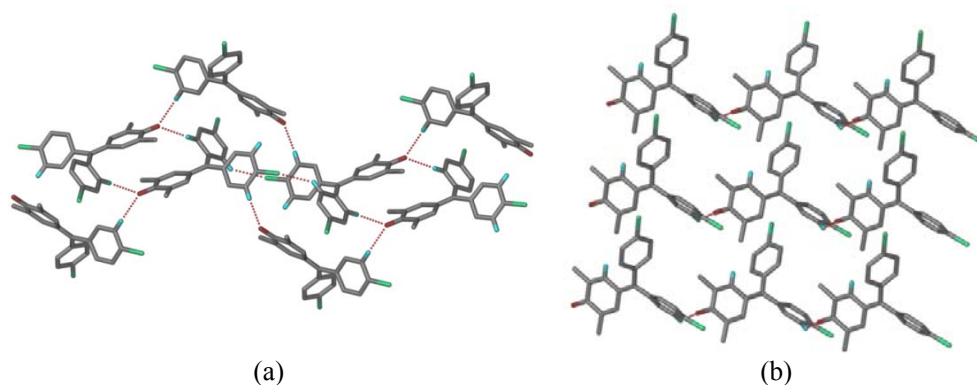


Figure 3.8 Intermolecular interactions and molecular packing in MCF-I. (a) C–H···O hydrogen bonded chains connected by C–H···O and C–H···Cl interactions. (b) Close pack of these zig zag chains to complete the structure. Hydrogens are deleted for clarity.

MCF-II: Centrosymmetric dimers formed by bifurcated C–H···O hydrogen bond (C9–H9···O1, 2.20 Å, 173.3° and C19–H19···O1, 2.27 Å, 133.0°) stack along the *a*-axis which are connected to nearest dimers by C–H···Cl interactions (C10–H10···Cl1, 2.64 Å, 141.3° and C15–H15···Cl2, 2.74 Å, 153.4°) in the crystal lattice (Figure 3.9).

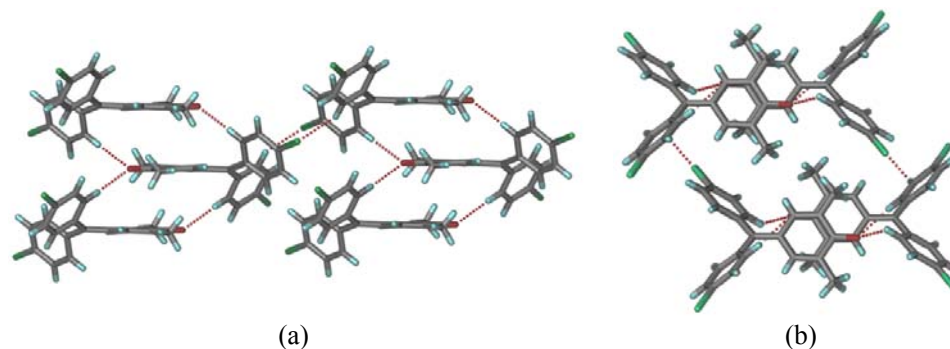


Figure 3.9 C–H···O hydrogen bonded dimers are connected by C–H···Cl interactions in MCF-II.

MCF-III: Centrosymmetric dimers formed by C–H $\cdots\pi$ interactions (C11–H11 $\cdots\pi$, 2.63 Å, 154.5°) stack along the *c*-axis. They are connected to the neighboring dimers through bifurcated C–H \cdots O hydrogen bonds (C12–H12B \cdots O1, 2.69 Å, 150.4°) (Figure 3.10).

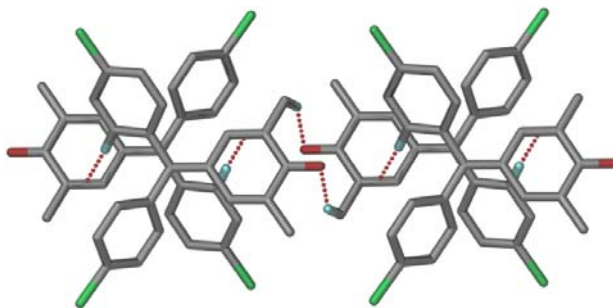


Figure 3.10 C–H $\cdots\pi$ dimers connected to neighboring dimers through weak C–H \cdots O hydrogen bonding in MCF-III.

TCF: No polymorphs were obtained for TCF even after several crystallization attempts. It has an entirely different crystal structure compared to other Fuchsones in the series. C–H \cdots O (C10–H10 \cdots O1, 2.27 Å, 133.9°) and Cl \cdots Cl type 2 interactions (Cl3 \cdots Cl4, 3.48 Å, 154.8°, 102.1°) connect the molecules in a 2D sheet which expands in 3D through C–H \cdots Cl (C13–H13 \cdots Cl4, 2.76 Å, 127.3°) and C=O $\cdots\pi$ interactions (3.15 Å, not shown in figure) (Figure 3.11).

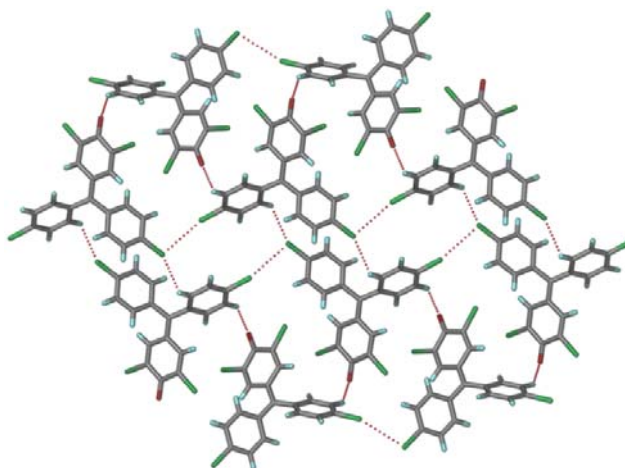


Figure 3.11 2D sheets formed by C–H \cdots O, C–H \cdots Cl and Cl \cdots Cl type II interactions in TCF.

C–H···O hydrogen bond metrics for all the crystal structures are listed in Table 3.3.

Table 3.3 Neutron normalized C–H···O hydrogen bond parameters.

Interaction	H···A/ Å	D···A/ Å	∠D–H···A/°	Symmetry code
TMF-I				
C(9)–H(9)···O(1)	2.29	3.256(2)	147.0	1-x,1-y,2-z
C(16)–H(16)···O(1)	2.39	3.280(2)	138.3	x,3/2-y,-1/2+z
TMF-II				
C(9)–H(9)···O(1)	2.23	3.304(1)	170.1	-x,2-y,1-z
C(15)–H(15)···O(1)	2.26	3.137(2)	136.3	1-x,2-y,1-z
TMF-III				
C(10)–H(10)···O(1)	2.25	3.283(4)	158.1	1-x,1/2+y,1/2-z
C(23)–H(23C)···O(1)	2.46	3.371(3)	141.0	1+x,y,z
C(22)–H(22B)···O1	2.55	3.545(3)	151.5	1-x, 1/2+y, 1/2+z
CMF-I				
C(9)–H(9)···O(1)	2.28	3.229(2)	145.2	1-x,-y,1-z
C(16)–H(16)···O(1)	2.40	3.308(2)	140.8	x,-1/2-y,1/2+z
CMF-II				
C(9)–H(9)···O(1)	2.19	3.264(2)	169.8	1-x,1-y,1-z
C(16)–H(16)···O(1)	2.50	3.284(2)	128.2	1-x,-1/2+y,3/2-z
CMF-d				
C(9)–H(9)···O(1)	2.37	3.206(4)	133.0	2-x,1-y,1-z
C(15)–H(15)···O(1)	2.39	3.393(3)	152.6	1-x,1-y,1-z
CMF-t				
C(9)–H(9)···O(1)	2.47	3.149(2)	127.9	1-x,-y,-z
C(15)–H(15)···O(1)	2.49	3.349(2)	150.9	-x,-y,-z
MCF-I				
C(9)–H(9)···O(1)	2.24	3.182(2)	143.9	1-x,2-y,1-z
C(18)–H(18)···O(1)	2.35	3.255(2)	139.9	x,3/2-y,-1/2+z
MCF-II				
C(9)–H(9)···O(1)	2.20	3.282(2)	173.3	2-x,-y,1-z
C(19)–H(19)···O(1)	2.27	3.106(2)	133.0	1-x,-y,1-z
TCF				
C(10)–H(10)···O(1)	2.277	3.128(4)	134.0	1/2+x,1/2-y,-1/2+z
TMF+CMF^a				
C(10)–H(10)···O(1)	2.407	3.299(2)	138.7	x,5/2-y,1/2+z
C(15)–H(15)···O(1)	2.290	3.254(2)	147.2	1-x,2-y,1-z
CMF+MCF^a				
C(10)–H(10)···O(1)	2.383	3.288(2)	140.2	x,1/2-y,-1/2+z
C(15)–H(15)···O(1)	2.257	3.202(2)	144.6	1-x,1-y,1-z
TMF+MCF-1^a				
C(9)–H(9)···O(1)	2.27	3.225(2)	145.5	2-x,1-y,-z
C(16)–H(16)···O(1)	2.37	3.267(2)	139.3	x,3/2-y,1/2+z
TMF+MCF-2^a				
C(9)–H(9)···O(1)	2.22	3.293(2)	171.5	2-x,1-y,1-z

C(15)–H(15)⋯O(1)	2.27	3.133(2)	135.3	1-x,1-y,1-z
TMF+MCF-4^a				
C(9)–H(9)⋯O(1)	2.26	3.205(2)	144.7	2-x,-y,-z
C(16)–H(16)⋯O(1)	2.35	3.256(2)	139.8	x,-1/2-y,1/2+z

^a = Solid solution

3.2.3 Chloro-methyl exchange and isostructurality

Crystal structure analysis of TMF-I, CMF-I and MCF-I shows that C–H⋯CH₃ contacts in TMF (C18–H18⋯C20, 2.83 Å, 169.8°, C3–H3⋯C21, 3.04 Å, 125.4° and C13–H13⋯C23, 2.76 Å, 141.6°) are exchanged by C–H⋯Cl interactions in CMF (C18–H18⋯Cl1, 2.79 Å, 169.0° and C3–H3⋯Cl2, 2.82 Å, 122.3°) and also in MCF (C13–H13⋯Cl2, 2.66 Å, 140.1°) to give isomorphous crystal structures. Again C–H⋯CH₃ contact in CMF (C13–H13⋯C21, 2.75 Å, 146.6°) is exchanged by C–H⋯Cl interaction in MCF (C13–H13⋯Cl2) and conversely, C–H⋯CH₃ contact in MCF (C16–H16⋯C20, 2.80 Å, 171.7°) is replaced by C–H⋯Cl interaction in CMF (C18–H18⋯Cl1). TMF-II and MCF-II are another isomorphous crystal pair in the Fuchsones and crystal structure revealed that C–H⋯CH₃ interactions in TMF (C19–H19⋯C22, 2.84 Å, 151.4°, C10–H10⋯C23, 2.74 Å, 141.4°) are exchanged by C–H⋯Cl interactions in MCF (C15–H15⋯Cl2, 2.74 Å, 153.4°, C10–H10⋯Cl1, 2.64 Å, 141.3°). TCF, wherein all the methyl groups are replaced by chlorine, has one crystal structure and its unit cell parameters and crystal structure are entirely different from all other structures in this series. Distances less than 3.5 Å for Cl⋯Cl interactions (less than the summation of van der Waals radii) may be considered as close contacts. Table 3.4 lists the Cl⋯Cl interactions which shows that TCF possess shortest Cl⋯Cl interaction (3.48 Å) whereas in the other crystal structures the Cl⋯Cl distances are comparatively longer. Therefore, in the crystal structures of the Fuchsones except TCF, Cl⋯Cl interactions are probably a result of close packing and have minimal structure directing role. The similarity of crystal structures of form I of TMF, CMF and MCF (TMF-I, CMF-I, MCF-I) and form II of TMF and MCF (TMF-II, MCF-II) is because the Cl atoms have less structure directing role as the crystal structure is mainly governed by C–H⋯O interactions. A different crystal structure of TCF is due to the presence of four Cl atoms which influence the crystal packing more than that in other compounds of this series. Therefore, chloro-methyl exchange is observed for the first three compounds

where Cl...Cl interactions are longer and in the last member in the series chloro-methyl exchange is not observed as close Cl...Cl interactions modifies the crystal packing.

Table 3.4 Cl...Cl interactions present in the crystal structures.

Compound	Interaction	D (Cl...Cl)	C-Cl...I-Cl	
			θ_1	θ_2
CMF-I	Cl1...Cl2	3.936	131.2	81.4
CMF-II	Cl1...Cl1	3.677	136.7	
	Cl1...Cl2	3.546	155.9	98.1
MCF-I	Cl2...Cl2	3.571	86.7	
MCF-II	Cl2...Cl2	3.877	107.7	
MCF-III	Cl1...Cl1	3.684	78.6	
TCF	Cl4...Cl4	3.845	107.5	
	Cl4...Cl3	3.476	154.8	102.1

3.2.4 Solid solutions of TMF, CMF and MCF

Solid solutions¹⁹ are solid state mixtures of one or more solutes in a crystalline environment. A necessary and sufficient condition for formation of solid solution is that the structure of the components must be isomorphous. Sometimes two structurally similar compounds possessing different crystal structures form solid solution due to conformational mimicry,^{9f,g,20} where the minor component is forced to adopt the conformation of the major component in the solid solution. Noting the isomorphous nature of TMF, CMF and MCF, solid solutions were attempted. TMF and MCF were crystallized in three different molar ratios to obtain isomorphous continuous series of solid solutions. The ratios of the starting materials in the solid solutions were inferred from the partial s. o. f. of the Cl and methyl groups in the crystal structure. When TMF and MCF were crystallized in 1: 1 molar ratio, a solid solution with TMF and MCF percentage ratio 55:45 was crystallized (TMF+MCF-1) in monoclinic space group $P2_1/c$ which is isomorphous with TMF-I, CMF-I and MCF-I. When 3:1 molar ratio of TMF and MCF was crystallized, solid solution with percentage ratio 75:25 of starting compounds was crystallized (TMF+MCF-2) in triclinic space group $P\bar{1}$ and is isomorphous with TMF-II and MCF-II. When TMF and MCF were crystallized in 1:3 molar ratio, two similar ratio solid solutions were concomitantly crystallized in different

space groups, one in monoclinic space group $C2/c$ (TMF+MCF-3) in percentage ratio 29:71 isomorphous with TMF-III and another in monoclinic space group $P2_1/c$ (TMF+MCF-4) isomorphous with TMF-I, CMF-I and MCF-I in the percentage ratio 30:70.

Crystallization of TMF and CMF in 1:1 molar ratio resulted a solid solution in monoclinic space group $P2_1/c$ isomorphous with TMF-I, CMF-I and MCF-I, where percentage ratio of TMF and CMF is 55:45. Similarly, crystallization of CMF and MCF in 1:1 molar ratio resulted solid solution in monoclinic space group $P2_1/c$ isomorphous with TMF-I, CMF-I and MCF-I with percentage ratio 44:56 of CMF and MCF. Attempts to crystallize solid solution of TCF with TMF, CMF and MCF did not result any crystalline product. All crystallizations were carried out in EtOAc solvent. Ratio of components in solid solutions is based on the partial site occupancy factors of Cl and CH_3 listed in Table 3.5.

Table 3.5 Percentage ratios of the components in solid solutions (SS) obtained and the molar ratios of starting materials (SM) used for crystallization.

Solid solution	Space group	S. o. f. Me/Cl	SM molar ratio	% ratio in SS
TMF+MCF-1	$P2_1/c$	0.554(2)/0.446(2)	1:1	55:45
TMF+MCF-2	$P\bar{1}$	0.752(2)/0.248(2)	3:1	75:25
TMF+MCF-3	$C2/c$	0.287(6)/0.713(6)	1:3	29:71
TMF+MCF-4	$P2_1/c$	0.301(3)/0.699(3)	1:3	30:70
TMF+CMF	$P2_1/c$	0.549(2)/ 0.451(2)	1:1	55:45
CMF+MCF	$P2_1/c$	0.5612(18)/ 0.4388(18) and 0.4388(18)/0.5612(18)	1:1	44:56

Formation of the solid solutions in various ratios and space groups indicates that infinite numbers of solid solutions are possible with varying ratios and in different space groups. TMF+MCF-3 crystallized in $C2/c$ space group in percentage ratio 29:71. TMF does not have a crystal structure in this space group $C2/c$ but forced to adopt the solid state arrangement of the major component MCF. Calculation of unit cell similarity index (Π)⁴ show the closeness of the unit cell parameters of the solid solutions and the polymorphs (Table 3.6). Π value close to zero indicates a good similarity in the cell parameters. Π can be expressed by the following equation

$$\Pi = \left| \frac{a+b+c}{a'+b'+c'} \right| - 1$$

where a, b, c and a', b', c' are the orthogonalized lattice parameters of related crystals.

Table 3.6 Unit cell similarity index (Π) of the isomorphous crystal structures.

Crystal Pair	Π
TMF-I and CMF-I	0.0015
TMF-I and MCF-I	0.0013
CMF-I and MCF-I	0.0002
TMF-II and MCF-II	0.0017
TMF+MCF-1 and TMF-I	0.0002
TMF+MCF-1 and CMF-I	0.0013
TMF+MCF-1 and MCF-I	0.0010
TMF+MCF-2 and TMF-II	0.0006
TMF+MCF-2 and MCF-II	0.0011
TMF+MCF-3 and MCF-III	0.0017
TMF+MCF-1 and TMF+MCF-4	0.0012
TMF+MCF-4 and TMF-I	0.0014
TMF+MCF-4 and MCF-I	0.0002
TMF+MCF-4 and CMF+MCF	0.0002
TMF+MCF-4 and TMF+CMF	0.0010

3.3 Color Polymorphism in CMF

Apart from various physico-chemical properties polymorphs can have different spectroscopic properties too. Relatively few examples are available where the polymorphism of an organic substance is associated with crystalline forms of different color.²¹ Hantzsch reported the first examples nearly 100 years ago in 1907.²² This phenomenon was originally called chromoisomerism, and later the term crystallochromy was coined by Klebe et al.²³ The well known example of color polymorphism is the “ROY” polymorphs with their characteristic red, orange and yellow colors. The color differences in “ROY” is due to the conformational differences associated with each polymorph.²⁴ All Fuchsones are colorful. Among the Fuchsones synthesized in this series, CMF polymorphs depict a special case of color polymorphism. CMF-I is orange colored whereas CMF-II is purple in color (Figure 3.12). The different colored polymorphs crystallized concomitantly from most of the solvents used for crystallization along with the solvated crystal structures. The orange colored polymorph

(CMF-I) was obtained concomitantly with CMF-t from toluene solvent but free from CMF-II, whereas, mesitylene solvent gave exclusively purple colored polymorph (CMF-II). Solid state UV-Vis spectra shows red shift of the absorption bands for CMF-II compared to CMF-I by 7 nm ($\pi \rightarrow \pi^*$) and 16 nm ($n \rightarrow \pi^*$). The absorption band due to $\pi \rightarrow \pi^*$ transition appeared at $\lambda_{\text{max}} = 274$ nm for CMF-I (orange) and 281 nm for CMF-II (purple), whereas absorption band due to $n \rightarrow \pi^*$ transition appears at $\lambda_{\text{max}} = 345$ nm for CMF-I and 361 nm for CMF-II (Figure 3.13).

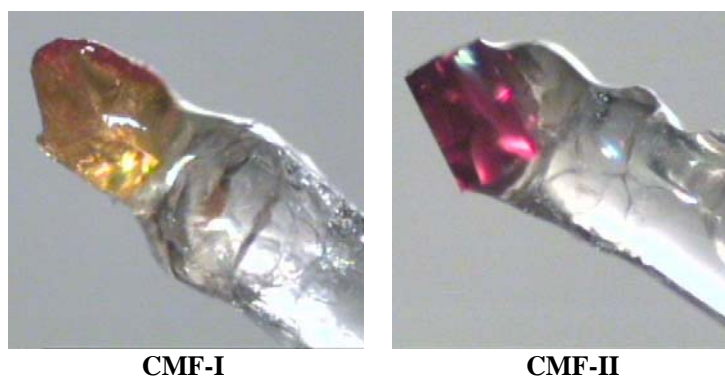


Figure 3.12 Color differences of the two polymorphs of CMF, orange and purple for CMF-I and CMF-II respectively.

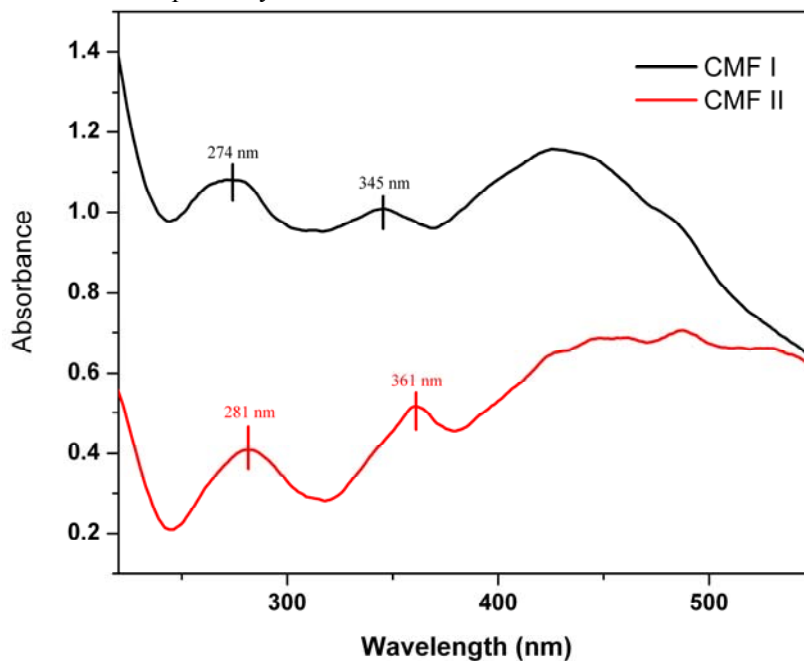


Figure 3.13 Solid state UV-Vis spectra of CMF-I and CMF-II.

As explained earlier crystal structure of CMF-I and CMF-II are very similar. The differences arises only in the extent of overlap of the quinoid rings of C–H···O hydrogen bonded dimer, the overlap is more in CMF-II compared to that in CMF-I. There is difference of torsion angle of about 9° between the two polymorphs, as shown in Figure 3.14, which may be a reason for color difference but further studies are required to determine the main cause behind it.

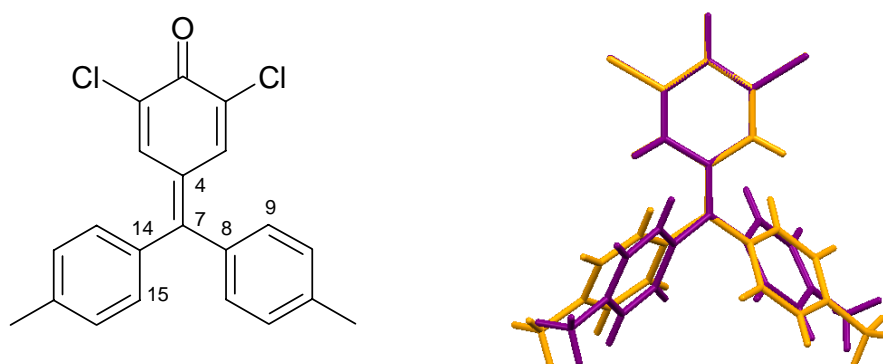
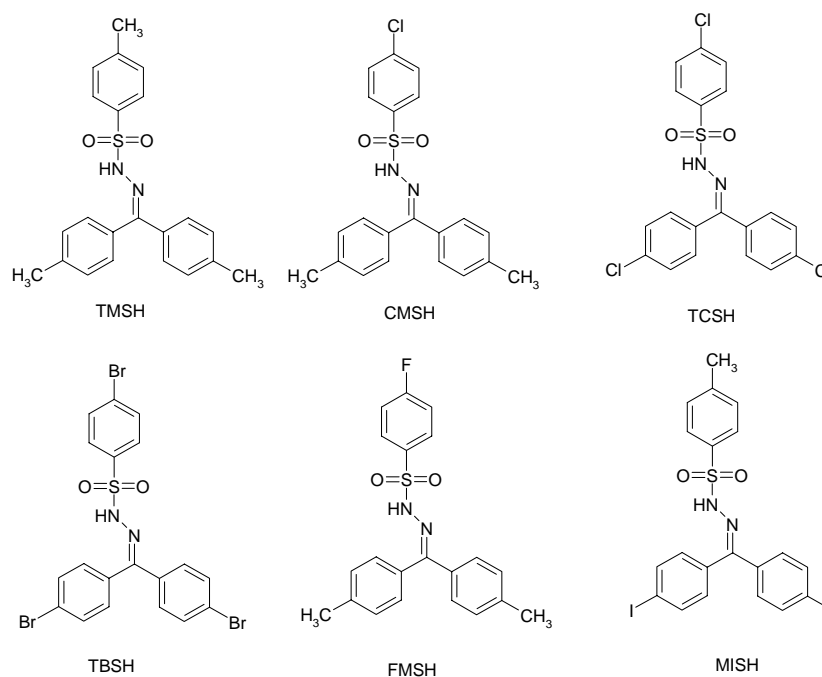


Figure 3.14 Overlay of the two conformers of CMF-I (orange) and CMF-II (purple). C4–C7–C8–C9 and C4–C7–C14–C15 torsion angles (in °) are 47.4(2), 43.2(2) for CMF-I and 38.4(2), 38.1(2) for CMF-II.

3.4 Polymorphism and Isostructurality in Sulfonylhydrazones

Five new derivatives of the trimorphic Bis(*p*-tolyl) ketone *p*-tosylhydrazone (TMSH, trimethylsulfonylhydrazone) were synthesized (detailed in Experimental section) with varying halogen substituents. As chloro-methyl or halogen-halogen exchange result isostructural crystal structures¹², therefore the three *p*-methyl groups in TMSH were replaced with halogens (F, Cl, Br and I) in varying ratios in order to achieve isostructural crystals. The molecules under study are shown in Scheme 3.4.



Scheme 3.4 Nangia et al. reported trimorphs of TMSH.¹² Halogen derivatives of TMSH synthesized are CSMH (chlorodimethylsulfonylhydrazone), TCSH (trichlorosulfonylhydrazone), TBSH (tribromosulfonylhydrazone), FMSH (fluorodimethylsulfonylhydrazone) and MISH (methyldiiodosulfonylhydrazone).

The compounds were crystallized from various solvents. CSMH crystallized as dimorphs (form I, CSMH-I and form II, CSMH-II) whereas TCSH, TBSH, FMSH and MISH have only one crystal structure each. Unit cell dimensions and crystal structure analysis demonstrated that CSMH-I, TCSH and TBSH have similar unit cell parameters, space group *C2/c* and possess the same crystal structure. Unit cell parameters and space group of FMSH are identical (orthorhombic space group *Pbca*) with CSMH-II. MISH has different unit cell parameters and crystal structure is different compared to other members in the series. Details of unit cell parameters are included in the Appendix.

3.4.1 Crystal structure analysis, isostructurality and polymorphism

CSMH crystallized in two polymorphic forms. Crystallization from nitromethane resulted single crystals which on X-ray data collection solved and refined in monoclinic space group *C2/c* with one molecule in the asymmetric unit, termed CSMH-I. Single crystals of Form II (CSMH-II) obtained from ethanol crystallized in orthorhombic space

group *Pbca* with one molecule in the asymmetric unit. The structural differences between the two polymorphs are illustrated in Figure 3.15.

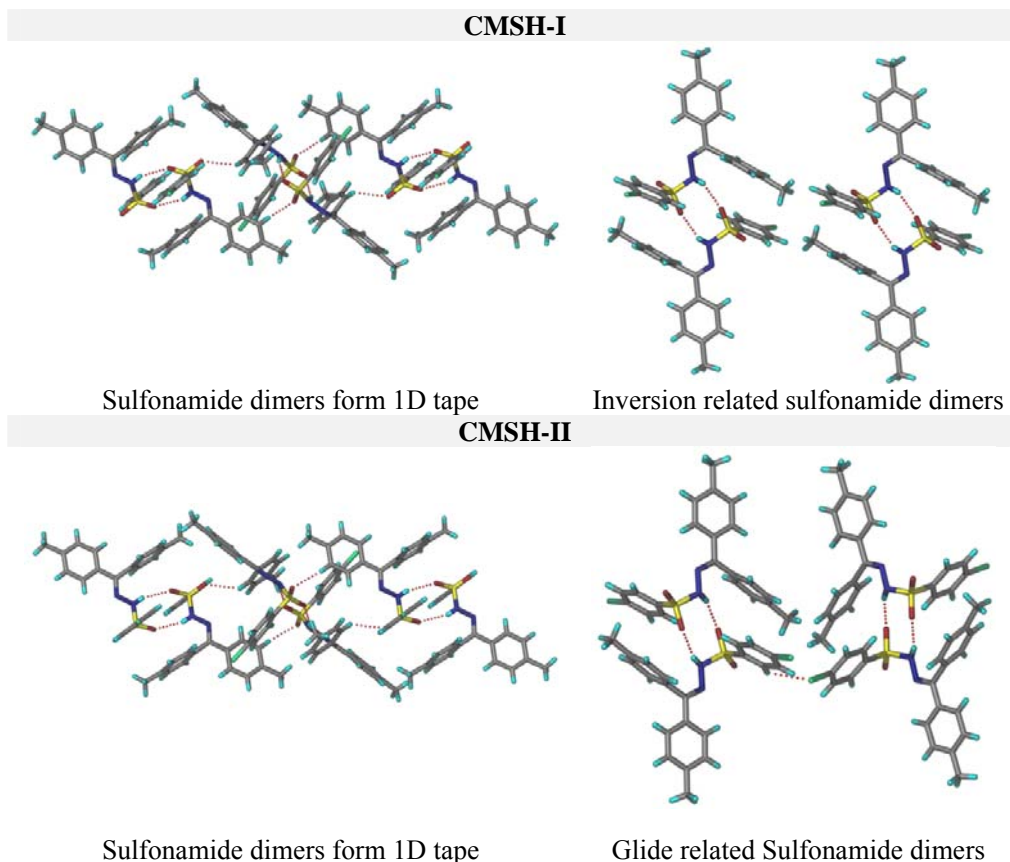


Figure 3.15 Both the polymorphs of CMSH contain the same sulfonamide N–H \cdots O dimer synthon (N1–H1A \cdots O2, CMSH-I, 2.05 Å, 153.6°, CMSH-II, 2.00 Å, 159.3°) of $R^2_2(8)$ graph set and the dimers are connected by C–H \cdots O hydrogen bonds (CMSH-I, C13–H13 \cdots O1, 2.52 Å, 125.3°; C16–H16 \cdots O1, 2.51 Å, 172.8° and CMSH-II, C12–H12 \cdots O2, 2.49 Å, 173.7°; C15–H15 \cdots O2, 2.50 Å, 135.1°) to form 1D tape. These tapes extend in 2D via C–H \cdots O hydrogen bond to give similar 2D structural unit for both the forms. The crystal structures are different in their 3D packing arrangement. C–H \cdots Cl interactions (C5–H5 \cdots Cl1, 2.80 Å, 127.7°) between two sulfonamide dimers complete the 3D packing in CMSH-II, whereas, in CMSH-I they are close packed. In CMSH-I two close packed dimers are inversion related whereas in CMSH-II the two connected dimers are glide related.

The six crystal structures are 2D isostructural due to the same 2D structural unit, in which tapes of sulfonamide dimers expand via C–H \cdots O hydrogen bonds (Figure 3.16).

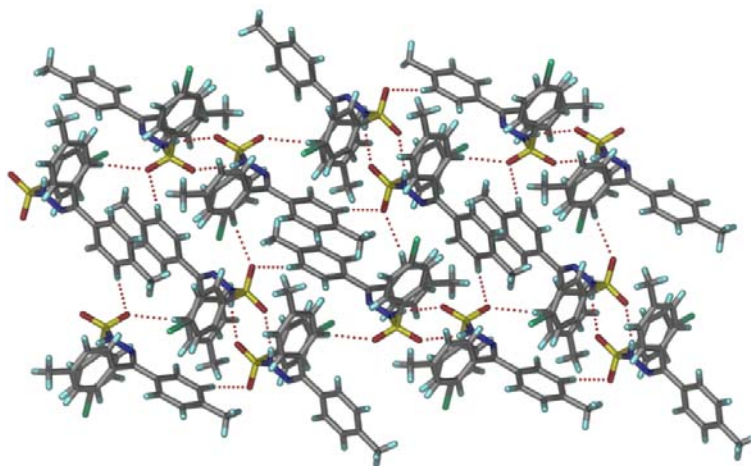
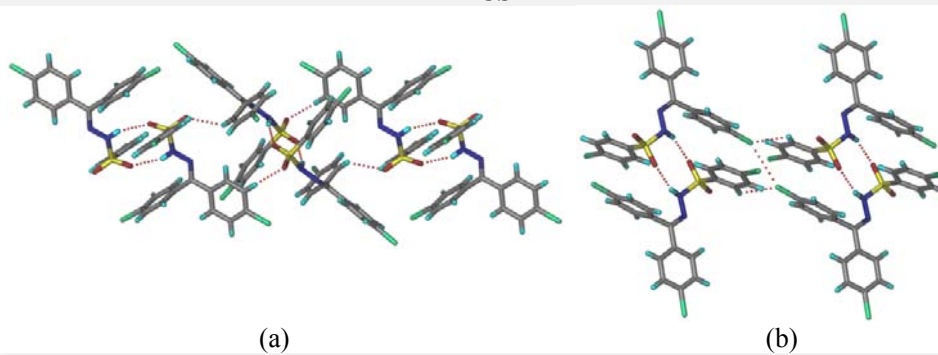


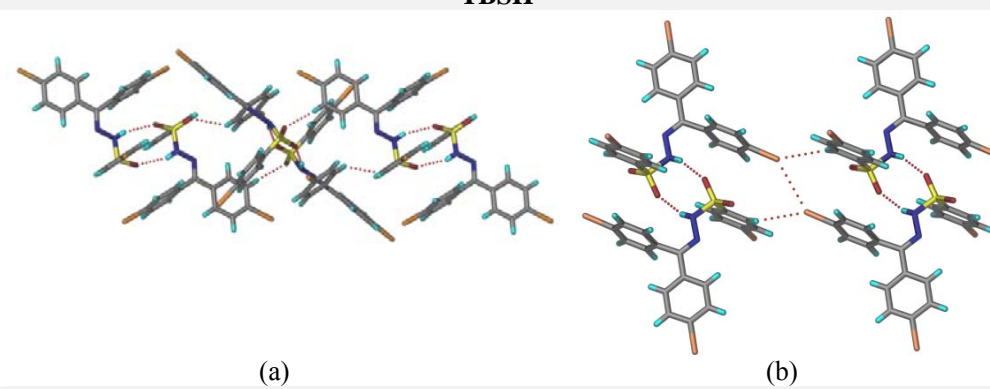
Figure 3.16 2D structural unit of CMSH-I formed by sulfonamide dimer tapes connected by C–H \cdots O hydrogen bonds. This 2D structural unit is present in all the crystal structures.

In the crystal structures of TCSH, sulfonamide dimers are connected by C–H \cdots Cl and type I Cl \cdots Cl interactions to complete the 3D pack. C–H \cdots Me (C3–H3 \cdots C20, 3.02 Å, 132.9°) and Me \cdots Me (C20 \cdots C20, 3.84 Å, 146.3°) contacts in CMSH-I are exchanged by C–H \cdots Cl (C3–H3 \cdots Cl2, 2.83 Å, 124.9°) and type I Cl \cdots Cl interactions (3.47 Å, 143.1°). The crystal structure of TBSH is similar to TCSH. In this crystal structure, C–H \cdots Cl and type I Cl \cdots Cl interactions of TCSH are exchanged by C–H \cdots Br (C5–H5 \cdots Br3, 2.95 Å, 122.4°) and type I Br \cdots Br interactions (3.59 Å, 142.3°). Therefore, CMSH-I, TCSH and TBSH are isomorphous with identical cell parameters, space group and crystal structures. Isostructurality in these cases is due to the Cl–Me, Br–Me and Cl–Br functional group exchange. In the crystal structure of FMSH two sulfonamide dimers related by glide plane are connected by C–H \cdots F contacts as in CMSH form II where two glide related sulfonamide dimers are connected by C–H \cdots Cl interaction. Therefore isostructurality in this case is due to Cl–F exchange. The 3D packing of MISH is different compared to other crystal structures due to relative offset of subsequent layers of molecules as shown in Figure 3.17. Hydrogen bond metrics are listed in Table 3.7.

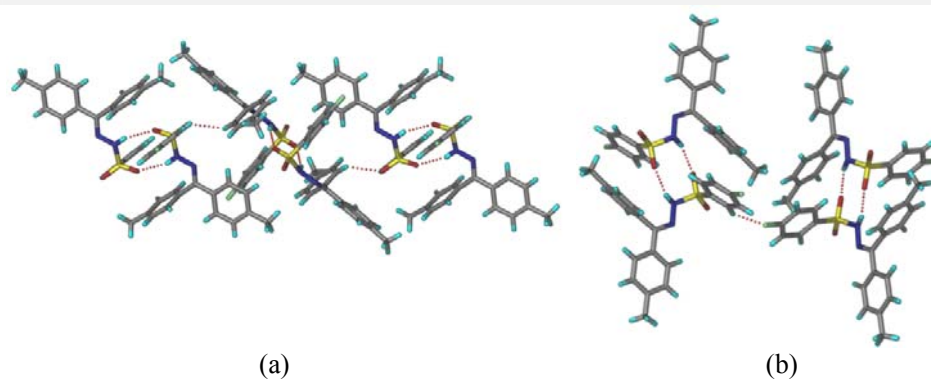
TCSH



TBSH



FMSH



MISH

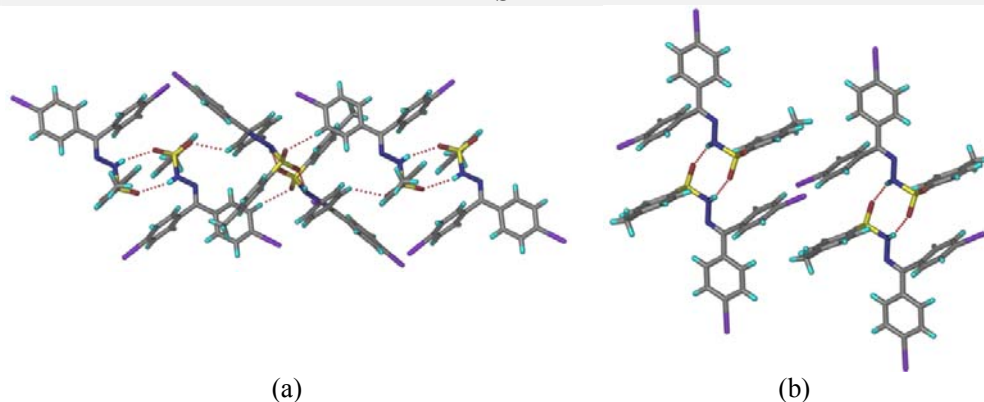


Figure 3.17 Crystal structures comparison of TCSH, TBSH, FMSH and MISH. TCSH and TBSH are isomorphous with CMSH-I in $C2/c$ space group, whereas, FMSH and CMSH-II are isomorphous crystal pairs in $Pbca$ space group. All these crystal structures are 2D isostructural and crystal structure of MISH has different 3D packing.

Table 3.7 Hydrogen bond metrics for Sulfonylhydrazones.

Interaction	H...A/ Å	D...A/ Å	$\angle D-H\cdots A/^\circ$	Symmetry code
CMSH-I				
N(1)–H(1A)···O(2)	2.05	2.985(2)	153.6	$1/2-x, 1/2-y, -z$
C(13)–H(13)···O(1)	2.52	3.272(2)	125.3	$1/2-x, 1/2+y, 1/2-z$
C(16)–H(16)···O(1)	2.51	3.589(3)	172.8	$x, -y, 1/2+z$
C(3)–H(3)···O(1)	2.48	2.888(3)	101.1	Intramolecular
CMSH-II				
N(1)–H(1A)···O(1)	2.00	2.965(3)	159.3	$1-x, -y, 1-z$
C(3)–H(3)···O(1)	2.44	3.451(3)	154.5	$1-x, -y, 1-z$
C(12)–H(12)···O(2)	2.49	3.577(3)	173.7	$1/2-x, -1/2+y, z$
C(15)–H(15)···O(2)	2.50	3.364(3)	135.1	$1/2+x, 1/2-y, 1-z$
C(5)–H(5)···O(2)	2.46	2.880(3)	101.8	Intramolecular
TCSH				
N(1)–H(1A)···O(2)	2.03	2.984(3)	157.7	$1/2-x, 1/2-y, -z$
C(13)–H(13)···O(1)	2.47	3.266(4)	129.5	$1/2-x, 1/2+y, 1/2-z$
C(16)–H(16)···O(1)	2.51	3.590(3)	174.0	$x, -y, 1/2+z$
C(5)–H(5)···O(2)	2.63	3.617(3)	151.1	$1/2-x, 1/2-y, -z$
C(3)–H(3)···O(1)	2.49	2.896(4)	101.0	Intramolecular
TBSH				
N(1)–H(1A)···O(1)	2.03	2.986(4)	158.0	$1/2-x, 1/2-y, 1-z$
C(5)–H(5)···O(2)	2.48	2.893(5)	101.1	Intramolecular
C(13)–H(13)···O(1)	2.47	3.266(4)	129.3	$1/2-x, -1/2+y, 1/2-z$
C(16)–H(16)···O(1)	2.51	3.590(4)	174.0	$x, -y, 1/2-z$
FMSH				
N(1)–H(1A)···O(1)	1.99	2.955(2)	158.5	$1-x, -y, 1-z$
C(9)–H(9)···O(2)	2.42	3.245(2)	131.5	$-1/2+x, 1/2-y, 1-z$
C(5)–H(5)···O(2)	2.47	2.888(3)	101.4	Intramolecular

C(3)–H(3)···O(1)	2.56	3.568(2)	153.1	1–x, –y, 1–z
MISH				
N(1)–H(1A)···O(2)	2.00	2.977(4)	162.6	2–x, 1–y, 1–z
C(3)–H(3)···O(1)	2.50	2.906(6)	101.0	Intramolecular
C(13)–H(13)···O(1)	2.51	3.322(4)	130.2	2–x, –1/2+y, 1/2–z
C(5)–H(5)···O(2)	2.59	3.611(4)	155.7	2–x, 1–y, 1–z

3.5 Comparison of Crystal Structures Using XPac Analysis

The XPac is a computer program, written by Dr. T. Gelbrich and Prof. Michael Hursthouse at the University of Southampton, UK to compare similarities and differences in crystal structures.²⁵ The XPac method allows the identification of similar packing arrangements in two given crystal structures and produces parameters which characterize their degree of similarity. In the XPac approach, each crystal structure is represented by a cluster of molecules, with a central core molecule and a shell of contacting molecules. The two clusters are then compared by computing the mean differences between the comprehensive (i.e. all possible combinations) sets of angles (δ_a) and interplanar angles (δ_p) respectively, between a chosen group of atoms in the core molecule and the corresponding atoms in one shell molecule (a double subunit) or two shell molecules (a triple subunit). The obtained δ parameters can be considered as reverse indicators of structural similarity. The focal point of the XPac procedure is that, subcomponents of two different crystal structures, i. e. ‘*supramolecular construct*’ are similar if they consist of molecules of the same type assembled in the same way. Any recurring periodic or discrete arrangement of molecules with its spatial characteristics may be called a supramolecular construct (SC). The concept of supramolecular construct differs from supramolecular synthon^{2g}; supramolecular construct implies only geometrical closeness, whereas supramolecular synthon implies an associated bonding involvement.

Each crystal structure can be explained as a cluster of molecules which consists of a central molecule (kernel) and all molecules surrounding it completing the coordination sphere. If two crystal structures contain a common fragment (i.e. a SC), then their clusters must also contain a common fragment which corresponds to this SC. Hence, the common SCs (if present) of two crystal structures can be identified by

comparing their representative clusters. A “corresponding ordered set of points” (COSP), i.e. a selection of atoms in the molecule is chosen to best represent its shape. The supramolecular construct of two structures can be discrete (0D, identical isolated units such as a hydrogen bonded dimer), extended 1D (identical chains), 2D (identical sheets) or 3D (similar arrangement of entire molecules).

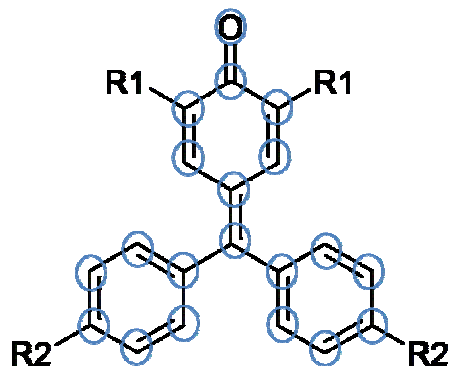
In the XPac plots of δ_p against δ_a , for a cluster of 15 molecules with one kernel (central molecule) and $n=14$ shell molecules (neighbour molecules), there are $n[1+(n-1)/2]=105$ data points and the position of each point characterizes the degree of similarity in a particular subunit of the cluster. Closer the (δ_a, δ_p) points to the origin of the coordinate system the better structural match of the two compounds. Thus, the quantitative dissimilarity index (X) computed as,

$$X = \sum_{i=1}^M \left(\delta_{a,i}^2 + \delta_{p,i}^2 \right)^{1/2}$$

Where X is the mean distance (in °) of all M data points from the origin and $\delta_{a,i}$ and $\delta_{p,i}$ are the coordinates of the i -th data point.

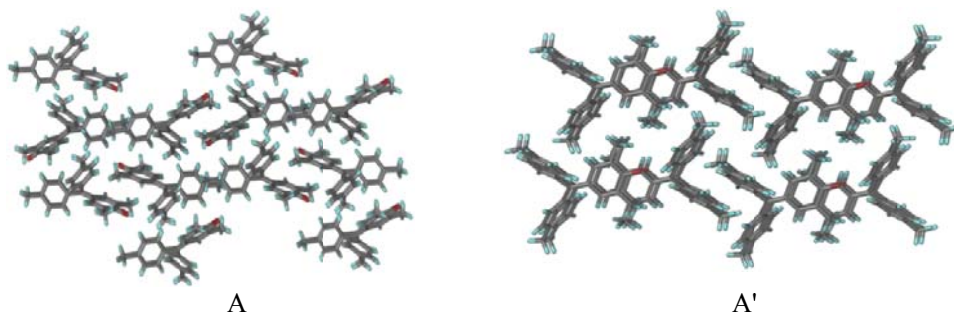
3.5.1 XPac analysis of Fuchsones

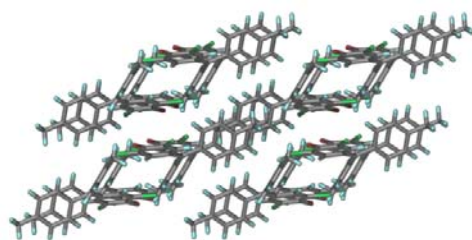
The principal molecular shape of the base molecule (Fuchson core) is maintained throughout the whole series of crystal structures. The shape of each independent molecule in each crystal structure was parameterized with an ordered set of points (OSP) consisting of twenty atomic positions, indicated with blue circles in Scheme 3.5. TMF-III, MCF-III and TCF were not considered as their crystal structures are entirely different and possess only 0D or 1D SCs. Crystal structures of the solid solutions are also not considered here to avoid large number of isomorphous crystal structures.



Scheme 3.5 Common set of points of Fuchsonone (indicated by blue circles) used for XPac analysis

From XPac analysis, 0D, 1D, 2D and 3D SCs were identified in the crystal structures of the Fuchsonone series. The isomorphous crystal structures are (i) TMF-I/CMF-I, (ii) CMF-I/MCF-I, (iii) TMF-I/MCF-I, (iv) TMF-II/MCF-II and (v) CMF-d/CMF-t. For these isomorphous crystal structures three different 3D SCs were identified (A, A' and A'') as described below (Figure 3.18). For crystal pairs (i) TMF-I/TMF-II, (ii) TMF-I/CMF-II, (iii) TMF-I/MCF-II, (iv) TMF-II/CMF-I, (v) TMF-II/CMF-II, (vi) TMF-II/MCF-II, (vii) CMF-I/CMF-II, (viii) CMF-I/MCF-II, (ix) CMF-II/MCF-I, (x) CMF-II/MCF-II and (xi) MCF-I/MCF-II 2D only one 2D SC (B) was observed (Figure 3.19). Crystal pairs (i) TMF-I/CMF-d, (ii) TMF-I/CMF-t, (iii) TMF-II/CMF-d, (iv) TMF-II/CMF-t, (v) CMF-I/CMF-d, (vi) CMF-I/CMF-t, (vii) CMF-d/MCF-I, (viii) CMF-d/MCF-II, (ix) CMF-t/MCF-I and (x) CMF-t/MCF-II, consist of two different 1D SCs C and C' (Figure 3.20). 0D SCs are found in the crystal pairs (i) CMF-d/CMF-II and (ii) CMF-t/CMF-II (Figure 3.21).





A''

Figure 3.18 3D SCs found in the crystal structures indicate the three dimensional similarity of the respective crystal structures. Crystal pairs TMF-I/CMF-I, CMF-I/MCF-I and TMF-I/MCF-I contain the SC A. SC A' was identified in the crystal pair TMF-II/MCF-II whereas SC A'' was found in the crystal pair CMF-d/CMF-t.

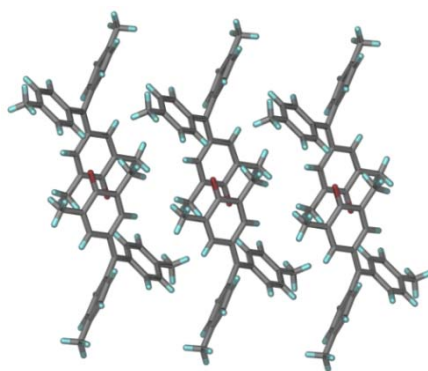
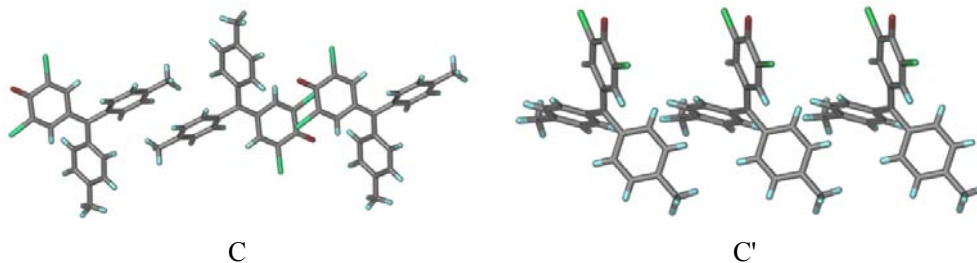


Figure 3.19 2D supramolecular construct (B) observed in the large number of crystal pairs of Fuchsones. The antiparallel molecules here are related by inversion symmetry.



C

C'

Figure 3.20 Crystal pairs CMF-d/CMF-I, CMF-d/TMF-I, CMF-t/CMF-I, CMF-t/MCF-I, CMF-t/TMF-I, CMF-d/MCF-I contain the 1D SC C whereas the crystal pairs CMF-d/MCF-2, CMF-d/TMF-II, CMF-t/MCF-II and CMF-t/TMF-II contain 1D SC C'.

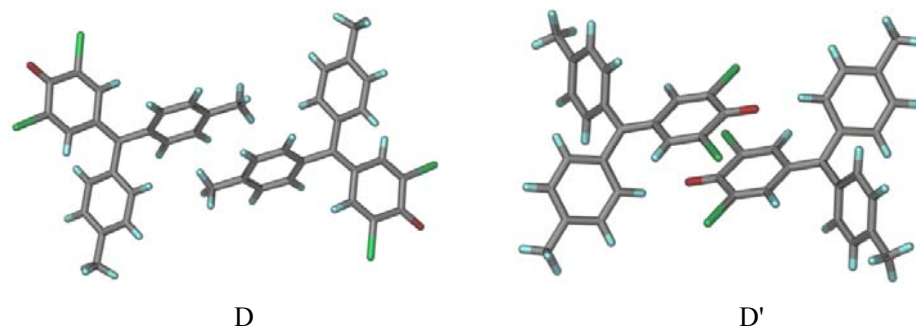
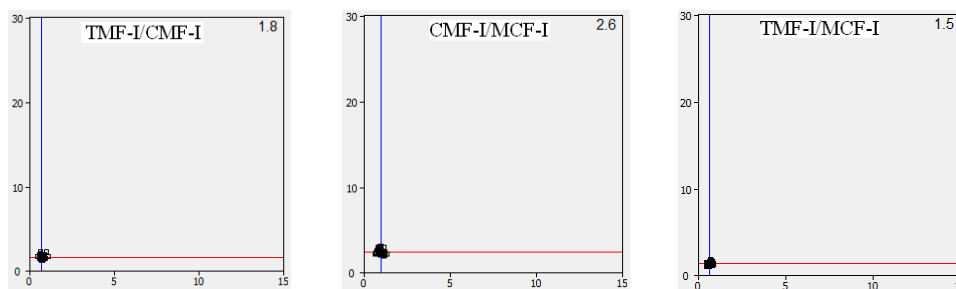


Figure 3.21 0D SC D and D' were observed for crystal pairs CMF-d/CMF-II and CMF-t/CMF-II respectively and in both the case molecules are inversion related.

Values of dissimilarity index X are listed below for 0D, 1D, 2D, 3D SCs present in the respective crystal structures. Color codes are dark red=3D, dark green=2D, blue=1D and orange=0D. A lower value of X indicates better match.

TMF-I							
TMF-II	6.8	TMF-II					
CMF-I	1.8	6.6	CMF-I				
CMF-II	13.0	11.4	12.4	CMF-II			
CMF-d	7.4	9.4	17.2	10.5	CMF-d		
CMF-t	8.0	7.6	6.1	10.4	2.7	CMF-t	
MCF-I	1.5	8.7	2.6	15.7	7.3	8.6	MCF-I
MCF-II	8.2	0.8	8.0	12.8	3.3	7.7	8.8

XPac plots of δ_p against δ_a shows the closeness of the XPac points. Few selected XPac plots are shown in Figure 3.22



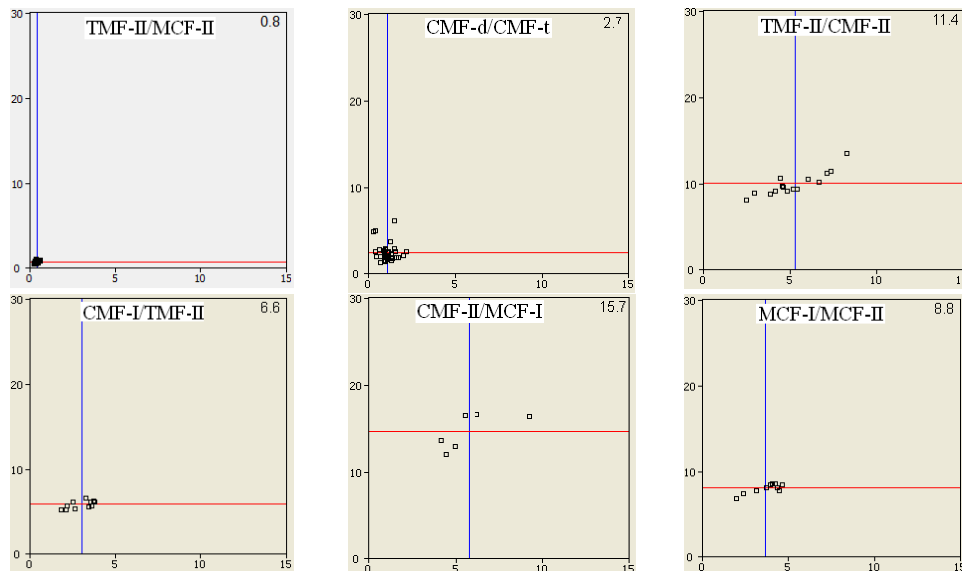
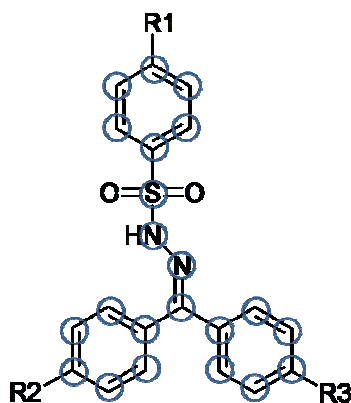


Figure 3.22 Selected XPaC plots of δ_p against δ_a (in $^\circ$), illustrating the degree of similarity exhibited by the different crystal structures Fuchsones. Upper right corner of each plot indicates the value of X .

3.5.2 XPaC analysis of Sulfonylhydrazones

For Sulfonylhydrazones the number of ordered set of points consists of 22 atomic positions as shown in Scheme 3.6 indicated by blue circles and it is retained for whole series of molecules.



Scheme 3.6 Common set of points of Sulfonylhydrazones (indicated by blue circles) used for XPaC analysis.

3D SCs were identified for the crystal pairs CMSH-I/TCSH, CMSH-I/TBSH, TCSH/TBSH, and CMSH-II/FMSH, whereas 2D SCs were identified for all other possible crystal pairs. Dissimilarity index X values are listed below for 2D and 3D SCs present in the respective crystal structures. Color codes are dark red=3D and dark green=2D. A lower value of X indicates better match.

	CMSH-I				
CMSH-II	4.5	CMSH-II			
TCSH	2.7	2.4	TCSH		
TBSH	3.5	2.0	1.1	TBSH	
MISH	5.0	2.9	2.6	2.0	MISH
FMSH	0.8	3.7	2.1	2.8	4.4

XPac plots of δ_p against δ_a shows the closeness of the XPac points and are shown in Figure 3.23.

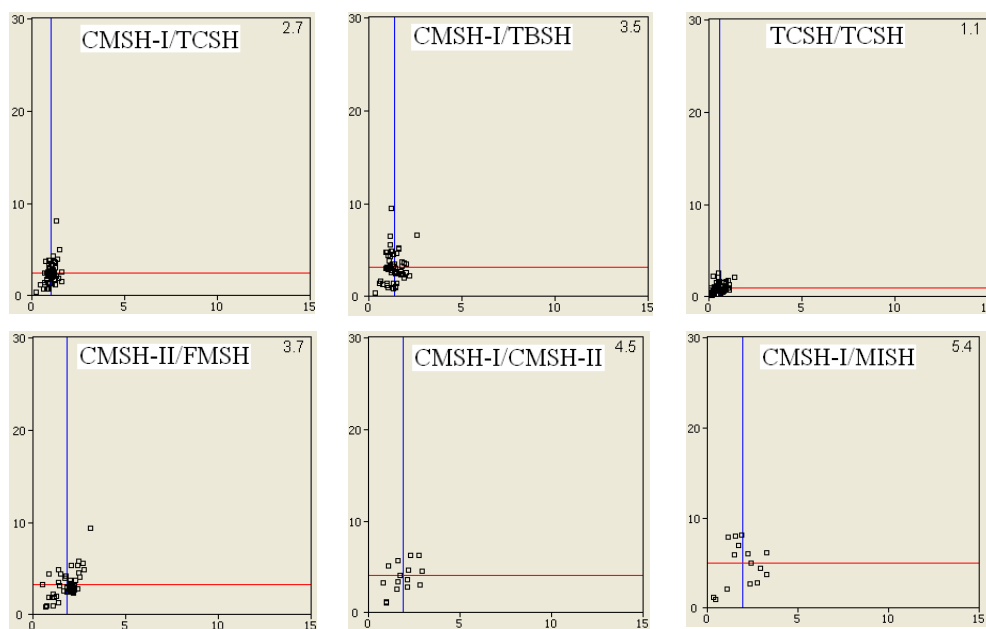


Figure 3.23 Selected XPac plots of δ_p against δ_a (in $^\circ$), illustrating the degree of similarity exhibited by the different crystal structures Sulfonylhydrazones. Upper right corner of each plot indicates the value of X .

3.6 Discussion

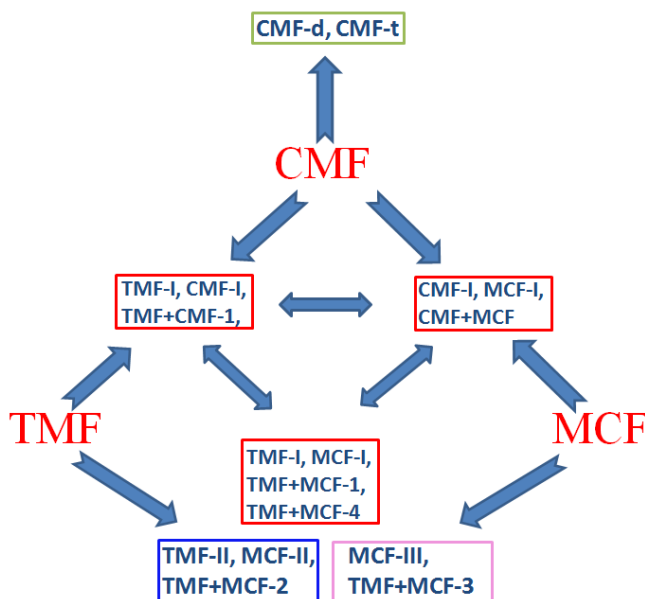
Isostructurality is observed in the two series of conformationally flexible molecules, Fuchsones, in which crystal structure is mainly governed by weak C–H···O interactions and in Sulfonylhydrazones, where crystal structures is mainly governed by strong N–H···O hydrogen bond and weak C–H···O interactions. Isostructurality is due to functional group exchangeability of halogen and methyl groups in both series of compounds. In CMF and MCF Cl-Me exchange is observed and structural role of Cl in these two compounds is mainly space filling like the methyl groups. But in the crystal packing of TCF, Cl group behaved differently playing crucial structural directing role resulting in an entirely different crystal structure. Cocrystallization of TMF, CMF and MCF resulted in continuous series of solid solutions and mostly they tend to crystallize like form I of the parent molecules. TMF+CMF, CMF+MCF, TMF+MCF-1, TMF+MCF-4 are isomorphous with TMF-I, CMF-I and MCF-I. Therefore the series of isostructural crystals obtained in Fuchsones are

Series 1: TMF-I↔CMF-I↔MCF-I↔TMF+CMF↔CMF+MCF↔TMF+MCF-1↔TMF+MCF-4

Series 2: TMF-II↔MCF-II↔TMF+MCF-2

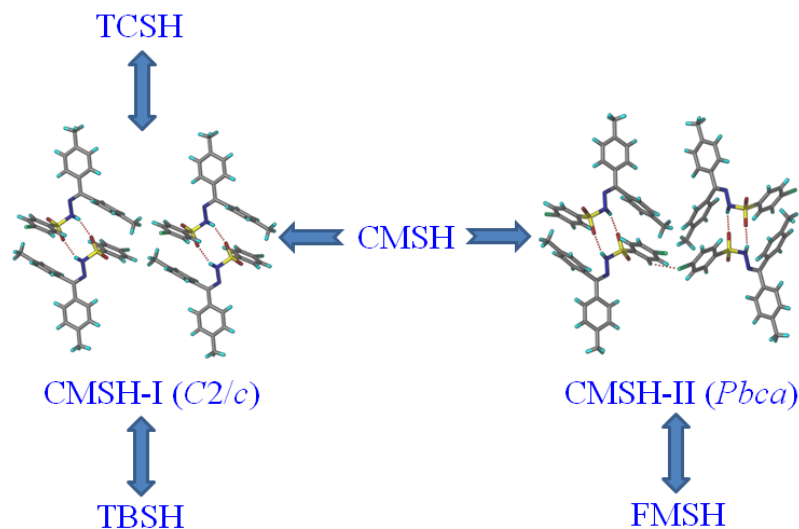
Isomorphous pairs are CMF-d↔CMF-t and MCF-III↔TMF+MCF-3.

These isomorphous crystal structures are interrelated as shown in Scheme 3.7.



Scheme 3.7 Interrelation of isostructurality and polymorphism among the crystal structures of Fuchsones. Isomorphous crystals resulting from two different starting materials (indicated by single headed arrows) are included in the different colored boxes. Crystal structures inside red boxes are isomorphous to each other (indicated by double headed arrows).

In Sulfonylhydrazones, conformational flexibility did not result in different packing arrangement instead the robust sulfonamide dimer synthon of graph set $R_2^2(8)$ governs the crystal packing resulting in 2D isostructurality for all six crystal structures. Cl-methyl, Br-methyl, Cl-Br and Cl-F functional groups proved to be structurally equivalent resulting in isomorphous crystals. Although examples are available for Cl-I or Br-I exchange, 3D packing of MISH is different compared to other members in the series indicating the effect of iodo group in the crystal packing. Polymorphism is found only in case of CMSH where form I is isomorphous with TCSH and TBSH and form II is isomorphous with FMSH. Therefore polymorphs of CMSH show a structural link in Sulfonylhydrazones. Scheme 3.8 depicts the isostructural relationship among Sulfonylhydrazones.



Scheme 3.8 Dimorphs of CMSH show a structural link among the crystal structures of Sulfonylhydrazones. Double head arrows are used here to indicate isomorphous nature.

Interestingly, despite being conformationally flexible the polymorphism in Sulfonylhydrazones is not conformational. They have similar torsion angles of the flexible parts in all the crystal structures. In Fuchsones, flexible torsions of the isostructural crystals scatter within a range of 1-5°. TMF-III and MCF-III have unique crystal structures and has quite different torsion angles compared to other crystal structures. Although TCF possess similar torsions as the isomorphous crystal structures, it has entirely different crystal packing because of the structural role of Cl group. Torsion angles of the flexible parts in case of the solid solutions are in between that of the individual components. Figure 3.24 shows overlay of the conformers observed in the crystal structures of Fuchsones and Sulfonylhydrazones. The corresponding torsion angles are included in Appendix. There is a variation of about 20° in torsion angles in the crystal structure of Fuchsones and for Sulfonylhydrazones conformers are almost identical.

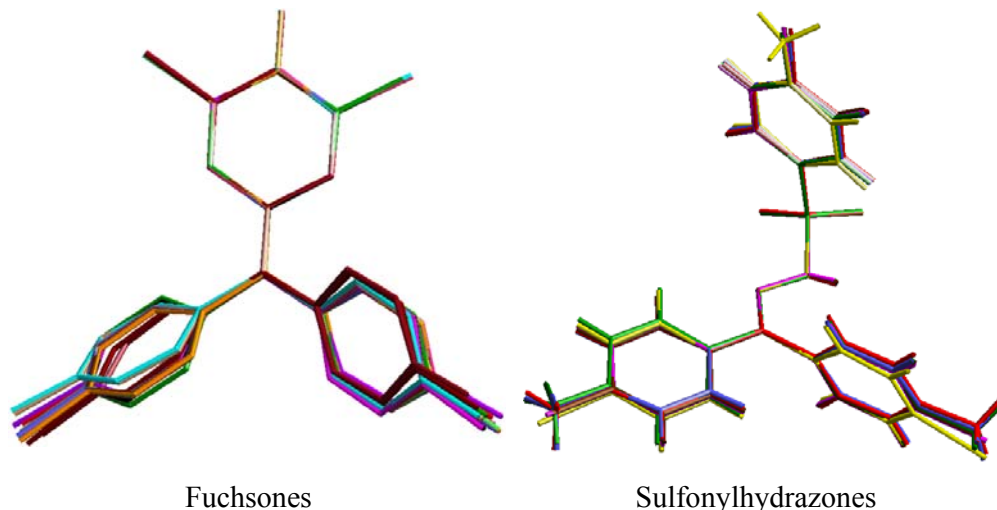


Figure 3.24 In Fuchsones, total 17 conformers were obtained for 4 molecules. These conformers are overlaid by keeping the quinoid ring fixed. Color codes are as follows TMF-I=dark grey, TMF-II=red, TMF-III=green, CMF-I=pink, CMF-II=dark red, CMF-III=light blue, CMF-IV=light brown, MCF-I=orange, MCF-II=purple, MCF-III=black, TCF=chocolate, TMF+CMF=dark blue, CMF+MCF=light green, TMF+MCF-1=blue, TMF+MCF-2=yellow, TMF+MCF-3=magenta and TMF+MCF-4=brown.

In Sulfonylhydrazones, a total of 6 similar conformers were obtained from five molecules under study. These conformers are overlaid by fixing Sulfonylhydrazone function group (S–N–N–C). Color codes are CMSH-I=red, CMSH-II=green, TCSH=brown, TBSH=magenta, FMSH=blue and MISH=yellow

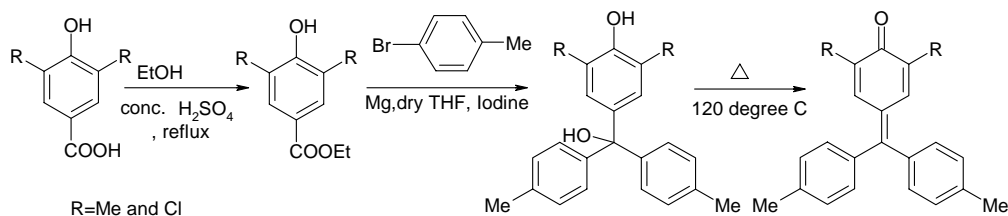
3.7 Conclusion

In summary, Cl-Me, Br-Me, Cl-Br and Cl-F exchanged isostructurality is observed in the two series of conformationally flexible polymorphic molecules. A total of seven isomorphous crystals in space group $P2_1/c$, three in space group $P\bar{1}$ and two in space group $C2/c$ were obtained for Fuchsones. Whereas in Sulfonylhydrazones three isomorphous crystal structures were obtained in space group $C2/c$ and two isomorphous crystals are in $Pbca$. Because of the isomorphous nature of the parent crystals infinite number of continuous series of isomorphous solid solutions is possible as evident from the formation of six solid solutions. Therefore in Fuchsones number of isomorphous crystals can be increased to infinity. The structure directing role of Cl is observed as TCF resulted in a different crystal structure. XPac is a useful tool to elucidate the similarity and differences and also to find common structure motif among several crystal

structures. 2D isostructurality in Sulfonylhydrazones is due to the presence of strong hydrogen bonding synthon sulfonamide dimer. Whereas various 0D, 1D and 2D supramolecular constructs were identified in the crystal structures of Fuchsones governed by weak C–H···O hydrogen bonds. The analysis demonstrated that common packing patterns occur frequently among polymorphs. Therefore the intriguing problem of finding and controlling the formation of isostructural crystals in conformationally flexible polymorphic molecules was successful to a great extent by invoking the idea of halogen-methyl and halogen-halogen functional group exchange.

3.8 Experimental Section

Synthesis: The four Fuchsones were synthesized using two different procedures, purified by column chromatography and characterized by FT-IR and ^1H NMR. Melting points were determined in Fischer Jones apparatus and DSC. DSC s were included in Appendix. TMF and CMF were synthesized^{16f} using Grignard reaction as shown in Scheme 3.9.



Scheme 3.9 Synthetic procedure of TMF and CMF.

TMF: A solution of 3, 5-dimethyl-4-hydroxybenzoic acid in absolute ethanol in presence of few drops of conc. H_2SO_4 was refluxed for 6 hours. The reaction mixture was poured in ice water to afford the corresponding ester as solid precipitate. The resulting material is purified by column chromatography. Mg turnings (50 mmol, 1.2 g) and dry THF (15 mL) were taken in a round bottomed flask under constant nitrogen atmosphere. A solution of 4-bromo toluene (50 mmol, 6 mL) in dry THF (10 mL) under nitrogen atmosphere was taken and 1 mL of it was added to RB flask containing Mg and dry THF under nitrogen followed by a tiny crystal of iodine. The remaining portion of 4-bromo toluene (60mmol) solution was added slowly over a period of 45 minutes. After the completion of the reaction a solution of ester (10 mmol, 1.83 g) in THF (20 mL) was added. The mixture was refluxed for 1 hour and the product was poured into a mixture of

crushed ice (~40 g) and conc. H₂SO₄ (1 mL) with stirring. The organic layer was separated and washed with water (10 mL), saturated sodium sulphate solution (10 mL) and again with water (10 mL) and dried to obtain a yellow colored oil which was purified using column chromatography to obtain the corresponding alcohol. The compound was heated at 120 °C for 2/3 hours to furnish colored Fuchson product.

¹H NMR (400 MHz, CDCl₃, δ ppm): 2.02 (6H, s), 2.4 (6H, s), 7.1 (4H, d, J 8), 7.1 (2H, s), 7.23 (4H, d, J 8).

FT-IR (KBr, cm⁻¹): 2909, 1632, 1611, 1493.

M. p.: 210-212 °C.

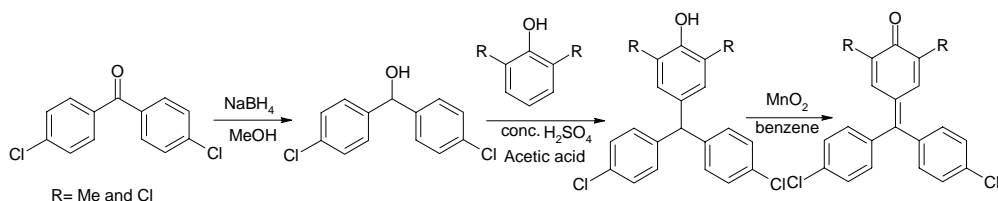
CMF: This molecule was synthesized using 3, 5-dichloro-4-hydroxybenzoic acid as the starting material and the above reaction procedure was used.

¹H NMR (400 MHz, CDCl₃, δ ppm): 2.46 (6H, s), 7.12 (4H, d, J 8), 7.25 (4H, d, J 8), 7.5 (2H, s).

FT-IR (KBr, cm⁻¹): 2932, 2839, 1630, 1590, 1506.

M. p.: 206-209 °C.

MCF: MCF was synthesized using the following procedure^{16f} (Scheme 3.10).



Scheme 3.10 Reaction scheme used to synthesize MCF and TCF.

4,4'-dichlorobenzophenone was reduced to the corresponding benzhydrol using NaBH₄ in methanol. Conc. H₂SO₄ (1 mL) was added to the stirred solution of 2,6-dimethylphenol (10 mmol, 1.20 g) and 4,4'-dichlorobenzhydrol (10 mmol, 2.53 g) in acetic acid (20 mL). The reaction mixture was stirred for 24 hours and poured in ice water to obtain the 4-hydroxyphenyldiphenylmethane as precipitate which was filtered

washed with water, dried and oxidized with MnO_2 in benzene to afford the Fuchsone product. The final product was purified by column chromatography.

^1H NMR (400 MHz, CDCl_3 , δ ppm): 1.94 (6H,s), 7.15-7.17 (2H,s) , 7.28 (4H, d, J 8 Hz), 7.43-7.41 (4H,d, J 8 Hz)

FT-IR (KBr, cm^{-1}): 2985, 2943, 2912, 1627, 1602, 1503

M. p.: 206-208 $^\circ\text{C}$.

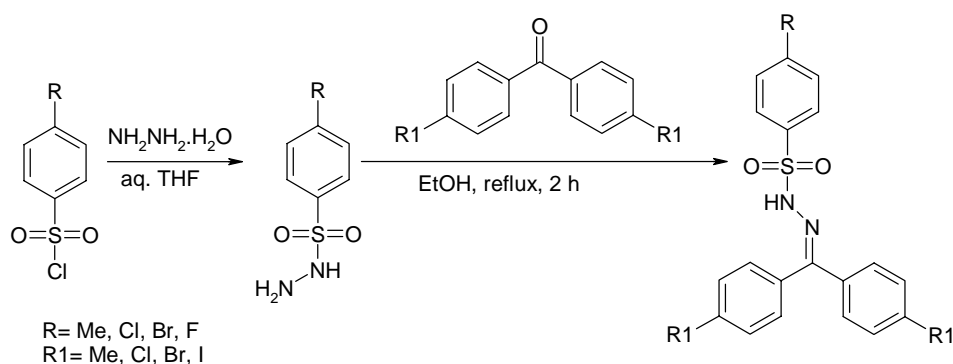
TCF: This compound was synthesized by using a modified technique of the above mentioned procedure. A homogeneous mixture of 2,6-dichlorophenol and 4,4'-dichlorobenzhydrol, produced by grinding both the materials, are dissolved in acetic acid and conc. H_2SO_4 (few drops) at 80/90 $^\circ\text{C}$ and rest of the procedure is same as was used for MCF.

^1H NMR (400 MHz, CDCl_3 , δ ppm): 7.19 (4H, d, J 8), 7.49 (6H, m)

FT-IR (KBr, cm^{-1}): 2923, 2852, 1624, 1092.

M. p.: 227-230 $^\circ\text{C}$.

Sulfonylhydrazones were synthesized²⁶ using the following procedure (Scheme 3.11) and purified by recrystallization from ethanol. Melting points were determined in Fischer-Jones apparatus.



Scheme 3.11 Reaction procedure used to synthesize Sulfonylhydrazones.

CMSH: To a stirred solution of *p*-chlorosulfonyl chloride (5.0 g, 23 mmol) in 25 mL THF was added hydrazine hydrate (2.5 g, 49 mmol) drop wise at 0°C. The reaction was continued for 30 min and the product extracted with ether to give *p*-chlorosulfonyl hydrazine. To a well stirred solution of *p*-chlorosulfonyl hydrazine (500 mg, 2.42 mmol) in 10 mL ethanol was added equimolar amount of 4,4'-dimethyl benzophenone (508.87 mg, 2.42 mmol) and was refluxed for 2 h. Cooling the reaction mixture afforded crystalline bis(*p*-tolyl)ketone *p*-Chlorosulphonylhydrazone as precipitate which was then filtered, washed with cold ethanol and recrystallized from hot ethanol.

¹H NMR (500 MHz, DMSO-D₆, δ ppm): 2.28 (3H, s), 2.39 (3H, s), 7.10 (2H, d, J 10), 7.32 (2H, d, J 10), 7.71 (2H, d, J 10), 7.91 (2H, d, J 10), 10.46 (1H, s).

FT-IR (KBr, cm⁻¹): 3188, 1585, 1346, 1167.

M. p.: 161-162 °C.

TCSH, TBSh, FMSH and MISH were synthesized using the above procedure.

TCSH:

¹H NMR (400 MHz, CDCl₃, δ ppm): 7.39 (2H, d, J 8), 7.52 (2H, d, J 8), 7.71 (2H, d, J 8), 7.90 (2H, d, J 8).

FT-IR (KBr, cm⁻¹): 3194, 1587, 1352, 1168.

M. p.: 203-205 °C.

TBSH:

¹H NMR (500 MHz, DMSO-D₆, δ ppm): 7.2 (2H, d, J 10), 7.55 (2H, d, J 10), 7.73 (2H, d, J 10), 7.8 (2H, d, J 10), 10.8 (1H, s).

FT-IR (KBr, cm⁻¹): 3192, 1589, 1346, 1170.

M. p.: 236-239 °C.

FMSH:

^1H NMR (400 MHz, CDCl_3 , δ ppm): 2.30 (3H, s), 6.98 (2H, d, J 8), 7.21 (2H, d, J 8), 7.41 (2H, d, J 8), 7.63 (2H, d, J 8).

FT-IR (KBr, cm^{-1}): 3184, 1585, 1317, 1176.

M. p.: 139-143 $^{\circ}\text{C}$.

MISH

^1H NMR (500 MHz, $\text{DMSO}-d_6$, δ ppm): 2.39 (1H, s), 7.41 (2H, d, J 10), 7.71 (2H, d, J 10), 7.77 (2H, d, J 10), 7.88 (2H, d, J 10), 10.66 (1H, s).

FT-IR (KBr, cm^{-1}): 3186, 1595, 1346, 1167.

M. p.: 249-253 $^{\circ}\text{C}$.

X-ray crystallography: X-Ray reflections for the Fuchsones (except CMF-d which is collected at 298 K) were collected at 100 K and Sulfonylhydrazones were collected at 298 K on Bruker SMART APEX CCD equipped with a graphite monochromator and Mo $\text{K}\alpha$ fine-focus sealed tube ($\lambda=0.71073$ Å). Data integration was done using SAINT.²⁷ Intensities for absorption was corrected using SADABS.²⁸ Structure solution and refinement was carried out using Bruker SHELXTL.²⁹ The hydrogen atoms were refined isotropically and the heavy atoms were refined anisotropically. N–H hydrogens were located from the electron density map and C–H hydrogens were fixed using HFIX command in SHELXTL. The experimental composition in solid solution crystal structures was determined by the variable site occupancy of C and Cl atoms in structure solution least-squares refinement cycles by using FVAR, EXYZ and EADP commands in SHELX-TL.

Solid state UV-Vis: Solid state UV-Vis spectra were recorded by Thermo Scientific Evolution 300 UV-Vis spectrophotometer. Experiments were carried out by mounting very thin homogeneous KBr discs with the help of quartz plates. Concentrations of the samples are ~0.8% (w/w).

DSC: DSC was performed for TMF-I, II, III, CMF-I, II, MCF-I, II and TCF on a Mettler Toledo DSC 822e module. Samples were placed in crimped but vented aluminum sample

pans with sample size is 4-6 mg. DSCs were performed at 5 °C min⁻¹ from 30 °C-250 °C. Samples were purged by a stream of dry nitrogen flowing at 150 mL min⁻¹. The DSCs are included in the Appendix.

3.9 References

1. (a) O. M. Yaghi, M. O’Keefe, N. W. Ockwig, H. K. Chae, M. Eddaoudi and J. Kim, *Nature*, 423, **2003**, 705. (b) G. R. Desiraju, *Angew. Chem., Int. Ed.*, 46, **2007**, 8342. (c) T. Friščić and L. R. MacGillivray, *Croat. Chem. Acta*, 79, **2006**, 327. (d) L. R. Mac-Gillivray, *CrystEngComm*, 67, **2004**, 77.
2. (a) J. L. C. Rowsell and O. M. Yaghi, *Angew. Chem., Int. Ed.*, 44, **2005**, 4670. (b) L. R. MacGillivray, G. S. Papefstathiou, T. Friščić, D. B. Varshney and T. D. Hamilton, *Top. Curr. Chem.*, 248, **2005**, 201. (c) M. J. Zaworotko, *Cryst. Growth Des.*, 7, **2007**, 4. (d) G. M. J. Schmidt, *Pure Appl. Chem.*, 27, **1971**, 647. (e) M. C. Etter, *J. Phys. Chem.*, 95, **1991**, 4601. (f) V. Peddy, J. A. McMahon, J. A. Bis and M. J. Zaworotko, *J. Pharm. Sci.*, 95, **2006**, 499. (g) G. R. Desiraju, *Angew. Chem., Int. Ed.*, 34, **1995**, 2311.
3. (a) S. L. Price, *Adv. Drug Delivery Rev.*, 2004, 56, 301; (b) R. J. Davey, *Chem. Commun.*, 2003, 1463; (c) S. R. Byrn, R. R. Pfeiffer, G. Stephenson, D. J. W. Grant and W. B. Gleason, *Chem. Mater.*, 1994, 66, 1148; (d) R. W. Lancaster, P. G. Karamertzanis, A. T. Hulme, D. A. Tocher, T. C. Lewis and S. L. Price, *J. Pharm. Sci.*, 2007, 96, 3419.
4. (a) A. Kálmán, L. Párkányi and G. Argay, *Acta Cryst.*, B49, **1993**, 1039. (b) L. Fábián and A. Kálmán, *Acta Cryst.*, B55, **1999**, 1099. (c) A. Kálmán and L. Párkányi, *Adv. Mol. Struct. Res.*, 3, **1997**, 189.
5. (a) P. G. Jones and F. Vancea, *CrystEngComm*, 2003, 5, 303; (b) L. Fábián, G. Argay, A. Kálmán and M. Báthori, *Acta Cryst.*, 58B, **2002**, 710. (c) A. Kálmán, L. Fábián and G. Argay, *Chem. Commun.*, **2000**, 2255.
6. (a) B. K. Saha and A. Nangia, *Heteroat. Chem.*, 18, 2007, 185. (b) A. Kálmán and L. Fábián, *Acta Cryst.*, B63, **2007**, 411. (c) C. M. Reddy, M. T. Kirchner, R. C. Gundakaram, K. A. Padmanabhan and G. R. Desiraju, *Chem.-Eur. J.*, 12, **2006**, 2222. (d) J. Kansikas and K. Sipilä, *Acta Cryst.*, B53, **1997**, 1127. (e) L.

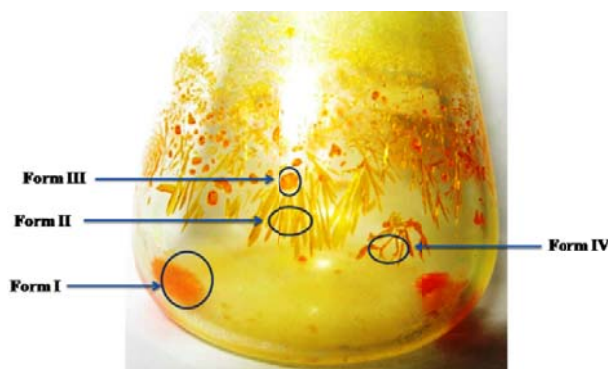
- Párkányi, A. Kálmán, S. Sharma and D. M. Nolen, *Inorg. Chem.*, 33, **1994**, 180.
- (f) S. Stankovic, J. Petrovic, D. Miljkovic, V. Pejanovic, R. Kovacevic, A. Stefanovic and M. Bruvo, *Acta Cryst.*, C48, 1992, 1248.
7. (a) G. R. Desiraju, *Science*, 278, 1997, 404. (b) G. R. Desiraju, *Nat. Mater.*, 1, **2002**, 77.
 8. I. Kitaigorodskii, *Organic Chemical Crystallography*, Consultant's Bureau, New York, **1961**.
 9. (a) J. A. R. P. Sarma and G. R. Desiraju, *Acc. Chem. Res.*, 19, **1986**, 222. (b) M. R. Edwards, W. Jones and W. D. S. Motherwell, *CrystEngComm*, 8, **2006**, 545. (c) J. van de Streek and S. Motherwell, *J. Appl. Cryst.*, 38, 2005, 694. (d) N. N. L. Madhavi, A. K. Katz, H. L. Carrell, A. Nangia and G. R. Desiraju, *Chem. Commun.*, **1997**, 1953. (e) R. Banerjee, R. Mondal, J. A. K. Howard and G. R. Desiraju, *Cryst. Growth & Des.*, 6, **2006**, 999. (f) M. R. Edwards, W. Jones, W. D. S. Motherwell and G. P. Shields, *Mol. Cryst. And Liq. Cryst.*, 356, 2001, 337. (g) G. R. Desiraju and J. A. R. P. Sarma, *Proc. Indian Acad. Sci. (Chem. Sci.)*, 96, **1986**, 599. (h) M. Polito, E. D'Oria, L. Maini, P. G. Karamertzanis, F. Grepioni, D. Braga and S. L. Price, *CrystEngComm*, 10, **2008**, 1848.
 10. (a) B. K. Saha and A. Nangia, *Heteroatom Chemistry*, 18, **2007**, 185. (b) T. Steiner, *J. Mol. Struct.*, 443, **1998**, 149. (c) I. Bar and J. Bernstein, *Tetrahedron*, 43, **1987**, 1299.
 11. S. Aitipamula and A. Nangia, *Chem. Commun.*, **2005**, 3159.
 12. S. Roy and A. Nangia, *Cryst. Growth & Des.*, 7, **2007**, 2047.
 13. V. S. S. Kumar, A. Addlagatta, A. Nangia, W. T. Robinson, C. K. Broder, R. Mondal, I. R. Evans, J. A. K. Howard and F. H. Allen, *Angew. Chem., Int. Ed.*, 41, 2002, 3848.
 14. S. K. Chandran, N. K. Nath, S. Roy and A. Nangia, *Cryst. Growth & Des.*, 8, **2008**, 140.
 15. (a) P. F. Gordon and P. Gregory, *Organic Chemistry In Colour*; Springer-Verlmg: New York, **1983**, pp 242. (b) L. S. Pratt, *The Chemistry And Physics Of Organic Pigments*; John Wiley: New York, 1947, pp 6. (c) D. F. Duxbury, *Chem. Rev.*, 93, **1993**, 381.

16. (a) A. Bistrzycki and C. Herbst, *Ber.*, 86, **1903**, 2335. (b) M. Gomberg and R. L. Jickling, *J. Am. Chem. Soc.*, 37, **1915**, 2575. (c) M. Gomberg and N. E. Van Stone, *J. Am. Chem. Soc.*, 38, **1916**, 1577. (d) T. W. Lewis, D. Y. Curtin and I. C. Paul, *J. Am. Chem. Soc.*, 101, **1979**, 5717. (e) H.-D. Becker and K. Gustafsson, *J. Org. Chem.*, 41, **1976**, 214. (f) H.-D. Becker, *J. Org. Chem.*, 32, **1967**, 2943.
17. J. Bernstein, *Polymorphism in Molecular Crystals*, Clarendon, Oxford, **2002**, pp-257-271.
18. P. Sanphui, B. Sarma and A. Nangia, *Cryst. Growth & Des.*, 10, 2010, 4550.
19. (a) A. I. Kitaigorodskii, *Mixed Crystals*, Springer-Verlag: Berlin, Heidelberg, **1984**. (b) J. A. R. P. Sarma and G. R. Desiraju, *J. Am. Chem. Soc.*, 108, **1986**, 2791. (c) A. Anthony, M. Jaskólski, A. Nangia and G. R. Desiraju, *Chem. Commun.*, **1998**, 2537. (b) F. C. Pigge, V. R. Vangala and D. C. Swenson, *Chem. Commun.*, **2006**, 2123.
20. G. R. Desiraju, *Crystal Engineering - The Design of Organic Solids*, Elsevier. Amsterdam, **1989**.
21. (a) D. Y. Curtin and S. R. Byrn, *J. Am. Chem. Soc.* 91, **1969**, 6102. (b) R. A. Fletton, R. W. Lancaster, R. K. Harris, A. M. Kenwright, K. J. Packer, D. N. Waters and A. J. Yeadon, *J. Chem. Soc. Perkin Trans. 2*, 170, **1986**, 1709. (c) G. A. Stephenson, T. B. Borchardt, S. R. Byrn, J. Bowyer, C. A. Bunnell, S. V. Snorek and A. L. Yu, *J. Pharm. Sci.*, 84, **1995**, 1385. (d) J. Bernstein and G. M. Schmidt, *J. Chem. Soc., Perkin Trans. 2*, **1972**, 951. (e) J. Bernstein and I. Izak, *J. Cryst. Mol. Struct.*, 5, **1975**, 257. (f) X. He, U. J. Griesser, J. G. Stowell, T. B. Borchardt and S. R. Byrn, *J. Pharm. Sci.*, 37, **2001**, 388. (g) H. Li, J. G. Stowell, T. B. Borchardt and S. R. Byrn, *Cryst. Growth Des.*, 246, **2006**, 2474. (f) G. R. Desiraju, I. C. Paul and D. Y. Curtin, *J. Am. Chem. Soc.*, 99, **1977**, 1594. (g) S. Chen, I. A. Guzei and L. Yu, *J. Am. Chem. Soc.*, 127, **2005**, 9881.
22. A. Hantzsch, *Angew. Chem.*, 20, **1908**, 1889.
23. B. Klebe, F. Graser, E. Hädicke and J. Berndt, *Acta Cryst.*, B45, **1989**, 69.
24. L. Yu, *J. Phys. Chem. A*, 106, **2002**, 544.
25. (a) T. Gelbrich and M. B. Hursthouse, *CrystEngComm*, 7, **2005**, 324. (b) T. Gelbrich and M. B. Hursthouse, *CrystEngComm*, 8, **2006**, 448. (c) T. Gelbrich,

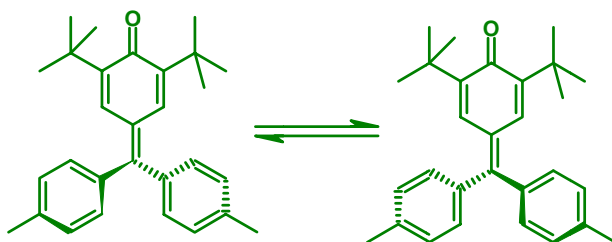
- D. S. Hughes, M. B. Hursthouse and T. L. Threlfall, *CrystEngComm*, 10, **2008**, 1328. (d) F. P. A. Fabbiani, B. Dittrich, A. J. Florence, T. Gelbrich, M. B. Hursthouse, W. F. Kuhs, N. Shankland and H. Sowa, *CrystEngComm*, 11, **2009**, 1396.
26. (a) L. Friedman, R. L. Litle and W. R. Reichle, *Organic Syntheses*, Wiley and Sons: New York, **1973**; Collect. Vol. V, p 1055. (b) V. P. Miller, Yang, T. M. Weigel, O. Han, H. Liu, *J. Org. Chem.*, 54, **1989**, 4175.
27. *SAINT-Plus*, version 6.45; Bruker AXS Inc.: Madison, WI, **2003**.
28. G. M. Sheldrick, SADABS, *Program for Empirical Absorption Correction of Area Detector Data*, University of Göttingen, Germany, 1997.
29. (a) *SMART (Version 5.625) and SHELX-TL (Version 6.12)*; Bruker AXS Inc.: Madison, WI, **2000**. (b) G. M. Sheldrick, *SHELXS-97 and SHELXL-97*; University of Göttingen, Germany, **1997**.

Chapter Four

Chiral and Racemic Tetramorphs of t-Butylfuchsone



Concomitant crystallization of four polymorphs Form I ($P2_1$), Form II ($P2_1/n$), Form III ($Pbca$) and Form IV ($C2/c$).



Chiral Conformations of t-Butylfuchsone

Conformational chirality leading to chiral crystallization was observed in two series of Fuchsones with varying substituents. Increasing steric influence around the hydrogen bond acceptor carbonyl group appears to be an important determinant in chiral crystallization.

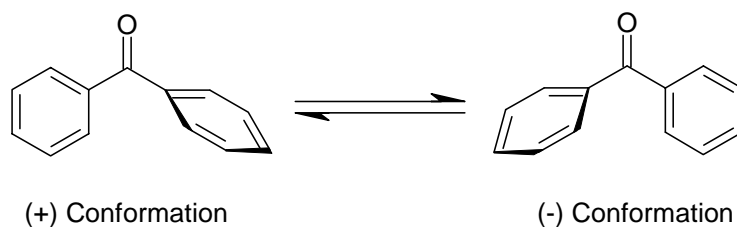
4.1 Introduction

The essential molecules of life exist in homochiral form. Living organisms consists of only right handed forms of sugars such as deoxyribose and ribose in DNA and RNA and left handed forms of amino acids that form the proteins.¹ The term chirality was first coined by Lord Kelvin in 1893,² which is used to describe an object that is non-superposable on its mirror image. A chiral molecule is a type of molecule that lacks an internal plane of symmetry and has a non-superposable mirror image. Molecular chirality is of interest because of its application to stereochemistry in inorganic chemistry, organic chemistry, physical chemistry, biochemistry, and supramolecular chemistry.³ Source of dissymmetry in organic molecules may be asymmetric carbon, silicon, nitrogen, sulfur and phosphorous, a chiral axis or a chiral plane.

Chiral molecules from an enantiomerically pure solution must crystallize in one of the 65 Sohncke space groups, i. e. space groups without mirror and inversion symmetry. Many organic compounds lacking stereogenic centres, planes of chirality, or atropoisomerism can also crystallize in Sohncke space groups. Recent CSD surveys showed that only 8-10% of achiral compounds crystallize in Sohncke space groups⁴ forming chiral crystals. Although Kitaigorodsky's model of close packing⁵ shows that molecules prefer to crystallize with a centre of inversion but still due to several reasons molecules lacking chiral centre, plane or axis can crystallize in Sohncke space groups.

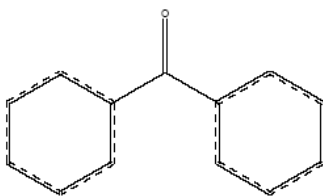
4.1.1 The spontaneous generation of chirality in achiral molecules

Generation of chirality in an achiral molecule⁴ can be due to three main reasons. Firstly, chirality is generated in a conformationally flexible molecule due to rotation of bonds, i.e. due to conformational chirality.⁶ Conformational flexible molecules which require high steric energy for the conversion of the structure to the mirror image is effectively chiral as it is conformationally locked and cannot convert to its mirror image. These molecules in liquid state or in solution can exist in a dynamic equilibrium of interconverting chiral conformations. An important class of molecules showing conformational chirality is benzophenone (Scheme 4.1). A CSD search revealed that out of 290 benzophenone molecules reported in CSD (version 1.12, Aug 2010 update)⁷, 32 (11%) of them crystallized in chiral space groups.



Scheme 4.1 Chiral conformations of benzophenone.

Total number of hits for the following substructure (Scheme 4.2) with only organics and 3D coordinate determined is 1488. Eliminating duplicates, salt, cocrystal, solvates, hydrates and benzene rings substituted by other rings, the number of hits were 290. Out of these 290 structures, 32 benzophenones crystallized in chiral space groups.



Scheme 4.2 Substructure used for CSD search

AMBZPH	BEHYAP	BEHYET	BERDOS	BERDUY
BIKCOO	BPHENO01	BROHBZ	CINYEE	COPKIB
FEVMUO	FINCEK	HESLAS	HIWNEH	HOBREV
HOBRIZ	HUZXOP	JACFUO	JIPXIQ	NELQOL
OBEXOI	OBEXUO	OBEYAV	RAYXIY	SATQUZ
TANSEG	TEL Ril	TOWBIQ	UGECUE	VOFVAN
WADBEI	XUMVOQ			

Secondly, helical arrangement of molecules⁸ leads to chiral crystallization. The helix is one of the most attractive and evocative expressions of chirality. One dimensional metallohelical chains are proved to be more efficient chiral precursors than oligohelicates. Numerous examples are available where achiral molecules including simple metal salts which crystallize in chiral space groups.⁹

Finally, the head-to-head stacking of molecules forming a columnar arrangement always plays an essential role in the chirality generation by either bond rotation or helical

arrangement. This kind of arrangement of molecules can be observed in chiral crystals of benzophenones and in phenanthridine.

4.1.2 Spontaneous resolution or spontaneous symmetry breaking

Mixtures of mirror-image configurations or conformations of a compound or a racemate may condense in three different ways (Figure 4.1)

- (i) Both enantiomers are present in the same condensate called a racemic mixture or racemate.
- (ii) The condensates comprise of only one enantiomer but the sample as a whole is neutral because it contains equal amounts of enantiomorphous condensates, called conglomerate. Separation of enantiomers forming conglomerate is called spontaneous resolution or spontaneous symmetry breaking.¹⁰
- (iii) The condensates may contain the two enantiomers in a non-ordered arrangement called pseudoracemate.

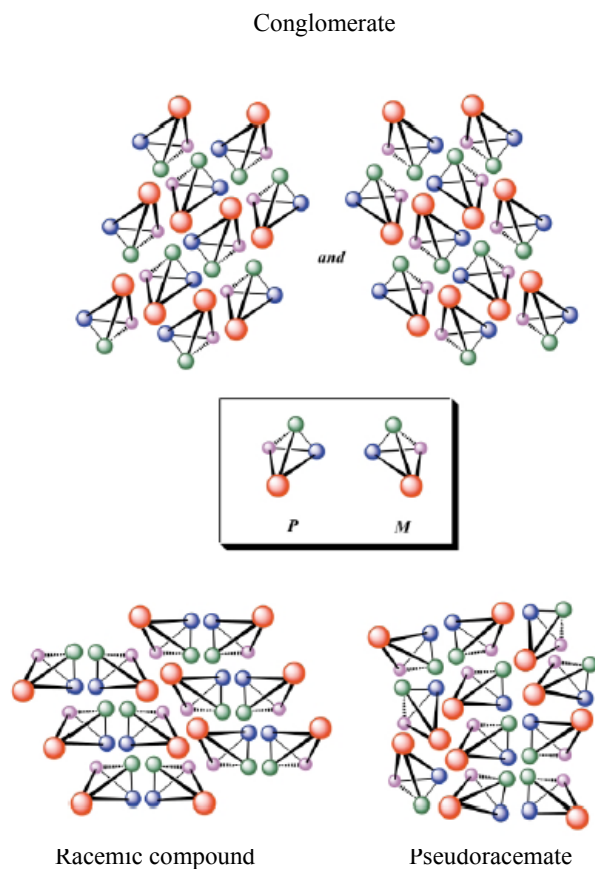


Figure 4.1 Model explaining conglomerate, racemic compound and pseudoracemate. This scheme is culled from Ref. 10a.

Louis Pasteur was the first to conduct spontaneous resolution when he discovered the concept of optical activity in the first place by the manual separation of left-handed and right-handed tartaric acid crystals in 1848.¹¹

Chiral crystals with non-centrosymmetric packing of molecules are important in many aspects such as electro-optic and nonlinear optical materials¹², asymmetric synthesis.¹³ An essential condition for molecules to show electro-optic modulation and second harmonic generation require noncentrosymmetric lattices having polar order. Furthermore, chiral crystallization is relevant to the origin of chiral compounds in nature.^{1,14}

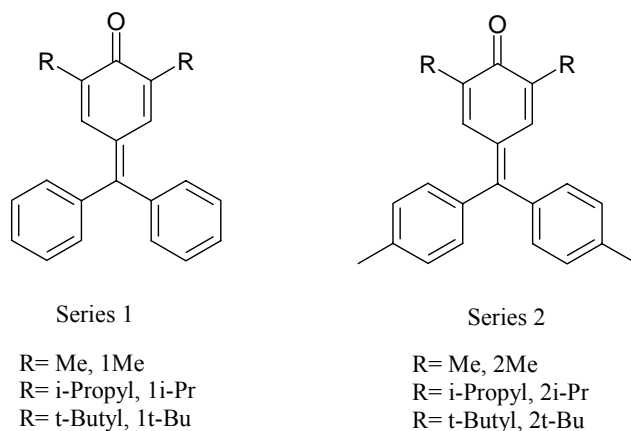
Polymorphism is the existence of the same chemical substance in more than one crystalline modification.¹⁵ When the rate of interconversion of enantiomers in liquid state is fast it gives rise to racemic and chiral crystals which can be termed as polymorphs. When the rate of interconversion is slow they are referred as different compounds viz. racemate and enantiomers (+ and –).¹⁶ There is no exact time frame defined for how fast or how slow interconversion must happen, so borderline cases are possible. Temperature is another factor which can change the interconversion rate.

When polymorphs crystallize simultaneously in the same flask under identical crystal growth conditions from the same solvent, they are termed as concomitant polymorphs.¹⁷ This phenomenon occurs when there are many metastable forms with almost similar energies which crystallize together.

4.2 Results and Discussion

Polymorphism in fuchsone family was reported from our group.¹⁸ Chiral crystallization was observed in two series of compounds (Scheme 4.3) viz. 1Me and 1t-Bu, along with their achiral polymorphs. Chirality arising in the solid state of fuchsones is due to its ability to exist in chiral conformations.⁶ Series 2 fuchsones (Scheme 4.3) were synthesized and crystallized as a continuation of series 1 by exchanging phenyl by p-tolyl group in order to tune chiral crystallization in different homologous series.

Crystallization of the 2t-Bu molecule resulted in a polymorph in non-centrosymmetric chiral space group with three other polymorphs in centrosymmetric space groups, whereas the other two derivatives in the series 2Me and 2i-Pr crystallize in centrosymmetric space groups. The role of t-Bu group over less bulky substituent on chiral crystallization is rationalized in the two series of fuchsone derivatives.



Scheme 4.3 Two series of fuchsones studied, Series 2 is obtained by exchanging phenyl groups of Series 1 by p-tolyl groups.

Series 2 fuchsones were synthesized, purified, characterized (detailed in experimental section) and crystallized from various organic solvents to obtain polymorphs. 2t-Bu shows chiral crystallization along with its racemic crystals whereas other members did not show chirality in solid state. 2Me crystallized as trimorphs in $P2_1/c$ and $P\bar{1}$ space groups from various solvents (detailed in chapter 3). Crystallization of 2i-Pr from different solvents, melting and sublimation techniques did not result a second polymorph. It crystallized in $P2_1/n$ space group with one molecule in the asymmetric unit.

4.2.1 The case of 2, 6-di-t-butyl ditolylfuchsones (2t-Bu)

2t-Bu was crystallized from various organic solvents. One specific crystallization batch of 2t-Bu afforded four polymorphs concomitantly named as form I, form II, form III and form IV according to the order they were characterized by single crystal X-ray diffraction. Form I crystallized in chiral $P2_1$ space group whereas form II, form III and form IV crystallized in centrosymmetric $P2_1/n$, $Pbca$ and $C2/c$ space groups respectively. The asymmetric unit of forms I-III contains one molecule whereas form IV contains half molecule. 2t-Bu molecule in form IV lies about the $C2$ rotational axis to give half molecule in the asymmetric unit. A comparison of unit cell parameters of all the polymorphs is listed in Table 4.1. Crystallization of 2t-Bu from various solvents yielded only form I. The crystallization condition to obtain a concomitant mixture of four

polymorphs is as follows: 2-3% EtOAc + Hexane solution (20 mL) of 2t-Bu in a round bottomed flask was evaporated in a rotary evaporator at 75-80° C. After partial/complete evaporation of the solvent, 5 mL hexane was added quickly and poured in a conical flask to dissolve the residue. After 7-10 hours crystals started appearing on the walls as thin plates (Form II, 2t-Bu-II), thick plates (Form III, 2t-Bu-III) and small needles (Form IV, 2t-Bu-IV). After complete evaporation of the solvent, block type crystals (Form I, 2t-Bu-I) appeared on the bottom of the flask (Figure 4.2).

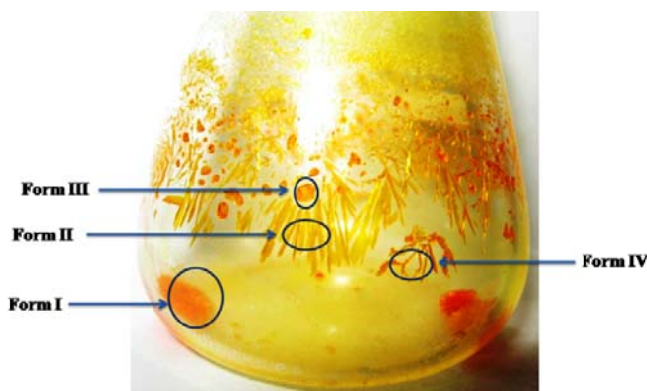


Figure 4.2 The crystallization batch showing all the four polymorphs crystallizing concomitantly.

Table 4.1 Comparison of the unit cell parameters of the four polymorphs of 2t-Bu.

	Form I	Form II	Form III	Form IV
Crystal system	Monoclinic	Monoclinic	Orthorhombic	Monoclinic
Space group	$P2_1$	$P2_1/n$	$Pbca$	$C2/c$
T/K	100	100	100	100
$a/\text{\AA}$	6.0525(8)	9.0435(8)	15.8153(14)	12.5468(14)
$b/\text{\AA}$	19.535(3)	16.2029(15)	17.4890(15)	23.813(3)
$c/\text{\AA}$	10.3567(14)	17.1008(16)	17.9924(16)	9.2568(10)
α°	90	90	90	90
β°	103.489(2)	95.993(2)	90	121.033(2)
γ°	90	90	90	90
Z	2	4	8	4
$V/\text{\AA}^3$	1190.7(3)	2492.1(4)	4976.6(8)	2369.8(4)
$R_1[I > 2\sigma(I)]$	0.0322	0.0586	0.0509	0.0550

4.2.2 Conformational chirality of 2t-Bu

Fuchsones can adopt chiral conformations. The molecule is achiral if it resides in a flat conformation, but in reality the two phenyl rings are twisted, because of steric overcrowding, in an asymmetric fashion to give two enantiomers which can interconvert rapidly in liquid state or in solution. These chiral conformations can be frozen in solid state either separately to give crystals of opposite chirality or racemic crystals where both enantiomers are present just like that in dimethylfuchstone.^{18, 19} Conformational chirality in 2t-Bu arises due to spatial arrangement of p-tolyl groups making it non-superimposable on its mirror image.

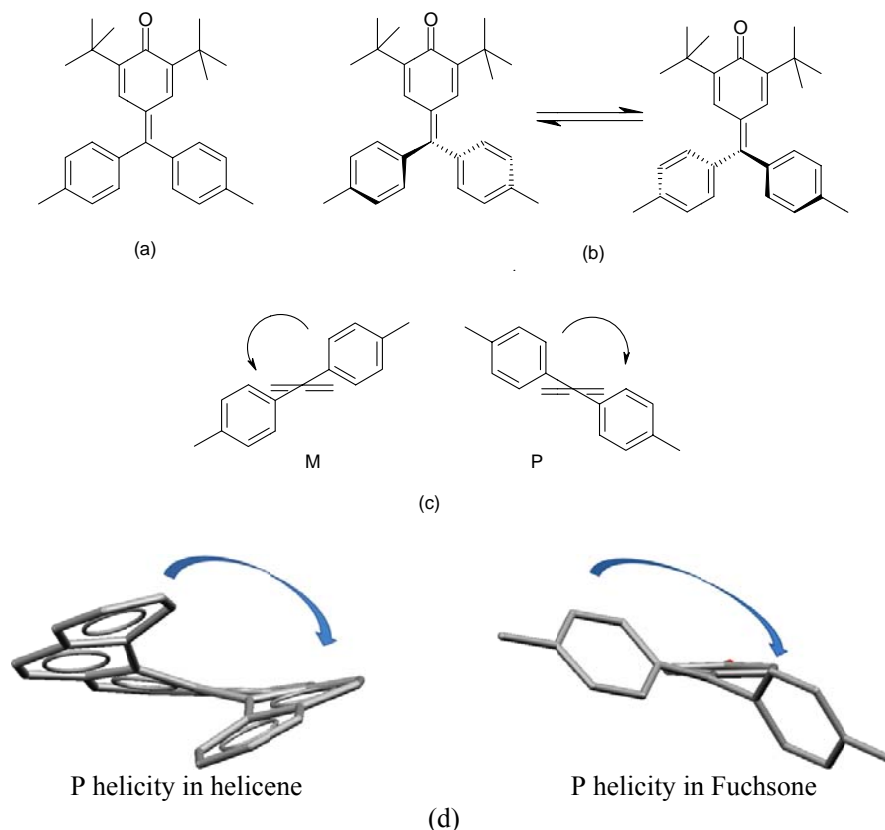


Figure 4.3 Flat conformation of 2t-Bu (a) which in practice exists as dynamic equilibrium between the two enantiomers in solution or in melt (b). (c) The enantiomers are named as P (plus) and M (minus). (d) Comparison of chirality of helicene with Fuchstone.

Chirality in this molecule can be compared with that in helicenes²⁰ by considering the benzoquinone ring lying in a plane in which case the p-tolyl groups reside either side of the plane giving rise to either right handed (plus=P) or left handed (minus=M) helicities (Figure 4.3).

Due to the presence of only one enantiomer in form I, single handed helices exist in the structure formed via C—H \cdots O hydrogen bond (C29—H29C \cdots O1, 2.41Å, 154.8°) between the molecules around 2₁ screw axis unlike in form II-IV where two opposite helices (right and left handed) are present (Figure 4.4).

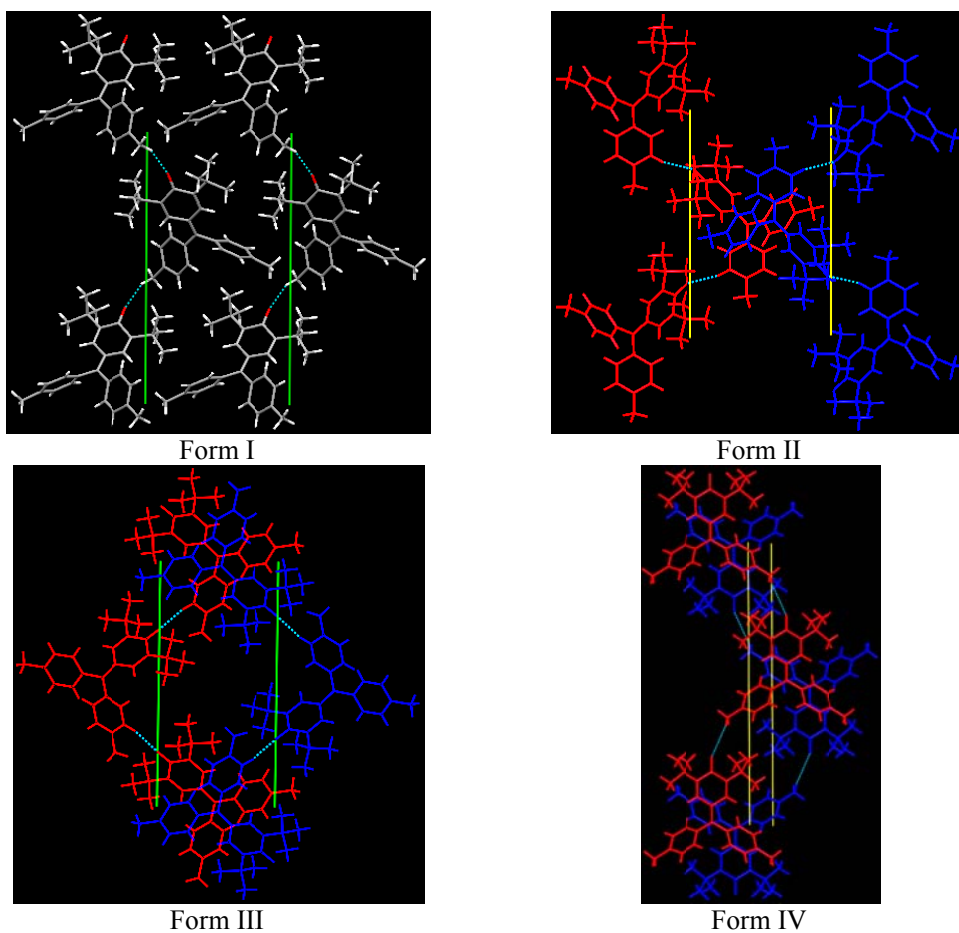


Figure 4.4 Form I contains only one handed helix whereas form II-IV contains opposite handed helices (shown in different colors) formed by both the enantiomers.

4.2.3 Crystal structure analysis

In the crystal structure of form I oxygen atom is involved in bifurcated C—H \cdots O hydrogen bonds (C29—H29C \cdots O1, 2.41 Å, 154.8° and C28—H29C \cdots O1, 2.56 Å, 176.8°) connecting two neighboring parallel helices. These helices are stacked one above the other via C—H \cdots π interaction (2.56 Å, 163.2°) completing the overall polar structure (Figure 4.5).

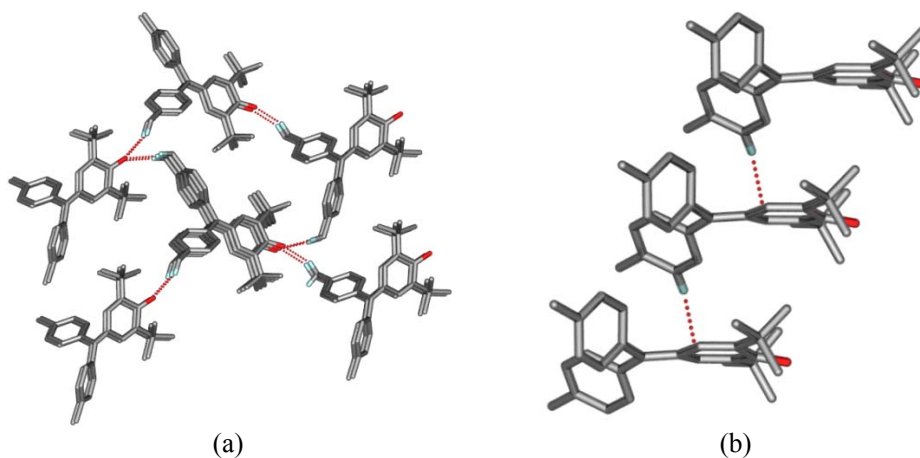


Figure 4.5 In form I, bifurcated C—H \cdots O hydrogen bond connects two helices (a), C—H \cdots π interaction between the molecules forms stacks of similar helices (b).

C—H \cdots O hydrogen bonded (C16—H16 \cdots O1, 2.22 Å, 158.4°) helices are connected to each other via various C—H \cdots π interactions (C13—H13 \cdots π , 2.65 Å, 147.0°; C19—H19 \cdots π , 2.77 Å, 124.6° and C9—H9 \cdots π , 2.70 Å, 167.1°) between inversion related molecules forming a cavity in the crystal structure of form II (Figure 4.6).

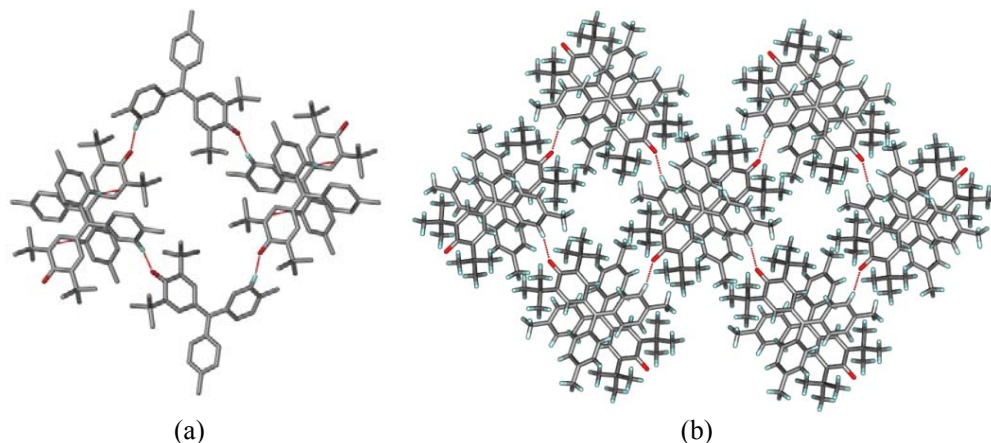


Figure 4.6 In form II, two antiparallel C—H \cdots O hydrogen bonded helices are connected by C—H \cdots π interactions between inversion related molecules (a). Bulky t-Butyl groups come closer to form a cavity (b).

Form III shows similar kind of interaction between two antiparallel C—H \cdots O hydrogen bonded (C16—H16 \cdots O1, 2.18 Å, 166.5°) helices as form II. Here also two opposite helices are connected by C—H \cdots π interactions (C13—H13 \cdots π , 2.71 Å, 137.3°) between the inversion related molecules forming a cavity. But the overall structure differs when another pair of antiparallel helices covers the cavity by close packing to complete the structure (Figure 4.7).

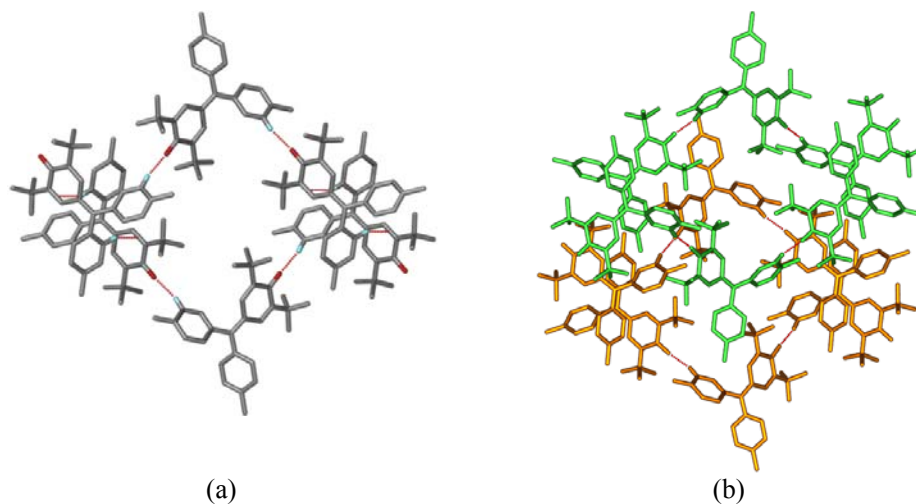


Figure 4.7 In form III, two opposite C—H \cdots O hydrogen bonded helices are connected by C—H \cdots π interaction between inversion related molecules forming cavity (a). Another pair of opposite helices covers the cavity (shown in different colors) (b).

The main structure governing interaction in the crystal structure of form IV is C—H $\cdots\pi$ (C11—H11 $\cdots\pi$ 2.76 Å, 176.6°) between two inversion related molecules which are stacked one above the other. Such stacks are connected to each other via weak C—H \cdots O interaction (C16—H16A \cdots O1, 2.98 Å, 137.0°) to complete the packing (Figure 4.8).

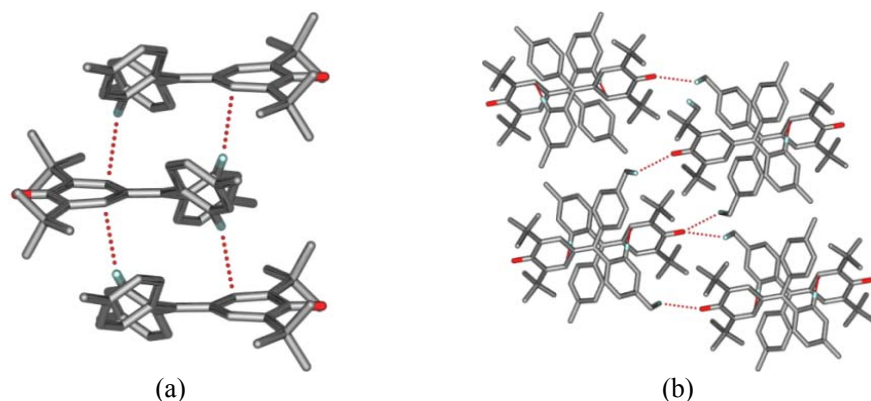


Figure 4.8 C—H $\cdots\pi$ dimers of form IV (a), connected by weak C—H \cdots O interaction (b).

In the crystal structure of 2i-Pr, the molecules form bifurcated C—H \cdots O hydrogen bond (C10—H10 \cdots O1, 2.29 Å, 152.1° and C27—H27C \cdots O1, 2.56 Å, 140.9°) with two inversion related molecules which are connected to each other via C—H $\cdots\pi$ interactions (C13—H13 $\cdots\pi$, 2.73 Å, 141.9°) forming stacks (Figure 4.9).

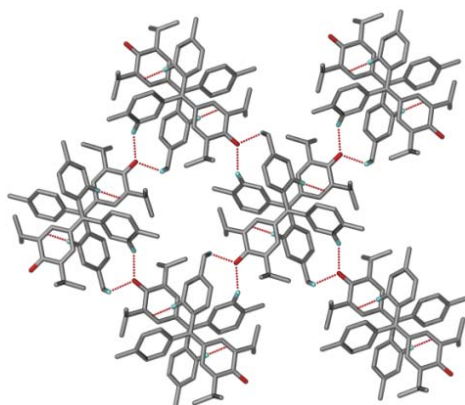


Figure 4.9 In 2i-Pr bifurcated C—H \cdots O hydrogen bonds connect inversion related molecules. The inversion related molecules are connected to each other via C—H $\cdots\pi$ interaction forming stacks.

Hydrogen bond parameters for 2t-Bu polymorphs and 2i-Pr are listed in Table 4.2.

Table 4.2 Neutron normalized hydrogen bond distances, angles and symmetry codes for 2t-Bu polymorphs and 2i-Pr.

Interaction	H...A/ Å	D...A/ Å	∠D-H...A/°	Symmetry code
2-tBu				
Form I				
C(29)—H(29C)···O(1)	2.41	3.421(2)	154.8	1-x,-1/2+y,2-z
C(28)—H(29C)···O(1)	2.561	3.643(2)	176.0	1-x, 1/2+y, 1-z
C(21)—H(21A)···O(1)	2.33	3.027(2)	120.3	Intramolecular
C(22)—H(22B)···O(1)	2.26	2.959(2)	120.5	Intramolecular
C(25)—H(25C)···O(1)	2.32	3.010(2)	119.8	Intramolecular
C(26)—H(26A)···O(1)	2.32	3.009(2)	119.5	Intramolecular
Form II				
C(16)—H(16)···O(1)	2.22	3.249(2)	158.4	1/2-x,-1/2+y,3/2-z
C(21)—H(21C)···O(1)	2.33	3.014(2)	119.6	Intramolecular
C(22)—H(22A)···O(1)	2.31	2.985(2)	119.1	Intramolecular
C(25)—H(25B)···O(1)	2.36	3.036(2)	119.3	Intramolecular
C(26)—H(26B)···O(1)	2.27	2.964(2)	120.2	Intramolecular
Form III				
C(16)—H(16)···O(1)	2.18	3.242(2)	166.5	-x,-1/2+y,1/2-z
C(21)—H(21B)···O(1)	2.34	3.018(2)	119.4	Intramolecular
C(22)—H(22B)···O(1)	2.29	2.984(2)	120.4	Intramolecular
C(25)—H(25A)···O(1)	2.31	2.990(2)	119.4	Intramolecular
C(26)—H(26C)···O(1)	2.30	2.991(2)	119.9	Intramolecular
Form IV				
C(16)—H(16)···O(1)	2.98	3.847(2)	137.0	1/2-x, -1/2+y, 1/2-Z
2i-Pr				
C(10)—H(10)···O(1)	2.29	3.287(2)	152.1	1/2-x,-1/2+y,1/2-z
C(27)—H(27C)···O(1)	2.56	3.467(2)	140.9	-1/2+x, 3/2-y, -1/2+z

When methyl group was exchanged with i-propyl group, i.e. 1i-Pr, two polymorphs, both in centrosymmetric space groups $P2_1/c$ and $Pbca$, were obtained. But with increase in the steric crowding around the carbonyl group by introducing t-butyl group in place of i-propyl group, i.e. 1t-Bu, the molecule crystallized in chiral space group $P2_1$ along with two centrosymmetric polymorphs (both in $P2_1/c$ space group). In the series 2 molecules, crystal structures of 2Me trimorphs (in space groups $P\bar{1}$ and $P2_1/c$), and 2i-Pr (in space group $P2_1/n$) are centrosymmetric. Interestingly, once again the t-butyl derivative, 2t-Bu, crystallized in chiral space group $P2_1$ along with three

centrosymmetric structures. Therefore, it can be concluded that on increasing the steric crowd around the carbonyl group, fuchsones tend to crystallize in non-centrosymmetric chiral space group.

4.2.4 Why t-butyl group?

A conformational flexible molecule lacking a chiral centre or axis can crystallize in chiral space group when there are high steric energy barriers to the conversion of the structure to its mirror image. In this case the molecule is conformationally locked and cannot convert to its mirror image making it effectively chiral. Conformational energy map for model compounds A and B (Figure 4.10) containing i-propyl and t-butyl group showed that higher energy is required for i-propyl group to convert from one conformer to another compared to t-butyl group by 1.5 kcal mol⁻¹.

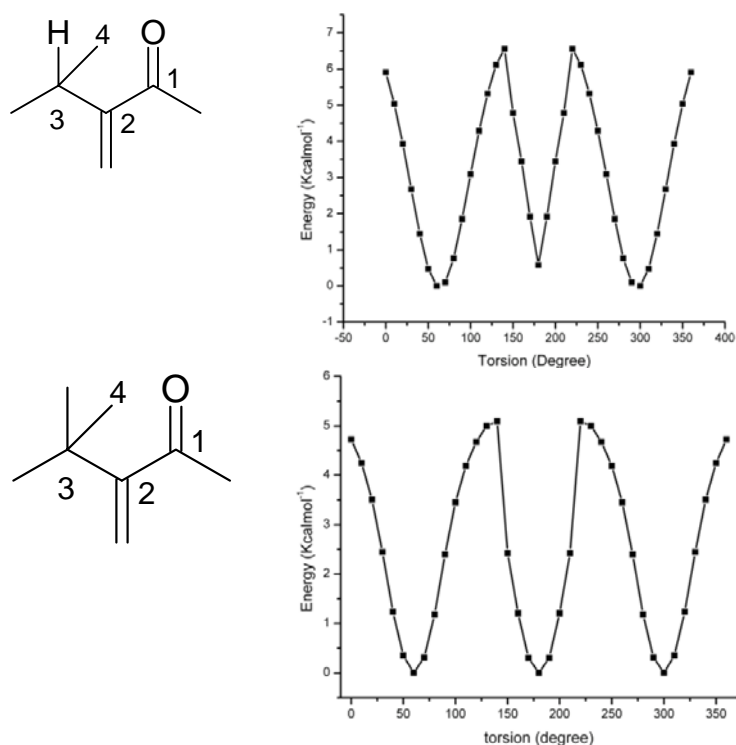


Figure 4.10 Conformer energies are plotted for every 10° change in i-Propyl and t-Butyl torsion angle τ_1 between 0 and 180°. The energy profile is symmetric about $\tau_1=180^\circ$. Conformer energies were calculated in Gaussian 03 (B3LYP/6-31G (d,p)).

This indicates molecules containing i-propyl group should have higher probability to crystallize in chiral space group. A CSD search (version 1.12, Aug 2010 update)⁷ on achiral molecules containing i-propyl and t-butyl groups shows that there are 13.5% achiral molecules containing i-propyl group having chiral/achiral polymorphic clusters whereas for t-butyl group the percentage is 7.5% which indicate that an achiral molecule containing i-propyl group has higher probability of chiral crystallization compared to molecules containing t-butyl group. Rotation of the phenyl or p-tolyl group around C–C single bond will experience about the same torsional barrier in all the molecules under study. But in the two series of fuchsones chiral crystallization is observed in t-butyl derivatives but not in i-propyl derivatives. Therefore no fair argument for the effects of substituents on chiral crystallization on t-butyl derivatives was immediately found.

4.2.5 Resolution of the enantiomers

Single crystal X-ray diffraction along with CD spectroscopy is useful in determining the absolute configuration of chiral crystals.²¹ Solid state CD spectroscopy is useful for compounds where enantiomers can interconvert rapidly in liquid state. Determination of flack parameter²² using single crystal XRD with Cu K α radiation on three single crystals from a batch of form I crystals (20% EtOAc +hexane mixture) show a value of 0.0(2) (Crystallographic data is in Appendix). The three crystal structures show the absolute configuration is M (minus). E. s. d. values of Flack's parameter are high because of the absence of heavy atom in the molecule. Solid state CD spectra (Figure 4.11) recorded on bulk sample of four different crystallization batches reveals the presence of only one enantiomer indicating significant enantiomeric excess. CD spectra of the opposite enantiomer could not be obtained which is not uncommon for compounds exhibiting conformational chirality.²³

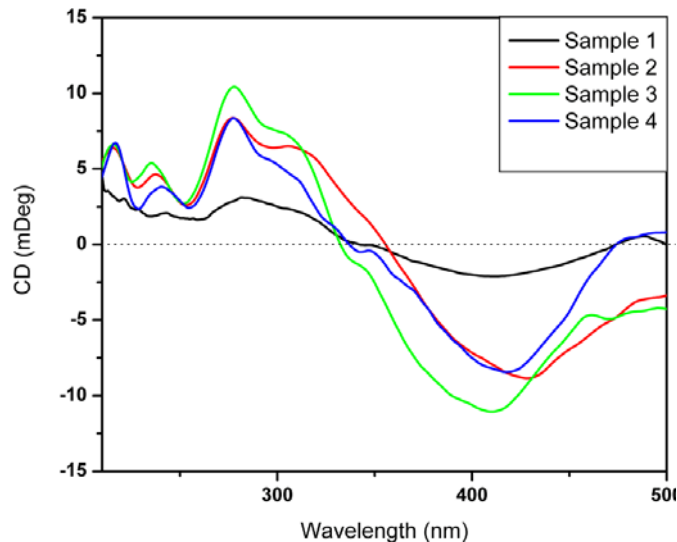


Figure 4.11 Solid state CD spectra of four different batches of crystallization showing optical activity for only one enantiomer. Sample 1= Form I obtained from Hexane, Sample 2= Form I obtained from CHCl_3 solvent, Sample 3= Form I obtained from EtOAc+hexane (10:90 mixture), Sample 4= Form I obtained from CH_3CN solvent.

4.3 Phase Transition Study

Polymorphs of 2t-Bu show phase transition upon heating. Hot stage microscopy, DSC and single crystal X-ray diffraction studies show that form II converts first to form III and finally to form I and form III converts to form I.

4.3.1 Hot stage microscopy (HSM) and single crystal XRD unit cell determination

HSM images of form II show change in the crystals at 130 °C which continued upto 140 °C. A second change was observed in the crystals at 160 °C which continued upto 176 °C and ultimately melted at 189 °C (Figure 4.12).

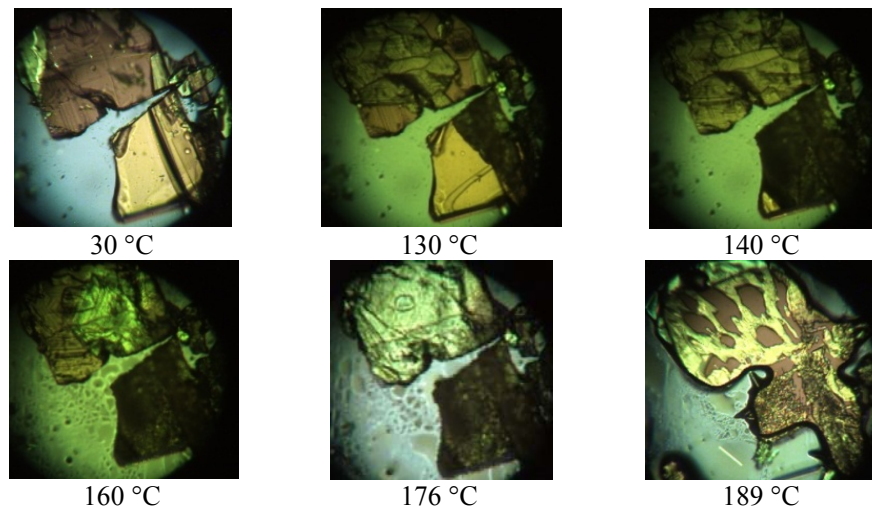


Figure 4.12 Hot stage microscopy images of form II, which show changes in the crystals at different temperatures.

Similarly, for form III, changes in crystals were observed at 146 °C in hot stage microscopy and at 189 °C crystals melted (Figure 4.13).

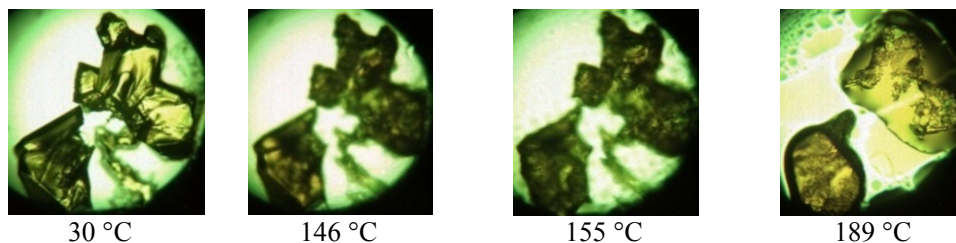


Figure 4.13 Hot stage microscopy images of form III, which show phase transition to form I from 146 °C.

In order to support this observation single crystal XRD experiments were carried out on form II and form III crystals. Few crystals of form II, which can be identified easily from their distinct morphology, and from unit cell determination were isolated and heated to 130 °C in controlled temperature hot air oven. After 6 hours crystals were taken out, allowed to cool down to room temperature and unit cell parameters determined on single crystal X-ray diffractometer which matched with form III. Again the same batch of crystals was heated to 165 °C for 6 hours and similarly the unit cell parameters were determined. It was found that crystals have now converted to form I. Therefore, the first change corresponds to the phase change form II→ form III and the 2nd change corresponds to form III→ form I phase transition.

Similarly, few crystals of form III were picked up and heated at 160 °C for 6 hours in a controlled temperature hot air oven and the cell values in X-ray diffractometer were determined. Unit cell parameters of these crystals indicated form III→ form I phase transition which is consistent with observation in the hot stage microscopy.

Hot stage microscopy experiment showed in form I some new crystals appear around 180 °C due to sublimation. Cell parameter determination revealed that sublimed crystals were form I and there were no phase transition (Figure 4.14).

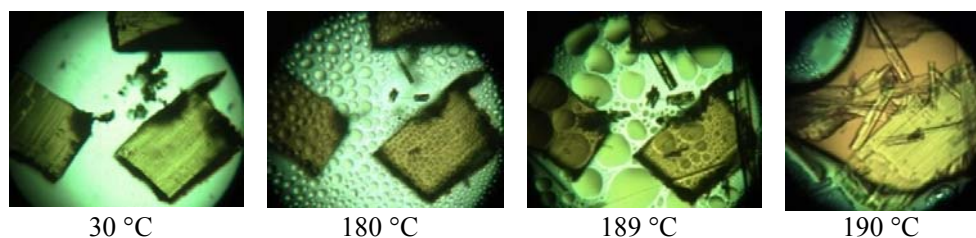


Figure 4.14 Hot stage microscopy images of form I, which show appearance of some crystals near the melting point which is due to sublimation.

Hot stage microscopy on crystals of form IV showed no phase transition and they melted at 185 °C (Figure 4.15).

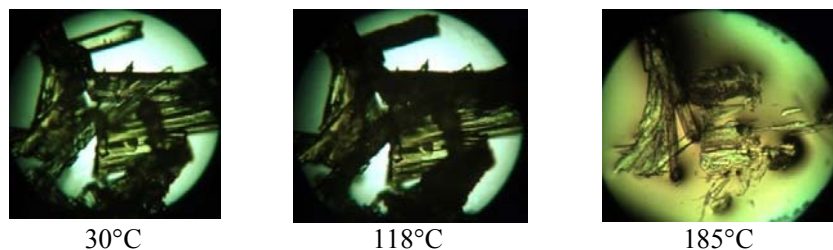


Figure 4.15 Hot stage microscopy images of form IV crystals.

4.3.2 Differential scanning calorimetry (DSC)

No phase transition is observed for form I in DSC thermo gram. In case of form II there are two weak endotherms, 1st one starts at 147.6 °C and 2nd one at 165 °C, which corresponds to the phase transitions that were observed in HSM and single crystal XRD experiments i.e. 1st endotherm corresponds to form II→ form III phase change and the 2nd endotherm corresponds to form III→ form I phase change. DSC thermogram of form III shows a weak endotherm which starts at 154.3 °C, corresponds to form III→ form I

phase change as is evident from similar experiments. Figure 4.16 shows DSC thermograms of form I, form II and form III. DSC on form IV crystals could not be performed because of less yield and difficulty in isolating this polymorph from other three. DSC of form I and form III were performed at $2\text{ }^{\circ}\text{C min}^{-1}$ from $30\text{--}210\text{ }^{\circ}\text{C}$, whereas DSC of form II was recorded at $0.5\text{ }^{\circ}\text{C min}^{-1}$ from $100\text{--}200\text{ }^{\circ}\text{C}$.

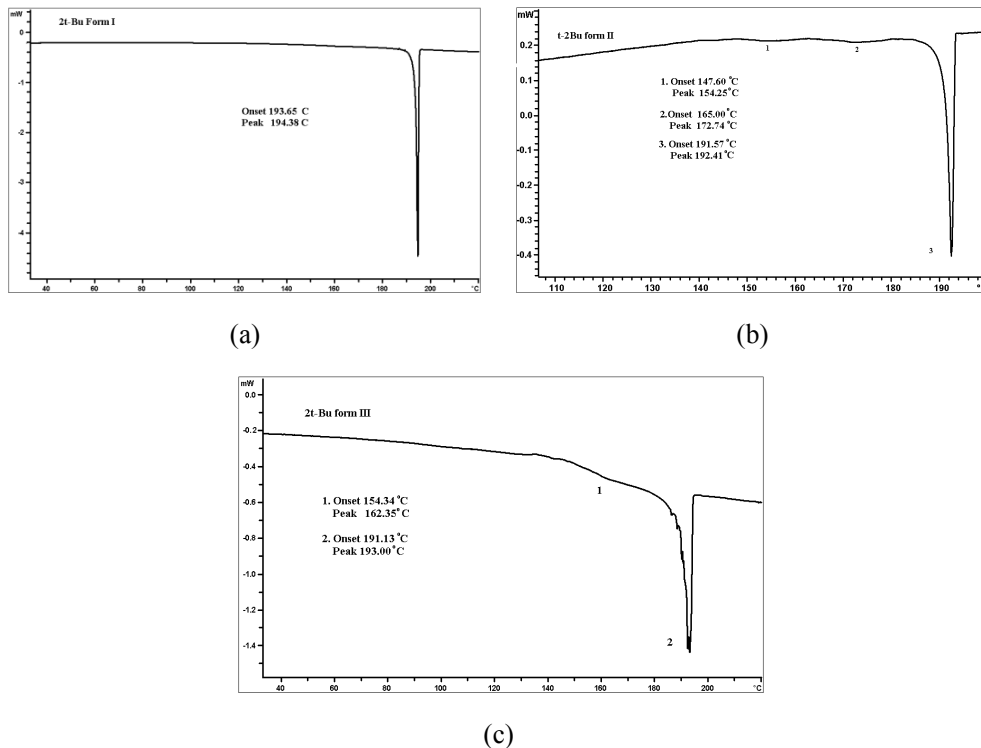


Figure 4.16 DSC thermo grams of form I (a), form II (b) and form III (c).

4.4 Stability of Four Polymorphs and Validity of Wallach's rule

Ostwald²⁴ stated that a system moves to equilibrium from an initial high-energy state through minimal changes in free energy. Therefore the polymorph that crystallizes first is one which possesses the lowest energy barrier (highest energy, metastable). This form would then transform to the next lower energy polymorph until a thermodynamically stable state is reached, the so-called Ostwald's Law of Stages. It was observed during crystallization of the four polymorphs that form II, III and IV crystallized first on the walls of the vessel and after complete evaporation of the solvent

form I appeared. Therefore according to Ostwald's law of stages form I is the thermodynamically stable polymorph and form II, III and IV are kinetically metastable. Table 4.3 shows values of packing fraction and density for the four polymorphs. Form I and IV have almost similar packing fraction and density and is greater than form II and III.

Table 4.3 Packing fraction and density of four polymorphs.

Form	Packing fraction	Density
Form I	65.8	1.112
Form II	62.7	1.062
Form III	62.8	1.064
Form IV	65.7	1.117

According to Wallach's rule²⁵ racemic crystals are more stable than the chiral counterparts. Brook and Dunitz²⁶ in 1991 did a CSD search to validate Wallach's rule and found that for chiral compounds (resolvable enantiomers), racemic crystals has greater average density compared to corresponding enantiomers and for achiral compounds forming chiral crystals (enantiomers interconvert rapidly in solution) difference of average density of chiral crystals to racemic crystals is not significant. In our case we have found that chiral crystal has more density and is more stable than the racemic crystals, which is against the Wallach's rule.

In 2t-Bu, greater density in case of chiral crystal is due to better molecular packing in crystal lattice compared to the racemic ones. In the crystal structure of form I hydrogen atom of p-methyl groups of tolyl ring is involved in bifurcated C—H \cdots O hydrogen bonding (C29—H29C \cdots O1 and C28—H28A \cdots O1) which leads to a better packing arrangement of the molecules in crystal lattice. Whereas in case of form II and form III hydrogen atom ortho position to p-methyl groups of tolyl ring are involved in C—H \cdots O hydrogen bonding (C16—H16 \cdots O1) because of which two bulky t-butyl groups comes close to give an open structure. But in form IV weak C—H \cdots O hydrogen bond is present which involves hydrogen atoms of p-methyl group like in form I (C16—H16A \cdots O1) (Figure 4.17). Because of this reason form IV has similar density and packing fraction as form I and form II and form III are less dense polymorphs.

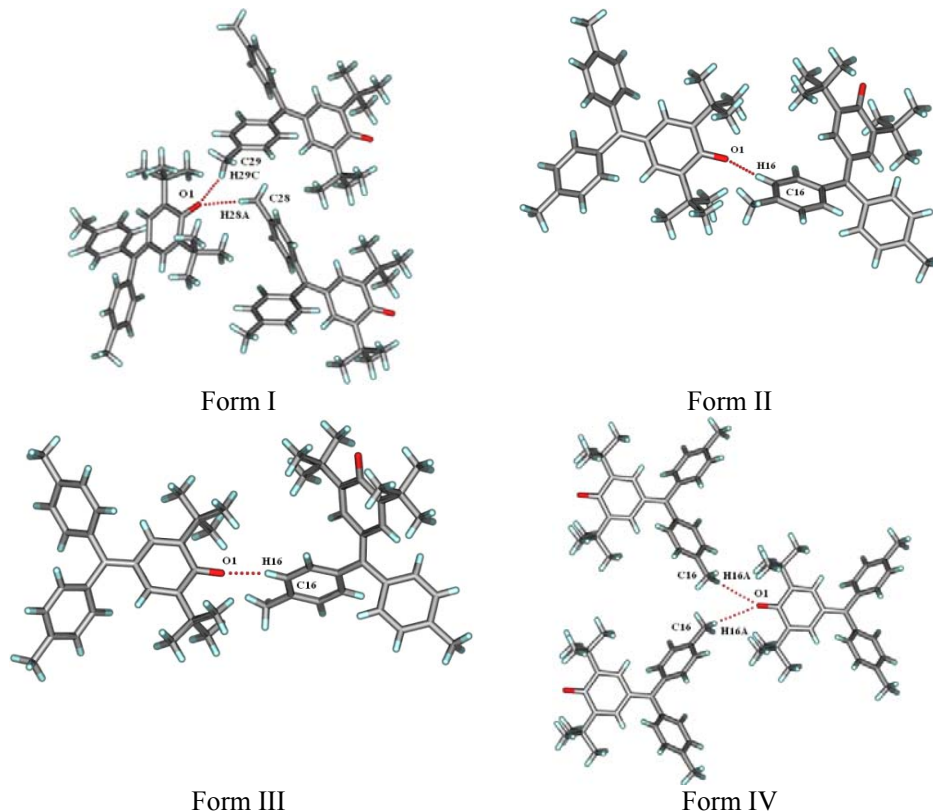


Figure 4.17 C—H...O hydrogen bonding in form I and form IV involves para methyl groups of tolyl ring whereas, in form II and form III hydrogen ortho to the methyl group of tolyl ring is involved.

4.5 CSD Search on Tetramorphic and Higher Polymorph Clusters

A CSD search (CCDC version 1.12, August 2010 update)⁷ using the search terms polymorph, form, phase or modification with 3D coordinate determined resulted in 14460 hits. Out of which there are 27 tetramorphic, 10 pentamorphic, 2 hexamorphic and 1 heptamorphic systems. The CSD ref codes for these polymorphic systems are as follows:

No of tetramorphs 27

ADULEQ	CBMZPN	PYRZIN	CERYAA
CILHIO	RUWYIR	WUWTOX	MOTNUF
BENZIE	HEYHUO	STARAC	TUWGEY
BIXGIY	KAXHAS	SLFNMB	ACRDIN
KELGEO	VISKAJ	MABZNA	WAMFAS

CDMSOR	POPGUX	TPEPHO	LCYSTN
XOFQOZ	QAHVIE	TOKSAO	
No of pentamorphs 10			
GLYCIN	IFULUQ	SUTHAZ	ZZZVXQ
BISMEV	DHANQU	KAXXAI	BEWKUJ
MELFIT	VIPKIO		
No of hexamorphs 2			
HMHO CN	BEDMIG		
No of heptamorphs 1			
QAXMEH			

Concomitant crystallization of four polymorphs is observed for molecules with refcodes RUWYIR²⁷ and HEYHUO²⁸ whereas there is only one concomitant pentamorphic system present that is trinitrobenzene (ZZZVXQ).²⁹

4.6 Conformational Differences

Conformational differences are observed among four polymorphs of 2t-Bu. Figure 4.18 shows the overlay of all the four conformations and Table 4.4 shows the torsion angles.

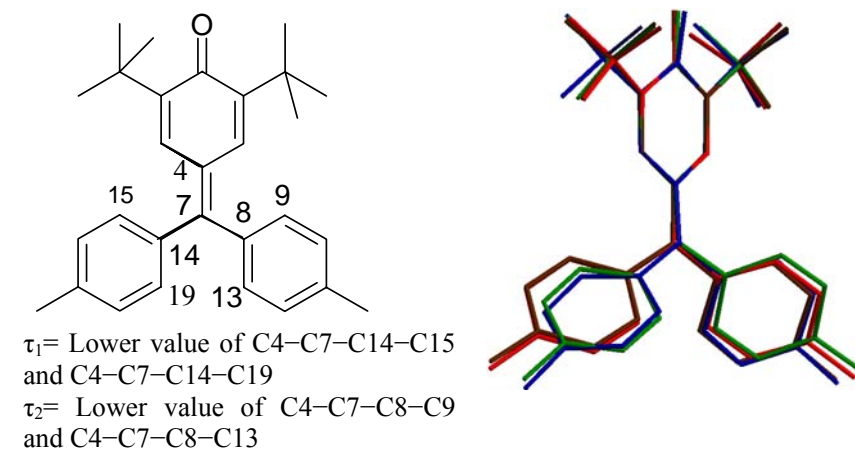


Figure 4.18 Overlay diagram showing four conformers form I (blue), form II (brown), form III (green) and form IV (red).

Table 4.4 Torsion angles for all the polymorphs of 2t-Bu

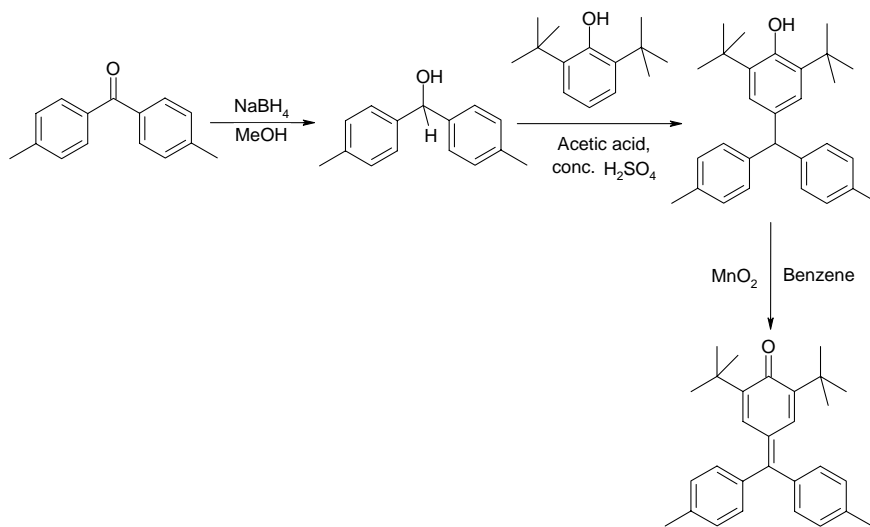
Polymorph	Torsion angles
Form I	C4–C7–C14–C15 = 38.6(2) and C4–C7–C8–C9 = 63.2(2)
Form II	C4–C7–C14–C15 = 35.6(3) and C4–C7–C8–C9 = 47.0(3)
Form III	C4–C7–C14–C15 = 42.3(2) and C4–C7–C8–C9 = 47.2(2)
Form IV	C4–C5–C6–C7 = 42.8(2)

4.7 Conclusion

Four concomitant polymorphs of 2t-Bu where one form is chiral and other three are racemic are discussed in this chapter. The ability of the t-butyl derivatives of fuchsones to crystallize in non-centrosymmetric chiral space groups is demonstrated. Occurrence of chiral crystallization of the achiral molecule is because of its ability to exist in chiral conformations. Crystallization of conformationally flexible fuchsones molecules in chiral space group are particularly important since there are no obvious barriers for their crystallization in space group with centre of inversion rather than in space group containing screw axis. Although the subtle factors behind the effect of substituents in chiral crystallization of fuchsones is not clear, however, increasing the steric influence of the substituents around the carbonyl group appears to be an important determinant. Overall, a controlled chiral crystallization is achieved due to the presence of t-butyl group in both the series of fuchsones. Thus, the molecular packing offered by the Sohncke space groups in 1t-Bu and 2t-Bu must be preferable to the more commonly observed centrosymmetric space groups.

4.8 Experimental Section

Synthesis: Scheme 4.4 shows the synthetic route of the fuchsones under study.³⁰



Scheme 4.4 Synthetic route of 2t-Bu.

4, 4'-dimethylbenzhydrol is synthesized from corresponding benzophenone (1.05 g, 5 mmol) by reaction with sodium borohydride (0.189 g, 5 mmol) in methanol. Conc. H₂SO₄ (5-6 drops) was added to a stirred solution of 2,6-di-tert-butylphenol (1.03 g, 5 mmol) and 4, 4'-dimethylbenzhydrol (1.06 g, 5 mmol) in acetic acid (15 mL). The precipitate obtained was filtered and dried to get 3,5-di-tert-butyl-4-hydroxyphenylditolymethane. A suspension of active MnO₂ (0.870 g, 10 mmol) and 3,5-di-tert-butyl-4-hydroxyphenylditolymethane (1.88 g, 5 mmol) in benzene (20 mL) was stirred for 12 h and filtered. The solvent was evaporated and dried to obtain 2t-Bu, which was purified by column chromatography in 1% EtOAc : hexane mixture.

¹H NMR (ppm): 7.21 (10H, m), 2.43 (6H, s), 1.26 (18H, s).

IR (cm⁻¹): 2956, 1629, 1602, 1515.

M. p.: 187 °C.

2i-Pr was synthesized using the above procedure with suitable starting materials.

¹H NMR (ppm): 7.25 (4H, d, J 8), 7.15 (6H, m), 3.25 (2H, m), 2.45 (6H, s), 1.09 (12H, d, J 8).

IR (cm⁻¹): 2957, 1628, 1595.

M. p.: 178 °C.

X-ray crystallography: Bruker SMART CCD diffractometer Mo-K α ($\lambda=0.71073$ Å) radiation was used to collect X-ray reflections on four polymorphs. Data reduction was performed using Bruker SAINT software.³¹ Intensities for absorption were corrected using SADABS.³² Structures were solved and refined using SHELXL-97.³³ Flack parameter was determined by collecting X-ray data on Oxford Diffraction Ltd., (Version 1.171.33.55) using Cu K α , ($\lambda=1.5418$ Å) radiation at 100 K. Data reduction was performed using CrysAlisPro, Oxford Diffraction Ltd., Version 1.171.33.55. OLEX2-1.0³⁴ and SHELXTL 97 were used to solve and refine the data. All non-hydrogen atoms were refined anisotropically, and C–H hydrogens were fixed. X-Seed³⁵ was used to prepare figures and packing diagrams.

Thermal analysis: DSC was performed on a Mettler Toledo DSC 822e module. Samples were placed in crimped but vented aluminum sample pans with sample size is 4–6 mg. DSC of form I and form III were performed at 2 °C min⁻¹ from 30 °C–210 °C, whereas DSC of form II was recorded at 0.5 °C min⁻¹ from 100 °C–200 °C. Samples were purged by a stream of dry nitrogen flowing at 150 mL min⁻¹. HSM was performed on a PolythermA Hot Stage and Heitzisch microscope supplied by Wagner & Munz. A Moticam 1000 (1.3 MP) camera supported by software Motic ImagePlus 2.0 ML is used to record images.

Solid state CD spectra: Solid state CD spectra were collected on JASCO 8.0 spectrometer. CD experiments were carried out by mounting KBr pellets of form I whose concentration ranges from 0.8% to 1%.

4.9 References

1. E. Broda, *Origins of Life*, 14, **1984**, 391. (b) L. Mörtberg, *Nature*, 232, **1971**, 105. (c) B. Norden, *Nature*, 266, **1977**, 567.
2. D. Z. Wang, *Mendeleev Commun.* **2004**, 244.
3. A. F. Casy, *Medicinal Chemistry*, 3rd ed.; Wiley-Interscience: New York, **1970**, Vol. I, pp. 81–87. (b) P. Friberger and G. Aberg, *Acta Pharm. Suec.* 8, **1971**, 361. (c) T. C. Daniels and E. C. Jorgensen, *Textbook of Organic, Medicinal and Pharmaceutical Chemistry*, 6th ed.; Lippincott: Philadelphia, **1971**, pp 31–33.

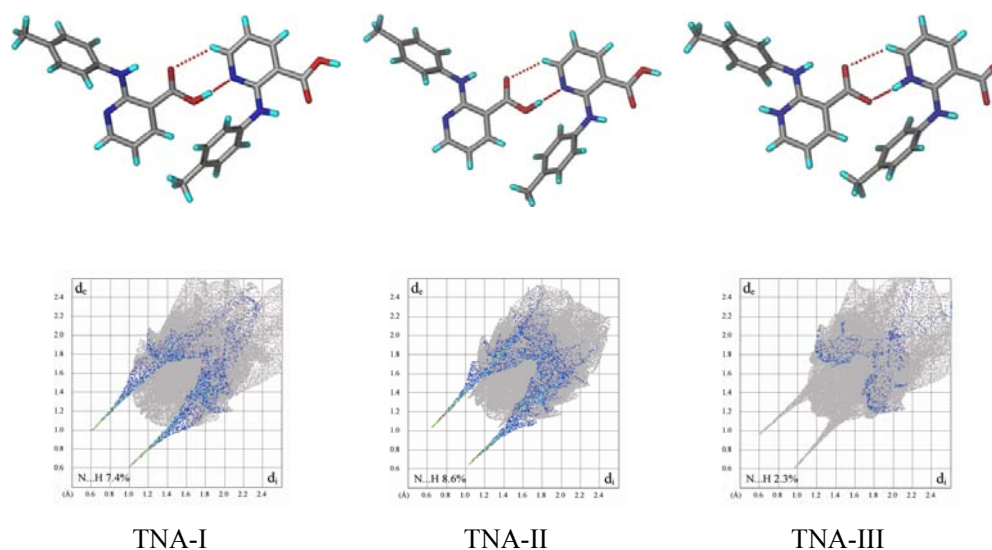
- (d) N. Himori, T. Ishimai and N. Taira, *Arch. Int. Pharmacodyn*, **242**, **1979**, 115.
- (e) P. Dayer, T. Leemann, J. Gut, T. Kronbach, A. Kupfer, R. Francis and U. Meyer, *Biochem. Pharmacol.* **343**, **1985**, 99. (e) I. W. Wainer and D. E. Drayer, *Drug Stereochemistry: Analytical Methods and Pharmacology*; Marcel Dekker: New York, **1988**.
4. E. Pidcock, *Chem. Commun.*, **2005**, 3457. (b) T. Matsuura and H. Koshima, *Journal of Photochemistry and Photobiology C: Photochemistry Reviews*, **6**, **2005**, 7.
 5. I. Kitaigorodskii, *Organic Chemical Crystallography*, Consultant's Bureau, New York, **1961**.
 6. (a) E. L. Eliel, *Stereochemistry of carbon compounds*, Tata Mcgraw-Hills, New Delhi, **1975**. (b) L. Lunazzi, M. Mancinelli, and A. Mazzanti, *J. Org. Chem.*, **73**, **2008**, 5354, (c) I. D. Cunningham, S. J. Coles and M. B. Hursthouse, *Chem. Commun.*, **2000**, 61. (d) K. C. W. Chong and J. R. Scheffer, *J. Am. Chem. Soc.* **125**, **2003**, 4040.
 7. Cambridge Crystallographic Data Center, www.ccdc.cam.ac.uk.
 8. (a) X.-Z. Li, M. Li, Z. Li, J.-Z. Hou, X.-C. Huang and D. Li, *Angew. Chem. Int. Ed.*, **47**, **2008**, 6371. (b) C. Piguet, G. Bernardinelli and G. Hopfgartner, *Chem. Rev.*, **97**, **1997**, 2005. (c) M. Albrecht, *Chem. Rev.*, **101**, **2001**, 3457. (d) L. Han and M.-C. Hong, *Inorg. Chem. Commun.*, **8**, **2005**, 406. (e) C. He, Y. Zhao, D. Guo, Z. Lin and C. Duan, *Eur. J. Inorg. Chem.* **2007**, 3451.
 9. (a) X.-C. Huang, J.-P. Zhang, Y.-Y. Lina and X.-M. Chen, *Chem. Commun.*, **2005**, 2232. (b) B. Moulton and M. J. Zaworotko, *Chem. Rev.*, **101**, **2001**, 1629. (c) X.-C. Huang, J.-P. Zhang and X.-M. Chen, *J. Am. Chem. Soc.*, **126**, **2004**, 13218. (d) T. Ezuhara, K. Endo and Y. Aoyama, *J. Am. Chem. Soc.* **121**, **1999**, 3279. (e) N. J. Babu and A. Nangia, *Cryst. Growth & Des.*, **6**, **2006**, 1995.
 10. (a) L. Pérez-García and D. B. Amabilino, *Chem. Soc. Rev.*, **31**, **2002**, 342. (b) M. Sakamoto, N. Utsumi, M. Ando, M. Saeki, T. Mino, T. Fujita, A. Katoh, T. Nishio and C. Kashima, *Angew. Chem. Int. Ed.*, **42**, **2003**, 4360. (c) D. Kondepudi, and K. Asakura, *Acc. Chem. Res.*, **34**, **2001**, 946. (d) X.-L. Tong, T.-L. Hu, J.-P. Zhao, Y.-K. Wang, H. Zhang and X.-H. Bu, *Chem. Commun.*, **2010**, 8543. (e) A. Collet, M.-J. Brienne and J. Jacques, *Chemical Reviews*, **80**, **1980**,

215. (f) E.-Q. Gao, S.-Q. Bai, Z.-M. Wang and C.-H. Yan, *J. Am. Chem. Soc.*, **125**, **2003**, 4984. (g) T. B. Norsten, R. McDonald and N. R. Branda, *Chem. Commun.*, **1999**, 719. (h) I. D. Cunningham, S. J. Coles and M. B. Hursthouse, *Chem. Commun.*, **2000**, 61. (i) M. A. Sephton, C. R. Emerson, L. N. Zakharov and P. R. Blakemore, *Chem. Commun.*, **2010**, 2094.
11. (a) L. Pasteur, *Ann. Chim. Phys.*, **24**, **1848**, 442. (b) M. Nakazaki, *Kagaku no Ryoiki*, **33**, **1979**, 951 (in Japanese). (c) Y. Tobe, *Mendeleev Communications*, **2003**, 1.
12. (a) D. Y. Curtin and I. C. Paul, *Chem. Rev.*, **81**, **1981**, 525. (b) *Non-linear Optical Properties of Organic Molecules and Crystals*; Eds. J. Zyss and D. S. Chemla, Academic Press: New York, **1987**, vols. 1 and 2.
13. (a) M. Sakamoto, *Chem. Eur. J.*, **3**, **1997**, 684. (b) T. Suzuki, T. Fukushima, Y. Yamashita and T. Miyashi, *J. Am. Chem. Soc.*, **116**, **1994**, 27933. (c) M. Sakamoto, S. Kobaru, T. Mino and T. Fujita, *Chem. Commun.*, **2004**, 1002. (d) H. Koshima, H. Kawanishi, M. Nagano, H. Yu, M. Shiro, T. Hosoya, H. Uekusa and Y. Ohashi, *J. Org. Chem.*, **70**, **2005**, 4490.
14. M. Avalos, R. Babiano, P. Cintas, J. L. Jiménez and J. C. Palacios, *Chem. Commun.*, **2000**, 887.
15. (a) W. C. McCrone, *Polymorphism in Physics and Chemistry of the Organic Solid State*, ed. D. Fox, M. M. Labes and A. Weissberger, Wiley-Interscience, New York, **1965**, 2, 725–767; (b) A. Nangia, *Acc. Chem. Res.*, **41**, **2008**, 595.
16. J. Bernstein, *Polymorphism in Molecular Crystals*, Clarendon, Oxford, **2002**, pp-3.
17. J. Bernstein, R. J. Davey and J.-O. Henck, *Angew. Chem. Int. Ed.*, **38**, **1999**, 3440.
18. S. K. Chandran, N. K. Nath and S. Roy, *Cryst. Growth Des.*, **8**, **2008**, 140.
19. (a) T. W. Lewis, I. C. Paul and D. Y. Curtin, *Acta Cryst.*, **B36**, **1980**, 70. (b) E.N. Duesler, T. W. Lewis, D. Y. Curtin and I. C. Paul; *Acta Cryst.*, **B36**, **1980**, 166.
20. P. S. Kalsi, *Stereochemistry Conformation and Mechanism*, New Age International (P) Limited Publishers, New Delhi, **2008**, 149.
21. (a) G. Pescitelli, S. D. Pietro, C. Cardellicchio, M. A. M. Capozzi and L. D. Bari, *J. Org. Chem.*, **75**, **2010**, 1143. (b) M. Minguet, D. B. Amabilino, K. Wurst and J.

- Veciana, *J. Chem. Soc., Perkin Trans. 2*, **2001**, 670. (c) H.-Q. Hao, W. -T. Liu, W. Tan, Z.-J. Lin and M.-L. Tong, *CrystEngComm*, **11**, **2009**, 967. (d) Q. Sun, Y. Bai, G. He, C. Duan, Z. Lin and Q. Meng, *Chem. Commun.*, **2006**, 2777.
22. H. D. Flack, *Acta Cryst.*, **A39**, **1983**, 876.
23. (a) A. Lennartson, T. Wiklund and M. Håkansson, *CrystEngComm*, **9**, **2007**, 856. (b) M. Vestergren, A. Johansson, A. Lennartson and M. Håkansson, *Mendeleev Commun.*, **2004**, 258. (c) A. Lennartson, M. Vestergren and M. Håkansson, *Chem.-Eur. J.*, **11**, **2005**, 1757.
24. W. F. Ostwald, *Z. Phys. Chem.*, **22**, **1897**, 289.
25. O. Wallach, *Liebigs Ann. Chem.*, **286**, **1895**, 90.
26. C. P. Brock, W. B. Schweizer and J. D. Dunitz, *J. Am. Chem. Soc.*, **1991**, **113**, 9811.
27. M. Morimoto, S. Kobatake and M. Irie, *Chem. -Eur. J.*, **9**, **2003**, 621.
28. V. S. S. Kumar, A. Addlagatta, A. Nangia, W. T. Robinson, C. K. Broder, R. Mondal, I. R. Evans, J. A. K. Howard and F. H. Allen, *Angew. Chem., Int. Ed.*, **41**, **2002**, 3848.
29. D. A. Parrish, J. R. Deschamps, R. D. Gilardi and R. J. Butcher, *Cryst. Growth Des.*, **8**, **2008**, 57.
30. H.-D. Becker, *J. Org. Chem.*, **32**, 1967, 2131.
31. *SAINT-Plus, version 6.45*; Bruker AXS Inc.: Madison, WI, **2003**.
32. G. M. Sheldrick, *SADABS, Program for Empirical Absorption Correction of Area Detector Data*, University of Göttingen, Germany, 1997.
33. (a) *SMART (Version 5.625) and SHELX-TL (Version 6.12)*; Bruker AXS Inc.: Madison, WI, **2000**. (b) G. M. Sheldrick, *SHELXS-97 and SHELXL-97*; University of Göttingen, Germany, **1997**.
34. O. V. Dolomanov, A. J. Blake, N. R. Champness and M. Schröder, *J. Appl. Cryst.* **36**, **2003**, 1283.
35. L. J. Barbour, X-Seed, *Graphical Interface to SHELX-97 and POV-Ray*, University of Missouri-Columbia, USA, **1999**.

Chapter Five

Neutral and Zwitterionic Polymorphs of 2-(*p*-Tolylamino) Nicotinic Acid (TNA)

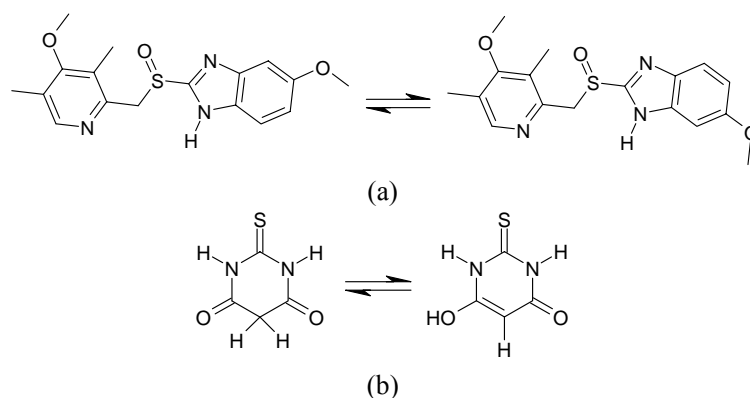


2D fingerprint plots for Hirshfeld surface show clear differences of $N\cdots H$ interactions of neutral polymorphs TNA-I, TNA-II and zwitterionic form TNA-III.

*Characterization of Neutral and Zwitterionic polymorphic cluster of 2-(*p*-tolylamino) nicotinic acid (TNA) is presented.*

5.1 Introduction

Polymorphism has been defined by many authors in literature¹, nevertheless, McCrone's definition is widely accepted i.e. "a solid crystalline phase of a given compound resulting from the possibility of at least two different crystalline arrangements of the molecules of that compound in the solid state".² The essence of all definitions is polymorphs involve different arrangements of the same molecule in the crystalline forms. For rigid molecules and with unambiguous crystal structures the meaning of the term polymorphism is not complicated. With the great number of crystal structures added to the 'Cambridge Structural Database' in recent years, the complexity of crystal structures has also increased side by side. Examples of few complications are, systems in which the dynamic isomers or tautomers are different molecules if the rate of interconversion is slow but are regarded as polymorphs if they interconvert rapidly in solution or in melt.^{1,3} Similarly, a racemate and a conglomerate would be considered as polymorphs if the rate of interconversion is fast and they are different compounds when the rate of interconversion is slow in liquid state.^{1,3} A case of racemic and chiral polymorphs was discussed in Chapter 4. But in borderline cases the distinction between polymorph and different compounds is still fuzzy. Two recent examples of tautomeric polymorphism are omeprazole⁴ and 2-thiobarbituric acid (Scheme 5.1).⁵



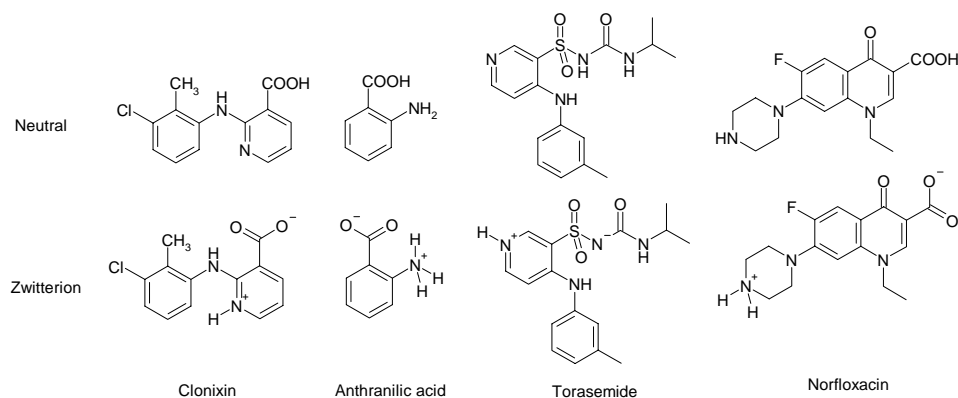
Scheme 5.1 (a) Two tautomers of omeprazole present in its tautomeric polymorphs. (b) These two tautomers are distributed among the five polymorphs of 2-thiobarbituric acid.

Nomenclature issue may arise due to intramolecular transfer of proton, i.e., neutral and zwitterionic nature of the molecules in the two polymorphs. Zwitterions contain both positive and negative formal charges on different atoms within the molecule

and are electrically neutral through a net cancellation of the formal positive and negative charges.⁶ In solution both the neutral and the zwitterionic form may exist and one form may predominate depending on the pH of the environment and the type of substituent present in the compound. These ambiguities occurring in order to qualify crystal structures as polymorphs are not only a matter of linguistics but may also have scientific and economic importance as well as patenting implications.^{4,7}

Ampholytes are amphoteric compounds contain both acidic and basic groups and exist as zwitterions in certain pH ranges. Amino acids are the classic example of zwitterions. In addition to amino acids, some other common types of zwitterions are buffers, detergents, dyes and drugs. Amphoteric compounds are frequently encountered in medicinal chemistry as drugs or drug metabolites and in biochemistry.⁸ Amphoteric drug molecules predominantly exist as charged species in physiological pH conditions and therefore these drugs can be used for specific targets.⁹ Because of the variable pH conditions in the digestive tract (varies from 1.2 to 6.8), an amphoteric drug can exist in zwitterionic as well as ionic states. This variable structure of the drug molecule results in differential physico-chemical behavior with respect to solubility, permeability and consequently bioavailability.

There are very few examples of molecules exhibiting both neutral and zwitterionic crystal structures. The Cambridge Structural Database (CSD ver 5.32, November 2010, May 2011 update) search showed that there are only four molecules (Scheme 5.2) which exhibit neutral and zwitterionic polymorphic clusters (solved X-ray crystal structure for single component organic systems). Clonixin¹⁰ form II (BIXGIY04) is zwitterionic whereas the other polymorphs of this tetramorphic compound are neutral (BIXGIY01, BIXGIY02, BIXGIY03). The monoclinic polymorph of Norfloxacin¹¹ is zwitterionic (VETVOG01) whereas the triclinic polymorph is neutral (VETVOG). Anthranilic acid¹² is trimorphic: neutral monoclinic (AMBACO08), neutral orthorhombic (AMBACO05) and zwitterionic orthorhombic (AMBACO07). Torasemide¹³ has one crystal structure that has one zwitterion and another neutral molecule (TORSEM02) while the second polymorph is fully zwitterionic (TORSEM04).



Scheme 5.2 Clonixin and Norfloxacin exhibit exclusive zwitterionic and neutral polymorphic cluster whereas anthranilic acid and torasemide exhibit partial zwitterionic polymorphs (both neutral and zwitterionic molecules are present in the same crystal structure).

Clonixin, a nonsteroidal anti-inflammatory drug, is tetramorphic and its form II is zwitterionic whereas other three forms are neutral (Figure 5.1).¹⁰

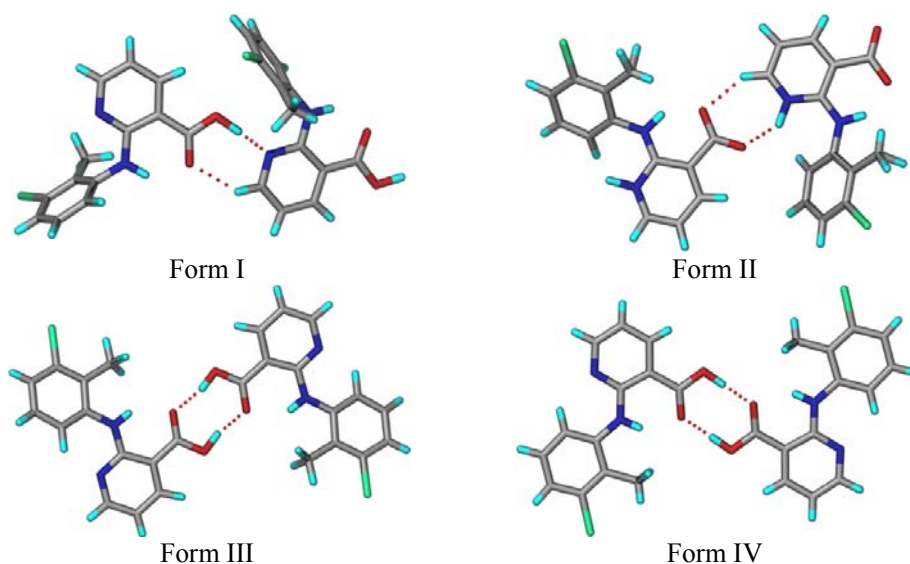


Figure 5.1 Clonixin form II is zwitterionic and contains ionic carboxylate-pyridinium synthon whereas the other three polymorphs are neutral.

Norfloxacin is a broad spectrum antibacterial drug and in the CSD two anhydrous crystal structures are reported, one in triclinic space group $P\bar{1}$ and another in monoclinic space group $P2_1/c$, both are named as form A. The monoclinic polymorph is zwitterionic whereas the triclinic polymorph is neutral.^{11,14}

Anthranilic acid form I contains one neutral and one zwitterionic molecule in the asymmetric unit. Form I contains $R_6^4(12)$ hydrogen bonding motif whereas form II and form III contain carboxylic acid dimer as major synthon. (Figure 5.2).^{12,15}

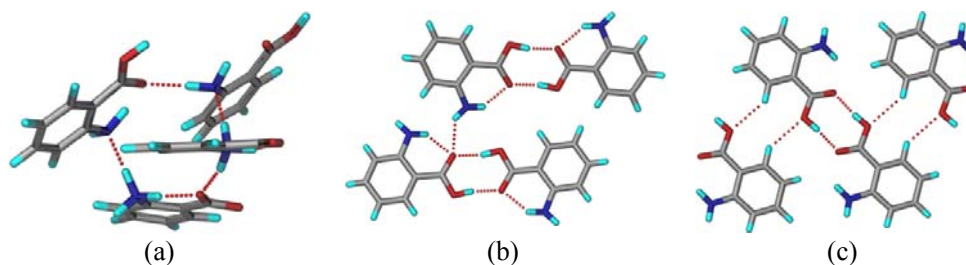
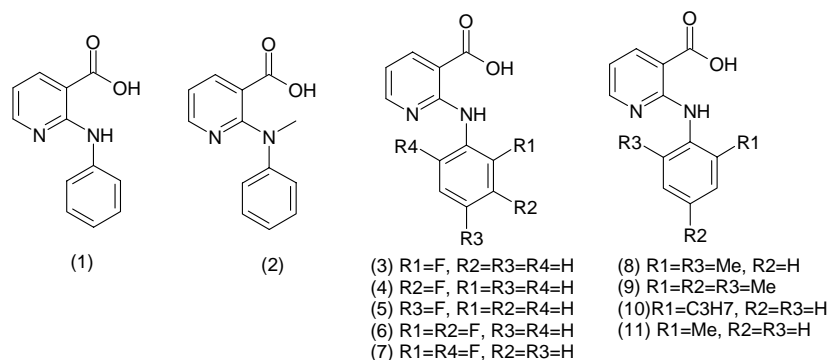


Figure 5.2 (a) $R_6^4(12)$ hydrogen bonding motif present in form I of Anthranilic acid whereas carboxylic acid is the main synthon in form II and form III.

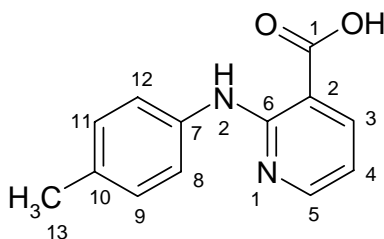
A similar example is Torasemide, a diuretic, which has three polymorphs in the CSD, named as form i, form ii and nonsolvated form T-N. The crystal structure of form i contains two molecules in the asymmetric unit, one is zwitterionic, proton being transferred from urea N to pyridine N, and other molecule is neutral. Form ii and form T-N contain two symmetry independent molecules each and are in zwitterionic form.^{13, 16}

Many diarylamines exhibit anti-inflammatory drug¹⁷ properties, eg., Niflumic acid, Clonixin, Mefenamic acid, Tolfenamic acid, Flufenamic acid Meclofenamic acid, Diclofenac etc. Most of these molecules exhibit polymorphic behavior.^{10,18} However, except clonixin, none of these compounds, including the recently reported pentamorphs of tolfenamic acid^{18e} illustrate an example of zwitterionic and neutral structures among the polymorphs. Tonglei Li et al¹⁹ have been working on the polymorphism of diaryl amine series. Scheme 5.3 shows the molecular structures of the compounds they have studied so far.



Scheme 5.3 The 11 Diaryl amines reported by Tonglei Li et al.

The synthon competition and cooperation among a series of carboxylic acids and amino pyridines in presence of different functional groups was studied by our group where proton transfer was found in all cases.²⁰ If both acid and pyridine functionalities are present in the same molecule, three possibilities may arise such as acid-acid homosynthon, acid-pyridine hetero-synthon which are most probable and intramolecular proton transfer to give carboxylate-pyridinium ionic synthon resulting a zwitterionic structure. All these possibilities may combine to give different polymorphic structures too. With this background, the nicotinic acid derivative 2-(p-tolylamino) nicotinic acid (TNA) was synthesized which falls in the category of diaryl amine (Scheme 5.4) and is an ampholyte. Extensive polymorph screening on TNA was performed using different crystallization techniques and was cocrystallized with carboxylic acid and pyridine derivatives.



Scheme 5.4 Molecular structure of 2-(p-tolylamino) nicotinic acid (TNA).

Even though the molecules studied by Tonglei Li et al. (Scheme 5.3) are structurally very close to TNA (particularly compounds a and b), the authors did not

disclose any example of neutral and zwitterionic polymorph sets in their series. Both 2-(phenylamino)nicotinic acid and 2-[methyl(phenyl)amino]nicotinic acid were found to be tetramorphic in their polymorph hunt.

5.2 Results and Discussion

TNA was synthesized (detailed in experimental section) and crystallized by various techniques such as slow evaporation, melting, sublimation, slow cooling, flash cooling and crystallization in presence of coformers to obtain three polymorphic modifications viz. form I (TNA-I) and form II (TNA-II) which are neutral and form III (TNA-III) which exist as zwitterion. TNA-I and TNA-II mostly crystallized concomitantly from acetone, methanol, ethanol, ethyl acetate, acetonitrile, chloroform and THF. TNA-II was obtained exclusively by melt crystallization. Zwitterionic form TNA-III was obtained when TNA was cocrystallized with 2-bromo-3-hydroxy pyridine, 2-amino pyridine, isonicotinic acid and nicotinic acid in CH₃CN solvent. The method could not be fully optimized since occasionally along with TNA-I or TNA-II or a molecular salt with 2-aminopyridine were also characterized. TNA-III could not be crystallized from solution crystallization in absence of pyridine type coformers. Solution crystallization of TNA and 2-aminopyridine from CH₃CN resulted in the corresponding molecular salt along with TNA-I or TNA-II and TNA-III. Other cocrystal formers such as dicarboxylic acids, 3-nitro benzoic acid etc. did not induce any zwitterion formation, instead cocrystal and molecular salt were obtained for these combinations. Cocrystallization of TNA with 3-nitrobenzoic acid in 1: 1 molar ratio resulted a cocrystal in 1:2 ratio where TNA is in zwitterionic form whereas 2-aminopyridine gave a 1:1 molecular salt. Crystallographic parameters of the three polymorphs are compared in Table 5.1. Detailed crystallographic parameters of all the crystal structures are listed in Appendix.

Table 5.1 Comparison of cell parameters of the three polymorphs to highlight the differences.

TNA	TNA-I	TNA-II	TNA-III (LT)	TNA-III (RT)
Crystal system	Monoclinic	Orthorhombic	Orthorhombic	Orthorhombic
Space group	<i>P2₁/n</i>	<i>Pbca</i>	<i>Pbca</i>	<i>Pbca</i>
T (K)	100	100	100	298

$a/\text{\AA}$	11.038(10)	14.2565(16)	9.0787(11)	9.250(4)
$b/\text{\AA}$	9.067(8)	10.7542(15)	14.2261(17)	14.207(4)
$c/\text{\AA}$	11.392(10)	14.769(3)	17.154(2)	17.509(10)
$\alpha/^\circ$	90	90	90	90
$\beta/^\circ$	101.860(14)	90	90	90
$\gamma/^\circ$	90	90	90	90
$V/\text{\AA}^3$	1115.8(17)	2264.3(6)	2215.6(5)	2301.1(17)
$D_{\text{calcd}} (\text{g cm}^{-3})$	1.359	1.339	1.369	1.318
Z/Z'	4/1	8/1	8/1	8/1
$R_1 [I > 2 \sigma(I)]$	0.0598	0.0497	0.0521	0.0646

5.2.1 Crystal structure analysis

TNA-I: Block morphology crystals of TNA-I obtained from acetone solvent were solved and refined in the monoclinic space group $P2_1/n$ with one molecule in the asymmetric unit ($Z'=1$). Chains of molecules linked by acid-pyridine two point synthon ($\text{O1-H1}\cdots\text{N1}$, 1.59 Å, 175.6° and $\text{C5-H5}\cdots\text{O2}$, 2.55 Å, 133.1°) are connected by $\text{C-H}\cdots\pi$ interaction ($\text{C4-H4}\cdots\text{C12}$, 2.88 Å, 145.8°) to make a planar sheet like structure. Such sheets are interlinked on either side by $\text{C-H}\cdots\pi$ interaction ($\text{C9-H9}\cdots\text{C3}$, 2.84 Å, 162.1°) and by $\text{C-H}\cdots\text{O}$ hydrogen bond ($\text{C12-H12}\cdots\text{O1}$, 2.58 Å, 174.7°) (Figure 5.3).

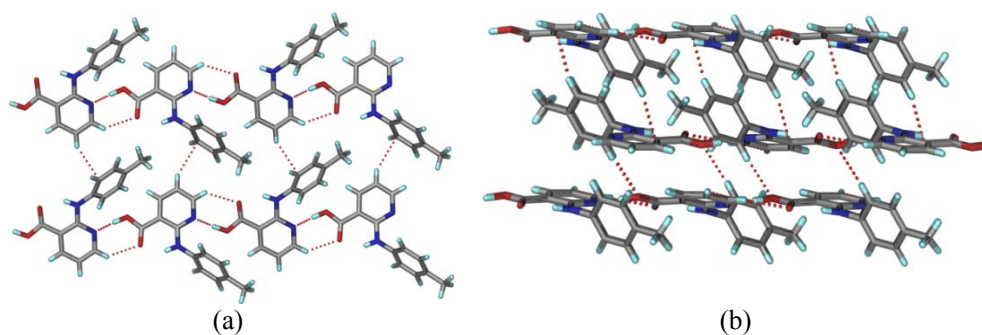


Figure 5.3 TNA-I. (a) $\text{C-H}\cdots\pi$ interactions connect chains of molecules formed by acid-pyridine synthon to result in 2D sheets. (b) These 2D sheets in turn complete the overall packing via formation of $\text{C-H}\cdots\pi$ and $\text{C-H}\cdots\text{O}$ interactions on either side.

TNA-II: Block morphology crystals of TNA-II obtained from methanol solvent were solved and refined in the orthorhombic space group $Pbca$ ($Z'=1$). In the crystal structure, acid-pyridine synthon ($\text{O1-H1}\cdots\text{N1}$, 1.68 Å, 174.7° and $\text{C5-H5}\cdots\text{O2}$, 2.49 Å, 136.1°) connects the molecules to form chains, which are interlinked by $\text{C-H}\cdots\text{O}$

(C13–H13A \cdots O2, 2.59 Å, 150.4°) hydrogen bond in 2D zigzag sheets. The 3D packing is completed by off-set $\pi\cdots\pi$ stack (3.39 Å) between pyridine rings (Figure 5.4).

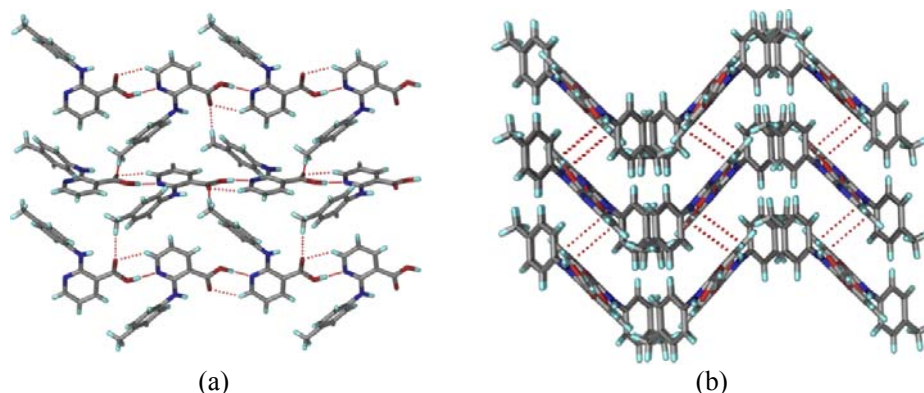


Figure 5.4 TNA-II. (a) 2D zigzag sheets formed by acid-pyridine synthon connected molecules. (b) These zigzag sheets are connected by $\pi\cdots\pi$ stack.

TNA-III: Block morphology crystals of TNA-III represent an interesting case where intramolecular proton transfer is observed. The proton migration is partial at room temperature and complete at 100 K as evident from room temperature (298 K) and low temperature (100 K) single crystal XRD data. Crystals of TNA-III were solved and refined in orthorhombic space group *Pbca* with one molecule in the asymmetric unit ($Z'=1$). The crystal structures at 298 K and 100 K datasets did not show any conformational and structural difference.

In the 100 K crystal structure of TNA-III, chains of molecules, formed by ionic carboxylate-pyridinium heterosynthon involving $N^+-H\cdots O^-$ ($N1^+-H1\cdots O1^-$, 1.59 Å, 170.9°) and auxiliary $C-H\cdots O$ hydrogen bond ($C5-H5\cdots O2$, 2.55 Å, 137.0°), are interlinked by $C-H\cdots O$ hydrogen bond ($C13-H13A\cdots O2$, 2.71 Å, 136.9°) and $C-H\cdots\pi$ interaction ($C4-H4\cdots C12$, 2.85 Å, 146.4°) result in 2D sheets. The structure is completed by $C-H\cdots O$ hydrogen bond ($C9-H9\cdots O2$, 2.46 Å, 164.0° and $C12-H12\cdots O1$, 2.52 Å, 172.4°) on either side of such 2D sheets (Figure 5.5).

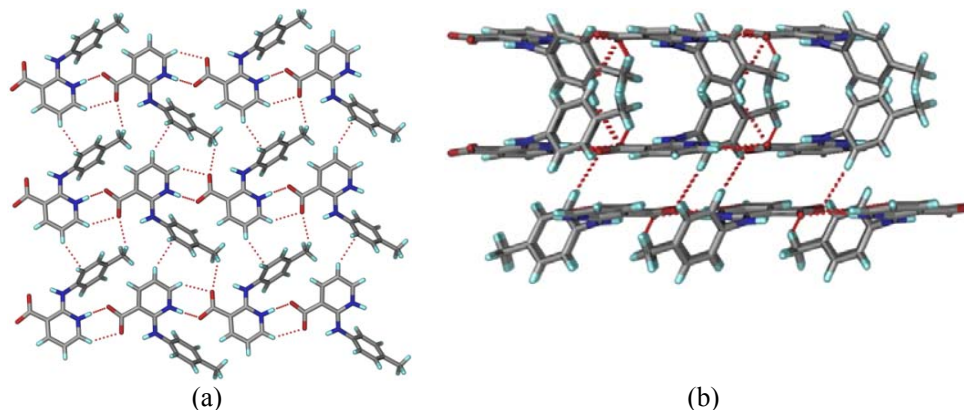


Figure 5.5 TNA-III. 2D sheets formed by chains connected by carboxylate-pyridinium heterosynthon. (b) 3D structure is completed by formation of C-H...O hydrogen bond on either side of such 2D sheets.

Cocrystal of TNA and 3-nitrobenzoic acid ($\text{NH}^+\text{-TNA-COO}^- \cdot 2\text{NBA}$): In the cocrystal of TNA with 3-nitrobenzoic acid intramolecular proton transfer has occurred in the TNA molecule but the expected carboxylate-pyridinium ionic synthon is replaced by pyridinium-nitro synthon ($\text{N1}^+\text{-H1}\cdots\text{O6}$, 2.17 Å, 152.5° and $\text{C5-H5}\cdots\text{O5}$, 2.53 Å, 138.8°). Carboxylate group of TNA is involved in O-H...O hydrogen bonding ($\text{O3-H3A}\cdots\text{O1}$, 1.66 Å, 170.1° and $\text{O8-H8A}\cdots\text{O2}$, 1.63 Å, 170.4°) with carboxylic acid group of 3-nitrobenzoic acid molecule as shown in Figure 5.6.

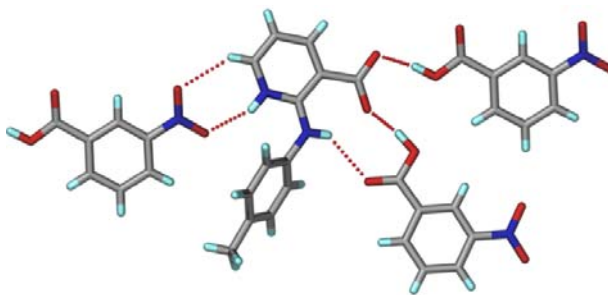


Figure 5.6 Hydrogen bond synthons in TNA•3-nitrobenzoic acid cocrystal where zwitterionic structure of TNA is present.

Molecular salt of TNA and 2-aminopyridine ($\text{AP-NH}^+\text{-TNA-COO}^-$): In this crystal structure proton transfer occurred from TNA to the 2-aminopyridine via a carboxylate...pyridinium synthon involving ionic $\text{N}^+\text{-H}\cdots\text{O}^-$ ($\text{N4}^+\text{-H4A}\cdots\text{O2}^-$, 1.74Å,

177.3°) and N–H···O[−] (N3–H3B···O1[−], 1.95 Å, 176.1°) hydrogen bonds whereas TNA pyN is free (Figure 5.7).

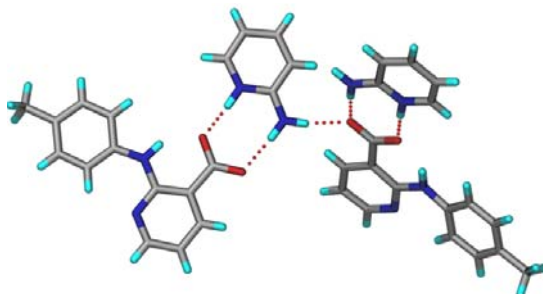


Figure 5.7 Synthons involved in the molecular salt of TNA and 2-aminopyridine.

Intramolecular N–H···O hydrogen bond is present in all the crystal structures (N2–H2···O2, 1.90, 147.3 TNA-I, 1.94, 141.7 for TNA-II, 1.84, 154.3 for TNA-III and in cocrystal 1.90, 139.1). Hydrogen bond parameters are listed in Table 5.2.

Table 5.2 Hydrogen bond distances, angles and symmetry codes of the crystal structures.

Interactions	H···A/ Å	D···A/ Å	∠D–H···A/°	Symmetry code
TNA-I				
N2–H2···O2	1.90	2.591(4)	147.3	Intramolecular
O1–H1···N1	1.59	2.591(4)	175.6	1/2+x, 1/2-y, 1/2+z
C3–H3···O1	2.34	2.672(5)	99.8	Intramolecular
C5–H5···O2	2.55	3.272(5)	133.1	-1/2+x, 1/2-y, -1/2+z
C12–H12···O1	2.58	3.526(5)	174.7	3/2-x, -1/2+y, 1/2-z
TNA-II				
O1–H1···N1	1.68	2.663(1)	174.7	-1/2+x, 1/2-y, 1-z
N2–H2···O2	1.94	2.669(1)	141.7	Intramolecular
C3–H3···O1	2.38	2.704(2)	100.2	Intramolecular
C5–H5···O2	2.49	3.222(2)	136.1	1/2+x, 1/2-y, 1-z
C13–H13A···O2	2.58	3.452(2)	150.4	1/2+x, y, 1/2-z
TNA-III at 100 K				
N1–H1···O1	1.76	2.631(2)	141.6	3/2-x, 1/2+y, z
N2–H2···O2	1.84	2.630(2)	154.3	Intramolecular
C3–H3···O1	2.39	2.722(3)	100.0	Intramolecular
C5–H5···O2	2.55	3.312(3)	137.0	3/2-x, 1/2+y, z
C9–H9···O2	2.46	3.379(3)	164.0	1-x, 1/2+y, 1/2-z
C12–H12···O1	2.52	3.463(3)	172.4	-1/2+x, 1/2-y, -z
TNA-III at 298 K				
N1–H1···O1	1.28	2.571(4)	164.2	3/2-x, -1/2+y, z
N2–H2···O2	1.91	2.644(4)	137.4	Intramolecular

C3–H3...O1	2.38	2.716(4)	101.0	Intramolecular
C5–H5...O2	2.52	3.273(4)	137.7	$3/2-x, -1/2+y, z$
C9–H9...O2	2.57	3.485(6)	166.5	$1-x, -1/2+y, 1/2-z$
NH⁺·TNA-COO⁻·2 NBA				
N1–H1...O6	2.17	2.962(2)	152.5	x, y, z
N2–H2...O2	1.91	2.621(2)	139.1	Intramolecular
N2–H2...O7	2.49	3.176(2)	137.2	$2-x, -y, 1-z$
O3–H3A...O1	1.66	2.568(2)	170.1	$-1+x, y, -1+z$
O3–H3...O2	2.58	3.056(2)	112.7	$-1+x, y, -1+z$
O8–H8A...O2	1.63	2.600(2)	170.4	$2-x, -y, 1-z$
C3–H3...O1	2.44	2.763(2)	100.3	Intramolecular
C5–H5...O5	2.53	3.286(2)	138.8	x, y, z
C5–H5...O10	2.33	3.041(2)	132.5	$1-x, 1-y, -z$
C8–H8...O1	2.40	3.316(2)	168.2	$2-x, 1-y, 1-z$
C12–H12...O9	2.53	3.447(2)	167.5	$x, y, 1+z$
C19–H19...O9	2.51	3.354(3)	151.9	$1-x, -y, -z$
C25–H25...O5	2.50	3.431(2)	177.0	$1-x, 1-y, -z$
C26–H26...O4	2.53	3.457(2)	174.0	$1-x, 1-y, -z$
AP-NH⁺·TNA-COO⁻				
N2–H2...O2	1.85	2.626(2)	146.2	Intramolecular
N3–H3A...O1	1.92	2.806(2)	169.5	$1/2+x, 3/2-y, 2-z$
N3–H3B...O1	1.94	2.843(2)	176.2	$1+x, y, z$
N4–H4A...O2	1.74	2.657(2)	177.2	$1+x, y, z$
C8–H8...N1	2.3217	2.919(2)	121.7	Intramolecular

The proton transfer was verified from the crystal structures by the analysis of C–O bond distances, O–C–O bond angles of carboxylic acid/ carboxylate group and C–N–C bond angles of the pyridine ring (Table 5.3). The length of the two C–O bond distances (C–O and C=O) in TNA-I (1.30 Å and 1.23 Å) and TNA-II (1.32 Å and 1.22 Å) indicate a neutral COOH group whereas the C–O bond distances being near equal (1.26 Å and 1.25 Å) in TNA-III imply a COO⁻ residue. Similarly, O–C–O and C–N–C bond angles argue in favor of a zwitterionic structure in TNA-III but neutral structures in TNA-I and TNA-II. There is a slight difference in the proton state between the crystal structures of TNA-III determined at 100 K and 298 K (referred to as LT and RT). The proton is fully located on the pyridine N and the carboxylate group is ionic in the LT crystal structure. The transfer of proton from COOH to pyridine N is slightly less so at RT. There is a partial proton occupancy near O and partial near N, though the values are almost impossible to assign from X-ray data. This slight drift of the proton towards the

neutral state is reflected more accurately by the bond distances and angles listed in Table 5.3. The difference between the C–O values increases slightly and the C–N–C angle shrinks by a degree.

Table 5.3 Comparison of C–O bond distances, O–C–O and C–N–C angles of the three polymorphs.

Polymorph	Bond distances(Å)	Angles (°)	
	C1–O1, C1–O2	O1–C1–O2	C5–N1–C6
TNA-I	1.303(4), 1.217(3)	123.9(3)	119.1(3)
TNA-II	1.316(2), 1.223(2)	123.3(1)	118.8(1)
TNA-III LT	1.261(3), 1.249(3)	125.9(2)	122.7(2)
TNA-III RT	1.269(5), 1.242(5)	125.7(3)	121.0(3)
NH ⁺ -TNA-COO ⁻ •2 NBA	1.245(2), 1.236(2)	125.6(1)	123.8(1)
AP-NH ⁺ •TNA-COO ⁻	1.252(2), 1.266(2)	118.2(2)	118.2(2)

5.2.2 Similarities and differences in the crystal structures of TNA-I and TNA-III

TNA-I and TNA-III possesses 2D isostructural sheets although they contain different synthons (TNA-I, acid-pyridine synthon whereas TNA-III contains carboxylate-pyridinium synthon), have different cell parameters and space groups but similar conformations. The calculated XRD lines of the two polymorphs show close peak positions (Figure 5.8a). TNA-II crystal structure is entirely different and its calculated XRD lines show clear differences from TNA-I and TNA-III (Figure 5.8b and c). The main structural difference between the structures of polymorph I and III is in the direction of the molecular layers in the identical 2D sheets. If the direction of TNA molecules connected by carboxylic acid–pyridine (in TNA-I) or carboxylate–pyridinium (in TNA-III) running in one direction (right to left) is designated as X and the opposite direction as Y, then the adjacent layers contain the motif YXYXYXY in TNA-I where the sequence is XXYXYXY in TNA-III (Figure 5.9). Thus the difference is more than just a shift of the proton, it is the tessellation of molecules in 3D that is different between TNA-I and III. A similar packing difference between the polymorphs of anti-inflammatory drug nimesulide was noted by our group recently.²¹

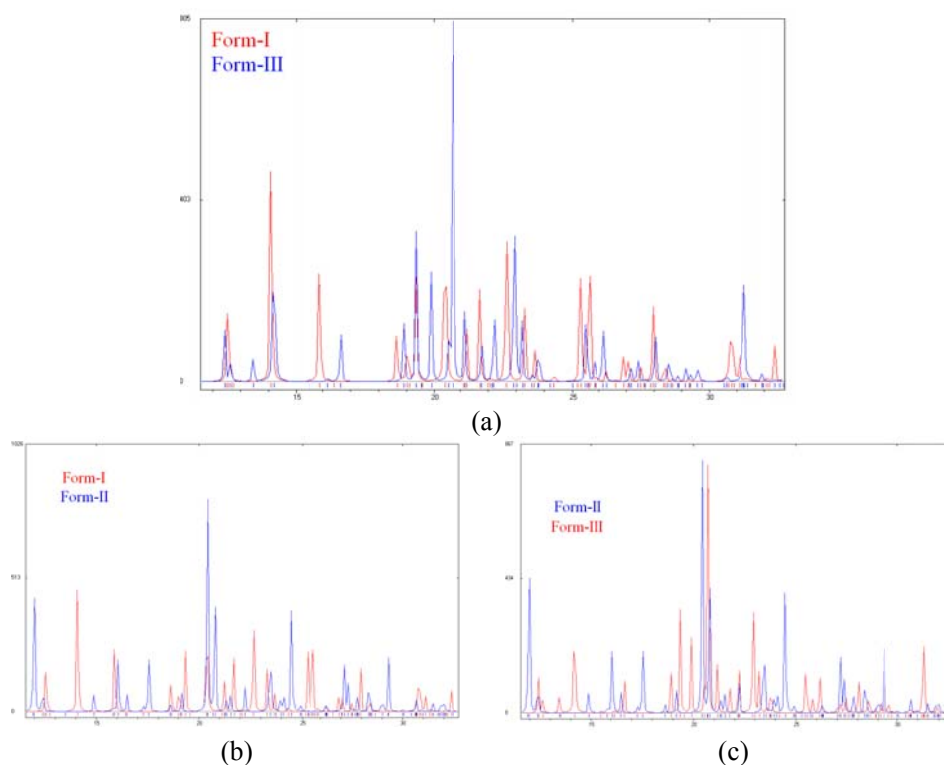
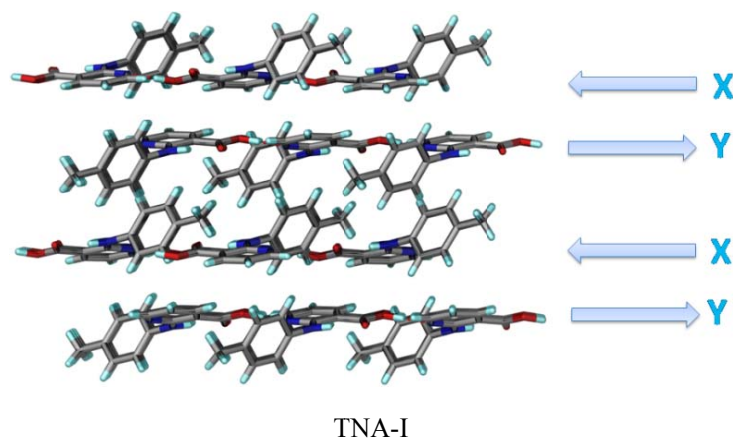
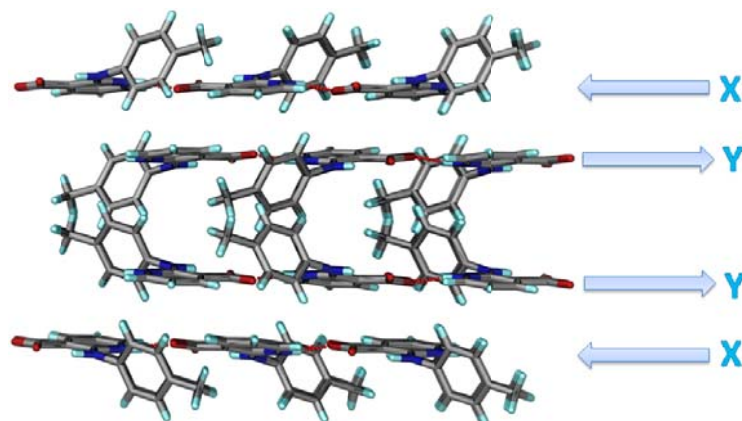


Figure 5.8 Overlay of calculated XRD lines of (a) TNA-I (red) and TNA-III (blue), (b) TNA-I (red) and TNA-II (blue) and (c) TNA-II (blue) and TNA-III (red).





TNA-III

Figure 5.9 Adjacent layer in the crystal structures of TNA polymorphs. The sequence is XYXYXYXY in TNA-I but XXYYXXYY in TNA-III. The other difference in hydrogen bonding is a neutral $\text{O}-\text{H}\cdots\text{N}$ hydrogen bond in TNA-I and ionic $\text{N}-\text{H}^+\cdots\text{O}^-$ in TNA-III.

5.2.3 XPac analysis of polymorphs I and III

The XPac method²² allows the identification of similar packing arrangements in two given molecular crystal structures and produces parameters which characterize their degree of similarity. XPac analysis of TNA structures I and III produced a 2D supramolecular construct (Figure 5.10a). The XPac plot (Figure 5.10b) of δ_p vs δ_a (in $^\circ$) shows the degree of similarity. δ_p and δ_a points lying close the origin indicate a closeness of the structures being compared. The XPac dissimilarity index X is 3.5%, given the similarity of the 2D supramolecular constructs in the two crystal structures.

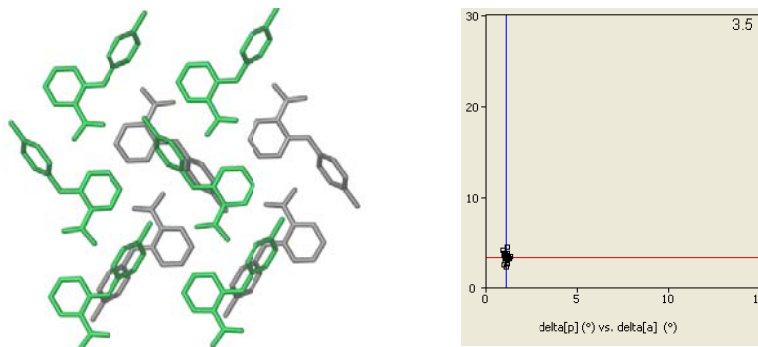


Figure 5.10 (a) 2D supramolecular construct identified by XPac analysis of TNA TNA-I and III. Molecules in different layers are shaded differently. (b) Plot of interplanar angular deviation (δ_p , x-axis) vs angular deviation (δ_a , y-axis) in degrees.

5.2.4 Thermal and spectroscopic characterization

Differential scanning calorimetry: The polymorphs of TNA were investigated by differential scanning calorimetry (DSC). No phase transition was observed among all the forms of TNA in DSC which indicates a monotropic relationship. TNA-I melted at 205 °C, TNA-II at 207 °C and TNA-III at 204 °C (Figure 5.11).

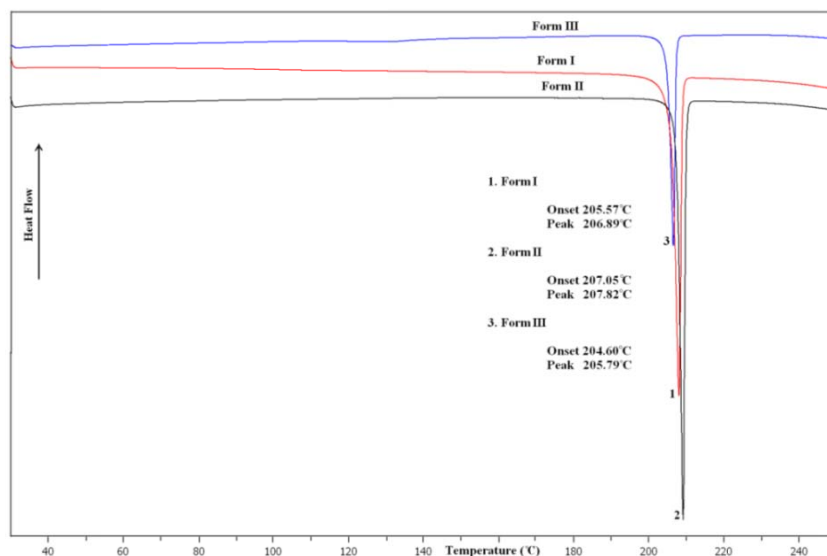


Figure 5.11 DSC thermograms of TNA-I (red), TNA-II (black) and TNA-III (blue).

FT-IR and FT-Raman spectroscopy: O–H and N–H group stretching frequencies are broad and the carbonyl stretching frequencies are significantly different for the three polymorphs of TNA. The infrared O–H and N–H group stretching frequencies of all the three polymorphs of TNA are broad and the carbonyl stretching frequencies are significantly different. The carbonyl stretch for TNA-III (1635 cm^{-1}) is at a lower wave number compared to TNA-I (1663 cm^{-1}) and TNA-II (1658.7 cm^{-1}), consistent with the carboxylate group vs carboxylic acid stretching frequency. Pyridine shows four skeletal vibrational bands in the range $1600\text{--}1430\text{ cm}^{-1}$. The four skeletal pyridine bands are close in TNA-I ($1602, 1579, 1518, 1459\text{ cm}^{-1}$) and TNA-II ($1602, 1578, 1518, 1459\text{ cm}^{-1}$) but different in TNA-III where fourth peak was not observed ($1604, 1564,$ and 1514 cm^{-1}). (Figure 5.12 and Table 5.4). The appearance of a broad O–H stretch band in the IR spectrum (centered at 3428 cm^{-1}) indicates partial proton transfer in TNA-III at

room temperature, which is consistent with the single crystal X-ray structure analysis at 298 K.

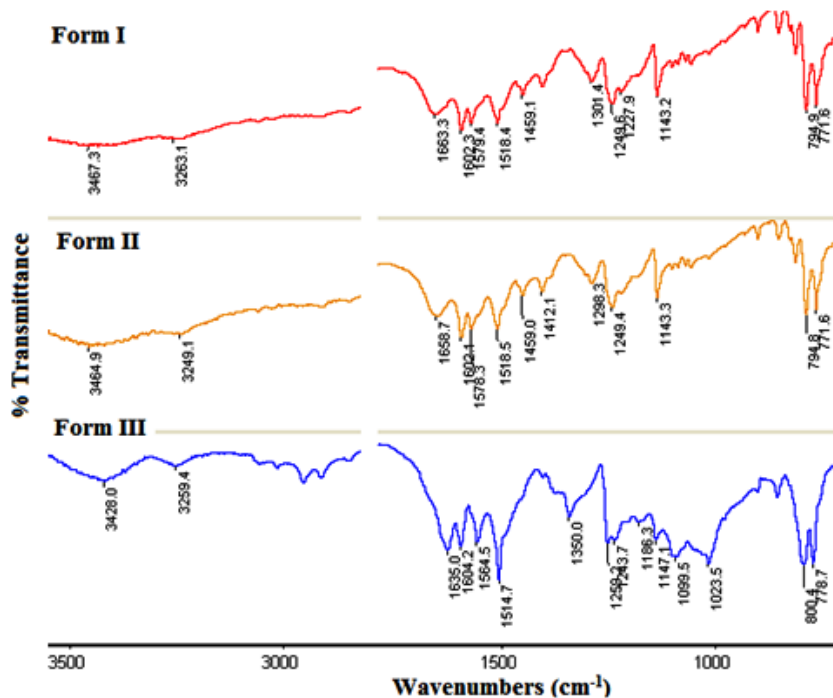


Figure 5.12 FT-IR comparison of TNA-I, TNA-II and TNA-III.

Table 5.4 FT-IR (KBr pellet) spectral bands of TNA polymorphs.

Polymorphs	O–H stretching (br) (cm ⁻¹)	N–H stretching (br) (cm ⁻¹)	C=O stretching (cm ⁻¹)	Pyridine Ring stretching(cm ⁻¹)
TNA-I	3467.3	3263.1	1663.3	1602, 1579.4, 1518, 1459
TNA-II	3464.9	3249.1	1658.7	1602, 1578, 1518, 1459
TNA-III	3428.0	3259.4	1635.0	1604, 1564, 1514

FT-Raman spectra of the three polymorphs have clear differences in the Raman shift values for carbonyl groups. A comparison of FT-Raman spectra is shown in Figure 5.13 and the Raman shifts values are summarized in Table 5.5

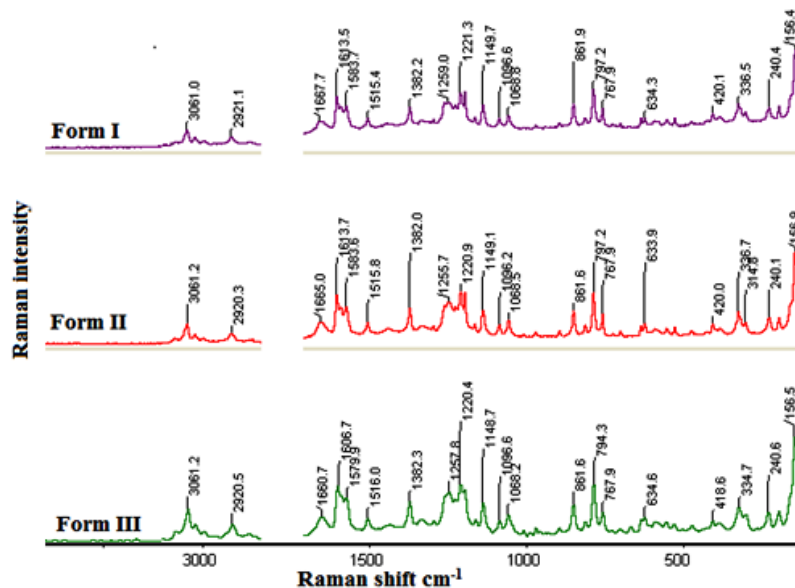


Figure 5.13 Comparison of Raman spectra of the three polymorphs of TNA.

Table 5.5 FT-Raman (neat solid) spectral bands of TNA polymorphs.

Polymorphs	Aromatic C–H stretching (cm ⁻¹)	Aliphatic C–H stretching (cm ⁻¹)	C=O stretching (cm ⁻¹)	N–H bending (cm ⁻¹)
TNA-I	3061.0	2921.1	1667.7	1583.7
TNA-II	3061.2	2920.3	1665.0	1583.6
TNA-III	3061.2	2920.5	1660.7	1579.9

¹³C and ¹⁵N ss-NMR: Solid state NMR is a useful technique to differentiate polymorphs. ¹⁵N and ¹³C SSNMR was performed on the three polymorphs of TNA. There is an up field shift ~1 ppm in ¹⁵N ss-NMR for pyridine N in TNA-III (–146.8 ppm) compared to TNA-I (–147.5 ppm), whereas for TNA-II the chemical shift is –143.0 ppm. Figure 5.14a shows the comparison of the ¹⁵N ss-NMR spectra of the polymorphs and the chemical shift values are listed in Table 5.6. Normally a large upfield chemical shift is expected as the free pyridine N becomes protonated (about 80-100 ppm). The reason for the same ¹⁵N chemical shift of TNA-I and III may be understood from the RT crystal structure. The RT structure represents an in-between situation of the neutral and ionic states. The LT structure is clearly zwitterionic. Since the ss-NMR was recorded at room

temperature, the chemical environment of the pyridine N is more neutral-like than ionic. Figure 5.14b shows the comparison of the ^{13}C ss-NMR spectra of the polymorphs and the chemical shift values are listed in Table 5.7.

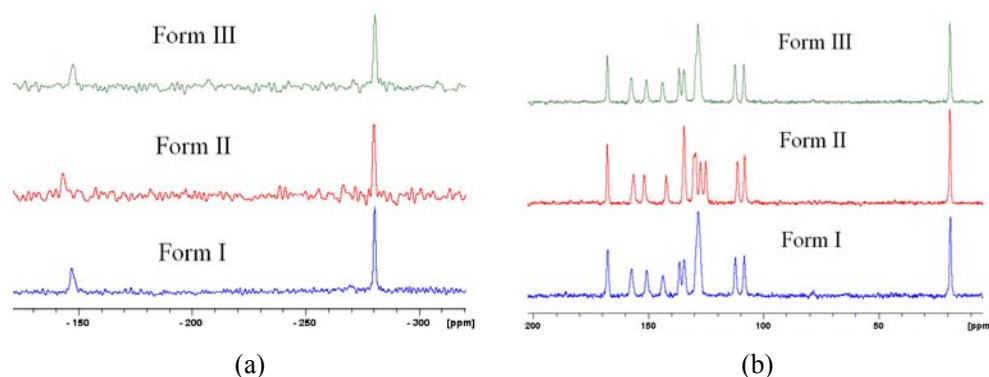


Figure 5.14 (a) ^{15}N ss-NMR and (b) ^{13}C ss-NMR for TNA-I, II and III.

Table 5.6 ^{15}N ss-NMR chemical shifts (in ppm) of the three polymorphs

Polymorph	Pyridine N	2° amine N
TNA-I	-147.6	-280.5
TNA-II	-143.0	-280.0
TNA-III	-146.8	-280.3

Table 5.7 ^{13}C ss-NMR chemical shifts (in ppm) of the three polymorphs

	TNA-I	TNA-II	TNA-III
C13	18.6	18.7	18.7
C2	108.2	108.0	108.3
C4	112.0	111.1	112.1
C8, C12	128.1	124.9	128.2
C10	Merged (C8, C12)	127.1	Merged (C8, C12)
C9, C11	134.3	129.3	134.3
C3	136.2	134.2	136.4
C7	143.5	142.0	143.6
C5	150.4	151.6	150.6
C6	157.1	156.2	157.2
C1	167.5	167.6	167.6

5.2.5 Conformational difference

TNA is flexible molecule and different torsions were observed in the crystal structures presented. TNA-I and TNA-III have similar torsions (packing polymorphs) around the p-tolyl group whereas p-tolyl torsion of TNA-II is significantly different compared to TNA-I and TNA-III (conformational polymorph). A nearly flat conformer is obtained in case of the molecular salt of $\text{AP-NH}^+\cdot\text{TNA-COO}^-$. Torsion angle for p-tolyl group (C6–N2–C7–C8) of all the conformers obtained is listed in Table 5.8. The overlay diagram of the all the conformations is shown in Figure 5.15. For a flat conformation of TNA, as in $\text{AP-NH}^+\cdot\text{TNA-COO}^-$ crystal structure, it is observed that the pyN atom remains inactive towards hydrogen bonding because of steric reason. Therefore, acid-acid dimer is also possible apart from the observed acid-pyridine synthon in the crystal structures of TNA.

Table 5.8 Torsion angles for all the conformations of TNA in its crystal structures.

Form	Torsion angle (°) (C6–N2–C7–C8)
TNA-I	68.0(4)
TNA-II	55.2(2)
TNA-III LT	66.5(3)
TNA-III RT	66.8(6)
$\text{NH}^+\text{-TNA-COO}^- \cdot 2 \text{ NBA}$	55.0(2)
$\text{AP-NH}^+\cdot\text{TNA-COO}^-$	11.1(3)

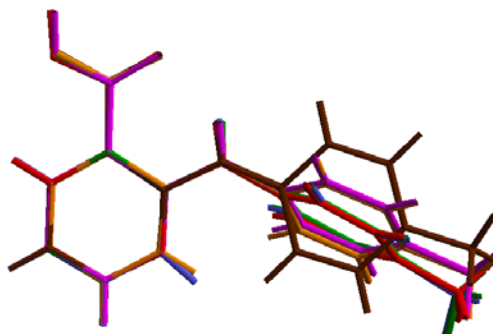


Figure 5.15 Overlay of all the conformations present in TNA crystal structures. Color codes are TNA-I= Red, TNA-II= Magenta, TNA-III LT = Blue, TNA-III RT = Green, $\text{NH}^+\text{-TNA-COO}^- \cdot 2 \text{ NBA}$ = Orange and $\text{AP-NH}^+\cdot\text{TNA-COO}^-$ = Brown.

5.2.6 CSD search

A search of the CSD (version 5.31, November 2010; May 2011 update)²³ was performed using the following functional groups as search criteria (Table 5.9), for all organic compounds with the word "form", "polymorph", "modification" and "phase" in the qualifier, excluding the entries for which 3D coordinates are not available. These searches resulted in only four zwitterionic and neutral polymorphic clusters for single component organic systems with solved X-ray crystal structures.

Table 5.9 Functional groups used to search the CSD and the number of hits retrieved.

Substructure	No. of hits	Substructures	No. of hits
N and COOH	411	NH ⁺ and COO ⁻	407
N and SO ₃ H	10	NH ⁺ and SO ₃ ⁻	118
N and PO ₄ H	31	NH ⁺ and PO ₄ ⁻	31
N and OH	1276	NH ⁺ and O ⁻	807
N and NC(=O)N	166	NH ⁺ and (NH ⁻)C(=O)N	3

5.2.7 Hirshfeld 2D fingerprint plot

2D Hirshfeld fingerprint plots²⁴ for the three polymorphs highlight the differences in intermolecular contacts (Figure 5.16). The sharp spikes for O^{...}H interactions for TNA-III near $d_e=d_i \approx 1.0$ indicates short O^{...}H contact in this crystal structure (strong N-H⁺...O⁻ hydrogen bond), whereas these protrusions are absent for TNA-I and TNA-II. The complementary situation in the polymorphs TNA-I and II of short N^{...}H contacts (strong O-H^{...}N hydrogen bond) is represented as sharp spikes near $d_e=d_i \approx 1.0$ whereas they are absent for TNA-III. The C-H^{...}O hydrogen bonds occur at longer distance of $d_e=d_i \approx 1.4$. These plots are yet another manifestation of neutral O-H^{...}N hydrogen bond in polymorphs I and II and ionic N-H⁺...O⁻ hydrogen bond in TNA-III. The π -stacking of linear hydrogen-bonded tapes in TNA-I and III structures is of the overlap region around $d_e=d_i \approx 2.5$ for inter-aromatic interactions, which less dense in TNA-II.

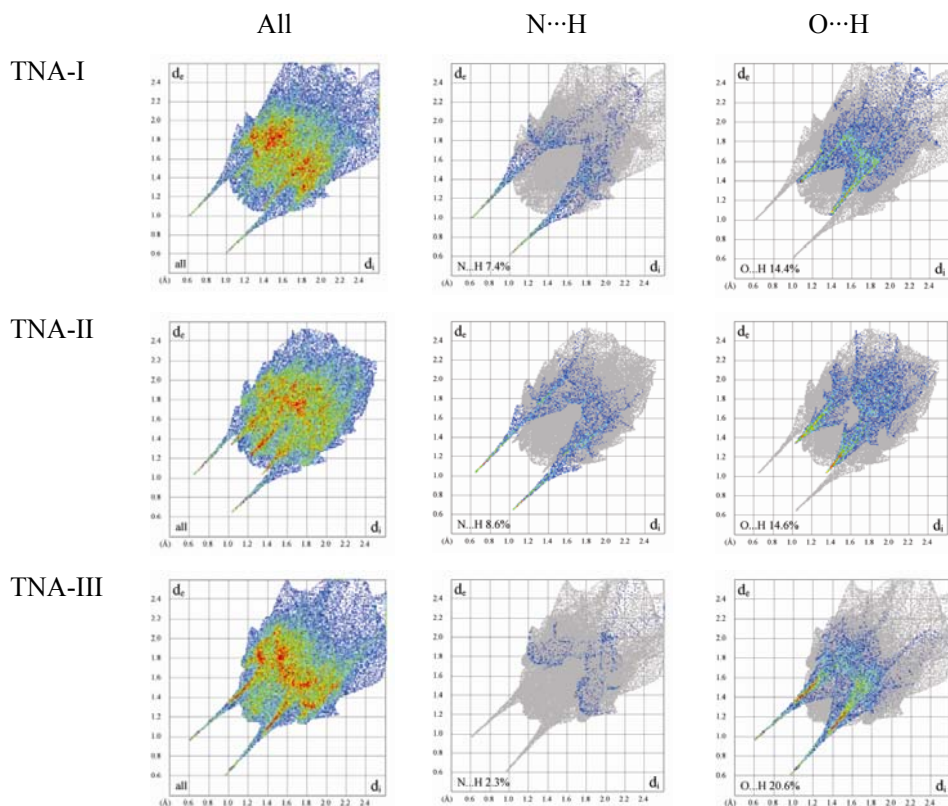


Figure 5.16 2D Hirshfeld fingerprint plots for three polymorphs.

The relative contribution of each interaction to the Hirshfeld surface is depicted in Figure 5.17. Contribution from N···H interaction to the Hirshfeld surface for TNA-I (7.4%) and TNA-II (8.6%) is higher compared to TNA-III (2.3%) whereas contribution from O···H interaction in TNA-III (20.6%) is more compared to TNA-I (14.4%) and TNA-II (14.6%). For the three polymorphs contribution due to C···C contacts negligible indicating the absence of $\pi\cdots\pi$ interaction in the polymorphs.

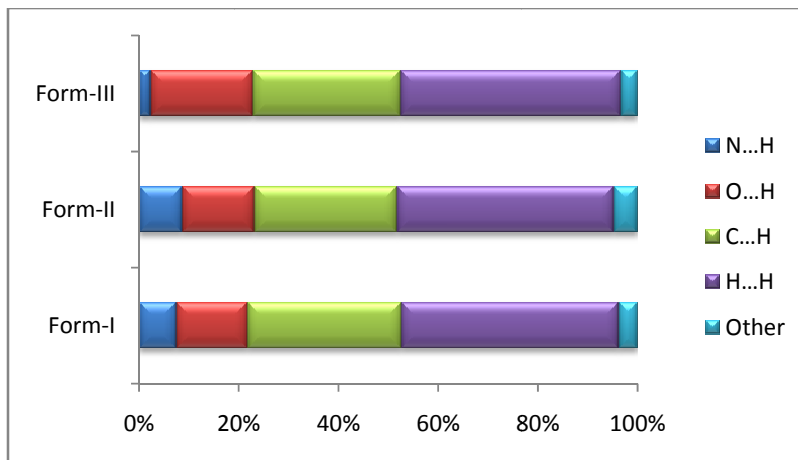


Figure 5.17 Contribution from major interactions to Hirshfeld surface.

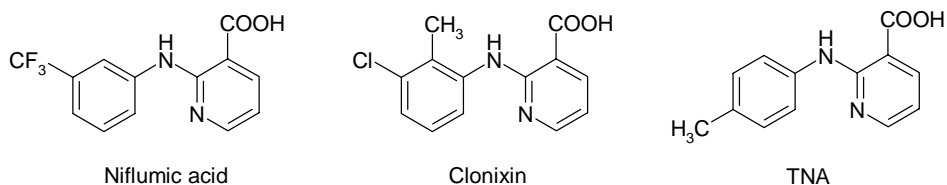
5.3 Discussion

5.3.1 Intramolecular proton transfer, ΔpK_a rule

For multi-component acid-base systems the question of proton transfer can be predicted using the “rule of 3”, which works quite well when $\Delta pK_a < 0$ and > 4 to give neutral hydrogen bond and proton transfer situations, respectively, in weakly acidic/basic and strong acid-base combinations.²⁵ However, predictions about neutral or ionic states are less reliable in the $0 < \Delta pK_a < 4$ range therefore ionization state of acid-base complexes cannot be correlated with pK_a in this transition range. An ampholyte can form zwitterion since the acidic and the basic groups can be simultaneously ionized and for zwitterionic ampholytes, the relation $pK_a^{\text{acidic}} < pK_a^{\text{basic}}$ is true.²⁶ When the two pK_a are relatively close (small value of ΔpK_a), it is not possible to decide which of the two protonated sites dissociates first.

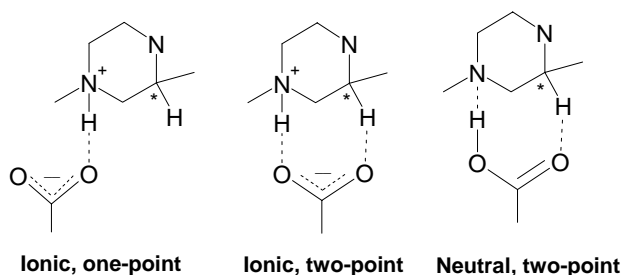
Calculated pK_a values for Clonixin are 1.69 and 4.80 which is comparable to the pK_a values for the closely related derivative Niflumic acid (1.70 and 4.71) (Scheme 5.5).²⁷ TNA being a similar molecule, pK_a values should be comparable with Clonixin and Niflumic acid. Since Clonixin and TNA can both exist as zwitterions and in neutral form in the solid state, one would expect similar acid base behavior from Niflumic acid. Cocrystallization of Niflumic acid and maleic acid ($pK_a=1.91$) resulted a molecular salt

structure,²⁷ therefore, although Niflumic acid has only one crystal structure (acid dimer), a zwitterionic structure is possible because pK_a of niflumic acid COOH group and maleic acid are close.



Scheme 5.5 Molecular structure of Niflumic acid, Clonixin and TNA.

Proton transfer is affected not only by the pK_a of the acid-base counterparts but also by the crystalline environment. Crystal structures of recently reported molecular salts of antidepressant drug Mirtazapine²⁸ revealed that proton transfer is not only because of pK_a difference more than 4 but also because of the hydrogen bonding motif present. In case of Mirtazapinium hemiadipate salt, although the pK_a difference lies in the middle region of salt and cocrystal, proton transfer occurred and was attributed due to the presence of stronger ionic two point synthon in the crystal structure rather than ionic one-point or neutral two point synthon (Scheme 5.6).



Scheme 5.6 Neutral and ionic two point synthons possible in Mirtazapine molecular salts.

Cocrystallization of TNA with NBA ($pK_a = 3.45$) resulted a cocrystal (NH^+ -TNA-COO $^-$ •2NBA) where zwitterionic structure was stabilized in the crystal structure. Here again the pK_a difference of NBA and TNA pyridine lies in the transition region of pK_a and the result was unexpected. On cocrystallization of TNA with 2-aminopyridine ($pK_a=6.86$) a molecular salt has resulted and the obvious reason is pK_a difference is more than 4.

In contrast to the crystal structures of related (phenylamino)nicotinic acids reported recently, neither a high Z' crystal structure nor the acid...acid homodimer was observed in TNA polymorphs. The observation of a zwitterionic polymorph for TNA suggest that several factors seem to operate in this family of structures at both the molecular and supramolecular level steric, electronic, conformation, hydrogen bonding, ΔpK_a , synthon competition, close packing, etc. and it is difficult to anticipate the crystal structure from the molecular diagram. A cocrystal containing similar acid-base functional groups was part of a recent Crystal Structure Prediction contest (4th blind test, 2007). The product in that case was a 1:1 cocrystal and its correct crystal structure was predicted by three research groups.²⁹ Crystal structures of salts have also been predicted³⁰ but not of a zwitterionic molecule. Molecular electrostatic potential is yet another tool to map out hydrogen bond strengths and preferences. Aakeröy³¹ concluded, from his crystallization outcome of amino-pyridines and carboxylic acids, that when the calculated electrostatic charge (MEPS in AM1 package) on the pyridine N is between -220 to -260 kJ/mol, a cocrystal is formed and when the value is between -270 to -290 kJ/mol a salt is the outcome. The MEP value for pyridine N in TNA is -268 kJ/mol (Figure 5.18) placing this molecule in the grey zone of difficult predictability. The fact that both neutral and ionic polymorphs of TNA are observed implies that kinetic factors could be important in the crystallization of these polymorphs.

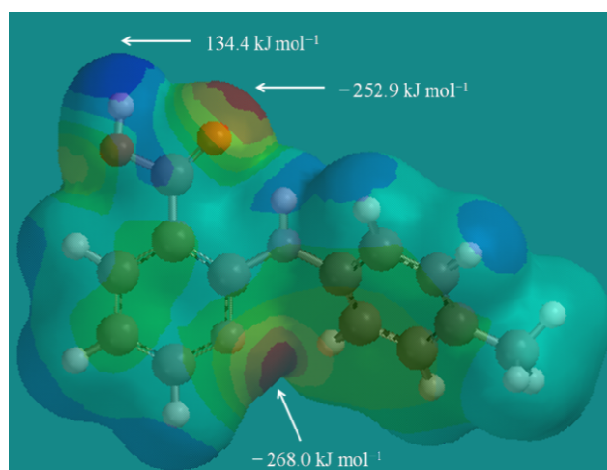
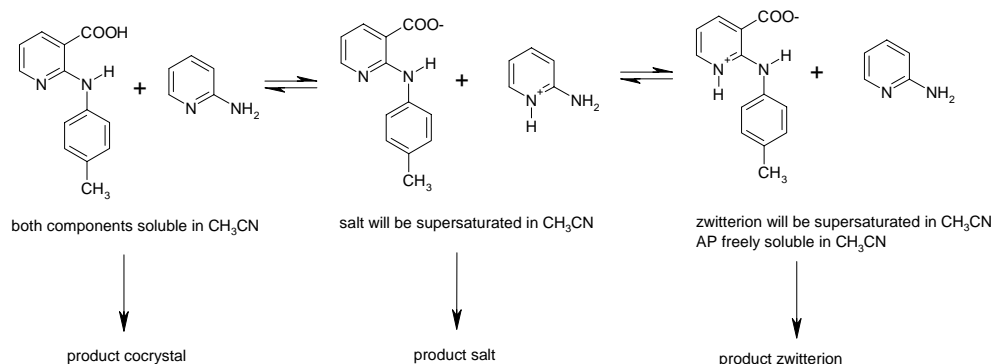


Figure 5.18 Electrostatic surfaces potential (ESP) calculated for TNA in Spartan (AM1). The molecular structure was constructed in GauessView 3.0 and optimized in Spartan '10 (Wavefunction, Inc.) using AM1.

5.3.2 What is the role of pyridine cofomers to give a zwitterionic structure of TNA?

There are several examples in the literature wherein a new polymorph was discovered during attempted co-crystallization.³² Although crystallization of TNA-III in presence of pyridine type cofomer does not represent an isolated case, yet, this is the first instance of a zwitterionic polymorph being crystallized in the presence of a cofomer additive. Despite the frequent occurrence of such reports, a general explanation for this phenomenon is still elusive. The crystallization of a salt structure with 2-aminopyridine wherein the TNA molecule exists as a carboxylate anion and the AP is a pyridinium cation could offer an explanation, at least in this instance. Since the pK_a of pyridine base would be similar, whether the moiety is present in TNA or AP, suggests that there could be a dynamic equilibrium between several species in solution (Scheme 5.7), a few neutral ones and others ionic. Depending on the solvent of co-crystallization, temperature, cofomer additive, supersaturation, etc, the concentration of the neutral adduct, salt and zwitterion will vary depending on the solubility of that species as part of the equilibrium in the crystallization medium. Since the species that is most supersaturated in a given solvent will precipitate first, the product of such a co-crystallization experiment will strongly depend upon the supersaturation conditions, and consequently on the crystallization parameters such as solvent, temperature, concentration, rate of cooling, etc. Since the selection of solvents for co-crystallization is usually a trial-and-error process, by testing the solubility of the components, the outcome often is a serendipitous result when a new polymorph of one of the components is discovered. Could a general recipe to obtain the zwitterionic polymorph of acid–base compounds be to use cofomers whose acidic/basic functional groups are of similar pK_a to the molecule? Those solvents in which the ionic form is likely to supersaturate will be preferred. The crystallization of zwitterionic polymorphs for acid–base drugs will have an immediate application for solubility improvement. Experiments are currently under way to establish a general protocol along these lines. These experimental design parameters will best operate in the grey zone of pK_a between 0 and 3. When $\Delta pK_a < 0$ or > 3 , the outcome is predictable.



Scheme 5.7 Equilibrium between soluble and supersaturated components, TNA and AP, in CH_3CN Solvent. This kind of equilibrium situation will most probably be present in solution when $0 < \Delta pK_a < 3$.

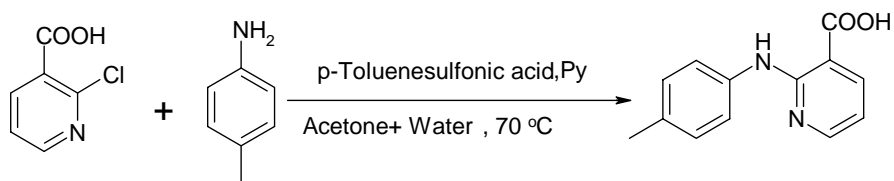
5.4 Conclusion

TNA stands as the 3rd example of a polymorphic system with zwitterionic and neutral polymorphs existing together after Clonixin and Norfloxacin. Anthranilic acid and torasemide are in a different category in that both neutral and zwitterionic molecules are present in the same crystal structure. Crystallization of the zwitterionic polymorph was observed in TNA only in the presence of coformers having pyridine moieties. Interestingly, with acidic coformers zwitterionic structure is cocrystallized. Therefore, in presence of pyridine coformers the zwitterionic polymorph is separating, whereas in presence of acidic 3-nitrobenzoic acid the zwitterionic molecule is separated out along with the coformer as a cocrystal. These preliminary observations suggest a role for the coformer in directing the crystallization towards a polymorph, a cocrystal, or a salt. Although solid state zwitterionic forms of organic molecules is common for compounds having both acidic and basic functionalities but occurrences of both neutral and zwitterionic forms for the same compound is not studied as much as other polymorphic systems. Crystal structure determination of the interesting zwitterionic form III of TNA in presence of specific coformers could provide a better understanding of crystal nucleation, the role of hydrogen bonding in crystallization.

5.5 Experimental Section

All solvents, reagents and coformers were purchased from commercial sources and used without further purification.

Synthesis: TNA was synthesized³³ by refluxing 2-chloronicotinic acid (315.3 mg, 2 mmol), p-toluidine (214.3 mg, 2 mmol), p-toluenesulfonic acid (95.0 mg, 0.5 mmol), and few drops of pyridine in water and acetone solution (1:4, 10 mL) at 70 °C overnight (about 8 h) (Scheme 5.8). The product obtained as precipitate was filtered and then purified by recrystallization from acetone to obtain pure 2(p-tolylamino)nicotinic acid (TNA) which was characterized by ¹H NMR, ¹³C NMR, and IR.



Scheme 5.8 Synthesis of 2(p-Tolylamino)nicotinic acid (TNA).

¹H NMR (CDCl₃, 400MHz): δ 9.99 (s, 1H), 8.39 (dd, 1H), 8.29 (dd, 1H), 7.52 (d, 2H), 7.19 (d, 2H), 6.72 (m, 1H), 2.33 (s, 3H).

IR (cm⁻¹): 3441.2, 3254.2, 3068.4, 1669.3, 1602.2, 1579.4, 1517.6, 1459.3, 1412.6, 1248.9, 1143.3, 795.5

M.p.: 205-207 °C.

X-ray crystallography: X-ray reflections for TNA-I, TNA-III LT and AP-NH⁺•TNA-COO⁻ were collected on Bruker SMART APEX CCD equipped with a graphite monochromator and Mo-Kα fine-focus sealed tube (λ = 0.71073 Å). Data integration was done using SAINT.³⁴ Intensities for absorption were corrected using SADABS.³⁵ Structure solution and refinement were carried out using Bruker SHELXTL.³⁶ X-ray reflection for TNA-II, TNA-III RT and NH⁺-TNA-COO⁻•2NBA were collected on Oxford Diffraction Ltd., (Gemini, Version 1.171.33.55) using Mo Kα, radiation. Data reduction was performed using CrysAlisPro, Oxford Diffraction Ltd., Version

1.171.33.55. OLEX2-1.0³⁷ and SHELXTL 97 were used to solve and refine the data. All non-hydrogen atoms were refined anisotropically. N–H and O–H hydrogens were located from difference electron density maps and C–H hydrogens were fixed. Packing diagrams were prepared in X-Seed.³⁸

Vibrational spectroscopy: Nicolet 6700 FT-IR spectrometer with an NXR FT-Raman module was used to record IR and Raman spectra. IR spectra were recorded on samples dispersed in KBr pellets. Raman spectra were recorded on solid samples contained in standard NMR diameter tubes or on compressed samples contained in a gold-coated sample holder.

ss-NMR: Solid state NMR spectra were recorded on a Bruker Avance spectrometer at 400 MHz. SSNMR experiments were carried out on Bruker 4mm double resonance CPMAS probe in zirconia rotors at 5.0 kHz with a cross-polarization contact time of 2.5 ms and a recycle delay of 8 s. ¹³C-CPMAS spectra recorded at 100 MHz were referenced to methylene carbon of glycine and then the chemical shifts were recalculated to the TMS scale ($\delta_{\text{glycine}} = 43.3$ ppm). Likewise, ¹⁵N-CPMAS spectra recorded at 40 MHz were referenced to glycine and then the chemical shifts were recalculated to nitromethane ($\delta_{\text{glycine}} = -347.6$ ppm).

Thermal analysis: DSC was performed on Mettler Toledo DSC 822e module. Samples were placed in crimped but vented aluminum sample pans. The typical sample size was 3–4 mg, and the temperature range was 30–250°C at heating rate of 5 °C min⁻¹. Samples were purged by a stream of dry nitrogen flowing at 150 mL min⁻¹.

5. 6 References

1. J. Bernstein, *Polymorphism in Molecular Crystals*, Clarendon, Oxford, **2002**, pp-2-4.
2. W. C. McCrone, in *Physics and Chemistry of the Organic Solid State*, ed. D. Fox, M. M. Labes and A. Weissberger, Wiley-Interscience, New York, vol. 2, **1965**, , pp. 725–767.
3. J. Dunitz, *Acta Cryst.* B51, **1995**, 619.
4. P. M. Bhatt and G. R. Desiraju, *Chem. Commun.*, **2007**, 2057.

5. M. R. Chierotti, L. Ferrero, N. Garino, R. Gobetto, L. Pellegrino, D. Braga, F. Grepioni and L. Maini, *Chem. Eur. J.*, 16, **2010**, 4347.
6. A. L. Lehninger, D. L. Nelson and M. M. Cox, *Principles of Biochemistry*, 2nd ed., Worth publishers; New York, **1993**, pp-81-83.
7. (a) G. R. Desiraju, *Crystal Growth & Design*, 8, **2008**, 3.
8. (a) A. Iwanade, D. Umeno, K. Saito and T. Sugo, *Biotechnology Progress*, 23, **2007**, 1425. (b) M. H. Abraham, K. Takaács-Novaák and R. C. Mitchell, *J. Pharm. Sci.*, 86, **1997**, 310. (c) V. I. Zaionts, *Pharmacokinetic optimization in drug research*, 13, **1980**, 1112. (d) N. Iwasaki, T. Ohashi, K. Musoh, H. Nishino, N. Kado, S. Yasuda, H. Kato and Y. Ito, *J. Med. Chem.*, 38, **1995**, 496.
9. (a) K. Y. Tam, A. Avdeef, O. Tsinman and N. Sun, *J. Med. Chem.*, 53, **2010**, 392. (b) D. F. Ranney, *Biochemical Pharmacology*, 59, **2000**, 105. (c) S. Marcus, M. Bernstein, G. Ziv, A. Glickman and M. Gipps, *Veterinary Research Communications*, 18, **1994**, 331.
10. M. Takasuka, H. Nakai and M. Shiro, *J. Chem. Soc., Perkin Trans.2* **1982**, 1061.
11. R. Barbas, R. Prohens and C. Puigjaner, *J. Therm. Anal. Cal.*, 89, **2007**, 687.
12. (a) C. J. Brown, *Proc. R. Soc. London, Ser. A*, 302, **1968**, 185. (b) C. J. Brown and M. Ehrenberg, *Acta Cryst.*, C41, **1985**, 441.
13. L. Dupont and G. Dive, *Bull. Soc. R. Sci. Liege*, 51, **1982**, 248.
14. S. Basavoju, D. Boström and S. P. Velaga, *Cryst. Growth & Des.*, 6, **2006**, 2699.
15. (a) C. D. G. Boone, J. L. Derissen and J. C. Schoone, *Acta Cryst.*, B33, **1977**, 3205. (b) G. E. Hardy, W. C. Kaska, B. P. Chandra and J. I. Zink, *J. Am. Chem. Soc.*, 103, **1981**, 1074. (c) H. Takazawa, S. Ohba and Y. Saito, *Acta Cryst.*, B42, **1986**, 1880. (d) T.-H. Lu, P. Chattopadhyay, F.-L. Liao and J.-M. Lo, *Anal. Sci.*, 17, **2001**, 905.
16. (a) L. Dupont, J. Lamotte, H. Campsteyn and M. Vermeire, *Acta Cryst.*, B34, **1978**, 1304. (b) L. Dupont, H. Campsteyn, J. Lamotte and M. Vermeire, *Acta Cryst.*, B34, **1978**, 2659. (c) A. Danilovski, D. Filic, M. Oresic and M.

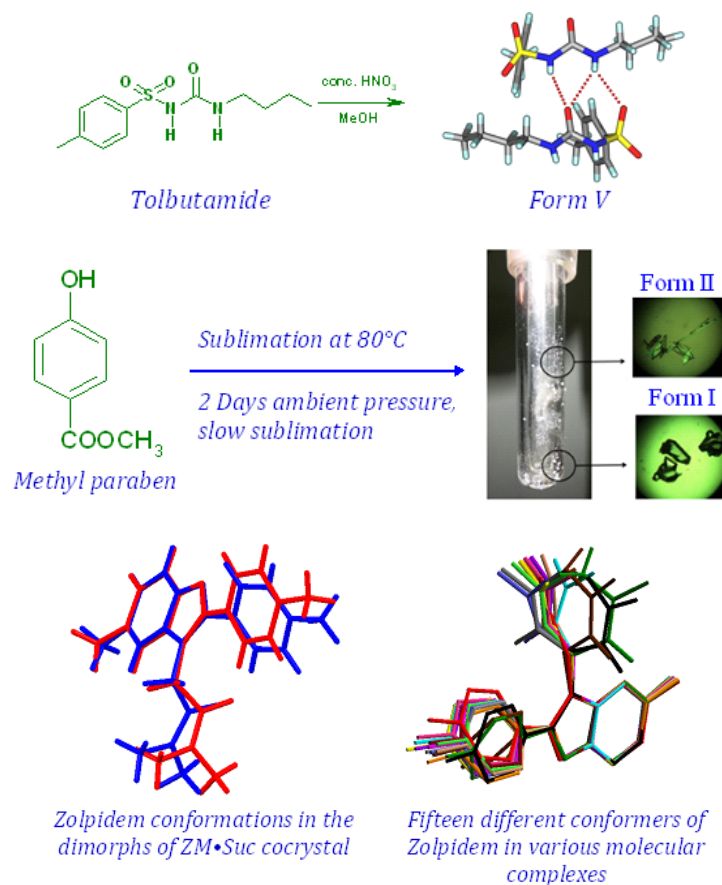
- Dumic, *Croat. Chem. Acta*, 74, **2001**, 103. (d) G. Bartolucci, B. Bruni, S. A. Coran and M. Di Vaira, *Acta Cryst.*, E65, **2009**, o972.
17. M. J. Thomas and J. A. Thomas, In *Modern Pharmacology with Clinical Applications*; 5th Ed., C. R. Craig, R. E. Stitzel, (Eds.) *Little Brown & Company*: Boston, **1997**.
18. (a) E. H. Lee, S. R. Byrn and M. T. Carvajal, *Pharm. Res.*, 23, **2006**, 2375. (b) J. F. McConnell and F. Z. Company, *Cryst. Struct. Commun.*, 5, **1976**, 861. (c) L. Fang, S. Numajiri, D. Kobayashi, H. Ueda, K. Nakayama, H. Miyamae and Y. Morimoto, *J. Pharm. Sci.*, 93, **2004**, 144. (d) K. V. Andersen, S. Larsen, B. Alhede, N. Gelting and O. Buchardt, *J. Chem. Soc., Perkin Trans.2*, **1989**, 1443. (e) V. Lopez-Mejias, J. W. Kampf and A. J. Matzger, *J. Am. Chem. Soc.*, 131, **2009**, 4554. (f) A. O. Surov, P. Szterner, W. Zielenkiewicz and G. L. Perlovich, *J. Pharm. Biomedical Anal.*, 50, **2009**, 831. (g) J. F. McConnell, *Cryst. Struct. Commun.*, 2, **1973**, 459. (h) M. H. K. Murthy, T. N. Bhat and M. Vijayan, *Acta Cryst.*, B38, **1982**, 315. (i) E. H. Lee, S. X. M. Boerrigter, A. C. F. Rumondor, S. P. Chamrthy and S. R. Byrn, *Cryst. Growth Des.*, 8, **2008**, 91. (j) E. H. Lee, S. X. M. Boerrigter and S. R. Byrn, *Cryst. Growth Des.* 10, **2010**, 518. (k) P. Moser, A. Sallmann and I. Wiesenberger, *J. Med. Chem.*, 33, **1990**, 2358. (m) D. K. Demertzi, D. Mentzafos and A. Terzis, *Polyhedron*, 12, **1993**, 1361. (n) C. Castellari and S. Ottani, *Acta Cryst.*, C53, **1997**, 794. (o) N. Jaiboon, K. Yos-In, S. Ruangchaithaweesuk, N. Chaichit, R. Thutivoranath, K. Siritaedmukul and S. Hannongbua, *Anal. Sci.*, 17, **2001**, 1465. (p) N. Muangsin, M. Prajuabsook, P. Chimsook, N. Chantarasiri, K. Siraleartmukul, N. Chaichit and S. Hannongbua, *J. Appl. Crystallogr.*, 37, **2004**, 288. (q) G. L. Perlovich, A. O. Surov, L. K. Hansen and A. B. Brandl, *J. Pharm. Sci.*, 96, **2007**, 1031. (r) A. O. Surov, I. V. Terekhova, A. Bauer-Brandl and G. L. Perlovich, *Cryst. Growth Des.* 9, **2009**, 3265.
19. (a) S. Long, S. Parkin, M. A. Siegler, A. Cammers and T. Li, *Cryst. Growth Des.* 8, **2008**, 4006. (b) S. Long and T. Li, *Cryst. Growth Des.*, 9, **2009**, 4993. (c) S. Long, T. Li, *Cryst. Growth Des.* 10, **2010**, 2465. (d) S. Long, S. Parkin, M. Siegler, C. P. Brock, A. Cammers and T. Li, *Cryst. Growth Des.* 8, **2008**,

3137. (e) S. Long, M. A. Siegler, A. Mattei, T. Li, *Cryst. Growth Des.*, **11**, **2011**, 414.
20. B. Sarma, N. K. Nath, B. R. Bhogala and A. Nangia, *Cryst. Growth Des.* **9**, **2009**, 1546.
21. P. Sanphui, B. Sarma, A. Nangia, *J. Pharm. Sci.*, **100**, **2011**, 2287.
22. (a) T. Gelbrich and M. B. Hursthouse, *CrystEngComm*, **7**, **2005**, 324. (b) T. Gelbrich and M. B. Hursthouse, *CrystEngComm*, **8**, **2006**, 448. (c) T. Gelbrich, D. S. Hughes, M. B. Hursthouse and T. L. Threlfall, *CrystEngComm*, **10**, **2008**, 1328. (d) F. P. A., Fabbiani, B. Dittrich, A. J. Florence, T. Gelbrich, M. B. Hursthouse, W. F. Kuhs, N. Shankland and H. Sowa, *CrystEngComm*, **11**, **2009**, 1396.
23. Cambridge Crystallographic Data Center, www.ccdc.cam.ac.uk.
24. (a) M. A. Spackman and D. Jayatilaka, *CrystEngComm*, **11**, **2009**, 19. (b) J. J. McKinnon, D. Jayatilaka, M. A. Spackman, *Chem. Commun.*, **2007**, 3814. (c) J. Bernstein, *Cryst. Growth Des.*, **11**, **2011**, 632.
25. (a) S. L. Johnson and K.A. Rumon, *J. Phys. Chem.* **69**, **1965**, 74. (b) W. Q. Tong and G. Whitesell, *Pharm. Dev. Technol.* **3**, **1998**, 215. (c) M. J. Bowker, *A Procedure for Salt Selection and Optimization. In Handbook of Pharmaceutical Salts*; P. H. Stahl and C. G. Wermuth, (Eds.); VHCA and Wiley-VCH: New York, **2002**.
26. A. Pagliara, P.-A. Carrupt, G. Caron, P. Gaillard and B. Testa, *Chem. Rev.*, **97**, **1997**, 3385.
27. S. L. Childs, G. P. Stahly, and A. Park, *Mol. Pharma.*, **4**, **2007**, 323.
28. B. Sarma, R. Thakuria, N. K. Nath and A. Nangia, *CrystEngComm*, DOI: 10.1039/C0CE00746C.
29. (a) M. A. Neumann, F. J. J. Leusen and J. Kendrick, *Angew. Chem. Int. Ed.* **47**, **2008**, 2427. (b) T. S. Thakur and G. R. Desiraju, *Cryst. Growth Des.*, **8**, **2008**, 4031.
30. (a) F. J. J. Leusen, *Cryst. Growth Des.*, **3**, **2003**, 189. (b) P. G. Karamertzanis and S. L. Price, *J. Phys. Chem. B*, **109**, **2005**, 17134.
31. C. B. Aakeröy, A. Rajbanshi, Z. J. Li and J. Desper, *CrystEngComm*, **12**, **2010**, 423.

32. (a) G. M. Day, A. V. Trask, W. D. S. Motherwell and W. Jones, *Chem. Commun.* **2006**, 54. (b) P. Sanphui, N. R. Goud, U. B. R. Khandavilli, S. Bhanothb and A. Nangia, *Chem. Commun.*, **2011**, DOI: 10.1039/c1cc10204d. (c) M. Rafilovich and J. Bernstein, *J. Am. Chem. Soc.*, 128, **2006**, 12185. (d) P. Vishweshwar, J. A. McMahon, M. Oliveira, M. L. Peterson, and M. J. Zaworotko, *J. Am. Chem. Soc.*, 127, **2005**, 16802. (e) A. D. Bond, K. A. Solanko, S. Parsons, S. Redder and R. Boese, *CrystEngComm*, 13, **2011**, 399. (f) M. Wenger and J. Bernstein, *Mol. Pharm.*, 4, **2007**, 355. (g) B. Lou, D. Boström and S. P. Velaga, *Cryst. Growth Des.*, 9, **2009**, 9, 1254. (h) X. Mei and C. Wolf, *Cryst. Growth Des.*, 4, **2004**, 1099.
33. P. C. Ting, J. J. Kaminski, M. H. Sherlock, W.C. Tom, J. F. Lee, R. W. Bryant, A. S. Watnick and A. T. McPhail, *J. Med. Chem.*, 33, **1990**, 2697.
34. *SAINT-Plus*, version 6.45, Bruker AXS Inc., Madison, WI, **2003**.
35. Sheldrick, G. M. *SADABS, Program for Empirical Absorption Correction of Area Detector Data*, University of Göttingen, Germany, **1997**.
36. (a) *SMART* (Version 5.625) and *SHELX-TL* (Version 6.12), Bruker AXS Inc., Madison, WI, **2000**. (b) G. M. Sheldrick, *SHELXS-97* and *SHELXL-97*, University of Göttingen, Germany, **1997**.
37. O. V. Dolomanov, A. J. Blake, N. R. Champness and M. Schröder, *J. Appl. Cryst.*, 36, **2003**, 1283.
38. L. J. Barbour, X-Seed, *Graphical Interface to SHELX-97 and POV-Ray*, University of Missouri-Columbia, USA, 1999.

Chapter Six

Polymorphism in Few Active Pharmaceutical Ingredients



Novel Form V of Tolbutamide, Form II of Methyl Paraben and cocrystal polymorphs of Zolpidem•Succinic acid are presented.

6.1 Introduction

There has been substantial research activity in the field of polymorphism driven by both fundamental scientific discovery and its importance in industries like agrochemicals, dyes, foodstuffs and especially in the pharmaceutical industry.¹ Discovery and characterization of polymorphs are crucial in the early stages of drug development, as unanticipated appearance or disappearance of a polymorph can impact the marketability of a drug, as in the case of ritonavir,² it can result in withdrawal of a commercial pharmaceutical product. Therefore, crystallization of a drug in various process conditions under a variety of crystallization methods has been particularly important. Despite its potential implications, the phenomenon of polymorphism is not always well understood, and even after many decades of research there is no proper clue what type of molecules exhibit polymorphism. Some molecules are highly polymorphic but some molecules like Benzoic acid do not show signs of polymorphism even after extensive research. Various approaches have been employed to control or to induce crystallization of novel polymorph which include altering the solvent of crystallization,³ templating with surface,⁴ polymer heteronuclei,⁵ tailor-made additives,⁶ crystallization from gel medium⁷ etc. Cocrystal formers that can potentially hydrogen bond with the drug are believed to play a role in producing a new crystal form. In 2006 a new polymorph of Maleic acid,⁸ 124 years after the first crystal form studied, was discovered during attempted cocrystallization with Caffeine. Two new polymorphs of curcumin⁹, a natural product with diverse pharmacological effects, was discovered during attempted cocrystallization with 4-hydroxy pyridine and 4,6-dihydroxypyrimidine. These experiments show that additives can induce the appearance of novel polymorphic forms. By now, there have been many reports of accidental generation of novel polymorphs of drug substances occurring during attempted cocrystallization in presence of coformers.¹⁰ Four polymorphs of benzidine^{10a} were isolated during cocrystallization. A new second polymorph of aspirin^{10b} was obtained in presence of amide coformers and now in presence of aspirin anhydride.^{10c} Novel polymorphs of other important compounds obtained serendipitously in presence of coformer are two new oxalic acid sesquihydrate polymorphs^{10d} crystallized in presence of asparagine or glutamine, form VI and VII of

acridine^{10f} was obtained in presence of terephthalic and *cis,trans*-muconic acid, and so on.

Most of the marketed pharmaceuticals are preferred in their stable crystalline forms. The arrangement of the molecules in a crystal determines its physical and chemical properties. In most cases, the crystallization of polymorphs often obeys Ostwald's Law of Stages¹¹ where the kinetically metastable form initially appears followed by its transformation to the more stable polymorph. Understanding the different factors¹² (e.g., solvent, temperature, agitation rate etc.) that affect the conversion between the forms is essential as these variables can facilitate or impede the transformation rate. A disadvantage of the thermodynamically stable form is that it is usually the least soluble and consequently has the lowest bioavailability. The differences in the solubility of various polymorphs are typically lower than a factor of two.¹³ In some cases a metastable crystalline phase may be purposely developed¹⁴ for the drug development when there is a significant increase in solubility and dissolution rate of metastable form (5 to 10 times) and thereby improving the absorption and/or bioavailability over the stable polymorph, for example, metastable form I is preferred than the stable form II of Ritonavir.² But it must be stabilised by special techniques such as addition of structurally related additives, substrates etc.

At the supramolecular level, further variation in the crystalline forms of a solid compound is possible. They may either exist as single molecular entities or multi-component species. Multi-component crystals include salts, hydrates, solvates and cocrystals of the drug molecule where a second component (counter-ion, water, solvent or a coformer respectively) is incorporated into the crystal lattice. Multi-component crystals can also exhibit polymorphism like single component systems. Polymorphism in multi-component systems¹⁵ is very recent and there are only few cocrystal polymorphs compared to single component polymorphic systems.

6.1.1 Modulated structure

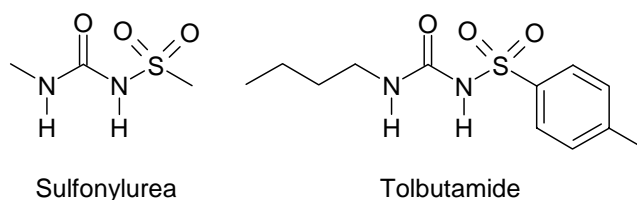
According to Steed¹⁶ some high Z' crystal structures are actually disorder averages of more symmetrical structures having superspace modulation. These modulations originate because conventional space group operations cannot accommodate

intermolecular interactions. The 1:2 complex of α -D-glucose and *p*-tolylboronic acid crystallized¹⁷ in glucofuranose form at room temperature in orthorhombic space group $P2_12_12_1$ with one molecule in the asymmetric unit ($Z' = 1$), however a modulated structure in monoclinic space group $P2_1$ was crystallized at 100 K with $Z' = 2$. A series of structurally related compounds, $M(H_2O)_2(15\text{-Crown-5})(NO_3)_2$, where $M = Cu, Mg, Zn$ and Co are the remarkable examples¹⁸ of modulated structures having $Z' > 1$.

6.2 Tolbutamide

Sulfonylurea functional group (Scheme 6.1), as the name indicates, contains both sulfonylamide and urea groups fused together. Sulfonylureas are a class of oral hypoglycemic agents (pills and capsules to lower the level of blood glucose) taken by people with type 2 diabetes.¹⁹ The sulfonylureas increase the secretion of insulin by the pancreas. The first-generation sulfonylureas include acetohexamide, chlorpropamide, tolazamide and Tolbutamide. The second-generation sulfonylureas include glipizide and glimepiride.

Tolbutamide (**TB**) (Scheme 6.1) is a first generation potassium channel blocker, sulfonylurea oral hypoglycemic drug sold under the brand name Orinase.



Scheme 6.1 Sulfonylurea functional group and molecular structure of Tolbutamide.

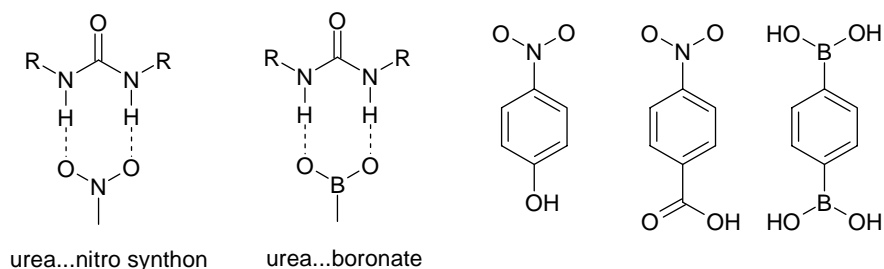
The first study on polymorphism of TB was reported in 1969 by Kuhnert-Brandstätter and Wunsch using hot-stage microscopy.²⁰ The existence of three polymorphic forms with melting points of 127, 117, and 106 °C were reported. Subsequently, the system was studied by Simmons et al.²¹, later by Burger who prepared four polymorphic forms (Forms I–IV).²² Hasegawa et al. analyzed the thermal behavior of Form I and showed that this form undergoes a reversible structural transformation to a new crystal form upon heating beyond 38 °C²³ named as Form I^H and the phase below 38

°C as Form I^L. Overall, there are five polymorphs of Tolbutamide reported in literature viz. form I^L, form I^H, form II, form III, and form IV. Recently, the crystal structures of all the four polymorphs were revisited²⁴ and the single crystal X-ray structure of three forms were determined and the crystal structure of the fourth polymorph was solved by powder X-ray diffraction.

There has been a report on the selective crystallization of a metastable form IV of TB in the presence of 2, 6-di-O-methyl- β -cyclodextrin.²⁵ Single crystal X-ray structure was determined for Tolbutamide β -cyclodextrine inclusion complex.²⁶ In addition there are also reports of the synthesis and characterization of Cd²⁺, Ag⁺, and Hg²⁺ complexes with deprotonated Tolbutamide.²⁷

6.2.1 Modulated high Z' structure of Tolbutamide

So far there is no cocrystal reported for TB in literature. With the idea that cocrystals can improve the physico-chemical properties of drugs,²⁸ novel cocrystals of TB were attempted. A synthon approach suggested *p*-nitrophenol, *p*-nitrobenzoic acid, and *p*-phenylenediboronic acid as potential coformers via the urea \cdots nitro²⁹ and urea \cdots boronate³⁰ heterosynthons (Scheme 6.2)



Scheme 6.2 The structure of Tolbutamide, urea \cdots nitro and urea \cdots B(OH)₂ synthons.

When TB was cocrystallized with *p*-nitrophenol and *p*-phenylenediboronic acid (p-NP and p-PDBA hereafter) in absolute EtOH solvent, single crystals, which on X-ray diffraction at 100 K solved as a new crystal structure of TB with 3 molecules in the asymmetric unit of *P*2₁/*n* space group, were obtained. When reflections were collected on the same crystal at 298 K, the structure solved with Z' = 1 but now the terminal carbon atoms of the butyl chain were disordered (Figure 6.1).

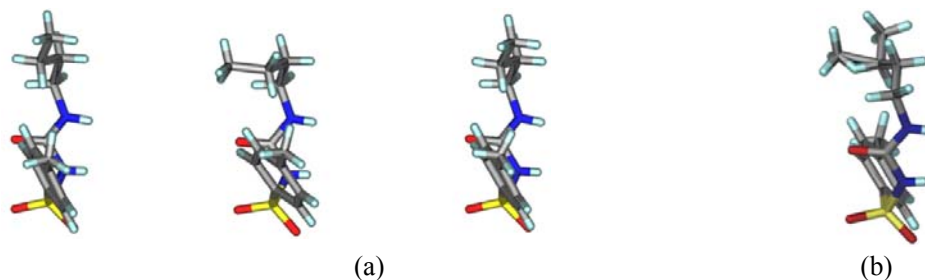


Figure 6.1 (a) The three symmetry independent molecules of TB differ in butyl chain conformations but the rest of the molecule overlays nicely. The middle molecule has gauche conformation whereas the two side molecules have anti conformation. (b) Room temperature structure ($Z'=1$) shows disorder at the terminal butyl chain.

The room temperature structure matches with that of form III in a recent X-ray diffraction study.²⁴ The unique b -axis is tripled in the 100 K data set compared to the 298 K measurement, 27.189(4) and 9.043(4) Å respectively. A close view of the reciprocal lattice in the RLATT program showed reflections for the triple size unit cell (Figure 6.2). A similar unit cell compared to the room temperature data can be visualized in the 100 K reflections by removing two rows of reflections, but this small unit cell structure did not refine properly ($R_1=0.1125$ and $\text{GoF}=1.114$). On the other hand, the correctly solved and refined crystal structures have lower R -factor and better GoF (0.0652, 0.963 at 100 K; 0.0714, 1.099 at 298 K). ORTEP diagrams of form III at 100 K and at 298 K are shown in Figure 6.3. The thermal ellipsoids are elongated for the crystal structure which is solved using 1/3 of the b -axis ($b=9.04$) indicating that the electron density is not accounted for completely in the crystal structure solution. Both the low temperature and room temperature structures have essentially the same packing arrangements of molecules except the small difference in the orientation of the butyl chain terminal carbon atoms in one of the three symmetry independent molecules.

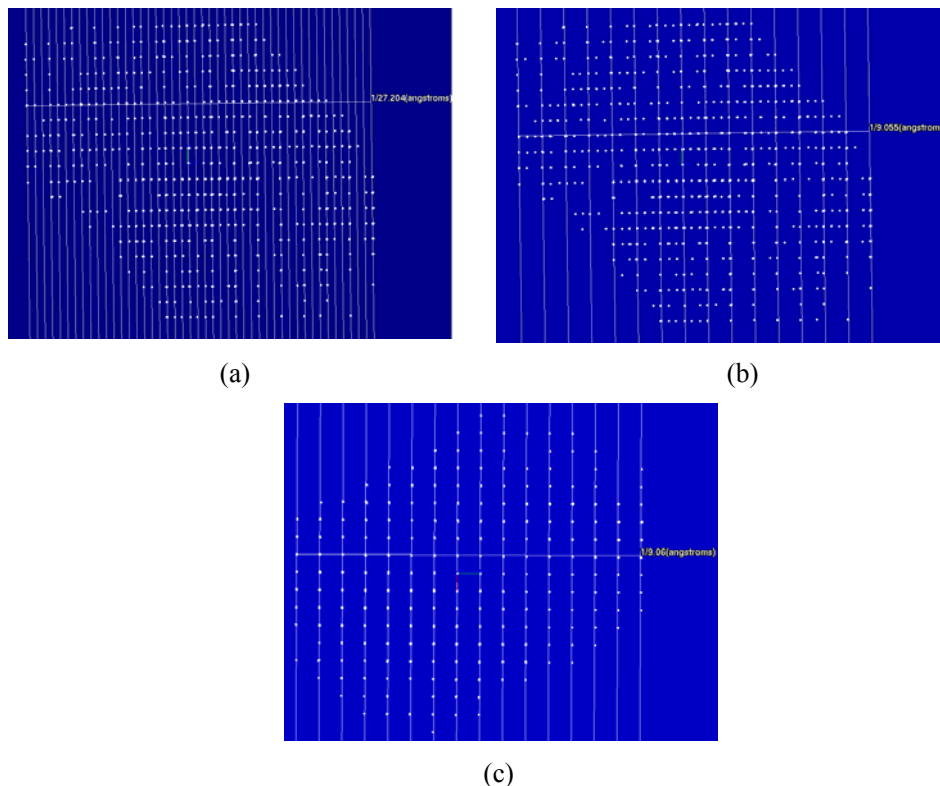


Figure 6.2 (a) Reflections of 100 K data viewed in RLATT software, (b) if only the reflections that are lying on the vertical lines are considered, cell dimensions with b axis = 9.0488(16) Å can be obtained, but this solution results in a comparatively bad structure. (c) Reflections at room temperature data viewed in RLATT software, from where it is not possible to obtain a cell with b axis of ~27 Å.

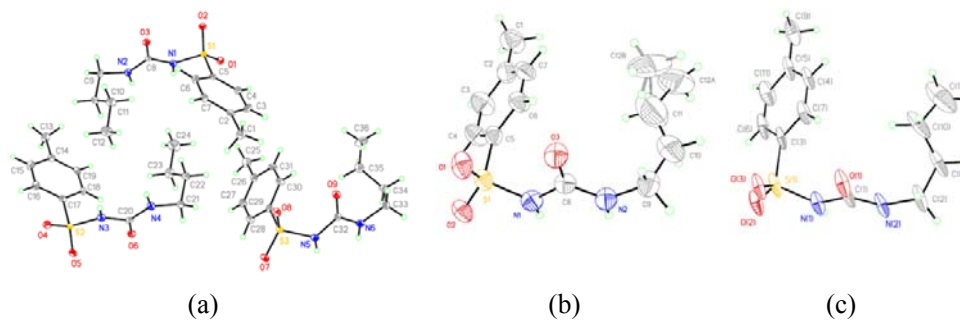


Figure 6.3 ORTEP diagrams at 35% probability of electron density in the ellipsoids. (a) Three symmetry independent molecules at 100 K of form III. (b) One molecule of form III with disorder in the butyl chain at 298 K. (c) 100 K data set solved using $\frac{1}{3}$ the b axis = 9.04 Å. The thermal ellipsoids are elongated indicating that the electron density is not accounted for correctly in the crystal structure solution.

The main synthon in both structures is the urea tape motif further stabilized by N–H···O=S hydrogen bond (Figure 6.4) (the metrics are listed in Table 6.1). There are possibilities that p-NP and p-PDBA may play a role in producing the high Z' modulated structure^{16,17,18} of TB form III because the known form I crystallized when the additive was absent. Figure 6.5 shows a putative scheme depicting the role of coformer in producing high Z' form III. The main lines of the calculated X-ray powder diffraction (XRPD) patterns of the $Z' = 1$ and the $Z' = 3$ structures overlay peak-to-peak (Figure 6.6) and hence they are called as modulated structures. The similarity of urea···boronate³⁰ hydrogen bonding to that of urea···nitro synthon²⁹ (Scheme 6.2) is a possible reason for these two molecules to give the same polymorphic result. However, even a trace of cocrystal formation was not detected in IR, NIR and Raman spectra and XRPD patterns of the solids.

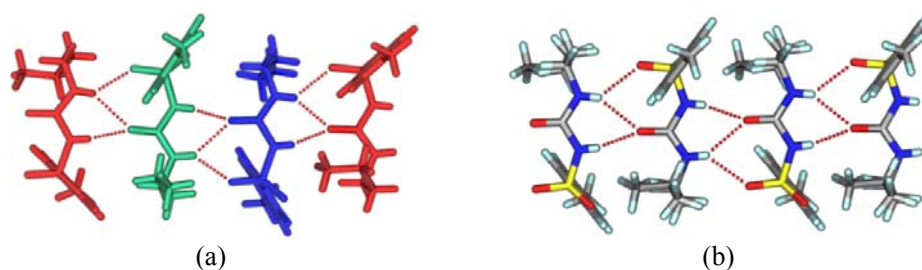


Figure 6.4 (a) Crystal structure of TB at 100 K. The three symmetry independent molecules form a urea tape like 1D chain structure along the b -axis. The terminal atoms of the butyl chain in two molecules is in anti conformation (green, blue) and one is in gauche conformation (red). (b) Urea tape motif in the room temperature structure. The butyl chain terminal atoms are disordered over two positions.

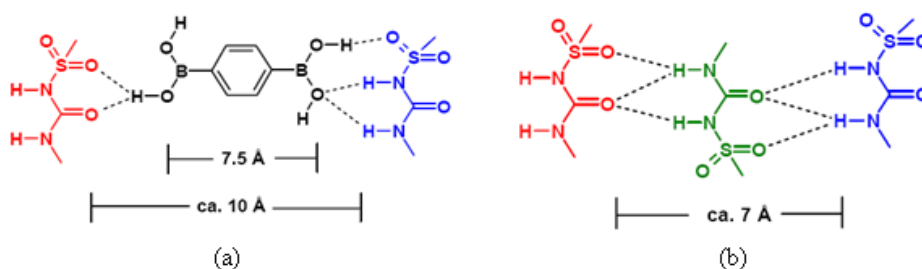


Figure 6.5 A putative scheme to show a hydrogen-bonded complex between TB and p-PDBA in solution (a) which gives way to the high Z' structure of form III (b). TB molecules in the same orientation are hydrogen bonded on both side of p-PDBA (placed in an inversion symmetry orientation) and a third TB molecule replaces the central linker molecule, but now with its sulfonyl group on the opposite side to give three symmetry independent molecules in the unit cell of TB form III ($Z' = 3$).

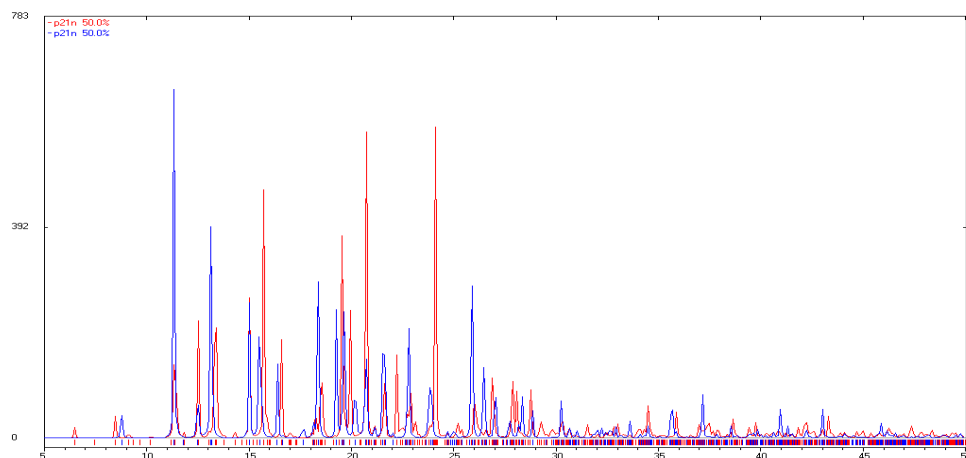


Figure 6.6 Overlay of calculated XRPD pattern of form III at room temperature (blue) and at 100 K (red).

Further efforts in this direction focused on cocrystallization of TB with *p*-nitrobenzoic acid, because the latter molecule has stronger hydrogen bonding COOH group compared to *p*-NP and *p*-PDBA, but the result was the known TB form IV.

6.2.2 Novel form V of Tolbutamide

There have been reports³¹ of sulfonylurea functional group interacting with nitrate ion via nitro...urea synthon as shown in Figure 6.7.

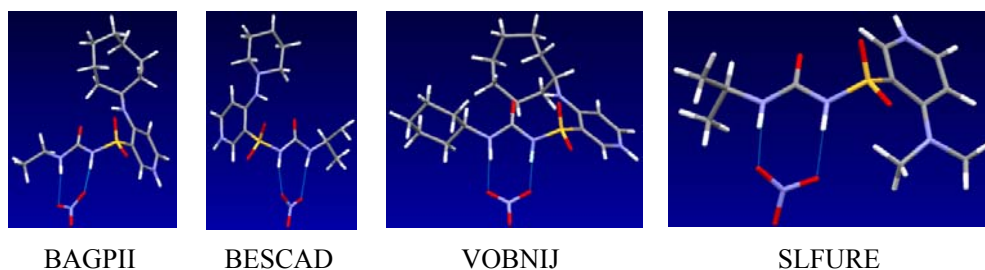


Figure 6.7 Urea...nitro synthon displayed by sulfonylurea and nitrate ion in four complexes. Ref. codes are BAGPII^{31b}, BESCAD^{31c}, VOBNIJ^{31d}, and SLFURE.^{31a}

Assuming this, when a nitrate anion was used as the complexing agent in the place of the nitro group to hydrogen bond with the urea functionality a serendipitous result was obtained. Crystallization of TB in methanol by adding a trace of conc. HNO₃ and allowing slow evaporation gave single crystals after 2 days that solved and refined in

Pbcn space group. As this is a new space group compared to the reported crystal structures of TB (form I *Pna*2₁, form II *Pc*, form III *P*2₁/*n*, and form IV *P*2₁/*c*), an indication that a new polymorph was crystallized, and hereafter called as form V.³² Crystals of form V were very unstable and converted to form I within a few hours. X-ray reflections were collected at room temperature because the crystal picked up moisture far more rapidly at 100 K and immediately transformed to form I. Attempts with intermediate temperature data collection also gave the same problem. The main synthon in this crystal structure is again the urea tape synthon (N–H···O=C: 1.84 Å, 157.7°; 2.29 Å, 141.2°) along the *b*-axis. The S=O group also engages in N–H···O hydrogen bond (2.22 Å, 138.7°) to stabilize the linear tape. A C–H···O=S hydrogen bond (2.76 Å, 132.0°) connects two such tapes and the overall structure is stabilized by close packing (Figure 6.8). Unlike the other three polymorphs (I, II and III), the tolyl group and the butyl chain are on the same side of the urea tape in this structure, similar to that in form IV. Hydrogen bond metrics are listed in Table 6.1.

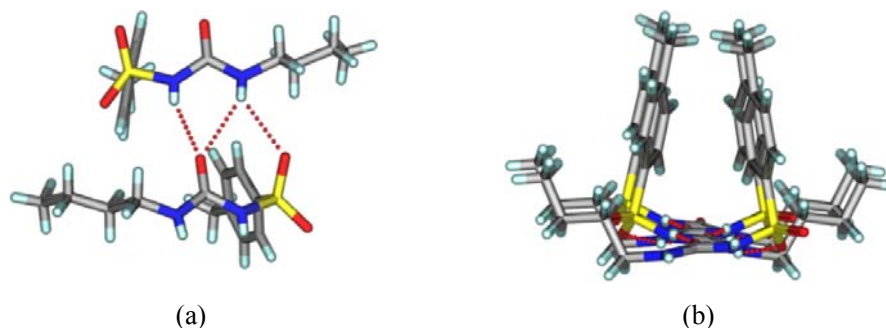


Figure 6.8 (a) Urea tape structure sustained by N–H···O hydrogen bonds in new form V of Tolbutamide. (b) The tolyl groups and butyl chains reside on the same side of the urea tape motif.

Table 6.1 Neutron normalized hydrogen bond parameters.

D–H···A	H···A (Å)	D···A (Å)	<D–H···A (°)	Symmetry code
Form III (100 K data)				
N–H1···O9	1.80	2.773(3)	161.6	1+x, y, z
N2–H2···O8	2.13	2.907(3)	132.4	1+x, y, z
N2–H2···O9	2.19	3.075(3)	145.7	1+x, y, z
N3–H3A···O3	1.77	2.764(4)	169.7	$\frac{1}{2}+x, \frac{1}{2}-y, -\frac{1}{2}+z$
N4–H4A···O2	2.06	2.893(4)	138.6	$\frac{1}{2}+x, \frac{1}{2}-y, -\frac{1}{2}+z$
N4–H4A···O3	2.41	3.263(4)	141.9	$\frac{1}{2}+x, \frac{1}{2}-y, -\frac{1}{2}+z$
N5–H5A···O6	1.78	2.781(4)	168.9	1–x, –y, 1–z
N6–H6A···O5	2.05	2.871(3)	137.5	1–x, –y, 1–z
N6–H6A···O6	2.35	3.209(4)	141.9	1–x, –y, 1–z
Form III (298 K data)				
N1–H1···O3	1.79	2.770(4)	163.8	$\frac{3}{2}-x, -\frac{1}{2}+y, \frac{1}{2}-z$
N2–H2···O1	2.14	2.946(4)	135.3	$\frac{3}{2}-x, -\frac{1}{2}+y, \frac{1}{2}-z$
N2–H2···O3	2.22	3.094(4)	143.4	$\frac{3}{2}-x, -\frac{1}{2}+y, \frac{1}{2}-z$
Form V (298 K data)				
N2–H1···O1	2.22	3.047(6)	138.7	$\frac{1}{2}-x, \frac{1}{2}+y, z$
N2–H1···O3	2.29	3.145(6)	141.2	$\frac{1}{2}-x, \frac{1}{2}+y, z$
N1–H2···O3	1.84	2.797(6)	157.7	$\frac{1}{2}-x, \frac{1}{2}+y, z$

The XRPD patterns of form IV and V calculated from the crystal structures were compared (Figure 6.9). The similarity of 1D urea tape motif and closeness of diffraction lines suggested a degree of similarity in these two structures. The molecular overlay in Mercury³³ showed good superposition, but only for 6 out of 15 molecules at the default settings of angle and distance tolerance of 20% between the structures being compared. However, when these tolerances were relaxed to 40% (to include more molecules in the overlay) the number of molecules being superposed increased to 10/15 and the differences between form IV and V structures showed up clearly (Figure 6.10). A good overlay of 15 nearest neighbor molecules (based on the close packing principle that any molecule is surrounded by 12 near neighbor molecules) is generally taken as an indicator of similarity between crystal structures. The main structural difference between form IV and V is in the direction of the two consecutive urea tapes. The two structures are 1D isostructural (same urea tape of molecules in similar conformations) but the difference lies in the direction of the urea tape in the two polymorphs (as detailed in the caption of Figure 6.11).

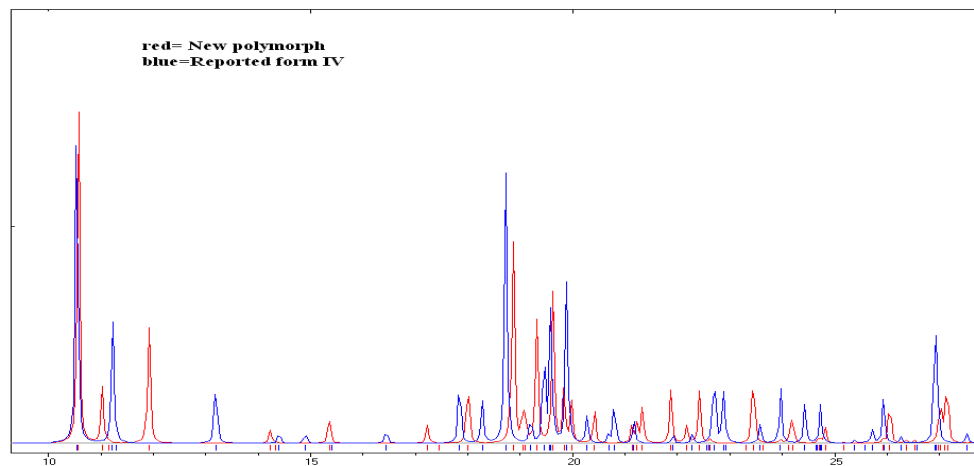


Figure 6.9 There are visible differences in the XRPDs of recently reported form IV (structure determined by powder data) and new form V.

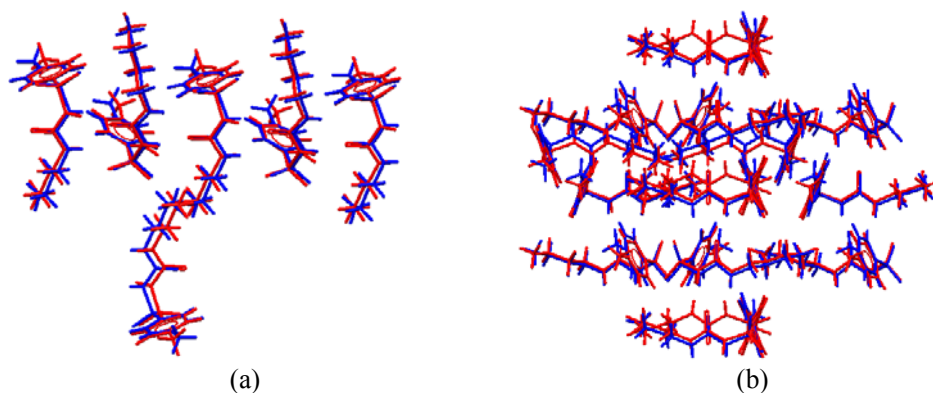


Figure 6.10 (a) Overlay of 6/15 near neighbor molecules at the default setting of 20% variance in bond angles and distances. The 6 molecule superposition is identical. (b) However, when the threshold is increased to 40% the number of molecules in overlay increases to 10/15 but the differences in molecular superposition show up clearly. Form V = blue, Form IV = red.

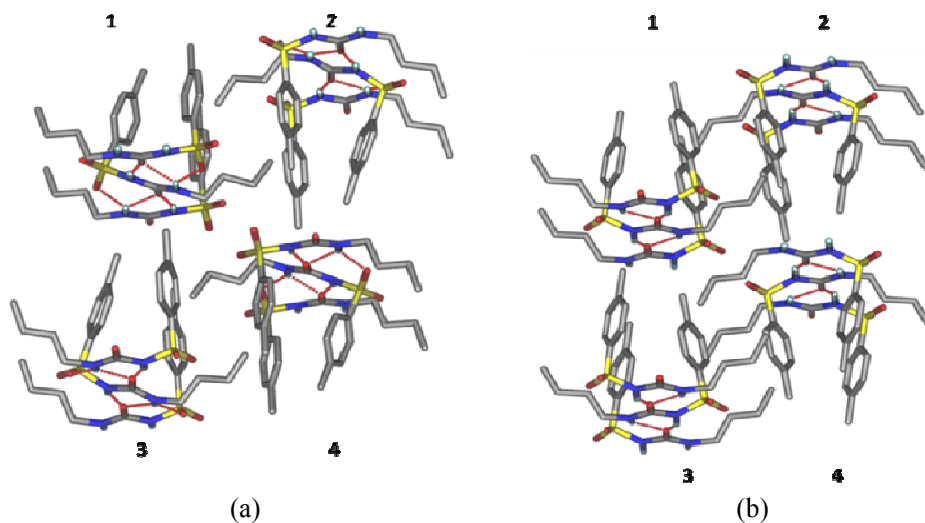


Figure 6.11 Difference in the direction of the urea tape in form V compared to form IV of TB. A molecular cluster of four adjacent urea tapes is shown in both cases (1, 2, 3 and 4). (a) In polymorph V the direction of urea tapes 1 and 2 are the same (carbonyl pointing away from the reader) but opposite for 3 and 4 (carbonyl group towards the reader). (b) In form IV urea tapes 1 and 3 are in the forward direction but 2 and 4 point away.

6.2.3 Characterization by FT-IR

The novel form V of TB was characterized by FT-IR. The N–H stretching frequency (3346 cm^{-1}) of form V is significantly different and S=O symmetric and asymmetric stretching frequencies (1345 and 1166 cm^{-1}) are slightly different compared to the values reported for polymorphs I-IV (Figure 6.12).

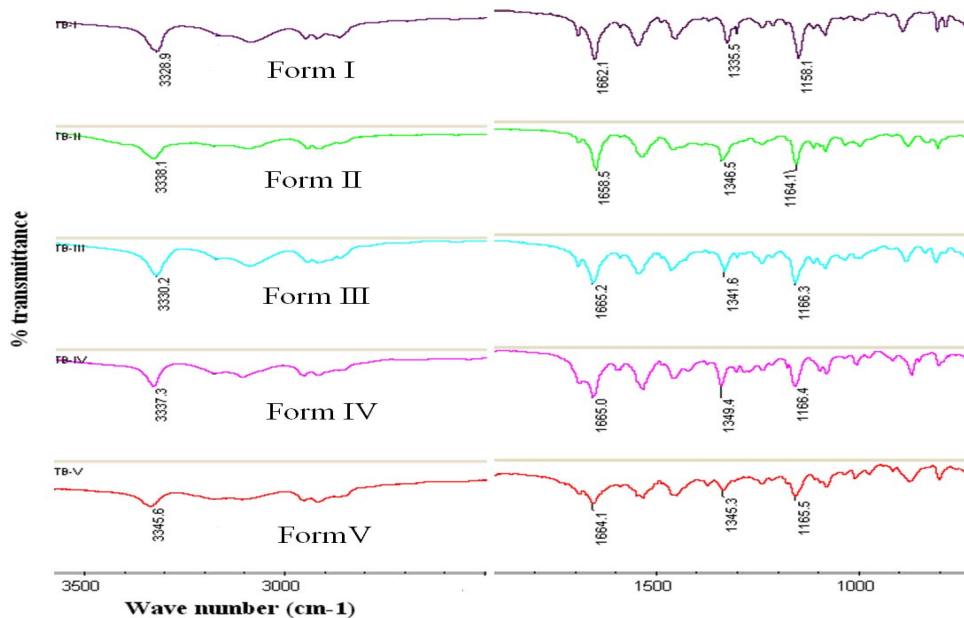


Figure 6.12 Comparison of FT-IR spectra of Tolbutamide new form V and reported polymorphs I-IV.

6.2.4 Phase transformation of form V

The metastable form V converted to the stable form I at room temperature upon storage under ambient conditions of temperature and humidity. Phase change was monitored by IR spectroscopy and optical microscopy.

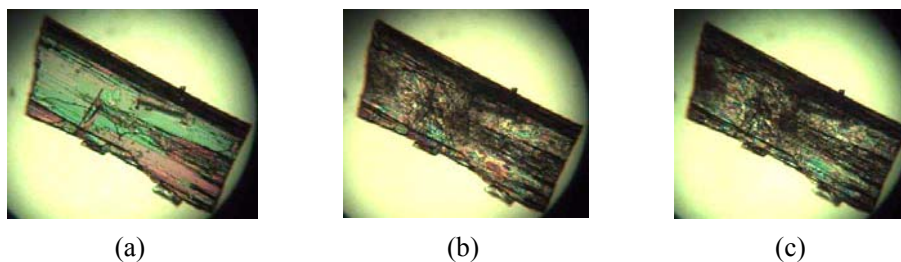


Figure 6.13 (a) TB form V crystal at room temperature, (b) the same crystal after two hours, and (c) transformation to form I after 24 hours.

Microscopy images of form V crystals showed the transformation to form I at room temperature within 2 h (Figure 6.13). The transformation of form V to form I was monitored by the diagnostic IR peaks (Figure 6.14).

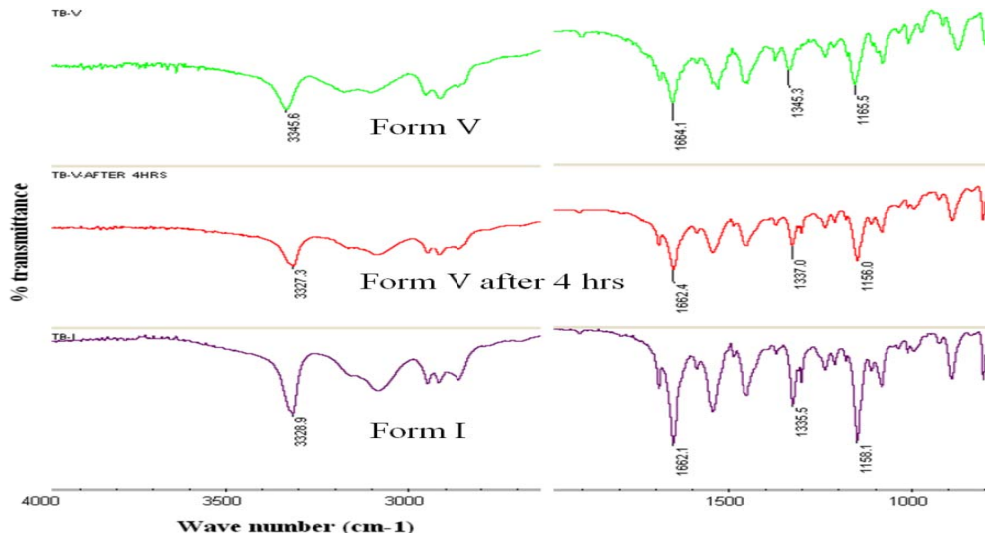
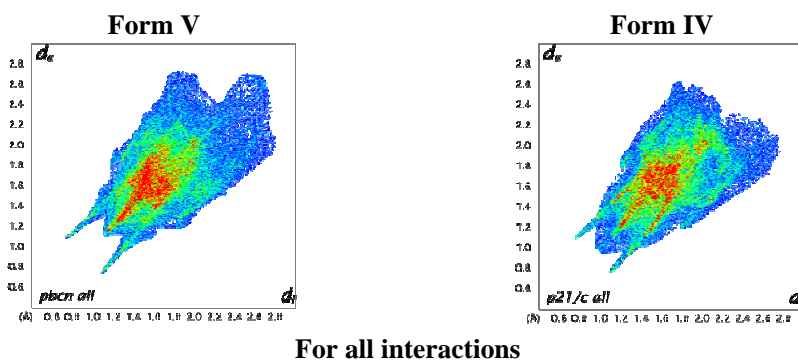


Figure 6.14 FT-IR spectra of TB form V (green), form V after 4 h at room temperature (red), and form I (magenta) confirm the metastable to stable polymorph phase transformation.

6.2.5 Hirshfeld fingerprint plots

2D Hirshfeld fingerprint plots³⁴ of the two polymorphs are also quite different. Figure 6.15 shows a comparison of 2D Hirshfeld fingerprint plots of form V and form IV for different interactions such as O \cdots H, H \cdots H and C \cdots H interactions.



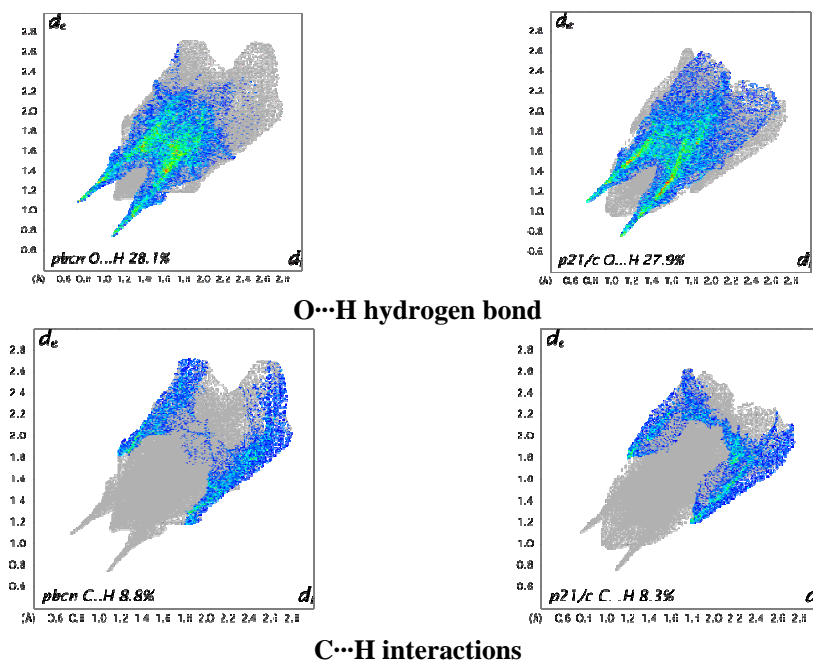
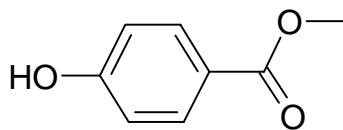


Figure 6.15 2D fingerprint Hirshfeld plots of Tolbutamide forms V and IV show clear differences in hydrogen bonding and hydrophobic interactions regions.

6.3 Crystal Structure of Methyl Paraben Polymorph II

Parabens³⁵ are a group of alkyl esters of *p*-hydroxybenzoic acid and typically include methyl paraben, ethyl paraben, propyl paraben, butyl paraben, heptyl paraben and benzyl paraben. The parabens or their salts are widely used as preservatives in cosmetics, toiletries, food and pharmaceuticals as they have a broad spectrum of antimicrobial activity. Methyl paraben (MP) (Scheme 6.3) is particularly important because of its high solubility (2.7 mg/mL in phosphate buffer)³⁶ compared to higher esters in the series. Methyl paraben is added as a preservative to skin creams, shampoos and eye makeup to protect users from infections, rashes, and microbial attacks. Approximately 30,000 lbs of methyl paraben is consumed annually in the USA. Basically, a huge percentage of the products for everyday use contain some form of paraben. Despite the extensive use of parabens they are under toxicological study, since parabens are known to be weak estrogen mimics.^{35,37}



Scheme 6.3 Molecular structure of Methyl paraben (MP).

Polymorphism in MP was first indicated by Fischer and Stauder in 1930³⁸ following which Kofler and Kofler investigated the phenomenon and discovered its two modifications.³⁹ Later in 1939 Lindpainter described six modifications of MP.⁴⁰ Methyl paraben was called *p*-oxybenzoic acid methyl ester in the older literature.

The X-ray structures for two modifications of β -cyclodextrin–methylparaben inclusion structures are reported.⁴¹ Cocrystal polymorphs of lamotrigine with methyl paraben were recently published.⁴² Methyl paraben also acts as a “molecular hook” for the selective separation of quinidine from its stereoisomer quinine based on its molecular specificity.⁴³ MP is known to interact with sugar and sugar alcohols.⁴⁴

6.3.1 Results and discussion

Three crystal structures of MP are archived in the Cambridge Structural Database⁴⁵ (ver. 1.12, August 2010 update; CSD Refcodes: CEBGOF,⁴⁶ CEBGOF01,⁴⁷ and CEBGOF02).⁴⁸ A new polymorph of MP was claimed by Vujovic and Nassimbeni⁴⁷ in 2006 but this was proved to be the same crystal structure by Threlfall and Gelbrich.⁴⁹ The latter authors commented that the shifts in the X-ray powder diffraction (XRPD) lines were due to lattice parameter changes with temperature. Another polymorph of MP with different *c*-axis and β -angle from that for Form I was claimed⁴⁸ in 2008, but the crystal structure, space group and Z values are the same. There is only one unique crystal structure of methyl paraben in the literature as of early 2011 based on the comparison of unit cell parameters, space group (Table 6.2), calculated XRD lines (Figure 6.16) and molecular packing (Figures 6.17). These single crystals were obtained by solution crystallization from alcoholic solvents (MeOH, EtOH) at room temperature.

A second polymorph of methyl paraben was successfully crystallized; hereafter Form II, and its X-ray crystal structure and molecular packing, thermal behavior, and Hirshfeld surface plots were compared with Form I.⁵⁰ A survey of the CSD suggested

that the other parabens, such as ethyl, propyl, allyl, *n*-hexyl, and benzyl, have only one crystal structure report each.

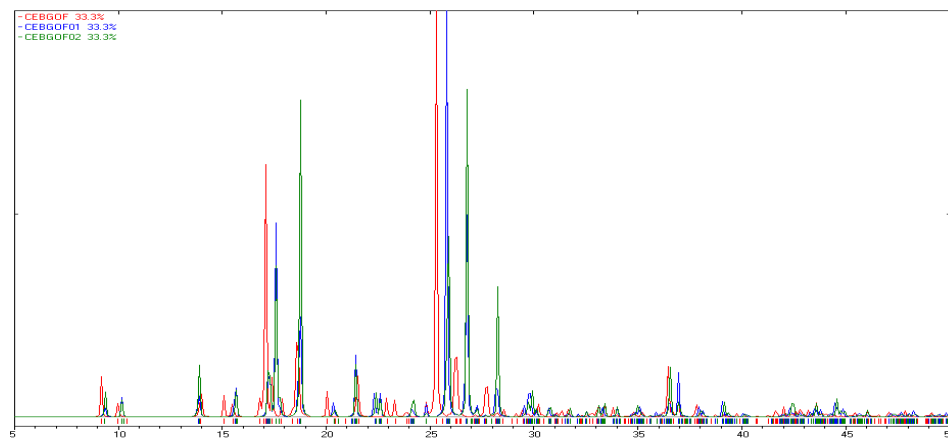


Figure 6.16 Overlay of calculated XRPD patterns from the crystal structure Refcode CEBGOF (red), CEBGOF01 (blue) and CEBGOF02 (green). Blue and green peaks are overlapping completely depicting the exact similarity in their crystal structures. These crystal structures were determined at different temperatures, and hence the overlay will not be perfect due to lattice expansion/ contraction.

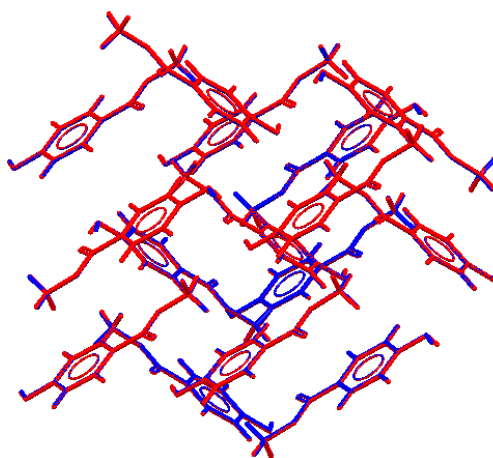


Figure 6.17 Overlay of 15 nearest neighbor molecules in the two crystal structures of Refcode CEBGOF01 (red) and CEBGOF02 (blue) at the default setting of 20% angle and distance tolerance in Mercury 2.3, a crystal structure visualization program distributed with the CSD. It shows complete overlap of all 15 molecules which proves crystal structures corresponding to the ref codes CEBGOF01 and CEBGOF02 are same.

Commercial methyl paraben was confirmed to be Form I by XRPD. Different techniques were used for polymorph screening such as crystallization from various

solvents at room temperature and low temperature, flash cooling, melting and sublimation. A second polymorph of methyl paraben was obtained in sublimation experiments as thin plate type crystals concomitantly with Form I (block crystals) when condensation was allowed to happen slowly over 2 days, as described in Experimental section. All other techniques and experiments gave Form I.

There are clear differences in the cell parameters of Form II and the reported crystal structure (Table 6.3) of different Z' value (Form I, $Z' = 3$; Form II, $Z' = 1$, ORTEP is shown in Figure 6.18). Among the three different structure reports for Form I, the crystal data of Vujovuc and Nassimbeni⁴⁷ (CEBGOF01) is considered for discussion because it has the lowest R -factor (0.033) and was determined at about the same temperature as the reflections data collected for form II (113 K, 100 K).

Table 6.3 Comparison of cell parameters of the best reported crystal structures of methyl paraben Form I with Form II.

Compound	Form II	CEBGOF	CEBGOF01	CEBGOF02
Reference	This work	Ref. 46	Ref. 47	Ref. 48
Crystal system	Monoclinic	Monoclinic	Monoclinic	Monoclinic
Space group	$P2_1/c$	Cc	Cc	Cc
T/K	100	283-303	113	100
$a/\text{\AA}$	4.8186(13)	13.568(5)	13.006(3)	12.9708(4)
$b/\text{\AA}$	14.630(4)	16.959(7)	17.261(4)	17.2485(7)
$c/\text{\AA}$	10.239(3)	12.458(6)	12.209(2)	10.8428(3)
$\beta/^\circ$	99.810(5)	130.10(3)	129.12(3)	119.260(1)
Z'/Z	1/4	3/12	3/12	3/12
$V/\text{\AA}^3$	711.3(3)	2192.710	2126.445	2116.316
$D_{\text{calc}}/\text{g cm}^{-3}$	1.421	1.382	1.426	1.433
$R_1[I > 2\sigma(I)]$	0.0801	0.054	0.033	0.0425

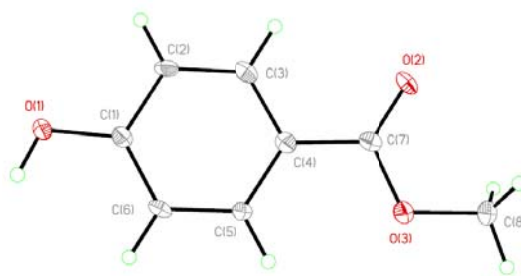


Figure 6.18 ORTEP Form II methyl paraben at 35% probability for heavy atom thermal ellipsoids. In contrast, Form I has three molecules in the asymmetric unit.

The yield of Form II was very low (~1%) and the quality of single crystals was poor compared to Form I crystals. Both polymorphs crystallized concomitantly on the cold finger of the sublimation apparatus (Figure 6.19). Crystals of Form II were found to be very unstable. Mechanical handling resulted in crystal deformation or phase change to Form I, and hence analytical measurements such as DSC, XRPD and ss-NMR could not be carried out on Form II.



Figure 6.19 Concomitant crystallization of Form I and Form II of methyl paraben by sublimation on the cold finger.

The crystal structure of Form I contains zigzag chains of O–H···O hydrogen bonds (1.79 Å, 174.0°; 1.77 Å, 165.3°; and 1.76 Å, 168.5°) along the *c*-axis, and such chains are connected via C–H···O (2.41 Å, 139.5°; 2.61 Å, 152.4°; and 2.47 Å, 137.8°) and C–H··· π (2.70 Å, 134.8°; 2.57 Å, 146.4°; 2.69 Å, 150.7°; and 2.61 Å, 133.8°) interactions (Figure 6.20, d and e). Whereas the molecules are coplanar in a molecular

dimer of Form II, they are nearly orthogonal in Form I (Figure 6.20, a and b). The main synthon in both structures is the O—H···O hydrogen bond from the hydroxyl O—H to the carbonyl oxygen. The sheet structure of Form II is sustained by O—H···O hydrogen bond (1.71 Å, 174.2°) and auxiliary C—H···O interactions (2.35 Å, 167.6°; 2.63 Å, 124.9 °). Adjacent layers are stacked at 3.23 Å distance. There are thus clear differences between the crystal structures of Form I (zigzag chain of molecules, 3D packing) and Form II (linear chain, lamellar packing), apart from the fact that their space groups, unit cell parameters and Z' values are different. The calculated XRD lines from the crystal structure show clear differences in peak positions for Form I and II (Figure 6.21).

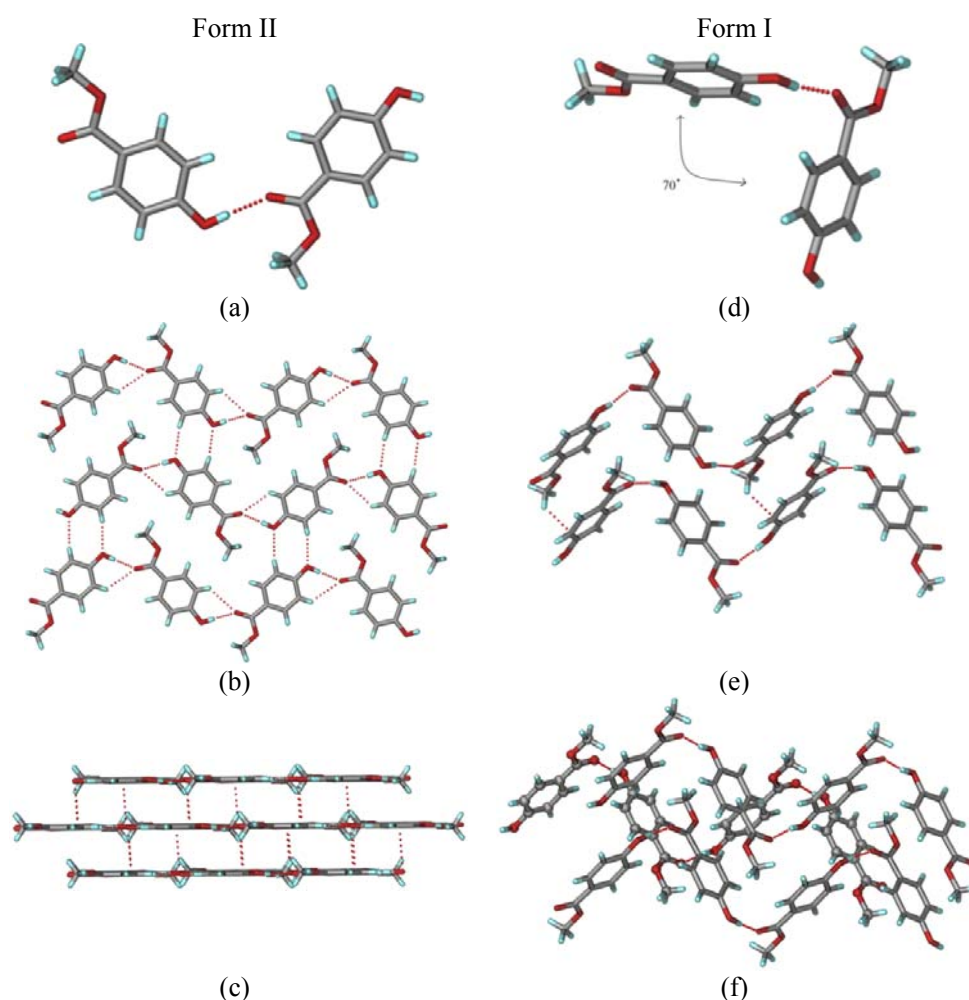


Figure 6.20 Hydrogen bonding and molecular packing in the crystal structures of MP. Form I (right panel) and Form II (left panel).

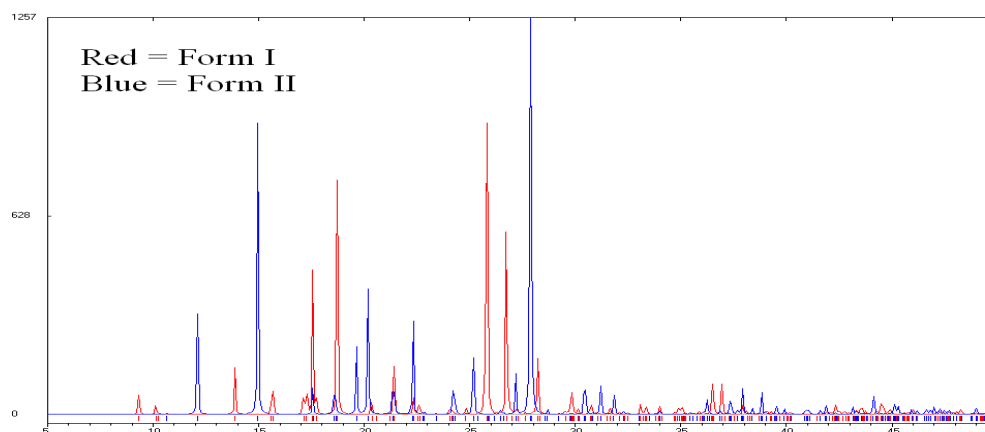


Figure 6.21 Calculated XRPD pattern of Form I (red) and Form II (blue).

IR stretching frequencies of O–H (Form I = 3314 cm^{-1} , Form II = 3416 cm^{-1}), C=O (Form I = 1681 cm^{-1} , Form II = 1686 cm^{-1}), and C–O (Form I = 1163 cm^{-1} and Form II = 1170 cm^{-1}) are different for the two polymorphs as shown in Figure 6.22.

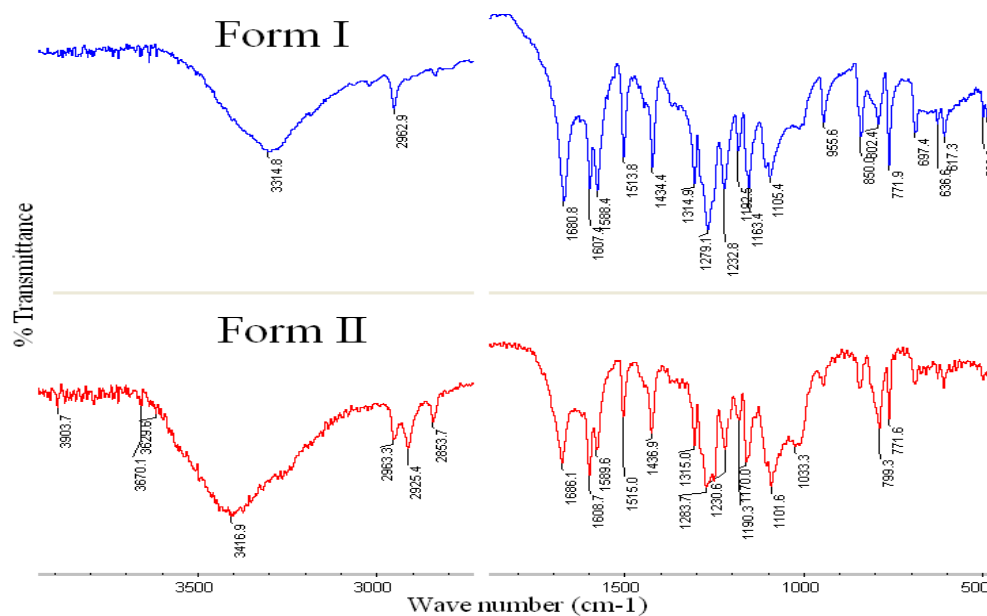


Figure 6.22 IR spectrum (KBr) of Form I and Form II show diagnostic peaks at different frequencies.

The crystal structure of Form II is similar to the crystal structure of ethyl paraben and propyl paraben⁵¹ (Figure 6.23), which has planar sheets with the ester ethyl and propyl groups projecting out of the layer, albeit more so than in the methyl analog. This leads to the thought:⁵² could ethyl and propyl paraben have a polymorphic structure similar to the 3D packing in Form I of methyl paraben?

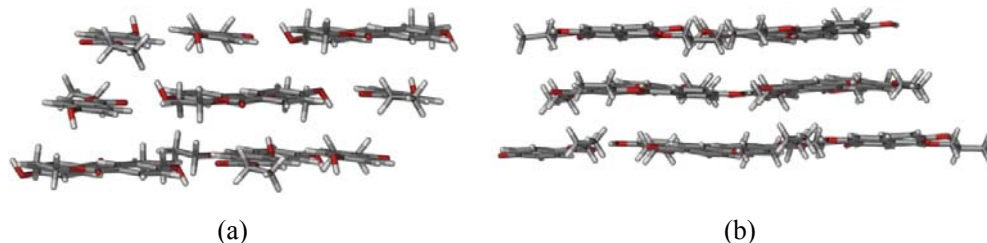


Figure 6.23 Layered crystal structure of ethyl paraben (hydrogens were generated in Mercury 2.3 software) (a) and propyl paraben (b).

The thermal events were visualized under a hot stage microscopy for both polymorphs. Form II crystals showed changes during heating which started at 68 °C and ultimately melted at 124 °C (Figure 6.24a), whereas sublimation of Form I crystals was observed which started at 100 °C and finally melted at 124 °C (Figure 6.24b).

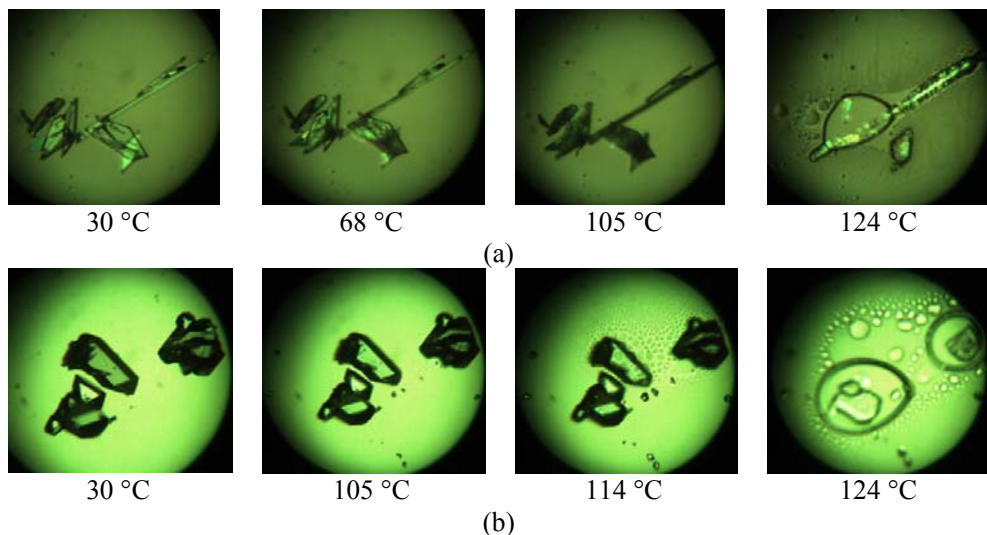


Figure 6.24 Hot stage microscopy images. (a) Form II crystals show changes (transparent to opaque nature) at about 68 °C. (b) Form I crystals begin sublimation at about 100 °C and then become liquid at 124 °C.

6.3.2 Hirshfeld fingerprint plots of MP form I and form II

The 2D fingerprint plots as Hirshfeld surface³⁴ for the two polymorphs display clear differences in the interactions even as the main structure governing O–H···O hydrogen bond is the same in both structures, which shows up as a pair of sharp spikes in the plots. The planar structure of Form II is depicted by the red region in the centre of the plot, which is due to a C=O group residing just above the phenyl ring centroid (3.43 Å) whereas the light red shade for the three molecules of Form I suggest the absence of stacking interactions. The C–H··· π interactions in Form I show up as wings in A and C molecule plots (C–H··· π 2.70 Å and 2.61 Å). The wings are not prominent for B molecule because the interaction is long (3.09 Å). The absence of C–H··· π interaction in the lamellar structure of Form II is demonstrated by the absence of wings in its 2D fingerprint plot (Figure 6.25). The relative contributions of each interaction to the Hirshfeld surface are depicted in Figure 6.26. Form II structure has less O···H and C···H contacts and more of H···H contacts compared to Form I. From the crystal structure and also from the Hirshfeld fingerprint plot it is evident that there is lower contribution of C···H contacts in Form II crystal structure compared to Form I.

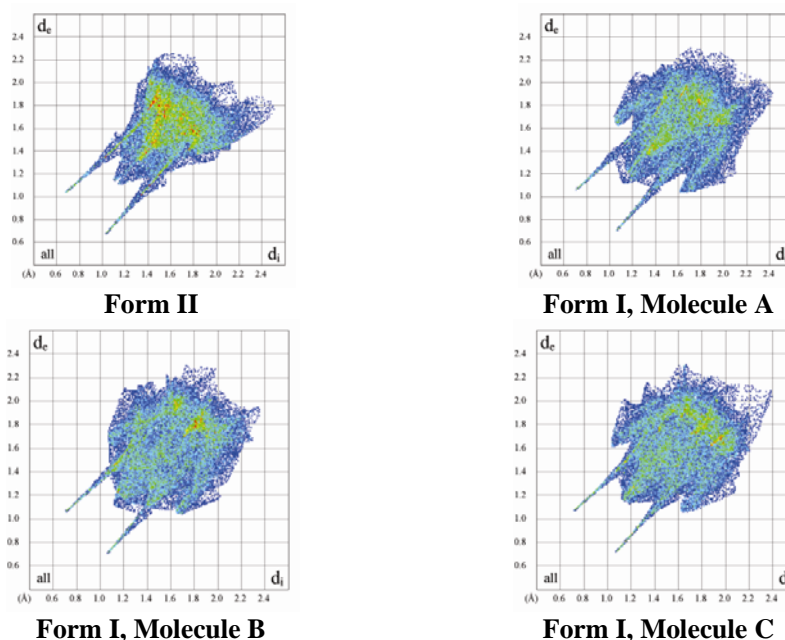


Figure 6.25 2D fingerprint plots of Form II and three molecules of Form I (A, B and C).

The density of MP polymorphs is very close (Table 6.3). From visual observation of crystal behavior upon manual handling it is clear that Form II is metastable. Lattice energy calculations⁵³ indicate the greater stability of Form I compared to Form II (Compass: -24.95, -24.90; Dreiding: -33.65; -31.22). The energy difference is larger in Dreiding calculations because this force field explicitly accounts for the hydrogen bond energy component whereas Compass calculates hydrogen bonds as an overall electrostatic term.

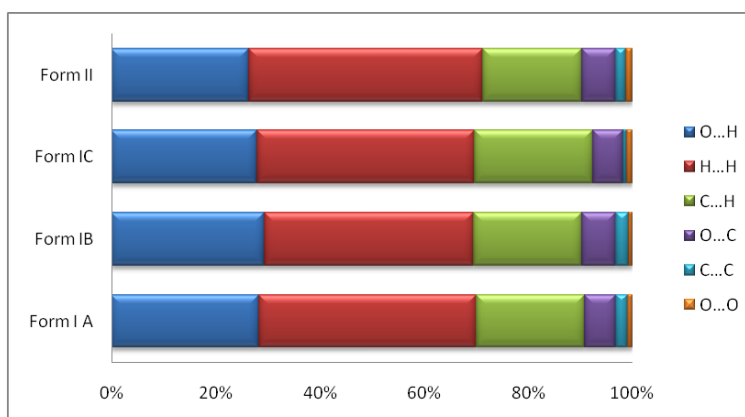


Figure 6.26 Relative contribution of different interactions to the Hirshfeld surface.

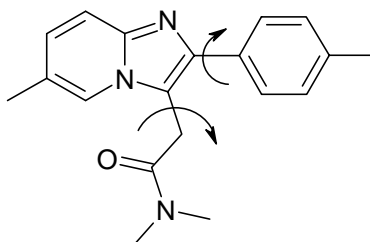
6.4 Conformational Polymorphism in Zolpidem•Succinic acid Cocrystal

Insomnia is a common condition that affects one's ability to sleep. Benzodiazepines⁵⁴ formed the mainline therapy for many years till the advent of newer nonbenzodiazepine group of drugs. The nonbenzodiazepines⁵⁵ are a class of psychoactive drugs whose pharmacological actions are similar but structurally unrelated to those of the benzodiazepines.

Zolpidem (ZM) is N,N-dimethyl-2-[6-methyl-2-(4-methylphenyl)imidazo[3,2-a]pyridin-3-yl]acetamide, an imidazo-pyridine, has been marketed in the US and elsewhere as immediate-release (IR) tablets containing 5 and 10 mg of Zolpidem tartarate under the tradename Ambien.⁵⁶ It is a class I drug according to the BCS classification system with the Do (min) and Do (max) of 0.002 and 0.004 respectively with a short half life of 2-3 hours.⁵⁷ Zolpidem becomes addictive if taken for extended periods of time.

Various salt forms of Zolpidem such as tartarate, tosylate, hydrochloride, mesylate and sulfate are reported in the patent literature⁵⁸ which include different hydrates, solvates, guest free and amorphous forms. In CSD (Version 5.31, August 2010 update), crystal structure of only one molecular salt, Zolpidemium saccharinate (Ref. code VAWQEQ), is reported. Solubility of Zolpidem free base is less (0.13mg/mL) compared to its salt forms (18.8 mg/mL for Zolpidem tartarate and 19.8 for Zolpidem hydrogen tartarate).^{58d} Crystal structures of Zolpidem free base and its hemitartrate hemihydrate and hydrogen tartarate were recently reported.⁵⁹

Existence of multiple crystal forms of a solid can be due to the possibility of existence of more than one supramolecular synthon, conformational flexibility of the molecule resulting in different conformers in solid state or differences in crystal packing. ZM has two flexible torsions (Scheme 6.4) and it has hydrogen bonding donor and acceptor groups. With these flexible torsions exist in this molecule, there are possibilities to discover multiple solid forms of the parent base or its salts or cocrystals. There are abundant numbers of crystal structures reported in CSD for benzodiazepine type of molecules but very less for nonbenzodiazepines. Therefore, a screening of multi-crystalline forms of this drug or its salt/cocrystals was carried out in order to study conformational variance and structure-property relationship in them which can be helpful for future development of drugs with new formulations.

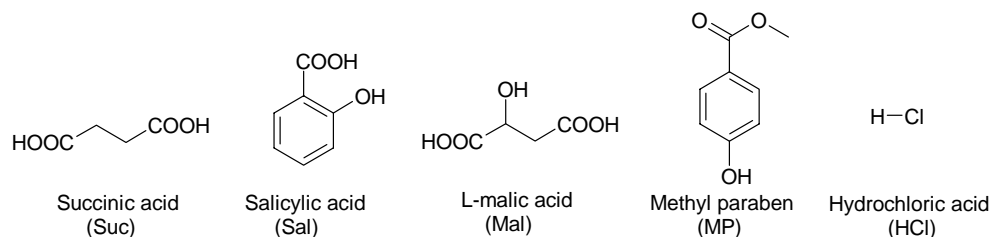


Scheme 6.4 Zolpidem (ZM) with two flexible torsions.

6.4.1 Results and discussion

Five cofomers were selected (Scheme 6.5) from GRAS list to make novel ZM molecular complexes and to screen novel polymorphs. Among these cocrystal formers succinic acid cocrystallized with ZM to give two cocrystal polymorphs whereas with

other conformers only hydrates and solvates with varying conformations of ZM were obtained.



Scheme 6.5 Coformers selected from GRAS list for cocrystallization.

6.4.2 Zolpidem•succinic acid cocrystal polymorphs (ZM•Suc)

Solution crystallization of ZM with succinic acid in 1:0.5 and 1:1 ratios resulted two cocrystal polymorphs in 1:0.5 ratios. Form I was crystallized from dry THF or dry dioxane whereas form II crystallized from CH₃CN, i-propanol, MeOH, n-propanol, EtOH, EtOAc, normal THF and dioxane.

In both the polymorphs, the primary synthon present is acid-COOH...N-imidazole (Figure 6.29a). ZM is conformationally flexible and in the crystal structures two mirror image conformers (non-superposable mirror image conformers) were observed (figure 6.28 a and b).

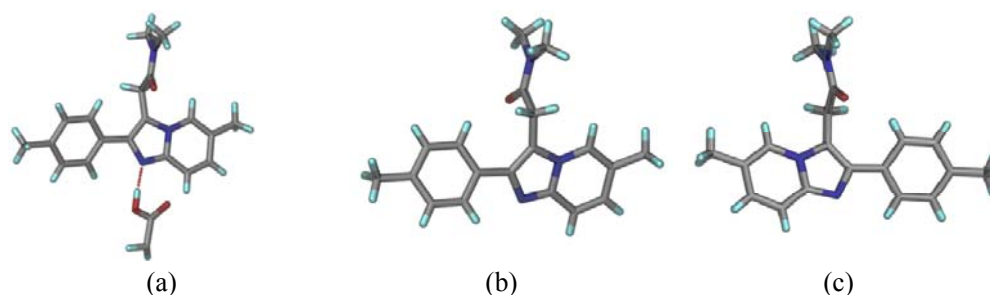


Figure 6.27 (a) Main synthon present in the cocrystal polymorphs of ZM•Suc. (b) and (c) represents the non-superposable mirror image conformers of ZM.

Crystal structure of form I (ZM•Suc-I): X-ray reflections collected on a needle morphology crystal of form I solved and refined in orthorhombic non-centrosymmetric space group *Iba*2 with one molecule of ZM and half molecule of Suc in the asymmetric

unit. The Suc molecule lies about the 2-fold rotation axis to result half molecule in the asymmetric unit. ZM molecules are stacked along *b*-axis via C–H···O hydrogen bonding (C16–H16B···O1, 2.29 Å, 150.5°) between methylene C–H and carbonyl oxygen. Such oppositely directing stacks (direction with respect to carbonyl group) are connected to each other via another C–H···O hydrogen bond (C3–H3···O1, 2.43 Å, 139.5°) and form a layer parallel to *bc* plane. Suc molecules act as a bridge between two such stacks of ZM molecules forming O–H···N hydrogen bond (O2–H2···N2, 1.63 Å, 174.9°) between Suc and imidazole N assisted by auxiliary C–H···O hydrogen bond (C6–H6···O3, 2.43 Å, 141.7°) completing the 3D packing (Figure 6.28).

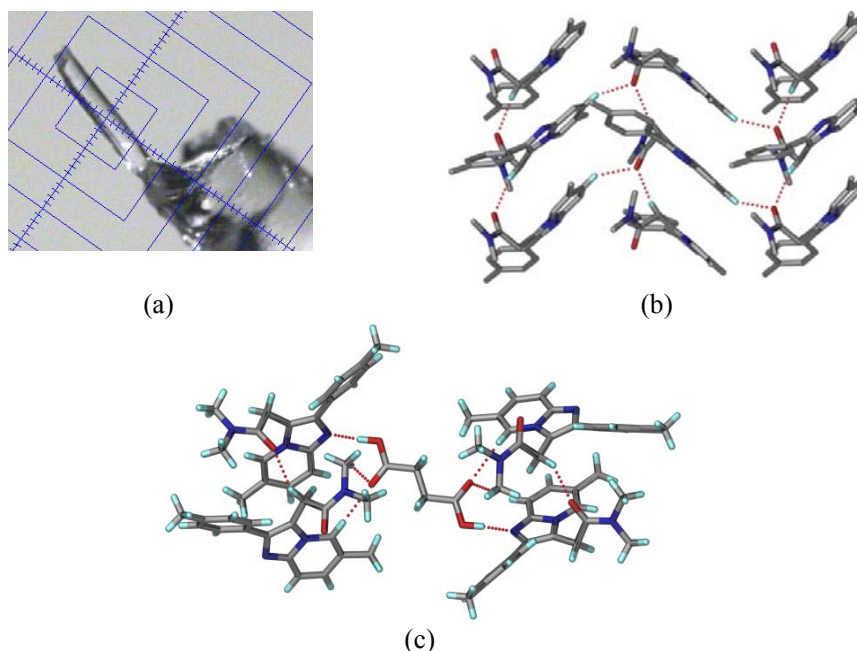


Figure 6.28 (a) Needle morphology single crystal of form I. (b) Oppositely directing stacks of ZM molecules connected by C–H···O interaction form layer. (c) Suc molecules connect two such layers.

Crystal structure of form II (ZM•Suc-II): Needle morphology crystals of form II were solved and refined in centrosymmetric monoclinic space group $P2_1/c$ with one molecule of ZM and half molecule of Suc, which lies about an inversion centre, in the asymmetric unit. ZM molecules are stacked one above the other, via trifurcated C–H···O hydrogen bonding between carbonyl oxygen and methylene CH₂ (C16–H16A···O1, 2.56 Å, 158.7°), C–H of N-dimethyl group (C18–H18A···O1, 2.26 Å, 164.4°) and aromatic C–H

(C6–H6···O1, 2.29 Å, 152.0°) from benzimidazole ring, along *c* axis. Other interactions such as C–H···N hydrogen bonding (C15–H15A···N3, 2.64 Å, 138.5°) involving CH₃ of tolyl group and pyrazole N (not shown in the figure) and π ··· π stacking between pyrazole and tolyl ring (3.29 Å) is also observed. Unlike form I, these stacks point towards the same direction with respect to carbonyl group and are not connected to each other directly but rather they are close packed. Two oppositely directing stacks of ZM molecules are connected by Suc via formation of O–H···N hydrogen bond (O2–H2···N2, 1.65 Å, 172.6°) between Suc COOH and imidazole N assisted by auxiliary C–H···O hydrogen bond (C18–H18B···O3, 2.48 Å, 153.9°) (Figure 6.29). Hydrogen bond metrics for both the forms are listed in Table 6.4 and crystallographic parameters are summarized in Appendix.

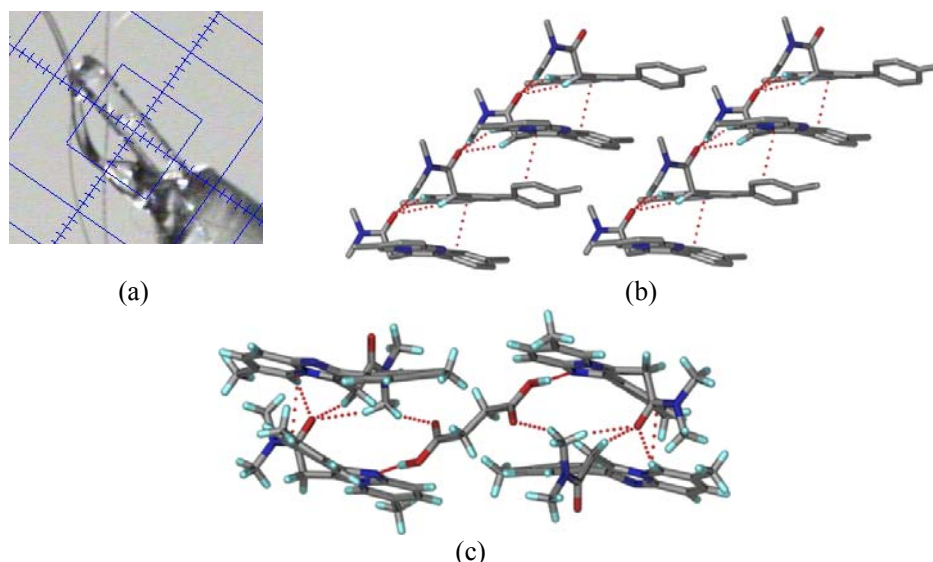


Figure 6.29 (a) Needle morphology crystal of form II. (b) Stacks of Zol molecules, directing along *c* axis, are close packed. (c) Suc molecules connect two oppositely directing stacks to complete the overall packing.

Table 6.4 Neutron normalized hydrogen bond distances, angles and symmetry codes.

Interaction	H···A/ Å	D···A/ Å	∠D–H···A/°	Symmetry code
Form I				
O(2)–H(2)···N(2)	1.63	2.615(3)	174.9	1/2–x, 1/2+y, z
C(3)–H(3)···O(1)	2.43	3.333(4)	139.5	1/2–x, 1/2–y, –1/2+z
C(6)–H(6)···O(3)	2.43	3.345(4)	141.7	x, y, z
C(16)–H(16B)···O(1)	2.29	3.275(4)	150.5	1/2–x, 1/2+y, z

C(18)–H(18A)···O(1)	2.33	2.724(4)	99.6	Intramolecular
Form II				
O(2)–H(2)···N(2)	1.65	2.628(2)	172.6	$x, 1/2-y, -1/2+z$
C(6)–H(6)···O(1)	2.29	3.283(2)	152.0	$x, 1/2-y, -1/2+z$
C(18)–H(18A)···O(1)	2.26	3.315(2)	164.4	$x, 1/2-y, -1/2+z$
C(18)–H(18B)···O(3)	2.48	3.489(2)	153.9	x, y, z
C(19)–H(19A)···O(1)	2.32	2.762(2)	102.6	Intramolecular

Polymorphism in ZM•Suc cocrystal is due to conformational differences of the p-tolyl group and N-dimethylacetamide group. In form I the torsion angles for p-tolyl and N-dimethylacetamide groups are 40.0(5) and 23.4(5) whereas for form II the values are 25.6(3) and 16.0(2). Figure 6.30 shows the overlay of the two conformers of form I and form II and corresponding torsion angles.

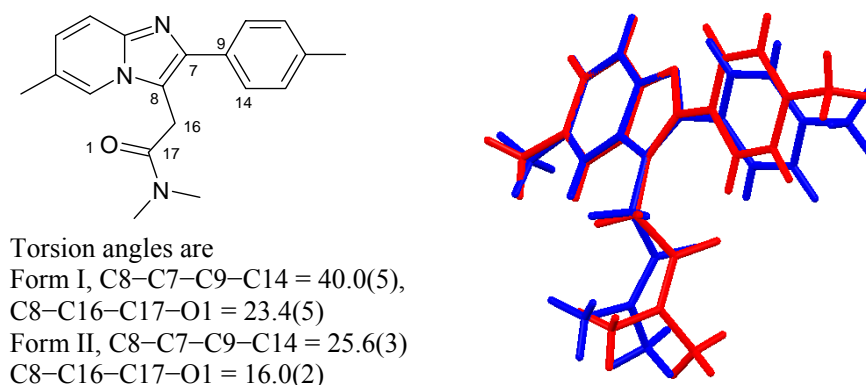


Figure 6.30 Overlay diagram shows the difference in the positions of the flexible parts of the ZM molecule in form I (blue) and form II (red).

6.4.3 Stability and phase transformation of form I and form II

Differential scanning calorimetry (DSC): DSC thermograms of both the polymorphs (Figure 6.31) did not show any phase transformation therefore two polymorphs are monotropically related. Form I melts at lower temperature (178 °C) with lower enthalpy of fusion 38.7 KJ mol⁻¹ compared to form II which melts at 184°C with an enthalpy of fusion value 40.2 KJ mol⁻¹. This establishes that the higher melting form II is thermodynamic polymorph whereas form I is metastable polymorph.

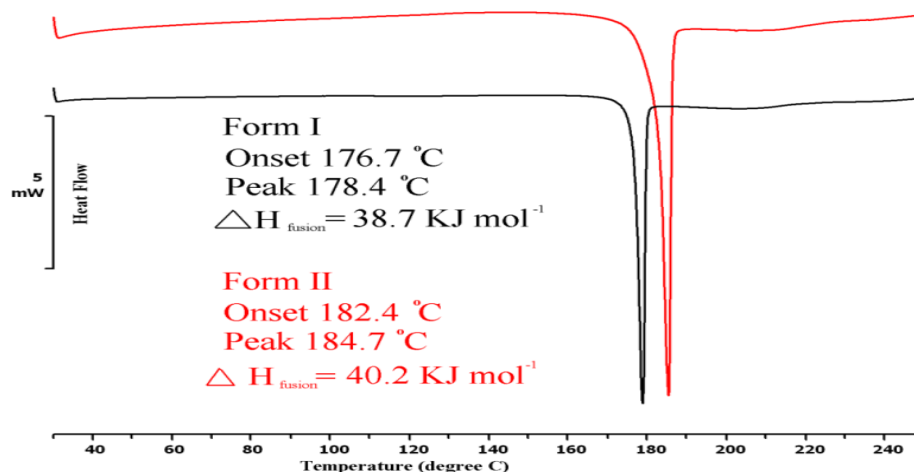


Figure 6.31 DSC thermograms of form I (black) and form II (red). Form II melts at higher temperature with higher enthalpy of fusion compared to form I.

Neat and liquid assisted grinding: Neat and liquid assisted grinding experiments were performed on the two polymorphs of ZM•Suc cocrystal in order to establish their stability relationship. When stoichiometric amounts of ZM and Suc were subjected to neat grinding, exclusive form II was obtained without any trace of form I. Neat grinding of form II did not induce any phase transformation to form I, whereas, the same on form I for 10/15 min resulted in phase transformation to form II. Liquid assisted grinding on stoichiometric amounts of starting materials resulted only in form II without any contamination of form I. Form I on liquid assisted grinding (solvents used are CH₃CN, THF, water) converted to form II whereas form II did not convert to form I. Therefore, as supported by DSC, form II is the stable polymorph whereas form I is the metastable one. Figure 6.32 shows a comparison of bulk material XRPD profiles of the two polymorphs overlayed with corresponding calculated XRPD lines.

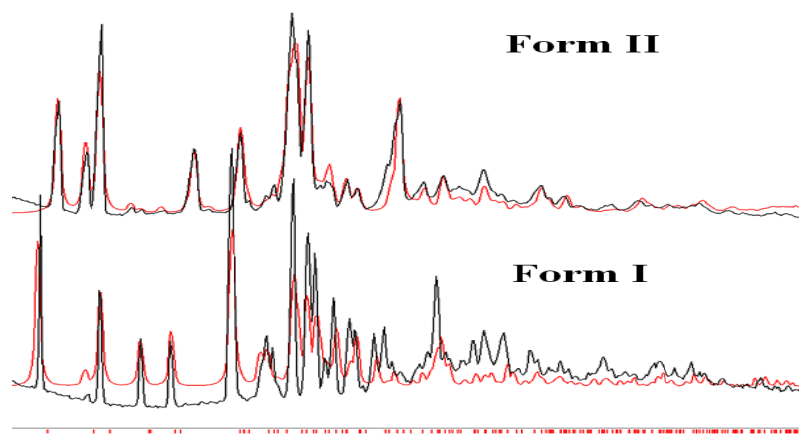


Figure 6.32 Comparison of calculated (red) and experimental (black) XRPDs of both the polymorphs which shows difference in peak position for both the polymorphs.

6.4.4 Spectral analysis of ZM•Suc polymorphs

The dimorphs of Zol.Suc were characterized by FT-IR, FT-Raman and by solid state ^{13}C NMR spectroscopy

FT-IR: IR stretching frequencies of C=O group (1643 and 1633 cm^{-1} for form I and form II respectively) are significantly different for the two polymorphs due to difference in hydrogen bonding pattern (Figure 6.33).

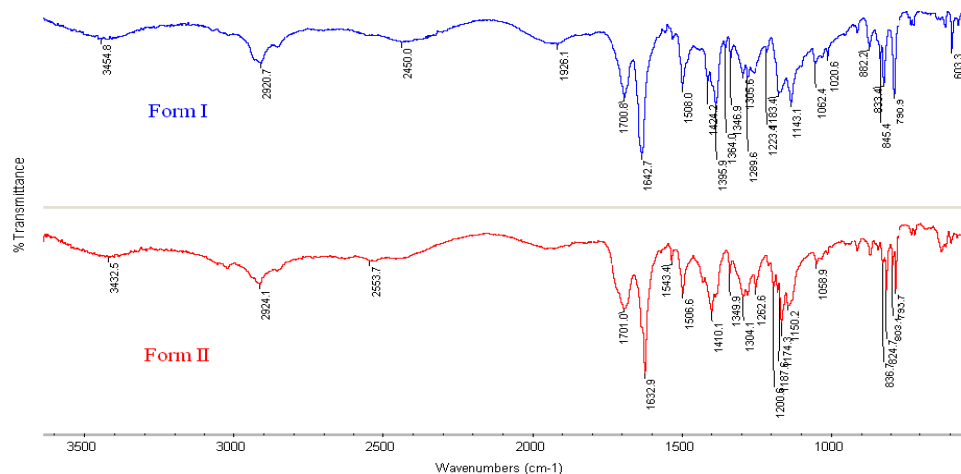


Figure 6.33 IR comparison of ZM•Suc form I and form II

FT-Raman: Raman shift for the C=O (1616cm^{-1} for form I and 1613 cm^{-1} for form II) and C–H stretching in both the polymorphs (2927cm^{-1} for form I and for form II 2925cm^{-1}) are different. Figure 6.34 depicts the differences in Raman shifts of the two polymorphs.

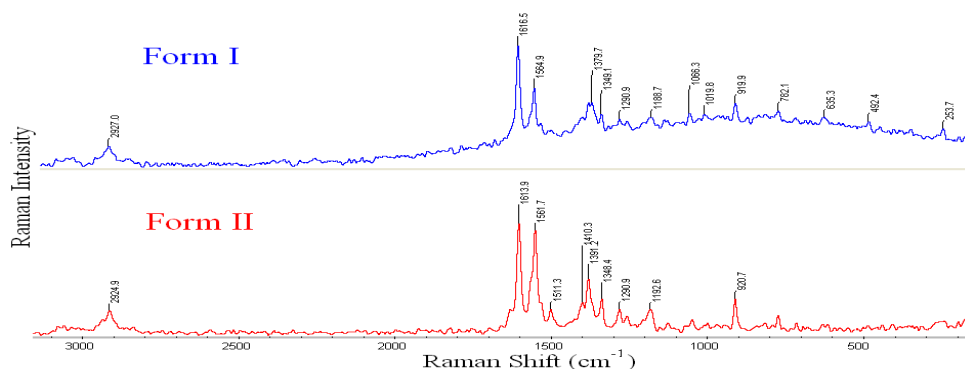


Figure 6.34 Comparison of FT-Raman spectra of form I (blue) and form II (red).

^{13}C ss-NMR: Solid state ^{13}C NMR of the two polymorphs showed clear differences in the peak positions. Figure 6.35 shows the comparison of the two spectra. Few extra peaks in the form I ss-NMR spectra are due to the presence of starting material (marked as circle in the Figure 6.36, which is a result of incomplete formation of cocrystal. Again in both the spectra few peaks were merged which are listed in Table 6.5.

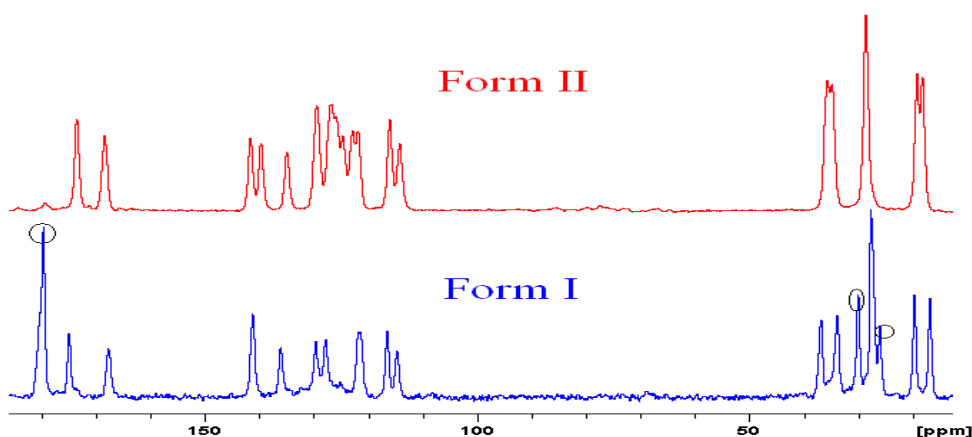
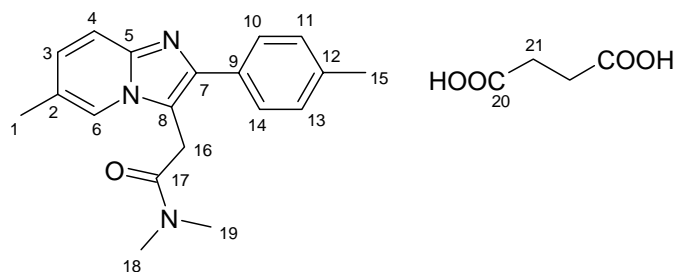


Figure 6.35 Comparison of ^{13}C ss-NMR spectra of the two polymorphs of ZM•Suc cocrystal. In the form I spectra few peaks due to starting material appeared (marked) which is due to incomplete formation of cocrystal.

Table 6.5 ^{13}C ss-NMR chemical shifts (in ppm) of the two polymorphs of ZM•Suc.



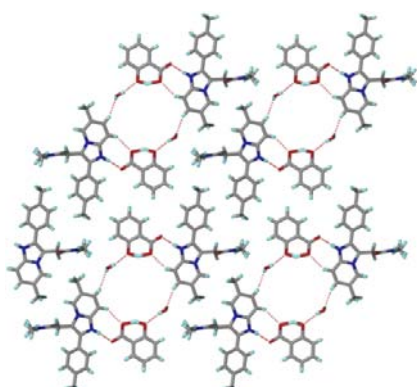
No.	Form I	Form II	No.	Form I	Form II
C15	16.6	18.1	C2	C2, C9, C8 and C3 are merged with the peaks at	124.5
C1	19.6	19.1	C9		125.8
C16	27.5	28.4	C8		126.7
C21	33.7	34.7	C3	127.6 and 129.4	129.3
C18, C19	36.7	35.5	C5	135.9	134.8
C4	114.6	114.1	C12	C12 and C6 are merged at 141.0	139.6
C7	116.4	115.9	C6		141.5
C10, C14	121.3	121.7	C17	167.6	168.2
C11, C13	121.6	122.8	C20	174.7	173.4

6.4.5 Conformational flexibility observed in crystal structures of ZM

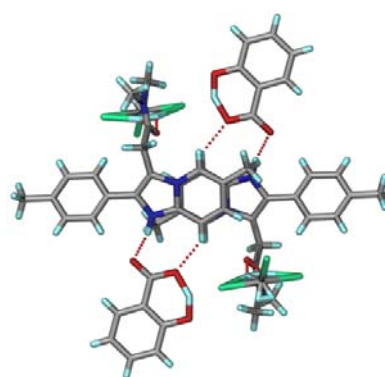
In literature, crystal structures of Zolpidemium saccharinate ($\text{ZM-NH}^+\cdot\text{Sac-N}^-$), Zolpidemium hydrogentartrate ($\text{ZM-NH}^+\cdot\text{HTar-COO}^-$) and Zolpidemium hemitartrate hemihydrates ($\text{ZM-NH}^+\cdot\text{Tar-COO}^-\cdot\text{H}_2\text{O}$) and ZM free base are reported.⁵⁹ In these crystal structures various conformations of p-tolyl and N-dimethylacetamide group were observed, so as in the ZM•Suc polymorphs. Hydrates, solvates and guest forms of other molecular complexes (Table 6.6) were crystallized and single crystal X-ray structures were determined to compare the torsional variance of ZM. Figure 6.36 depicts the crystal structures of these molecular complexes.

Table 6.6 Molecular complexes obtained during cocrystallization with different GRAS conformers.

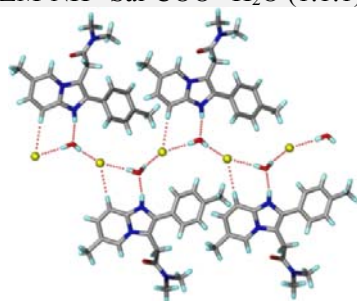
Components	Molecular complexes	Crystalline forms obtained	
ZM and Sal	Molecular salt hydrate	ZM-NH ⁺ •Sal-COO ⁻ •H ₂ O (1:1:1)	2ZM-NH ⁺ •2Sal-COO ⁻ •CH ₂ Cl ₂ (2:2:1)
ZM and HCl	Salt Hydrate	ZM-NH ⁺ •Cl ⁻ •H ₂ O (1:1:1)	ZM-NH ⁺ •Cl ⁻ •2CH ₃ CN (1:1:2)
ZM and Mal	Molecular salt hydrate	2ZM-NH ⁺ •2Mal-COO ⁻ •2H ₂ O (2:2:2)	-----
ZM and MP	Cocrystal	ZM•MP (1:1)	-----



ZM-NH⁺•Sal-COO⁻•H₂O (1:1:1)



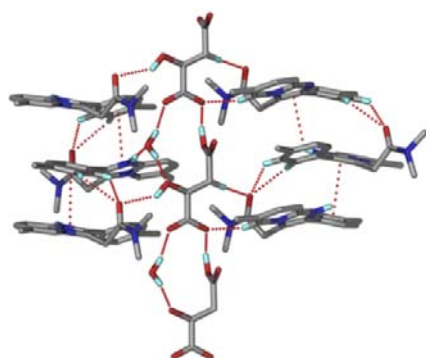
2ZM-NH⁺•2Sal-COO⁻•CH₂Cl₂ (2:2:1)



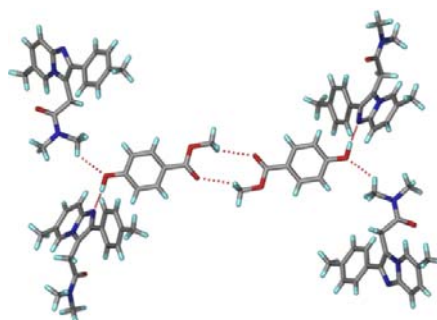
ZM-NH⁺•Cl⁻•H₂O (1:1:1)



ZM-NH⁺•Cl⁻•2CH₃CN (1:1:2)



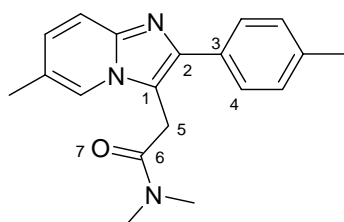
2ZM-NH⁺•2Mal-COO⁻•2H₂O (2:2:2)



ZM•MP (1:1)

Figure 6.36 With salicylic acid ZM resulted two crystalline salt forms, a hydrate (in 1:1:1 ratios) and a DCM solvate (in 2:2:1 ratios). Hydrate has planar sheet structure whereas the DCM solvate possesses 3D packing. Hydrochloride salt of Zolpidem crystallized as a hydrate in 1:1:1 ratios and as CH₃CN solvate in 1:1:2 ratios. With L-malic acid one salt hydrate (2:2:2 ratios) crystal structure and with methyl paraben a cocrystal (1:1 ratios) were obtained. Crystallographic parameters and DSC, TGA plots of these molecular complexes are included in the Appendix.

In these crystal structures the two specified torsion angles (Figure 6.37), torsion 1 varies between 4° to 45° whereas the torsion 2 varies between 0° to 24°. A total of fifteen conformers obtained for ZM are overlayed by fixing the benzimidazole ring (Figure 6.38) and the corresponding values are listed in Table 6.7.



Torsion 1=1-2-3-4

Torsion 2= 1-5-6-7



Figure 6.37 Flexible torsions of ZM molecule and overlay of 15 conformers present in different molecular complexes.

Color codes are, ZM•Suc, form I = Light Blue, ZM•Suc, form II = Orange, ZM-NH⁺•Cl⁻•H₂O = Yellow, ZM-NH⁺•Cl⁻•2CH₃CN = Blue, ZM-NH⁺•Sal-COO⁻•H₂O = Light Green, 2ZM-NH⁺•2Sal-COO⁻•CH₂Cl₂, conformer 1 = Pink, 2ZM-NH⁺•2Sal-COO⁻•CH₂Cl₂, conformer 2 = Dark Red, ZM•MP= Light Brown, 2ZM-NH⁺•2Mal-COO⁻•2H₂O, conformer 1 = Magenta, 2ZM-NH⁺•2Mal-COO⁻•2H₂O, conformer 2 = Brown, ZM-NH⁺•Tar-COO⁻•H₂O, conformer 1 = Red, ZM-NH⁺•Tar-COO⁻•H₂O,

conformer 2 = Green, ZM-NH⁺•HTar-COO⁻•H₂O = Black, ZM-NH⁺•Sac-N⁻ = Dark Grey, ZM = Purple.

Table 6.7 Torsion angles (°) for fifteen conformers found in the crystal structures.

ZM molecular complexes	1	2	ZM molecular complexes	1	2
ZM•Suc, form I	40.0(5)	23.4(5)	ZM•Suc, form II	25.6(3)	16.0(2)
ZM-NH ⁺ •Cl ⁻ •H ₂ O	30.3(2)	17.2(2)	ZM-NH ⁺ •Cl ⁻ •2CH ₃ CN	16.8(3)	16.4(3)
ZM-NH ⁺ •Sal-COO ⁻ •H ₂ O	34.8(3)	4.3(3)	ZM•MP	34.1(5)	6.1(4)
2ZM-NH ⁺ •2Sal-COO ⁻ •CH ₂ Cl ₂ conformer 1	44.6(4)	1.8(4)	2ZM-NH ⁺ •2Sal-COO ⁻ •CH ₂ Cl ₂ conformer 2	37.6(4)	0.1(4)
2ZM-NH ⁺ •2Mal-COO ⁻ •2H ₂ O conformer 1	35.1(7)	13.8(6)	2ZM-NH ⁺ •2Mal-COO ⁻ •2H ₂ O conformer 2	32.5(7)	1.6(6)
ZM-NH ⁺ •Tar-COO ⁻ •H ₂ O conformer 1	31.1(3)	16.0 (3)	ZM-NH ⁺ •Tar-COO ⁻ •H ₂ O conformer 2	17.9(6)	20.6(11)
ZM-NH ⁺ •HTar-COO ⁻ •H ₂ O	12.7(2)	7.2(15)	ZM-NH ⁺ •Sac-N ⁻	4.2(4)	4.2(3)
ZM	23.5(3)	7.1(3)			

6.5 Conclusion

Polymorphism in three important cases viz. Tolbutamide, Methyl paraben and Zolpidem•Succinic acid cocrystal have been discussed. Novel form V of Tolbutamide was obtained serendipitously in presence of trace amount of conc. HNO₃. Formation of modulated high Z' structure of form III TB in presence of coformers indicate the fact that the coformer could act as a template in this crystallization as the known form I was obtained in the absence of any additives. The role of tailored additives and structural mimics in the selective growth of metastable polymorphs is well known.⁶⁰ An essential, daily use bulk chemical methyl paraben afforded single crystals of a second polymorph under specially optimized sublimation conditions of slow condensation. This polymorph is metastable compared to the well known and commercial crystalline material. The search of drug polymorphs in the metastable zone is important because kinetic forms generally have enhanced solubility and bioavailability compared to the thermodynamic

phase. Hence there is a need for methods to crystallize kinetic polymorphs of drugs and also to stabilize them in the crystal lattice. The pair of methyl paraben structures adds to the now growing number of polymorph sets⁶¹ wherein the stable crystal structure has multiple molecules in the asymmetric unit. Cocrystal polymorphs of ZM•Suc were characterized by single crystal XRD, XRPD, thermal and spectroscopic techniques and their stability order was established. The densities of the two polymorphs are very close and there is no phase transition upon heating as indicated by DSC. Neat and solvent assisted grinding experiments proved the stability order as form II is more stable than form I, which is in accordance with the enthalpy of fusion values for both the forms. Therefore form II is the thermodynamic polymorph whereas form I is metastable. Molecular conformation of organic solid is important as it provides almost ideal systems to the study of structure/property relationships. Crystal structures were determined for few other molecular complexes of ZM and compared with the reported crystal structures which showed the flexibility of the *p*-tolyl group to give rise total 15 conformers. Despite having such torsional flexibility in molecular complexes, the parent base ZM was not found to be polymorphic, although, possibility of polymorphism cannot be ruled out.

6.6 Experimental Section

TB was purchased from Sigma-Aldrich and *p*-phenylenediboronic acid and *p*-nitrophenol from Alfa-Aesar, and MP and *p*-nitrobenzoic acid from S. D. Fine Chemicals and ZM was a gift from a friend.

Crystallization details: TB Form III: A 1:1 molar ratios of tolbutamide and the appropriate coformer (*p*-phenylenediboronic acid, *p*-nitrophenol or *p*-nitrobenzoic acid) were grinded in a mortar-pestle for 30 min and dissolved in absolute EtOH in separate experiments. Crystals appear after 2/3 days. The product was Tolbutamide form III high Z' crystal structure with the first and second two coformers, and form IV crystallized in the third case.

TB Form V: 0.5 mL of conc. HNO₃ was added to 10 mL of MeOH and cooled to –20 °C for 30 min. 30 mg of tolbutamide was dissolved in 10 mL of MeOH in a separate flask and cooled to –20°C. 1 mL of the acidified MeOH was added to the cooled tolbutamide

solution and left for undisturbed crystallization at room temperature. Crystals of form III appeared after 2d.

MP form II: 50 mg MP was placed in a sublimation apparatus and was heated at 80°C under ambient pressure for two days. No cooling device was used to condense the sublimed material as its presence resulted only form I crystals. After two days form II crystallized in very low yield along with block crystals of form II.

ZM•Suc, form I: ZM and Suc were taken in 1:1 (30.7 mg of ZM and 11.8 mg of Suc) or 1:0.5 (30.7mg of ZM and 5.9 mg of Suc) molar ratios in a conical flask and dissolved in dry THF or dry dioxane by sonication, filtered and left for crystallization at ambient temperature by covering with aluminum foil. Single crystals of Form I appeared after 4/5 days. THF and dioxane were dried using Na and benzophenone.

ZM•Suc, form II: ZM and Suc were taken in 1:1 (30.7 mg of ZM and 11.8 mg of Suc) or 1:0.5 (30.7mg of ZM and 5.9 mg of Suc) molar ratios in a conical flask and dissolved in suitable solvent by gentle heating and left for crystallization at ambient temperature. Solvents used for crystallization are CH₃CN, i-propanol, MeOH, n-propanol, EtOH, EtOAc, THF (normal) and dioxane (normal). Single crystals of suitable size for X-ray diffraction appeared after 4/5 days.

Other molecular complexes of ZM: Single crystals of ZM-NH⁺•Sal-COO⁻•H₂O was obtained by dissolving equimolar amounts of both the components in MeOH, whereas, 2ZM-NH⁺•2Sal-COO⁻•CH₂Cl₂ was obtained when crystallization was carried out using DCM solvent. ZM-NH⁺•Cl⁻•H₂O was crystallized when 5/6 drops of methanol acidified with conc. HCl (1 mL of conc. HCl added to 10 mL of MeOH) was added to a methanolic solution of ZM and left for crystallization under ambient temperature conditions. Single crystals of ZM-NH⁺•Cl⁻•2CH₃CN were obtained when the anhydrous molecular complex was crystallized from CH₃CN solvent. Single crystals of 2ZM-NH⁺•2Mal-COO⁻•2H₂O and ZM•MP were obtained by dissolving equimolar amounts of individual components in MeOH and subsequent crystallization after 2 days.

X-ray crystallography: X-ray reflections were collected on Bruker SMART CCD and Oxford Gemini diffractometer (Version 1.171.33.55). Mo-K α (λ =0.71073 Å) radiation

was used to collect X-ray reflections on the single crystals. Data reduction was performed using Bruker SAINT software.⁶² Intensities for absorption were corrected using SADABS⁶³ Structures were solved and refined using SHELXL-97.⁶⁴ For datasets collected on Oxford Gemini diffractometer (Version 1.171.33.55), data reduction was performed using CrysAlisPro, Oxford Diffraction Ltd., Version 1.171.33.55 and OLEX2-1.0⁶⁵ was used for structure solution and refinement. All non-hydrogen atoms were refined anisotropically and C–H hydrogens were fixed.

Thermal analysis: DSC was performed on a Mettler Toledo DSC 822e module. Samples were placed in crimped but vented aluminum sample pans with sample size is 4–6 mg. DSCs were performed at 5 °C min^{−1} from 30 °C–250 °C. Samples were purged by a stream of dry nitrogen flowing at 150 mL min^{−1}.

Vibrational spectroscopy: Nicolet 6700 FT-IR spectrometer with an NXR FT-Raman module was used to record IR and Raman spectra. IR spectra were recorded on samples dispersed in KBr pellets. Raman spectra were recorded on solid samples contained in standard NMR diameter tubes or on compressed samples contained in a gold-coated sample holder.

ss-NMR: Solid state ¹³C NMR spectra were recorded on a Bruker Avance spectrometer at 400 MHz. ss NMR experiments were carried out on Bruker 4 mm double resonance CPMAS probe in zirconia rotors at 5.0 kHz with a cross-polarization contact time of 2.5 ms and a recycle delay of 8 s. ¹³C-CPMAS spectra recorded at 100 MHz were referenced to methylene carbon of glycine and then the chemical shifts were recalculated to the TMS scale ($\delta_{\text{glycine}} = 43.3$ ppm).

6.7 References

1. (a) S. R. Byrn, R. R. Pfeiffer and J. G. Stowell, *Solid-State Chemistry of Drugs*; SSCI: West Lafayette, IN, **1999**. (b) J. Bernstein, *Polymorphism in Molecular Crystals*, Clarendon, Oxford, **2002**. (c) R. Hilfiker, *Polymorphism in the Pharmaceutical Industry*, Wiley–VCH, Weinheim, **2006**. (d) H. G. Brittan, *Polymorphism in Pharmaceutical Solids*, Marcel Dekker, New York, **1999**.

2. (a) J. Bauer, S. Spanton, R. Henry, J. Quick, W. Dziki, W. Porter and J. Morris, *Pharma. Res.* **2001**, 18, 856. (b) S. R. Chemburkar, J. Bauer, K. Deming, H. Spiwek, K. Patel, J. Morris, R. Henry, S. Spanton, W. Dziki, W. Porter, J. Quick, P. Bauer, J. Donaubauer, B. A. Narayanan, M. Soldani, D. Riley and K. McFarland, *Org. Process Res. Dev.* **2000**, 4, 413.
3. (a) M. Trifkovic, S. Rohani and M. Mirmehrabi, *Org. Process Res. Dev.*, 11, **2007**, 138. (b) M. M. Parmar, O. Khan, L. Seton and J. L. Ford, *Cryst. Growth Des.*, 7, **2007**, 1635.
4. (a) C. A. Mitchell, L. Yu and M. D. Ward, *J. Am. Chem. Soc.*, 123, **2001**, 10830. (b) R. Hiremath, S. W. Varney and J. A. Swift, *Chem. Commun.* **2004**, 2676.
5. (a) C. P. Price, A. L. Grzesiak and A. J. Matzger, *J. Am. Chem. Soc.*, 127, **2005**, 5512. (b) M. D. Lang, A. L. Grzesiak and A. J. Matzger, *J. Am. Chem. Soc.*, 124, **2002**, 14834.
6. (a) P. K. Thallapally, R. K. R. Jetti, A. K. Katz, H. L. Carrell, K. Singh, K. Lahiri, S. Kotha, R. Boese and G. R. Desiraju, *Angew. Chem., Int. Ed.*, 43, **2004**, 1149. (b) X. He, J. G. Stowell, K. R. Morris, R. R. Pfeiffer, H. Li, G. P. Stahly and S. R. Byrn, *Cryst. Growth Des.*, 1, **2001**, 305.
7. (a) J. A. Foster, M.-O. M. Piepenbrock, G. O. Lloyd, N. Clarke, J. A. K. Howard and J. W. Steed, *Nature Chem.*, 2, **2010**, 1037. (b) R. I. Petrova, R. Patel and J. A. Swift, *Cryst. Growth Des.*, 6, **2006**, 2709.
8. G. M. Day, A. V. Trask, W. D. S. Motherwell and W. Jones, *Chem. Commun.* **2006**, 54.
9. P. Sanphui, N. R. Goud, U. B. R. Khandavilli, S. Bhanothb and A. Nangia, *Chem. Commun.*, 47, **2011**, 5013.
10. (a) M. Rafilovich and J. Bernstein, *J. Am. Chem. Soc.*, 128, **2006**, 12185. (b) P. Vishweshwar, J. A. McMahon, M. Oliveira, M. L. Peterson, and M. J. Zaworotko, *J. Am. Chem. Soc.*, 127, **2005**, 16802. (c) A. D. Bond, K. A. Solanko, S. Parsons, S. Redder and R. Boese, *CrystEngComm*, 13, **2011**, 399. (d) M. Wenger and J. Bernstein, *Mol. Pharm.*, 4, **2007**, 355. (e) B. Lou, D. Boström and S. P. Velaga, *Cryst. Growth Des.*, 9, **2009**, 9, 1254. (f) X. Mei and C. Wolf, *Cryst. Growth Des.*, 4, **2004**, 1099.

11. W. F. Ostwald, *Z. Phys. Chem.*, **22**, **1897**, 289.
12. H. G. Brittan, *J. Pharm. Sci.*, **2007**, *96*, 705.
13. M. Pudipeddi and A. T. M. Serajuddin, *J. Pharm. Sci.*, *94*, **2005**, 929.
14. (a) M. Allesø, F. Tian, C. Cornett and J. Rantanen, *J. Pharm. Sci.*, *99*, **2010**, 3711. (b) D. Singhal and W. Curatolo, *Adv. Drug. Del. Rev.*, *56*, **2004**, 335.
15. (a) N. J. Babu, L. S. Reddy, S. Aitipamula and A. Nangia, *Chem. Asian J.*, *3*, **2008**, 1122. (b) B. R. Sreekanth, P. Vishweshwar and K. Vyas, *Chem. Commun.* **2007**, 2375. (c) J. A. Bis, P. Vishweshwar, R. A. Middleton and M. J. Zaworotko, *Cryst. Growth Des.*, *6*, **2006**, 1048. (d) S. L. Childs and K. I. Hardcastle, *Cryst. Growth Des.*, *7*, **2007**, 1291. (e) J. A. Bis, P. Vishweshwar, D. Weyna and M. J. Zaworotko, *Mol. Pharma.*, *4*, **2007**, 401. (f) W. W. Porter III, S. C. Elie and A. J. Matzger, *Cryst. Growth Des.*, *1*, **2008**, 14. (g) N. Schultheiss, S. Bethune and J.-O. Henck, *CrystEngComm*, *12*, **2010**, 2436. (h) M. L. Peterson, M. K. Stanton, R. C. Kelly, R. Staplesc and A. Chenga, *CrystEngComm*, *13*, **2011**, 1170. (i) S. Aitipamula, P. S. Chow and R. B. H. Tan, *CrystEngComm*, *12*, **2010**, 3691. (j) S. Aitipamula, P. S. Chow and R. B. H. Tan, *CrystEngComm*, *11*, **2009**, 1823.
16. J. W. Steed, *CrystEngComm*, *5*, **2003**, 169.
17. S. K. Chandran and A. Nangia, *CrystEngComm*, *8*, **2006**, 581.
18. X. Hao, M. A. Siegler, S. Parkin and C. P. Brock, *Cryst. Growth Des.* *5*, **2005**, 2225.
19. (a) M. J. Thomas and J. A. Thomas in *Modern Pharmacology with Clinical Applications*, ed. C. R. Craig and R. E. Stitzel, Little Brown & Company, Boston, 5th edn, **1997**, pp. 763–77. (b) <http://www.drugbank.ca/drugs/DB01124>.
20. M. Kuhnert-Brandstätter and S. Wunsch, *Mikrochim Acta (Wien)*, *6*, **1969**, 1297.
21. D. L. Simmons, R. J. Ranz, N. D. Gyanchandani and P. Picotte, *Can. J. Pharm. Sci.*, *7*, **1972**, 121.
22. A. Burger, *Sci. Pharm.*, *43*, **1975**, 161.
23. G. Hasegawa, T. Komasa, R. Bando, Y. Yoshihashi, E. Yonemochi, K. Fujii, H. Uekusa and K. Terada, *Int. J. Pharm.*, *369*, **2009**, 12.

24. S. Thirunahari, S. Aitipamula, P. S. Chow and R. B. H. Tan, *J. Pharm. Sci.*, **99**, **2010**, 2975.
25. Y. Sonoda, F. Hirayama, H. Arima, Y. Yamaguchi, W. Saenger and K. Uekama, *Cryst. Growth Des.*, **6**, **2006**, 1181.
26. A. Paulidou, D. Maffeo, K. Yannakopoulou and I. M. Mavridis, *CrystEngComm*, **12**, **2010**, 517.
27. D. P. Kessissoglou, G. E. Manoussakis, A. G. Hatzidimitriou and M. G. Kanatzidis, *Inorg. Chem.*, **26**, **1987**, 1395.
28. W. Jones, W.D. S. Motherwell and A. V. Trask, *Mrs Bulletin*, **31**, **2006**, 875.
29. (a) L. S. Reddy, S. K. Chandran, S. George, N. J. Babu and A. Nangia, *Cryst. Growth Des.*, **7**, **2007**, 2675. (b) M. C. Etter, Z. Urbańczyk-Lipkowska, M. Zia-Ebrahimi and T. W. Panunto, *J. Am. Chem.Soc.*, **112**, **1990**, 8415.
30. Q. Li, F. Xue and T. C. W. Mak, *Inorg. Chem.*, **8**, **1999**, 4142.
31. (a) L. Dupont, O. Dideberg and J. Delarge, *Cryst. Struct. Commun.*, **10**, **1981**, 89. (b) L. Dupont, K. Lewinski, K. Stadnicka and J. Delarge, *Cryst. Struct. Commun.*, **10**, **1981**, 925. (c) L. Dupont, O. Dideberg, J. Delarge, G. Dive and L. Thunus, *Acta Cryst.*, B38, **1982**, 1495. (d) L. Dupont, O. Dideberg, B. Masereel, J. Delarge, M. Schynts, B. Pirotte, *Acta Cryst.*, B47, **1991**, 2152.
32. N. K. Nath and A. Nangia, *CrystEngComm*, **13**, **2011**, 47.
33. Mercury is a crystal structure visualization and display program distributed by the Cambridge Crystallographic Data Center (CCDC) with the Database package (<http://www.ccdc.cam.ac.uk>); another CCDC product, the COSET program, may also be used for crystal structure overlay.
34. (a) M. A. Spackman and D. Jayatilaka, *CrystEngComm*, **11**, **2009**, 19. (b) J. J. McKinnon, D. Jayatilaka and M. A. Spackman, *Chem. Commun.* **2007**, 3814. (c) J. Bernstein, *Cryst. Growth Des.*, **11**, **2011**, 632.
35. (a) M. G. Soni, S. L. Taylor, N. A. Greenberg and G. A. Burdock, *Food Chem. Toxicol.*, **40**, **2002**, 1335. (b) S. Mizuba and W. Sheikh, *J. Ind. Microbiol.*, **1**, **1987**, 363.
36. F. Tajarobi, S. Abrahmsén-Alami and A. Larsson, *J. Pharm. Sci.*, **100**, **2011**, 275.
37. M. S. Reisch, *C&EN*, **83**, **2005**, 25.

38. V. R. Fischer and F. Stauder, *Mikrochemie*, 8, **1930**, 330.
39. V. L. Kofler and A. Kofler, *Mikrochemie*, 9, **1931**, 45.
40. E. Lindpaintner, *Mikrochemie*, **1939**, 27, 21.
41. M. R. Cairra, E. J. C. de Vries and L. R. Nassimbeni, *Chem. Commun.* **2003**, 2058.
42. M. L. Cheney, N. Shan, E. R. Healey, M. Hanna, L. Wojtas, M. J. Zaworotko, V. Sava, S. Song and J. R. Sanchez-Ramos, *Cryst. Growth Des.*, 10, **2010**, 394.
43. M. Khan, V. Enkelmann and G. Brunklaus, *J. Am. Chem. Soc.*, 132, **2010**, 5254.
44. M. Ma, T. Lee and E. Kwong, *J. Pharm. Sci.*, 91, **2002**, 1715.
45. Cambridge Crystallographic Data Center, www.ccdc.cam.ac.uk.
46. L. Xianti, *Chin. J. Struct. Chem.*, 2, **1983**, 213.
47. D. Vujovic, L. R. Nassimbeni, *Cryst. Growth Des.*, 6, **2006**, 1595.
48. H.-K. Fun, S. R. Jebas, *Acta Cryst.*, E64, **2008**, o1255.
49. T. L. Threlfall, T. Gelbrich, *Cryst. Growth Des.*, 7, **2007**, 2297.
50. N. K. Nath, H. Aggarwal and A. Nangia, *Cryst. Growth Des.*, 11, **2011**, 967.
51. (a) L. Xianti, *Chin. J. Struct. Chem.* 5, **1986**, 281. (b) Y. Zhou, G. Matsadiq, Y. Wu, J. Xiao and J. Cheng, *Acta Cryst.*, E66, **2010**, o485.
52. N. K. Nath, B. K. Saha and A. Nangia, *New J. Chem.*, 32, **2008**, 1693.
53. Cerius²: Module for crystal lattice energy and structure prediction, www.accelrys.com.
54. (a) L. H. Sternbach, *J. Med. Chem.*, 22, **1979**, 1. (b) F. Watjen, R. Baker, M. Engelstoff, R. Herbert, A. MacLeod, A. Knight, K. Merchant, J. Moseley, J. Saunders, C. J. Swain, E. Wong and J. P. Springer, *J. Med. Chem.*, 32, **1989**, 2282.
55. B. E. Tomczuk, C. R. Taylor, L. M. Moses, D. B. Sutherland, Y. S. Lo, D. N. Johnson, W. B. Kinnier and B. F. Kilpatrick, *J. Med. Chem.*, 34, **1991**, 2993.
56. E. A. Zannou, P. Li and W.-Q. Tong in *Developing Solid Oral Dosages Form: Pharmaceutical Theory and Practice*, ed. Y. Qiu, Y. Chen, G. Zhang, L. Liu and W. Porter, Academic Press Elsevier, 1st edition 2009, pp-916.
57. (a) T. Takagi, C. Ramachandran, M. Bermejo, S. Yamashita, L. X. Yu and G. L. Amidon, *Mol. Pharm.*, 3, 2006, 631. (b) N. A. Kasim, M. Whitehouse, C.

- Ramachandran, M. Bermejo, H. Lennernäs, A. S. Hussain, H. E. Junginger, S. A. Stavchansky, K. K. Midha, V. P. Shah and G. L. Amidon, *Mol. Pharm.*, **1**, **2003**, 85. (c) <http://69.20.123.154/services/bcs/results.cfm>.
58. (a) A. Judith, D. Ben-Zeon, K. Marco, L. David, M.-S. Erzebt, S. Szaboles, S. Anchel, S. Csaba and Z. Shlomo, WO 80857, **2001**. (b) Y. Kumar, P. Mohan, A. Nath, T. Chandrashekhar, R. Santhakumar and S. Ganguli, US 0262025 A1, **2008**. (b) B. K. Cheng, US 0293946 A1, **2008**. (c) A. J. Basu, K. B. Rao, G. S. Babu and K. Sabapathy, WO 122576 A1, **2010**. (d) G. J. B. Ettema, J. M. Lemmens, T. H. A. Peters and F. Picha, US 6,242,460 B1, **2001**.
59. (a) I. Halasz and R. E. Dinnebier, *J. Pharm. Sci.*, **99**, **2010**, 871. (b) D. R. Vega, R. Baggio, M. Roca and D. Tombari, *J. Pharm. Sci.*, **100**, **2011**, 1377.
60. (a) I. Weissbuch, L. Addadi, M. Lahav and L. Leiserowitz, *Science*, **253**, **1991**, 637. (b) R. J. Davey, N. Blagden, G. D. Potts and R. Docherty, *J. Am. Chem. Soc.*, **119**, **1997**, 1767.
61. (a) N. Zencirci, T. Gelbrich, D. C. Apperley, R. K. Harris, V. Kahlenberg, U. J. Griesser, *Cryst. Growth Des.*, **10**, **2010**, 302. (b) N. J. Babu, S. Cherukuvada, R. Thakuria and A. Nangia, *Cryst. Growth Des.*, **10**, **2010**, 1979. (c) B. Sarma, P. Sanphui and A. Nangia, *Cryst. Growth Des.*, **10**, **2010**, 2388. (d) S. Mahapatra, T. S. Thakur, S. Joseph, S. Varughese and G. R. Desiraju, *Cryst. Growth Des.*, **10**, **2010**, 3191. (e) M. Rafilovich and J. Bernstein, *J. Am. Chem. Soc.*, **128**, **2006**, 12185. (f) S. Long, M. A. Siegler, A. Mattei, L. Tonglei, *Cryst. Growth Des.*, **11**, **2011**, 414.
62. *SAINT-Plus, version 6.45*; Bruker AXS Inc.: Madison, WI, **2003**.
63. G. M. Sheldrick, SADABS, *Program for Empirical Absorption Correction of Area Detector Data*, University of Göttingen, Germany, 1997.
64. (a) *SMART (Version 5.625) and SHELX-TL (Version 6.12)*; Bruker AXS Inc.: Madison, WI, **2000**. (b) G. M. Sheldrick, *SHELXS-97 and SHELXL-97*; University of Göttingen, Germany, **1997**.
65. O. V. Dolomanov, A. J. Blake, N. R. Champness and M. Schröder, *J. Appl. Cryst.* **36**, **2003**, 1283.

Chapter Seven

Conclusion

This thesis covers the identification and characterization of three different aspects of polymorphism: (1) polymorphism in isostructural molecules (Chapter 2 and 3), (2) polymorphism of two special cases (by definition) viz. chiral/racemic (Chapter 4) and neutral/zwitterionic (Chapter 5) and finally, (3) polymorphism in active pharmaceutical ingredients (Chapter 6).

7.1 Polymorphism in Isostructural molecules

The importance of isostructurality and polymorphism has been discussed in Chapter 1. Chapters 2 and 3 depict the isostructurality and polymorphism in three series of compounds.

Chapter 2 focuses on the polymorphism and isostructurality among the triiodohydroxy compounds viz. triiodophenol (TIP), triiodoresorcinol (TIR) and triiodophloroglucinol (TIG). Polymorphism was expected in the series of compounds after analyzing their crystal structures. The terminal members TIP and TIG crystallized in orthorhombic space group $P2_12_12_1$ and are isomorphous whereas the middle member TIR crystallized in monoclinic space group $P2_1/n$ with a different crystal structure. This led to the idea that the middle member TIR should also be able to crystallize in the orthorhombic space group $P2_12_12_1$ similar to the terminal members. Hetero-seeding technique resulted in the desired polymorph of TIR. The same concept pointed towards the possibility of polymorphism in TIP and TIG too. Although TIP is still monomorphic, in contrast, TIG crystallized in monoclinic space group $P2_1/n$ and is isomorphous with the monoclinic polymorph of TIR. Interestingly, in the crystal structures, TIR mimics TIG because of positional disorder of the OH groups in TIR and that is one of the reasons why polymorphism was observed in both the molecules. A set of crystal structures, retrieved from CSD, where molecules contain halogens at 1, 3 and 5 positions revealed that these compounds are traditionally well known in orthorhombic space group $P2_12_12_1$ and are isostructural with orthorhombic polymorphs of TIR and TIG except triiodotrifluorobenzene which is isostructural with monoclinic polymorphs of TIR and TIG (Figure 7.1).

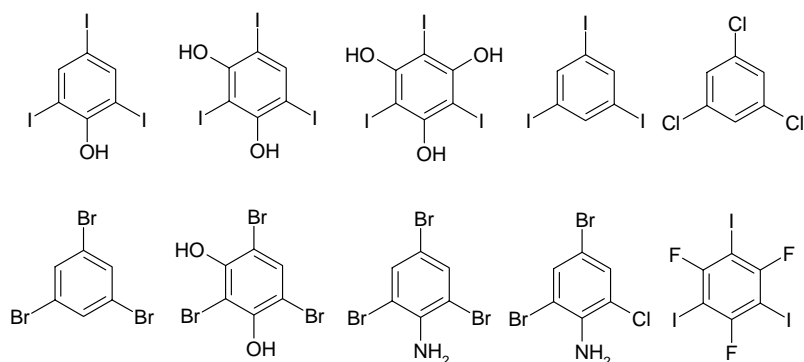


Figure 7.1 Isostructural series of molecules of this work (first three) and from CSD (rest).

In addition to polymorphism and isostructurality on rigid molecules in Chapter 2, study on these phenomena in conformational molecules viz. Fuchsones and Sulfonylhydrazones (Figure 7.2) was carried out and discussed in Chapter 3. Fuchsones and Sulfonylhydrazones are known to crystallize as conformational polymorphs. Isostructurality in conformationally flexible molecules is a challenge because such molecules often lead to different crystalline packing arrangements due to the presence of several conformers in solution.

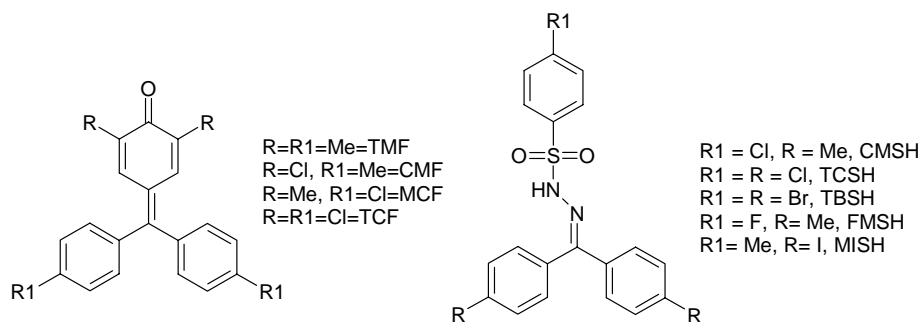


Figure 7.2 Fuchsones and Sulfonylhydrazones studied in Chapter 3.

Despite the enormous polymorphism in Fuchsones, form I of TMF, CMF and MCF are isostructural whereas form II of TMF and MCF form an isostructural pair. Cocrystallization of TMF, CMF and MCF resulted in continuous series of solid solutions viz. TMF+CMF, CMF+MCF, TMF+MCF-1, TMF+MCF-2, TMF+MCF-3 and TMF+MCF-4. The series of isostructural crystals obtained in Fuchsones are

Series 1: TMF-I \leftrightarrow CMF-I \leftrightarrow MCF-I \leftrightarrow TMF+CMF \leftrightarrow CMF+MCF \leftrightarrow TMF+MCF-1 \leftrightarrow
TMF+MCF-4

Series 2: TMF-II \leftrightarrow MCF-II \leftrightarrow TMF+MCF-2.

Sulfonylhydrazones, where the structure was mainly governed by sulfonamide dimer synthon, were expected to be polymorphic but only CSMH crystallized as dimorph (CSMH-I and CSMH-II). Isostructurality was observed among the crystal structures and CSMH polymorphs form a structural link. CSMH-I is isomorphous with TCSH and TBSH (in monoclinic space group *C2/c*) and CSMH-II is isomorphous with FMSH (in orthorhombic space group *Pbca*).

Therefore, isostructurality was observed in three different series of polymorphic compounds and number of isostructural crystals in Fuchsones can theoretically be increased to infinity by solid solution formation.

7.2 Polymorphism in Two Special Cases: Chiral Vs Racemic and Neutral Vs Zwitterionic polymorphs

The modern definition of polymorphism was given by McCrone and can be stated in a simple way as the phenomenon which involves differential arrangement of the same molecule in its crystalline forms. But complications arise in case of a racemate and a conglomerate. Another example of such a situation is when there is an intramolecular transfer of substituent in one (or more) of the crystal structures compared to others where there are no such transfer. Tautomers and zwitterions fall in the second category. In such a situation crystal structures can be considered as polymorphic when the rate of interconversion (+ enantiomer \rightleftharpoons - enantiomer or neutral \rightleftharpoons zwitterion) is rapid in solution.

Chapter 4 focuses on the concomitant polymorphism in a conformationally chiral molecule ditertiarybutylditolylfuchstone (t-BuF) where one polymorph is chiral (in non-centrosymmetric space group *P2₁*) and other three polymorphs are achiral (in centrosymmetric space groups *P2₁/n*, *Pbca* and *C2/c*). These tetramorphs can be called polymorphs as the conformational enantiomers interconvert rapidly in liquid state. One

of the reasons for generation of chirality in an achiral molecule is the ability of a molecule to exist as chiral conformers. The ability of the t-butyl derivatives, in two series of Fuchsones, to direct crystallization in non-centrosymmetric chiral space group $P2_1$ is established. Although the subtle factors behind the effect of substituents in chiral crystallization of Fuchsones is not clear, however, increasing the steric influence of the substituents around the carbonyl group appears to be an important factor. This observation perhaps finds application in non linear optical materials because materials that crystallize in non-centrosymmetric space group is a requirement for second harmonic generation.

Chapter 5 describes the polymorphism in an ampholyte 2-(*p*-tolylamino) nicotinic acid (TNA), which exists as at least three polymorphic modifications, two are neutral (Form I and form II) whereas form III is zwitterionic. There are very few examples of molecules exhibiting both neutral and zwitterionic polymorphs. The neutral polymorphs crystallized concomitantly during solution crystallization whereas the zwitterionic polymorph crystallizes only in presence of a pyridine based coformer such as 2-aminopyridine or 2-bromo-3-hydroxypyridine. Crystal structure determination of the zwitterionic polymorph provides better understanding of crystal nucleation and role of hydrogen bonding in presence of specific coformers. A general method to crystallize zwitterionic polymorphs of nicotinic acids will have a pharmaceutical application.

7.3 Polymorphism in Active Pharmaceutical Ingredients

Polymorphism in pharmaceutical compounds is well-known and has important implications in drug formulation. It is important to characterize these forms according to their stability because the metastable forms have greater solubility/dissolution compared to the thermodynamically stable form. Chapter 6 focuses on the polymorphism in three pharmaceutically important molecules viz. Tolbutamide, Methyl Paraben and Zolpidem.

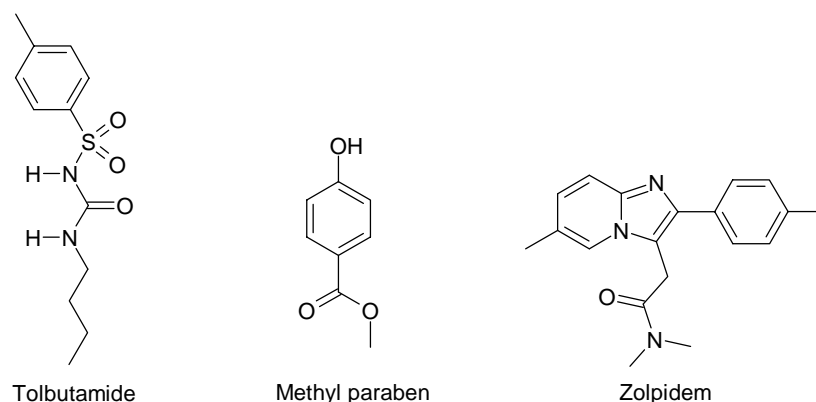


Figure 7.3 The three pharmaceutically active molecules studied in Chapter 6.

Tolbutamide, a sulfonylurea drug exhibiting hypoglycaemic activity, is known to exist as five different polymorphs viz. Form I^L, Form I^H, Form II, Form III and Form IV. However, no cocrystal of this drug is reported. With the idea that cocrystals can improve the physicochemical properties of drugs, novel cocrystals of Tolbutamide were attempted. A synthon approach suggested *p*-nitrophenol, *p*-nitrobenzoic acid, and *p*-phenylenediboronic acid as potential coformers via the urea⋯nitro and urea⋯boronate heterosynthons.

Manual and mechanical grinding and solution crystallization techniques did not result any cocrystal. A modulated crystal structure of the known Form III of Tolbutamide was obtained when *p*-nitrophenol and *p*-phenylenediboronic acid were used as coformers. The *b*-axis of this new crystal structure (at 100 K) is tripled ($P2_1/n$, 27.189(4) vs. 9.043(4) Å) and there are 3 symmetry-independent molecules in the unit cell. The butyl chain C atoms are fully ordered in the low temperature form III crystal structure ($Z' = 3$) compared to a disordered butyl group in the reported room temperature structure ($Z' = 1$). When nitrate anion was used as the complexing agent in place of the nitro group to hydrogen bond with the urea functionality, a serendipitous result happened. Crystallization of Tolbutamide with a trace amount of nitric acid in methanol afforded a novel polymorph V of Tolbutamide in $Pbcn$ space group.

Methyl paraben is extensively used in day to day life. Approximately 30,000 lbs of methyl paraben is consumed annually in the USA. There has been a recent controversy

regarding polymorphism in methyl paraben. A second genuine polymorph was crystallized by slow sublimation at ambient pressure at 80 °C and its crystal structure, thermal behavior and Hirshfeld fingerprint plots were compared with the three reported crystal structures of form I which were earlier claimed to be different polymorphs.

Pharmaceutical co-crystals are attracting immense interest both in academics and industry as they can improve many properties of API like solubility, dissolution rate, stability, crystallinity and many more. Cocrystal polymorphs of Zolpidem, an insomnia drug, were characterized using X-ray diffraction, thermal methods and by spectroscopy and their stability relationship was established. Conformational flexibility of the drug molecule around C–C single bond resulted in different packing arrangement in the two polymorphs. Fifteen different conformations were obtained for a total of ten molecular complexes and the parent API (six are from this work and four were reported).

The marketed form of zolpidem is its tartarate salt. A comparison of physicochemical properties of the cocrystal polymorphs or other novel molecular complexes with that of the marketed product may lead to the discovery of alternate solid forms for drug development.

Appendix

Crystallographic data for the crystal structures discussed in this thesis:

Crystal Data	TIP	TIR-O	TIR-M
Emp. Formula	C ₃ H ₃ I ₃ O	C ₆ H ₃ I ₃ O ₂	C ₆ H ₃ I ₃ O ₂
Formula wt.	471.78	486.78	486.78
Crystal system	Orthorhombic	Orthorhombic	Monoclinic
Space group	<i>P</i> 2 ₁ 2 ₁ 2 ₁	<i>P</i> 2 ₁ 2 ₁ 2 ₁	<i>P</i> 2 ₁ / <i>n</i>
T [K]	100	100	100
<i>a</i> [Å]	4.3695(5)	4.4949(7)	14.8819(10)
<i>b</i> [Å]	14.6940(15)	13.958(2)	4.3317(3)
<i>c</i> [Å]	14.1839(15)	15.036(2)	15.5848(11)
α [°]	90	90	90
β [°]	90	90	108.4950(10)
γ [°]	90	90	90
<i>Z</i> / <i>Z</i>	1/4	1/4	1/4
Volume [Å ³]	910.68(17)	943.3(3)	952.77(11)
<i>D</i> _{calc} [g cm ⁻³]	3.441	3.427	3.394
μ /mm ⁻¹	10.231	9.890	9.793
Reflns. collected	4958	5135	8909
Unique reflns.	1797	1861	1878
Observed reflns	1788	1800	1853
<i>R</i> ₁ [<i>I</i> > 2 σ (<i>I</i>)], <i>wR</i> ₂	0.0290, 0.0700	0.0582, 0.1346	0.0277, 0.0696
GOF	1.126	1.256	1.187
Diffractionmeter	Smart Bruker	Smart Bruker	Smart Bruker

TIG-O	TIG-M	TIP+TIR-O	TIR+TIG-O
C ₆ H ₃ I ₃ O ₃	C ₆ H ₃ I ₃ O ₃	C ₆ H _{1.50} I ₃ O _{1.50}	C ₆ H ₃ I ₃ O _{2.50}
503.78	503.78	478.27	495.78
Orthorhombic	Monoclinic	Orthorhombic	Orthorhombic
<i>P</i> 2 ₁ 2 ₁ 2 ₁	<i>P</i> 2 ₁ / <i>n</i>	<i>P</i> 2 ₁ 2 ₁ 2 ₁	<i>P</i> 2 ₁ 2 ₁ 2 ₁
100	100	100	100
4.6376(4)	14.582(4)	4.4419(3)	4.5607(3)
13.5291(11)	4.5004(13)	14.3683(9)	13.6484(8)
15.3446(12)	15.507(5)	14.5730(9)	15.3485(9)
90	90	90	90
90	107.569(4)	90	90
90	90	90	90
1/4	1/4	1/4	1/4
962.76(14)	970.2(5)	930.09(10)	955.39(10)
3.476	3.449	3.416	3.447
9.705	9.631	10.024	9.773
5921	8806	9609	9686
1805	1859	1846	1889

1800	1719	1834	1884
0.0241, 0.0602	0.0488, 0.1115	0.0215 , 0.0535	0.0225, 0.0544
1.108	1.187	1.197	1.178
Smart Bruker	Smart Bruker	Smart Bruker	Smart Bruker

TMF-I	TMF-II	TMF-III	CMF-I
C ₂₃ H ₂₂ O	C ₂₃ H ₂₂ O	C ₂₃ H ₂₂ O	C ₂₁ H ₁₆ Cl ₂ O
314.41	314.41	314.41	355.24
Monoclinic	Triclinic	Monoclinic	Monoclinic
<i>P</i> 2 ₁ / <i>c</i>	<i>P</i> $\bar{1}$	<i>P</i> 2 ₁ / <i>c</i>	<i>P</i> 2 ₁ / <i>c</i>
100	100	100	100
7.6297(5)	7.4822(6)	12.869(3)	7.5479(5)
12.5889(8)	8.1328(6)	17.255(4)	12.4908(9)
18.2064(11)	15.3014(11)	7.960(2)	18.3342(13)
90	97.5620(10)	90	90
95.4670(10)	101.0460(10)	99.436(5)	95.9850(10)
90	102.9920(10)	90	90
1/4	1/2	1/4	1/4
1740.76(19)	875.49(11)	1743.6(7)	1719.1(2)
1.200	1.193	1.198	1.373
0.071	0.071	0.071	0.382
17000	9080	16414	17449
3233	3406	3085	3389
3089	3235	2472	3105
0.0498, 0.1300	0.0430, 0.1107	0.0755, 0.1665	0.0324, 0.0823
1.056	1.066	1.113	1.051
Smart Bruker	Smart Bruker	Smart Bruker	Smart Bruker

CMF-II	CMF-d	CMF-t	MCF-I
C ₂₁ H ₁₆ Cl ₂ O	C ₂₃ H ₁₆ Cl ₂ O ₂	C _{24.50} H ₁₆ Cl ₂ O	C ₂₁ H ₁₆ Cl ₂ O
355.24	395.26	397.27	355.24
Monoclinic	Triclinic	Triclinic	Monoclinic
<i>P</i> 2 ₁ / <i>c</i>	<i>P</i> $\bar{1}$	<i>P</i> $\bar{1}$	<i>P</i> 2 ₁ / <i>c</i>
100	298	100	100
8.1079(5)	7.222(2)	7.2779(7)	7.5638(16)
17.6794(12)	12.034(4)	11.8390(11)	12.612(3)
12.3042(8)	12.859(4)	12.4604(11)	18.207(4)
90	102.963(5)	101.2630(10)	90
107.3880(10)	102.420(5)	103.8560(10)	96.092(3)
90	92.363(5)	91.1900(10)	90
1/4	1/2	1/2	1/4
1683.12(19)	1058.9(6)	1019.73(16)	1727.0(6)
1.402	1.240	1.294	1.366
0.390	0.320	0.330	0.380
17199	10898	10683	17374
3306	4157	4000	3369

3068	2518	3422	3208
0.0292, 0.0786	0.0540, 0.1489	0.0396, 0.1082	0.0328, 0.0856
1.040	0.979	1.048	1.059
Smart Bruker	Smart Bruker	Smart Bruker	Smart Bruker

MCF-II	MCF-III	CMF+MCF	TMF+CMF
C ₂₁ H ₁₆ Cl ₂ O	C ₂₁ H ₁₆ Cl ₂ O	C ₂₁ H _{13.25} Cl ₂ O	C ₂₂ H _{19.25} Cl O
355.24	355.24	352.47	335.07
Triclinic	Monoclinic	Monoclinic	Monoclinic
<i>P</i> $\bar{1}$	<i>C</i> 2/ <i>c</i>	<i>P</i> 2 ₁ / <i>c</i>	<i>P</i> 2 ₁ / <i>c</i>
100	100	100	100
7.5140(7)	19.8402(15)	7.5735(6)	7.5966(8)
8.1314(7)	10.8101(8)	12.5391(11)	12.5450(13)
15.2380(14)	7.7823(6)	18.2526(16)	18.2688(18)
97.0260(10)	90	90	90
101.4830(10)	90.00	95.7320(10)	95.684(2)
104.0540(10)	90	90	90
1/2	0.5/4	1/4	1/4
870.71(14)	1669.1(2)	1724.7(3)	1732.4(3)
1.355	1.414	1.357	1.285
0.377	0.393	0.380	0.225
8918	8341	17571	17513
3344	1630	3402	3416
3001	1562	3173	3174
0.0365, 0.0935	0.0334, 0.0880	0.0423, 0.1093	0.0378, 0.0932
1.039	1.071	1.110	1.077
Smart Bruker	Smart Bruker	Smart Bruker	Smart Bruker

TMF+MCF-1	TMF+MCF-2	TMF+MCF-3	TMF+MCF-4
C ₂₂ H _{19.25} Cl _{0.75} O	C _{22.50} H _{20.50} Cl _{0.50} O	C _{21.50} H _{17.75} Cl _{1.50} O	C _{21.50} H _{17.75} Cl _{1.50} O
326.21	324.61	345.28	345.28
Monoclinic	Triclinic	Monoclinic	Monoclinic
<i>P</i> 2 ₁ / <i>c</i>	<i>P</i> $\bar{1}$	<i>C</i> 2/ <i>c</i>	<i>P</i> 2 ₁ / <i>c</i>
100	100	100	100
7.6140(5)	7.4976(7)	19.853(3)	7.6040(6)
12.5924(8)	8.1301(7)	10.8323(15)	12.5706(11)
18.2117(12)	15.2759(13)	7.8131(11)	18.1989(15)
90	97.4970(10)	90	90
95.6060(10)	101.2120(10)	90.00	95.8030(10)
90	103.2220(10)	90	90
1/4	1/2	0.5/4	1/4
1737.8(2)	874.13(13)	1680.3(4)	1730.7(2)
1.247	1.233	1.365	1.325
0.186	0.147	0.311	0.302
17702	8980	7930	17520
3447	3381	1500	3422

3288	3284	1402	3214
0.0392, 0.0999	0.0450, 0.1110	0.0579, 0.1163	0.0479, 0.1034
1.091	1.145	1.319	1.208
Smart Bruker	Smart Bruker	Smart Bruker	Smart Bruker

CMSH-I	CMSH-II	TCSH	TBSH
C ₂₁ H ₁₉ Cl N ₂ O ₂ S	C ₂₁ H ₁₉ Cl N ₂ O ₂ S	C ₁₉ H ₁₃ Cl ₃ N ₂ O ₂ S	C ₁₉ H ₁₃ Br ₃ N ₂ O ₂ S
398.89	398.89	439.72	573.10
Monoclinic	Orthorhombic	Monoclinic	Monoclinic
<i>C2/c</i>	<i>Pbca</i>	<i>C2/c</i>	<i>C2/c</i>
298	298	298	298
22.305(2)	11.726(5)	22.655(4)	23.334(8)
12.0112(12)	15.488(7)	11.6004(18)	11.594(4)
15.3336(15)	22.317(10)	15.428(3)	15.600(5)
90	90	90	90
100.953(2)	90	101.926(3)	103.035(5)
90	90	90	90
1/8	1/8	1/8	1/8
4033.1(7)	4053(3)	3967.2(11)	4112(2)
1.314	1.307	1.472	1.852
0.311	0.309	0.584	6.005
20658	40435	15441	20670
3992	4096	3923	4031
3164	3097	2454	2569
0.0514, 0.1270	0.0451, 0.1141	0.0516, 0.1124	0.0399, 0.0836
1.039	1.050	1.016	1.003
Smart Bruker	Smart Bruker	Smart Bruker	Smart Bruker

FMSH	MISH	2t-Bu-I	2t-Bu-II
C ₂₁ H ₁₉ F N ₂ O ₂ S	C ₂₀ H ₁₆ I ₂ N ₂ O ₂ S	C ₂₉ H ₃₄ O	C ₂₉ H ₃₄ O
382.44	602.21	398.56	398.56
Orthorhombic	Monoclinic	Monoclinic	Monoclinic
<i>Pbca</i>	<i>P2₁/c</i>	<i>P2₁</i>	<i>P2₁/n</i>
298	298	100	100
11.939(2)	11.6335(16)	6.0525(8)	9.0435(8)
15.261(3)	11.6089(16)	19.535(3)	16.2029(15)
21.322(4)	15.843(2)	10.3567(14)	17.1008(16)
90	90	90	90
90	96.670(2)	103.489(2)	95.993(2)
90	90	90	90
1/8	1/4	1/2	1/4
3884.9(12)	2125.1(5)	1190.7(3)	2492.1(4)
1.308	1.882	1.112	1.062
0.194	3.075	0.065	0.062
33011	21633	12340	23016
3843	4235	4703	4358

3047	3678	4580	3719
0.0428, 0.1138	0.0390, 0.1003	0.0322, 0.0812	0.0586, 0.1176
1.048	1.064	1.060	1.146
Smart Bruker	Smart Bruker	Smart Bruker	Smart Bruker

2t-Bu-III	2t-Bu-IV	2i-Pr	TNA-I
C ₂₉ H ₃₄ O	C ₂₉ H ₃₄ O	C ₂₇ H ₃₀ O	C ₁₃ H ₁₂ N ₂ O ₂
398.56	398.56	370.51	228.25
Orthorhombic	Monoclinic	Monoclinic	Monoclinic
<i>Pbca</i>	<i>C2/c</i>	<i>P2₁/n</i>	<i>P2₁/n</i>
100	100	100	100
15.8153(14)	12.5468(14)	8.5454(9)	11.038(10)
17.4890(15)	23.813(3)	15.2329(16)	9.067(8)
17.9924(16)	9.2568(10)	17.3166(18)	11.392(10)
90	90	90	90
90	121.033(2)	98.015(2)	101.860(14)
90	90	90	90
1/8	0.5/4	1/4	1/4
4976.6(8)	2369.8(4)	2232.1(4)	1115.8(17)
1.064	1.117	1.103	1.359
0.062	0.065	0.065	0.094
45143	11335	22712	10196
4412	2104	4407	2190
3767	1708	3747	1987
0.0509, 0.1169	0.0550, 0.1137	0.0610, 0.1425	0.0598, 0.1827
1.116	1.063	1.095	1.188
Smart Bruker	Smart Bruker	Smart Bruker	Smart Bruker

TNA-II	TNA-III (100 K)	TNA-III (298 K)	NH⁺-TNA-COO⁻•2 NBA
C ₁₃ H ₁₂ N ₂ O ₂	C ₁₃ H ₁₂ N ₂ O ₂	C ₁₃ H ₁₂ N ₂ O ₂	C ₂₇ H ₂₂ N ₄ O ₁₀
228.25	228.25	228.25	562.49
Orthorhombic	Orthorhombic	Orthorhombic	Triclinic
<i>Pbca</i>	<i>Pbca</i>	<i>Pbca</i>	<i>P1</i>
100	100	298	298
14.2565(16)	9.0787(11)	9.250(4)	7.8000(8)
10.7542(15)	14.2261(17)	14.207(4)	13.0415(16)
14.769(3)	17.154(2)	17.509(10)	14.0098(15)
90	90	90	64.870(11)
90	90	90	86.132(9)
90	90	90	85.992(9)
1/8	1/8	1/8	1/2
2264.3(6)	2215.6(5)	2301.1(17)	1286.0(3)
1.339	1.369	1.318	1.453
0.092	0.094	0.091	0.113
10798	20081	5988	9618

4319	2160	2097	5273
2306	2005	866	3625
0.0497/0.1026	0.0521/0.1475	0.0646 /0.1350	0.0399/ 0.1033
0.872	1.185	0.929	1.039
Oxford Diffraction	Smart Bruker	Oxford Diffraction	Oxford Diffraction

AP-NH⁺•TNA-COO⁻	TB-III, LT	TB-III, RT	TB-V
C ₁₈ H ₁₈ N ₄ O ₂	C ₁₂ H ₁₈ N ₂ O ₃ S	C ₁₂ H ₁₈ N ₂ O ₃ S	C ₁₂ H ₁₈ N ₂ O ₃ S
322.36	270.34	270.34	270.34
Orthorhombic	Monoclinic	Monoclinic	Orthorhombic
<i>P</i> 2 ₁ 2 ₁	<i>P</i> 2 ₁ / <i>n</i>	<i>P</i> 2 ₁ / <i>n</i>	<i>Pb</i> cn
298	100	298	298
6.8022(8)	11.5613(17)	11.787(5)	15.851(6)
10.4120(12)	27.189(4)	9.043(4)	9.288(4)
23.206(3)	13.556(2)	13.955(6)	19.691(8)
90	90	90	90
90	102.803(2)	104.644(7)	90
90	90	90	90
1/4	3/12	1/4	1/8
1643.6(3)	4155.2(11)	1439.2(10)	2899.2(19)
1.303	1.296	1.248	1.239
0.088	0.236	0.227	0.226
15003	39777	14600	25042
3220	7363	2846	2568
3101	5713	2304	1647
0.0420, 0.0928	0.0652, 0.1505	0.0714, 0.1679	0.0784, 0.2086
1.162	0.963	1.099	1.062
Smart Bruker	Smart Bruker	Smart Bruker	Smart Bruker

MP-II	ZM•Suc-I	ZM•Suc-II	ZM-NH⁺•Cl⁻•H₂O
C ₈ H ₈ O ₃	C ₂₁ H ₂₄ N ₃ O ₃	C ₂₁ H ₂₄ N ₃ O ₃	C ₁₉ H ₂₄ Cl N ₃ O ₂
152.14	366.43	366.43	361.86
Monoclinic	Orthorhombic	Monoclinic	Orthorhombic
<i>P</i> 2 ₁ / <i>c</i>	<i>I</i> ba2	<i>P</i> 2 ₁ / <i>c</i>	<i>P</i> bca
100	100	100	100
4.8186(13)	24.520(3)	9.0697(15)	18.1812(12)
14.630(4)	9.6118(10)	21.307(3)	9.9506(7)
10.239(3)	16.4739(17)	9.7325(16)	19.7751(13)
90	90	90	90
99.810(5)	90	90.265(17)	90
90	90	90	90
1/4	1/8	1/4	1/8
711.3(3)	3882.5(7)	1880.8(5)	3577.6(4)
1.421	1.254	1.294	1.344
0.109	0.085	0.088	0.232

7072	19301	10355	35151
1370	3833	3796	3534
1252	3430	2432	3331
0.0801, 0.1564	0.0631, 0.1326	0.0433/0.0877	0.0397, 0.0940
1.339	1.187	0.885	1.088
Smart Bruker	Smart Bruker	Oxford Diffraction	Smart Bruker

ZM-NH⁺•Cl⁻•2CH₃CN	ZM-NH⁺•Sal-COO⁻•H₂O	2ZM-NH⁺•2Sal-COO⁻•CH₂Cl₂	2ZM-NH⁺•2Mal-COO⁻•2H₂O
C ₂₃ H ₂₈ Cl N ₅ O	C ₂₆ H ₂₉ N ₃ O ₅	C ₅₃ H ₅₆ Cl ₂ N ₆ O ₈	C ₄₆ H ₅₈ N ₆ O ₁₄
425.95	463.52	975.94	918.98
Monoclinic	Triclinic	Monoclinic	Monoclinic
<i>P</i> 2 ₁ / <i>c</i>	<i>P</i> $\bar{1}$	<i>P</i> 2 ₁ / <i>n</i>	<i>P</i> 2 ₁
100	100	100	100
9.6386(19)	8.4804(10)	16.6441(10)	15.0976(16)
8.9405(17)	10.9715(13)	17.7017(8)	7.2495(8)
26.169(5)	13.4688(16)	16.7517(11)	20.519(2)
90	90.248(2)	90	90
96.052(3)	106.839(2)	91.009(6)	90.900(2)
90	106.470(2)	90	90
1/4	1/2	2/8	2/4
2242.5(7)	1145.1(2)	4934.8(5)	2245.5(4)
1.262	1.344	1.314	1.359
0.195	0.094	0.193	0.101
22425	10855	16194	21233
4406	3958	7071	7672
4054	3452	3865	6084
0.0599, 0.1337	0.0512, 0.1265	0.0462, 0.0804	0.0727, 0.1279
1.210	1.041	0.833	1.071
Smart Bruker	Smart Bruker	Oxford Diffraction	Smart Bruker

ZM•MP
C ₂₇ H ₂₉ N ₃ O ₄
459.53
Orthorhombic
<i>Pbca</i>
100
7.2702(5)
21.8256(16)
30.082(2)
90
90
90
1/8
4773.2(6)
1.279

0.087
 46601
 4695
 3501
 0.0898, 0.1378
 1.205
 Smart Bruker

Crystal data of 2t-Bu-1 under Cu K α radiation

Crystal Data	Crystal 1	Crystal 2	Crystal 3
Emp. Formula	C ₂₉ H ₃₄ O	C ₂₉ H ₃₄ O	C ₂₉ H ₃₄ O
Formula wt.	398.56	398.56	398.56
Crystal system	Monoclinic	Monoclinic	Monoclinic
Space group	<i>P</i> 2 ₁	<i>P</i> 2 ₁	<i>P</i> 2 ₁
T [K]	100	100	100
<i>a</i> [Å]	6.0544(2)	6.05834(13)	6.0578(3)
<i>b</i> [Å]	19.5688(5)	19.5652(4)	19.5697(9)
<i>c</i> [Å]	10.3671(3)	10.3736(2)	10.3728(6)
α [°]	90	90	90
β [°]	103.518(3)	103.512(2)	103.561(5)
γ [°]	90	90	90
Z'/Z	2	2	2
Volume [Å ³]	1194.24(6)	1195.57(4)	1195.39(11)
<i>D</i> _{calc} [g cm ⁻³]	1.108	1.107	1.107
μ /mm ⁻¹	0.491	0.491	0.491
Reflns. collected	8558	10219	10119
Unique reflns.	4642	4534	4210
Observed reflns	4606	4525	4207
<i>R</i> ₁ [<i>I</i> >2 σ (<i>I</i>)], <i>wR</i> ₂	0.0336, 0.0907	0.0353, 0.0923	0.0313, 0.0850
GOF	1.067	1.083	1.045
Flack	0.0(2)	0.0(2)	0.0(2)
Radiation source	Cu	Cu	Cu
Diffractometer	Oxford Diffraction	Oxford Diffraction	Oxford Diffraction

DSCs of Fuchsones:

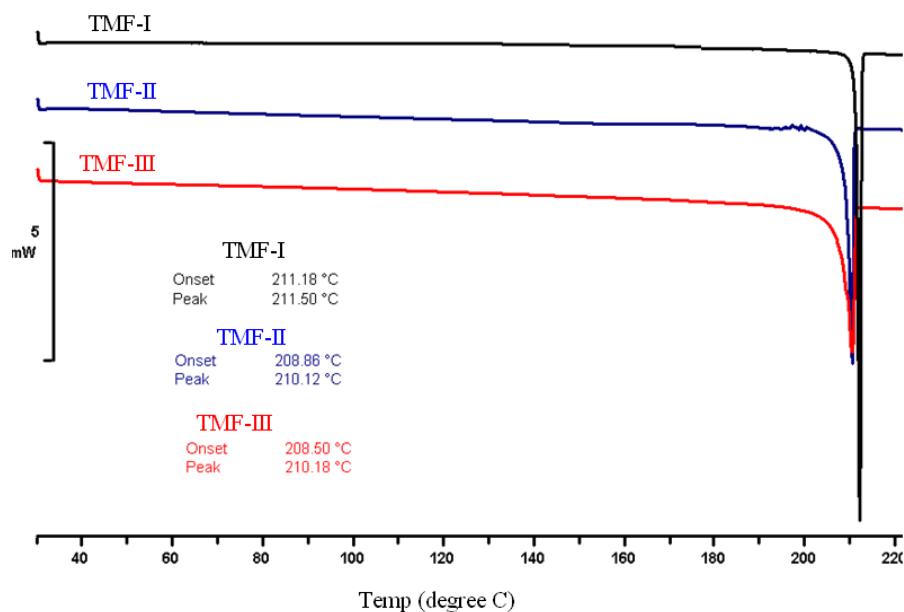


Figure A1 DSC thermograms of TMF polymorphs.

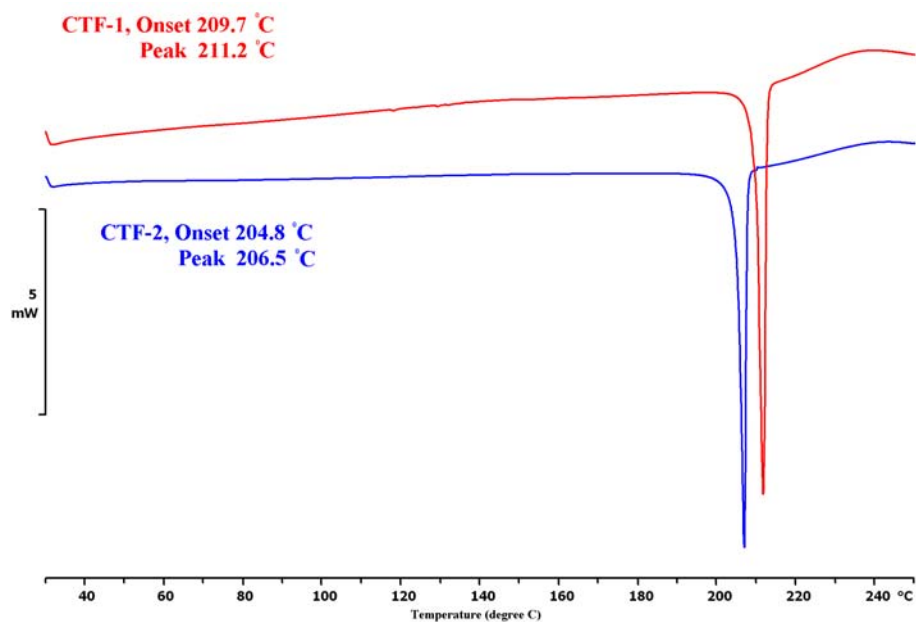


Figure A2 DSC thermograms of CTF polymorphs.

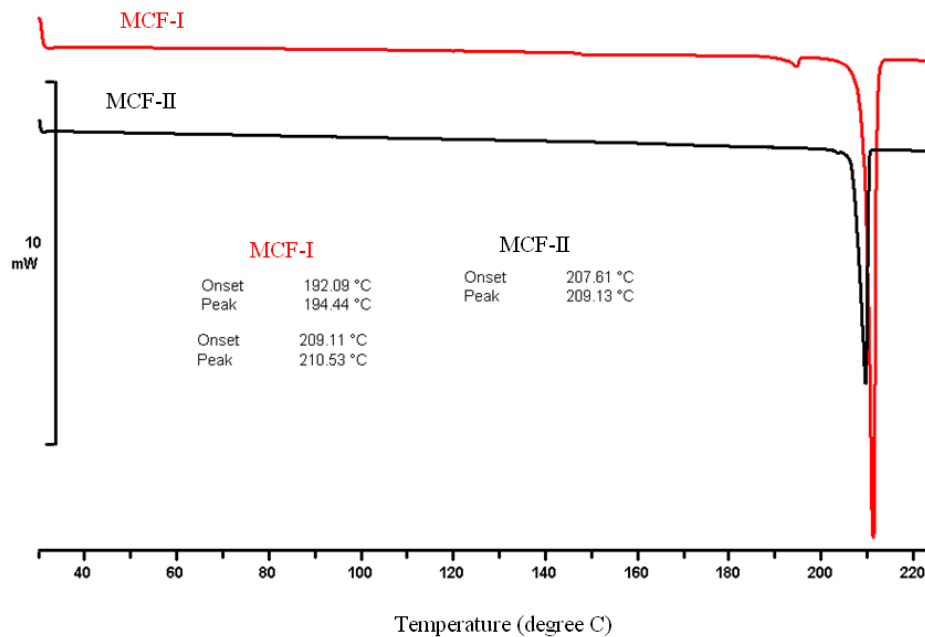


Figure A3 DSC thermograms of MCF-I and MCF-II. MCF-III could not be obtained in pure form.

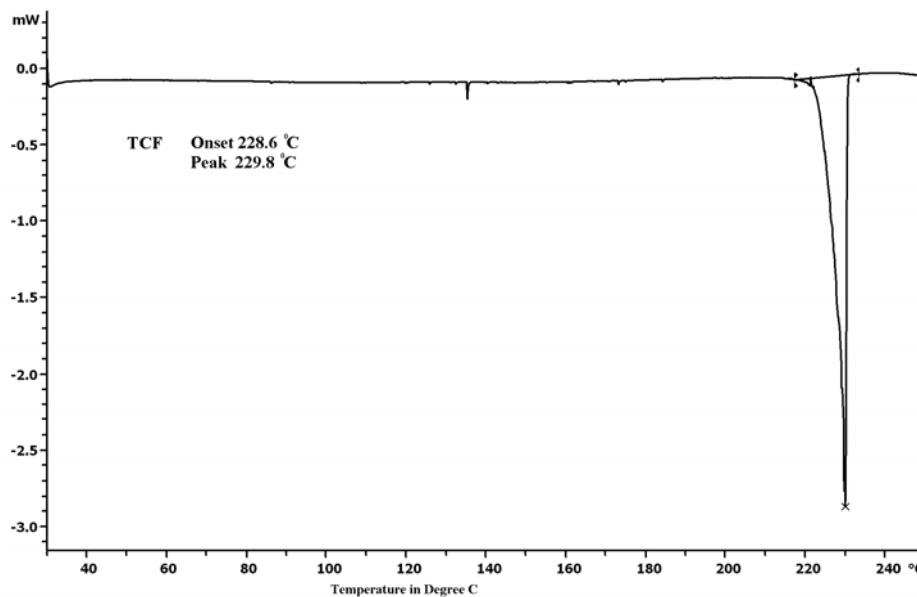


Figure A4 DSC thermogram of TCF.

DSC and TGA of molecular complexes of Zolpidem:

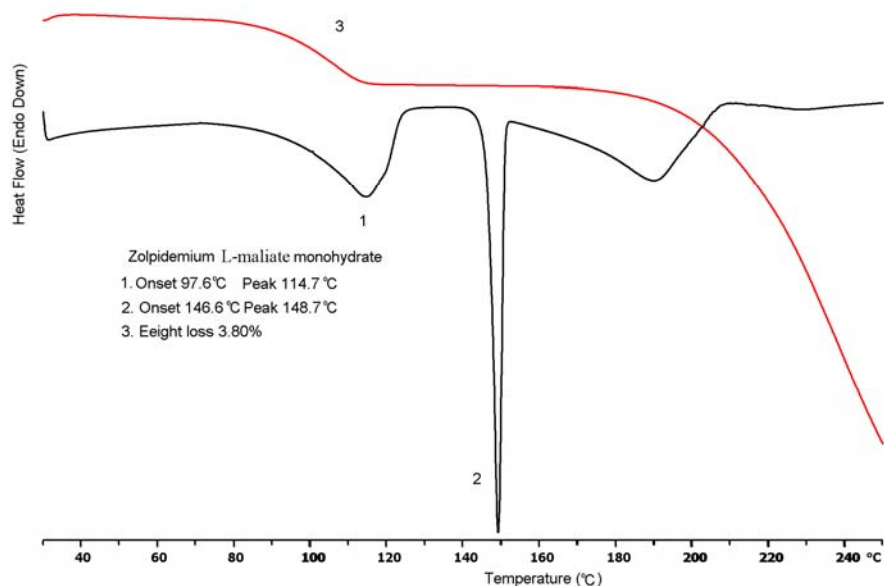


Figure A5 DSC (black) and TGA (red) of $2\text{ZM-NH}^+\cdot 2\text{Mal-COO}^-\cdot 2\text{H}_2\text{O}$. TGA shows a weight loss of 3.80% starting at 97 °C corresponding to the theoretical weight loss of 3.92%. The molecular complex melted at 146 °C.

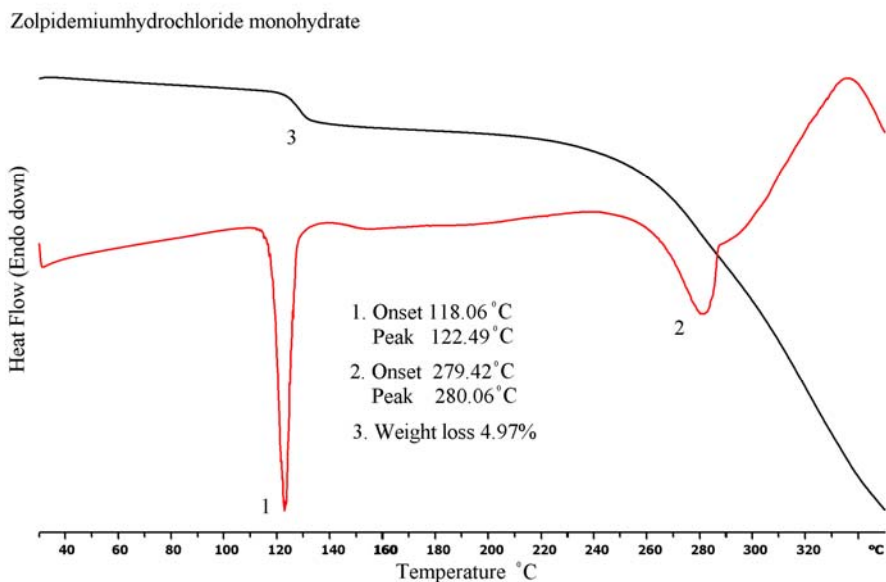


Figure A6 DSC (red) and TGA (black) of $\text{ZM-NH}^+\cdot \text{Cl}^-\cdot \text{H}_2\text{O}$. TGA shows a weight loss of 4.97% at 118 °C of corresponding to the theoretical weight loss of 4.99%. The molecular complex melted at 279 °C.

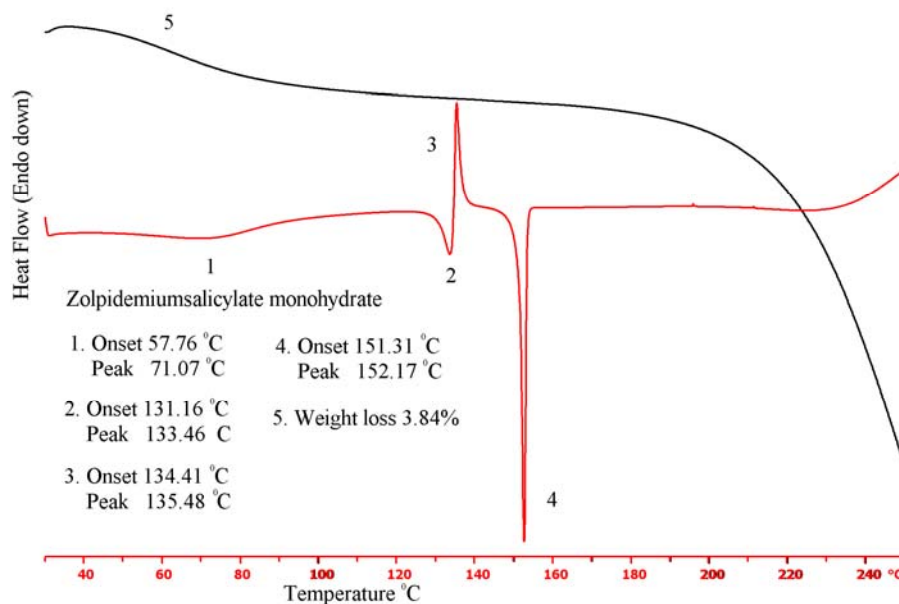


Figure A7 DSC (red) and TGA (black) of $\text{ZM-NH}^+\cdot\text{Sal-COO}^-\cdot\text{H}_2\text{O}$. TGA shows a weight loss of 3.84% at 57 °C corresponding to the theoretical weight loss of 3.88%. The molecular complex melted at 151 °C.

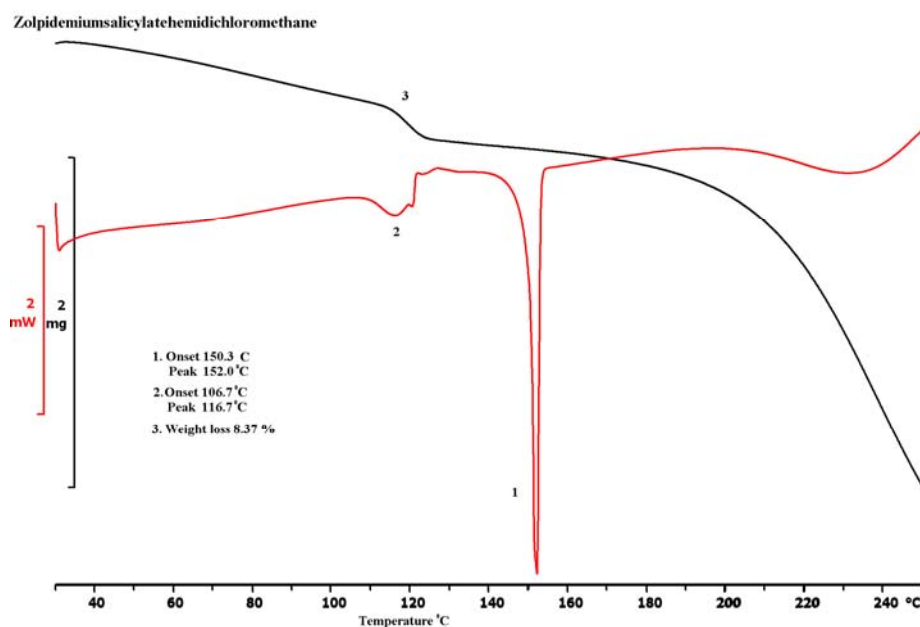


Figure A8 DSC (red) and TGA (black) of $\text{ZM-NH}^+\cdot\text{Sal-COO}^-\cdot 0.5\text{CH}_2\text{Cl}_2$. TGA shows a weight loss of 8.37% at 106 °C corresponding to the theoretical weight loss of 8.70%. The molecular complex melted at 150.3 °C.

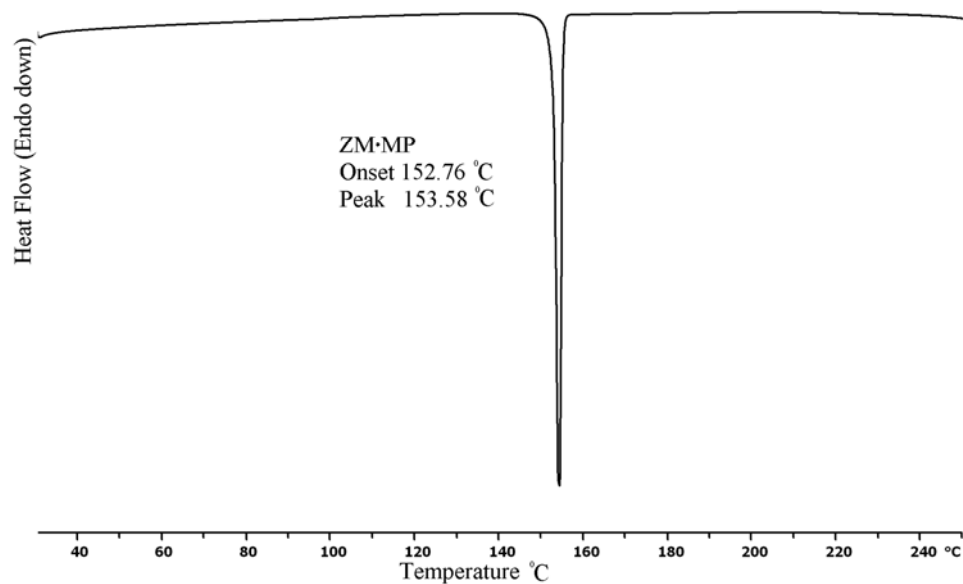


Figure A9 DSC thermogram of ZM•MP cocrystal which melted at 152 °C.

Comparison of calculated and experimental XRPDs of molecular complexes of Zolpidem: molecular complexes:

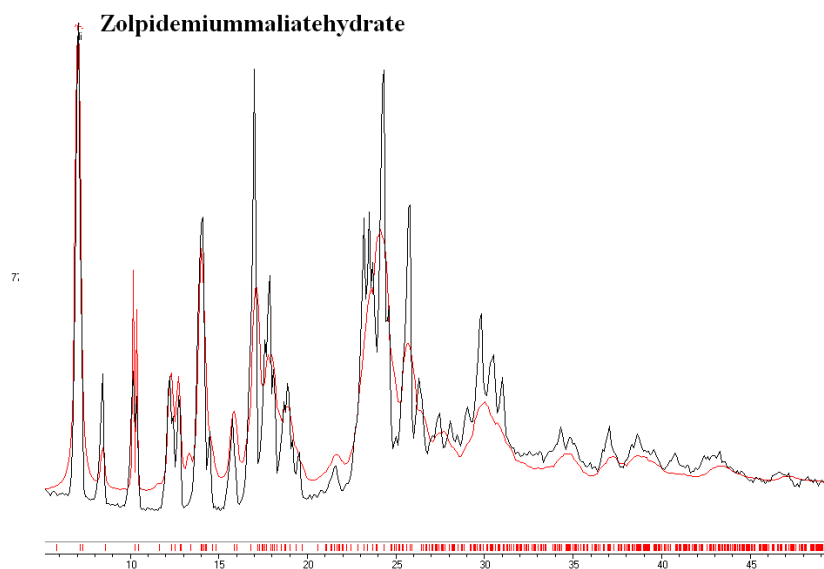


Figure A10 Comparison of calculated (red) and experimental (black) XRPD patterns of the molecular complex $2\text{ZM-NH}^+ \cdot 2\text{Mal-COO}^- \cdot 2\text{H}_2\text{O}$.

Zolpidemiumsalicylatemonohydrate

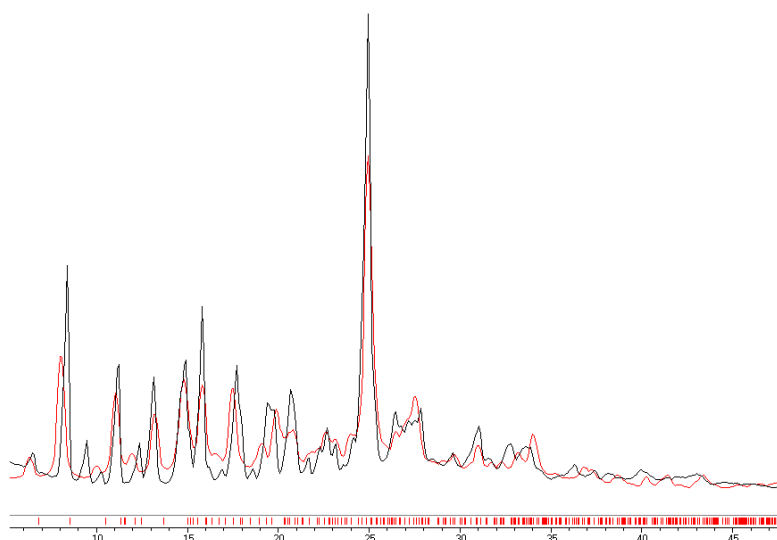


Figure A11 Comparison of calculated (red) and experimental (black) XRPDs of ZM-NH⁺•Sal-COO⁻•H₂O.

ABOUT THE AUTHOR

Naba Kamal Nath, youngest son of Mr. Bholā Ram Nath and Ms. Ranima Nath, was born in Jorhat, District of Assam, India, in 1981. He received his primary education from 133 No. Bongal Pukhuri Adarsha Prathamīc Vidyalā and completed his secondary school education at Jorhat Govt. Boys H. S. & M. P. School, Jorhat. He then completed his Intermediate education and B. Sc. from J. B. College, Jorhat, Assam. After the completion of his M.Sc. (Inorganic Chemistry as Special Paper) from Gauhati University, Guwahati, he joined School of Chemistry, University of Hyderabad, to pursue PhD in 2006 under the supervision of Prof Ashwini Nangia. He qualified CSIR-UGC-National Eligibility Test for Junior Research Fellowship (JRF) held in June 2005 and was awarded research fellowship by the University Grant Commission (UGC) for 2006-2011 (JRF and SRF).

LIST OF PUBLICATIONS

1. Isostructural Polymorphs of Triiodophloroglucinol and Triiodoresorcinol
Naba K. Nath, Binoy K. Saha and Ashwini Nangia
New J. Chem., **2008**, 32, 1693–1701. (Special issue on Polymorphism and Crystal forms)
2. Polymorphism in Fuchsones
Sreekant K. Chandran, **Naba K. Nath**, Saikat Roy, and Ashwini Nangia
Cryst Growth & Des., **2008**, 8, 140-154. (Special issue on Facets of Polymorphism in Crystals)
3. Synthon Competition and Cooperation in Molecular Salts of Hydroxybenzoic Acids and Aminopyridines
Bipul Sarma, **Naba K. Nath**, Balakrishna R. Bhogala, and Ashwini Nangia
Cryst Growth & Des., **2009**, 9, 1546-1557.
4. N–H···N(pyridyl) and N–H···O(urea) Hydrogen bonding and Molecular Conformation of N-aryl-N'-pyridylureas
Sreekanth K. Chandran, **Naba K. Nath**, Suryanarayan Cherukuvada, Ashwini Nangia
J. Mol. Struct., **2010**, 968, 99-107.
5. Novel form V of Tolbutamide and a high Z' crystal structure of form III
Naba K. Nath and Ashwini Nangia
CrystEngComm, **2011**, 13, 47–51. (Structure of the week in Crystal Growth & Design Network)
6. Crystal structures of Mirtazapine molecular salts
Bipul Sarma, Ranjit Thakuria, **Naba K. Nath** and Ashwini Nangia
CrystEngComm, **2011**, 13, 3232-3240.
7. Crystal Structure of Methyl Paraben Polymorph II
Naba K. Nath, Himanshu Aggarwal and Ashwini Nangia
Cryst Growth & Des., **2011**, 11, 967.
8. Chiral and racemic tetramorphs of t-Butylfuchsone
Naba K. Nath and Ashwini Nangia

(Manuscript in preparation)

9. Neutral and zwitterionic polymorph of 2-(p-tolylamino)nicotinic acid (TNA)

Naba K. Nath, Sudalai Kumar S. and Ashwini Nangia

(Manuscript in preparation)

10. Chloro-methyl exchange and polymorphism in Fuchsones

Naba K. Nath and Ashwini Nangia

(Manuscript in preparation)

11. Crystal structures of molecular complexes of Zolpidem

Naba K. Nath and Ashwini Nangia

(Manuscript in preparation)



CERTIFICATE

This is to certify that the thesis entitled “**Isostructurality and Polymorphism in Model Compounds and Active Pharmaceutical Ingredients**” submitted by **Naba Kamal Nath** bearing Regd. No. CH05PH25 in partial fulfillment of the requirements for the award of Doctor of Philosophy in Chemistry is a bonafide work carried out by him under my supervision and guidance.

The thesis has not been submitted previously in part or in full to this or any other University or Institution for the award of any degree or diploma.

Dean
School of Chemistry

Prof. Ashwini Nangia
Thesis Supervisor

DECLARATION

I **Naba Kamal Nath** hereby declare that this thesis entitled “**Isostructurality and Polymorphism in Model Compounds and Active Pharmaceutical Ingredients**” submitted by me under the guidance and supervision of **Professor Ashwini Nangia** is a bonafide research work. I also declare that it has not been submitted previously in part or in full to this University or any other University of Institution for the award of any degree or diploma.

Name: **Naba Kamal Nath**

Date:

June 2011

Hyderabad

Signature of the Student

Regd. No. 05CHPH25

ACKNOWLEDGEMENT

It is my immense pleasure to express my sincere gratitude to my Ph. D. supervisor **Prof. Ashwini Nangia**, for his constant cooperation, encouragement, kind guidance and for introducing me to this research field. It has been great pleasure and fortune to work with him. I am also indebted to him for the work freedom he has given me during my Ph D tenure.

I would like to thank the Prof. M. V. Rajasekharan, Dean, School of Chemistry, and former Deans, for their constant inspiration and for allowing me to avail the available facilities.

I am extremely thankful individually to all the faculty members of the School, Dr. S. M. Ahmed and Mr. Murthy of Central Instrument Laboratory (CIL) and non teaching staff for their various help and cooperation on various occasions.

I wish to record my thanks to UGC for fellowship support. I also would like to thanks the DST-PURSE programme for funding my visit to NTU, Singapore to attend CGOM9 conference.

I would like to acknowledge Prof. Michael Hursthouse and Dr. T. Gelbrich, School of Chemistry, University of Southampton, Southampton, UK, for providing us the “XPac program” free of cost. I sincerely thank Dr. Sanjay Nilapwar, Experimental Officer, Biomolecular Interactions and Protein Production Facility Manchester Interdisciplinary Centre, The University of Manchester, UK, for recording the solid state CD spectra of Fuchsone samples. My sincere thanks to Dr. Saikat Roy and Mr. Ranjit Thakuria for synthesizing and collecting single crystal X-ray data of Sulfonylhydrazones.

I am deeply indebted to all my teachers starting from my elementary school to M. Sc., especially late Dadu Dutta, late Dibakar Mahanta sir, Dr. Arpan Barooah, Dr. Prashanta Barooah sir Dr. Diganta K. Deka and Dr. Pradeep Phukan sir for their wonderful teaching and education throughout my academics.

I would like to acknowledge my lab seniors Dr. Srinivasulu Aitipamula, Dr. Sreenivas Reddy, Dr. Malla Reddy, Dr. Bala Krishna Reddy, Dr. Binoy K. Saha, Dr. Saikat Roy, Mr. Sreekanth Chandran, Dr. N. Jagadeesh Babu and Dr. Bipul Sarma for their help and encouragement at various stages of my Ph. D. My sincere thanks to my labmates Ranjit, Palash, Surya, Rajesh, Kalyan, Maddileti, Sudalai Kumar, Geetha, Suresh, Venkat, Arghya, Babu, Satyanarayana, Moumita, Snigdha, Gautom, Himanshu, Kanishka, Sumanth, Uday, Sreenu Kishore and Swarupa for maintaining a friendly and cooperative atmosphere in the lab.

Words are not enough to express my appreciation, gratitude and earnest feelings to my friend Mousumi for giving me her constant mental support and encouragement throughout my Ph.D. life. My pleasant association with some friends in UOH such as Swarnali ba, Bornali, Jayashree, Supria, Munmi, Neelam, Kakoli, Poli, Premanka, Sanjeev, Tridib, Abdul, Sapan, Sashanka, Indu, Rava, Mujjafar, Jayanta and Ticken is unforgettable. I would like to acknowledge few of my beloved seniors in UOH, roommate Abhik da, Moloy da, Subhash da, Rahul da, Dinu da, Teja bhai, Prashant da, Manab da, Utpal da, Suparna di, Anindita di, Bhaswati di, Bashudhara di and Rumpa. I would also like to thank few of my friends in School of Chemistry Arindam, Arun, Sandeep, Sudhanshu, Malkappa, Shuvra, Ramkumar, Ghanta, Tapta, Mehboob, Dinu, Sanghamitra, Venu, Sajna, Ramsuresh, Nayan, Tulika, Gupta, Durgaprasad, Hari, Anji, Ravi, Srinivas, G. D. P, Rambabu, D. K., Krishna, Anand, Prabeen, Swami, and Prabhu. I would like to thank my M Sc and B Sc seniors and friends Khirud da, Lakhindra da, Babita ba, Pabitra da, Anshuman, Rajib, Partha, Bibek, Abhisek, Kalyan Bulon, Lakhya, Kuldeep and Kundu.

I thank my dada, nobou and little Ria, cousins Tulu, Babu, Akanmani, Pulak, mahi, moha, mama, mami and aita for their support and encouragement.

The blessings and best wishes of my parents keep me active throughout my life. They made me what I am and I owe everything to them. Dedicating this thesis to them is a minor recognition for their invaluable support and encouragement.

Naba Kamal Nath

SYNOPSIS

This thesis entitled “**Isostructurality and Polymorphism in Model Compounds and Active Pharmaceutical Ingredients**” consists of seven chapters.

CHAPTER ONE

Introduction

Solid state chemistry in the modern era has gained significance in the isolation, identification and characterization of different crystal forms of the same molecule or of aggregates of molecules with other molecules due to scientific, materials, regulatory, and intellectual property reasons. These crystalline forms can be polymorphs, solvates/hydrates, salts and cocrystals. The importance of multi-crystalline forms originate due to the fact that they can exhibit a range of different physico-chemical properties of the solid material.

McCrone defined polymorphism as “*a solid crystalline phase of a given compound resulting from the possibility of at least two different crystalline arrangements of the molecules of that compound in the solid state*”. Depending on the differences between polymorphs they can be classified as conformational polymorph, due to differences in molecular conformations, synthon polymorph, due to differences in hydrogen bonding, and packing polymorph, where the difference is in the overall packing of molecules. Polymorphism has immense importance in pharmaceutical industry, dyes and pigment, agrochemicals, explosive materials etc. due to its ability to alter the melting point, color, compressibility, filterability, stability, solubility etc. of the solid material. Polymorphism is very common in pharmaceutical solids, with estimates of 30-50% in drug-like molecules, compared to 4-5% polymorphic compounds for organic solids in the Cambridge Structural Database.

Isostructurality is another phenomenon, inversely related to polymorphism, which refers to identical or a nearly identical crystal packing arrangement of chemically related compounds in the crystal lattice. This phenomenon has substantial importance in solid state development which can be employed to find out desired crystal forms of a

drug by replacing one molecule with another without disturbing the crystalline order. Two crystals are said to be isomorphous if (a) they have the same space group and unit cell dimensions and (b) the types and the positions of atoms in both structures are the same except for a replacement of one or more atoms in one molecule with different types of atoms in the other. Two isomorphous substances can form a continuous series of solid solutions. On the other hand, two crystals are said to be isostructural if they have the same crystal structure, but not necessarily the same unit cell dimensions nor the same chemical composition, and with a comparable variability in the atomic coordinates to that of the cell dimensions and chemical composition. Isostructural materials can be designed from molecules with exchange of functional groups such as halogen exchange, halogen→methyl, O–H→C–H, N–H→C–H, P=O→P (lp), H→t-Bu, etc.

CHAPTER TWO

Isostructural Polymorphs of Triiodoresorcinol and Triiodophloroglucinol

The twin phenomena of polymorphism and isostructurality typify almost opposite molecule to crystal structure behavior in the organic solid-state. Triiodoresorcinol (TIR, 2,4,6-triiodoresorcinol) and triiodophloroglucinol (TIG, 2,4,6-triiodophloroglucinol) crystallized as orthorhombic (TIR-O and TIG-O in $P2_12_12_1$) and monoclinic (TIR-M and TIG-M in $P2_1/n$) polymorphs mediated via inter-halogen I⋯I interactions. The orthorhombic polymorphs are isostructural and in turn similar to the crystal structure of 1,3,5-triiodobenzene (TIB). The isostructural monoclinic polymorphs are similar to the structure of 1,3,5-trifluoro-2,4,6-triiodobenzene (TIF). Triiodophenol (TIP) crystallized in a single orthorhombic form only. TIG-M and TIR-M have tandem O–H⋯O hydrogen bonds in addition to inter-iodine interactions. The isomorphous nature of crystal structures was confirmed by the formation of 1: 1 binary solid-solutions, TIP + TIR-O and TIR + TIG-O, in orthorhombic space group $P2_12_12_1$. Dimorphs of TIR and TIG establish a structural link in the triiodobenzene series TIB ($P2_12_12_1$) - TIP ($P2_12_12_1$) - TIR ($P2_12_12_1$ and $P2_1/n$) - TIG ($P2_12_12_1$ and $P2_1/n$) - TIF ($P2_1/n$). The search for new

polymorphs was initiated after analyzing the isostructurality relationship in the series of compounds.

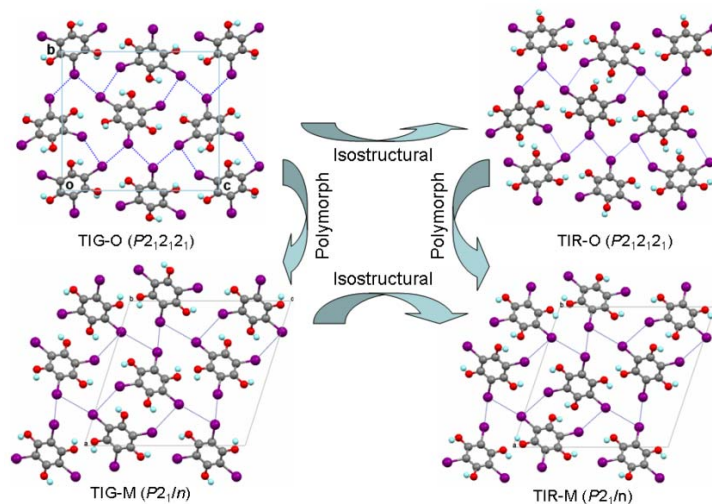


Figure 2.1 Isostructural orthorhombic and monoclinic pairs of TIG and TIR polymorphs.

CHAPTER THREE

Isostructurality and Polymorphism in Fuchsones and Sulfonylhydrazones

One of the approaches to study the structural aspects of packing motifs in organic solids is to vary systematically the mode of substitution on a particular molecule and to investigate the subsequent similarities and differences in the crystal structures. The similarity in volume of the methyl group and the chlorine atom has led to the idea that they could be interchanged. This is called chloro-methyl exchange. In the Cambridge Structural Database (CSD) about 30% of the 105 pairs of molecules differing only by the substitution of a methyl group for a chlorine atom are found to be isostructural. Isostructurality among the polymorphs of the two chloro-methyl exchanged compounds is rare in literature. A study of isostructurality based on chloro-methyl exchange rule among the polymorphs of a series of Fuchsones is presented in this chapter. Molecular acronyms TMF, CMF, MCF and TCF stand for tetramethylfuchsones,

dichlorodimethylfuchstone, dimethyldichlorofuchstone and tetrachlorofuchstone (Figure 3.1).

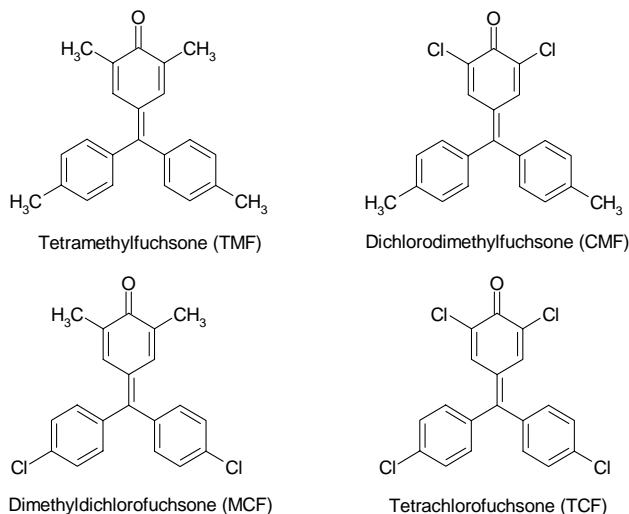


Figure 3.1 Series of Fuchstones where methyl group is exchanged with chloro.

TMF crystallized as trimorph, form I (TMF-I), form II (TMF-II) and form III (TMF-III); CMF crystallized as dimorph, form I (CMF-I), form II (CMF-II) along with two solvated crystal structures dioxane (CMF-d) and toluene (CMF-t); MCF as trimorph, form I (MCF-I), form II (MCF-II) and form III (MCF-III). But for TCF only one crystal structure was obtained. Comparison of cell parameters, space group and crystal structure analysis revealed that TMF-I, CMF-I and MCF-I form an isomorphous crystal triplet and TMF-II and MCF-II are isomorphous crystal pair. The two solvated crystal structures CMF-d and CMF-t also form an isomorphous crystal pair. Isomorphism in the polymorph series is further confirmed by the formation of solid solution. Different stoichiometric ratio solid solutions were obtained which crystallized in the same space groups of the polymorphs of the three compounds (TMF+CMF, CMF+MCF, TMF+MCF-1, TMF+MCF-2, TMF+MCF-3 and TMF+MCF-4). Isostructurality and polymorphism in Fuchstones can be interrelated as shown in Scheme 3.2.

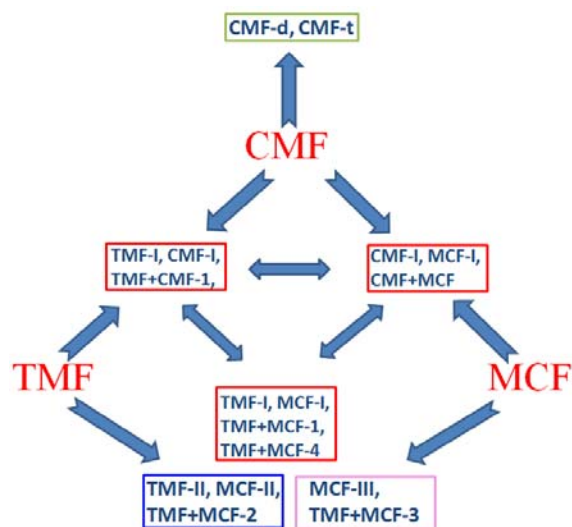


Figure 3.2 Interrelation of isostructurality and polymorphism among the crystal structures of Fuchsones. Isomorphous crystals resulting from two different starting materials (indicated by single headed arrows) are included in the different colored boxes. Crystal structures inside red box are isomorphous to each other (indicated by double headed arrows).

Sulfonylhydrazones are conformationally flexible molecules. Halogen-methyl exchange and inter halogen exchanged isostructurality was studied in this series. The following halogen and methyl derivatives were synthesized and crystal structures were determined to find polymorphs and isostructurality among them.

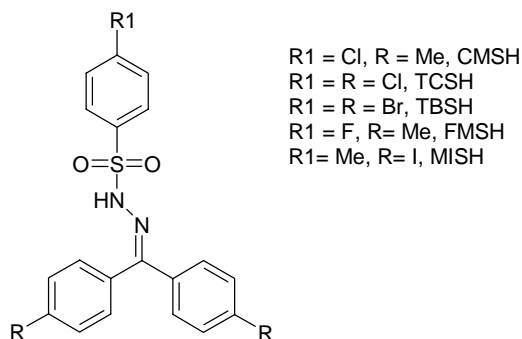


Figure 3.3 Sulfonylhydrazone derivatives selected for this study.

Summary of polymorphism and isostructurality in Sulfonylhydrazones is as follows.

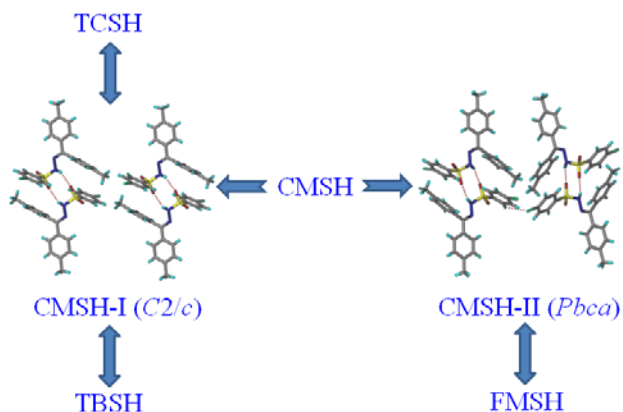


Figure 3.4 Sulfonylhydrazones exhibiting isostructurality and polymorphism. CMSH-I and CMSH-II represents polymorph 1 and polymorph 2 of CMSH. The double headed arrows relate the isomorphous crystal structures. Polymorphs of CMSH establish a structural link in the series.

CHAPTER FOUR

Chiral and Racemic Tetramorphs of *t*-Butylditolylfuchsone

Optically active molecules must crystallize in chiral space groups, but in solution a racemic mixture of a chiral molecule may aggregate either to form an achiral racemic crystal (more common) or undergo a spontaneous resolution where the two enantiomers crystallize separately into a conglomerate of enantiopure crystals (rare). Achiral molecules can also crystallize in chiral space groups. Conformationally flexible achiral molecules in liquid state or in solution can exist in a dynamic equilibrium of interconverting chiral conformations. When the rate of interconversion of enantiomers in liquid state is fast it gives rise to racemic and chiral crystals and they are termed as polymorphs. When the rate of interconversion is slow they are different compounds, viz. racemate and enantiomers (+ and –).

Crystal structures with non-centrosymmetric packing of molecules are important in many aspects such as in electro-optic and nonlinear optical materials, asymmetric synthesis and is relevant to understanding of the origin of life.

The title compound 4-(α,α -ditolylmethylene)-2,6-di-*t*-butyl-1,4-benzoquinone (*t*-Butylditolylfuchsonone) which can exhibit conformational chirality, was synthesized and crystallized as a concomitant mixture of four polymorphs. Form-I crystallized in chiral space group $P2_1$, however, form-II, III, and IV crystallized in centrosymmetric space groups $P2_1/n$, $Pbca$, and $C2/c$ respectively. Conformational chirality in the title molecule and the effect of *t*-Bu groups on the crystallization in non-centrosymmetric chiral space group was noted in two series of Fuchsonone derivatives (Figure 4.1). Phase transition from racemic to chiral polymorph was monitored by thermal techniques and single crystal X-ray diffraction.

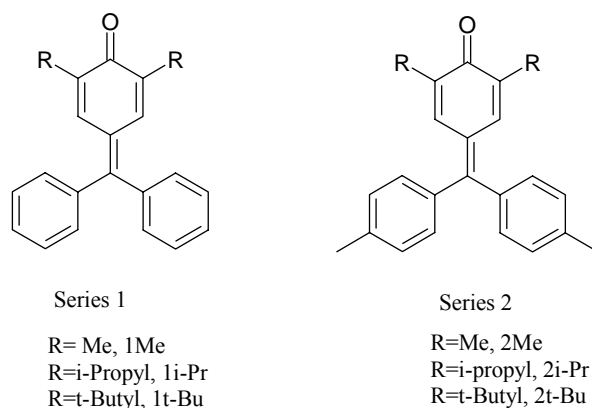


Figure 4.1 Moving from Me→i-Pr→t-Bu in the above two series of Fuchsones exhibit chiral crystallization.

CHAPTER FIVE

Neutral and Zwitterionic Polymorphs of 2-(*p*-Tolylamino) Nicotinic Acid (TNA)

Ampholites are amphoteric compounds which contain both acidic and basic groups and exist as zwitterion in certain pH ranges. Amino acids are the commonest examples of amphoteric compounds. Zwitterions contain both positive and negative charges on different atoms within the molecule and are electrically neutral through a net cancellation of formal positive and negative charges. Amphoteric drug molecules

predominantly exist as charged species in physiological pH conditions therefore these drugs are better suited for targets situated in plasma.

Molecules exhibiting both neutral and zwitterionic crystal structures are not common. To our knowledge, there are only four molecules in CSD which exhibit neutral and zwitterionic polymorphs. Clonixin form II and Norfloxacin form A exist as zwitterions along with their neutral polymorphs, whereas anthranilic acid form I and Torasemide form-i are in part zwitterionic (both neutral and zwitterionic molecules are present in the asymmetric unit) in nature.

Many diarylamines exhibit anti-inflammatory drug properties. Common examples are niflumic acid, clonixin, mefenamic acid, tolfenamic acid, flufenamic acid meclofenamic acid, diclofenac etc. and most of them are polymorphic. A nicotinic acid derivative, 2-(p-tolylamino) nicotinic acid (TNA) which falls under the category of diaryl amines (an ampholite) was synthesized and crystallized as conformational trimorphs with two neutral (Form I and Form II) and one zwitterionic polymorphs (Form III). Crystal structures of form I and form III are 2D isostructural whereas form II has completely different crystal structure through a different molecular conformation. Partial intramolecular proton transfer is observed in the room temperature crystal structure of form III whereas proton transfer is complete at 100 K. Polymorphs were characterized by FT-IR, FT-Raman, ss-NMR, DSC, and single crystal X-ray diffraction. 2D finger print plots of Hirshfeld surface shows the difference in the hydrogen bonding interactions for all the three polymorphs (Figure 5.1).

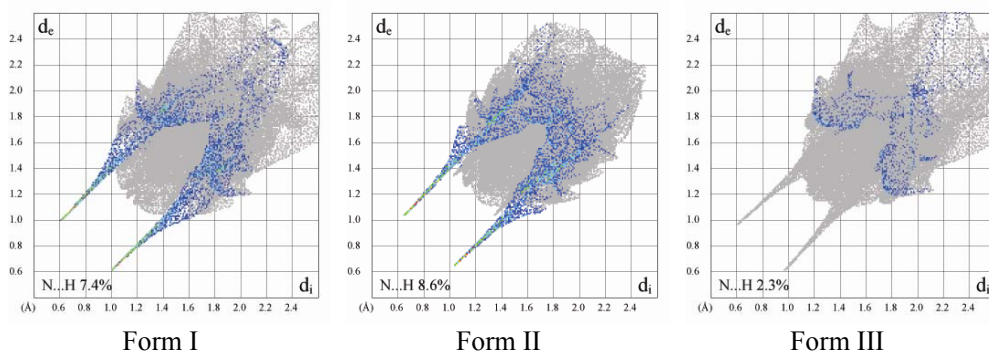


Figure 5.1 2D fingerprint plots for Hirshfeld surface shows clear differences of N...H interactions of form I and form II from zwitterionic form III.

CHAPTER SIX

Polymorphism in Few Active Pharmaceutical Ingredients

There are several examples from the pharmaceutical industry where the appearance of a new crystal form significantly affected the performance of a product, sometimes with serious clinical effects. Important legal factors related to patent issues are also involved since new polymorphs extend patent coverage and confer legal protection of drug products. Also cocrystal is an emerging topic in pharmaceutical industry with respect to improving drug properties.

Tolbutamide (TB) is a sulfonylurea drug to control blood sugar levels in patients with type 2 diabetes. Five polymorphs of this drug (Form I^H, Form I^L, Form II, Form III and Form IV) are reported in the literature. In an attempt to design novel cocrystal of sulfonylurea functional group, Tolbutamide was cocrystallized with *p*-nitrophenol and *p*-phenylenediboronic acid in EtOH solvent. Single crystals were obtained that resulted in a new crystal structure of TBM with 3 molecules in the asymmetric unit of $P2_1/n$ space group at 100 K. When X-ray data was collected on the same crystal at 298 K a crystal structure with the cell values matching with the reported form III of Tolbutamide was obtained but the terminal carbon atom of butyl chain was disordered indicating a modulated structure of form III. When Tolbutamide was crystallized from methanol with a trace of conc. HNO_3 added, a new crystal structure with different cell parameters and space group ($Pbcn$) compared to the previously reported forms of the molecule was obtained which is termed novel form V of Tolbutamide.

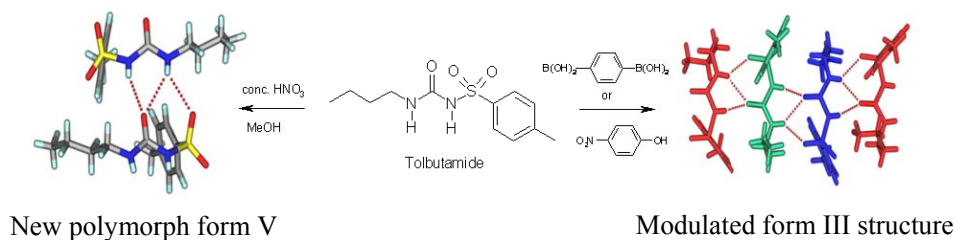


Figure 6.1 Novel form V and a high Z' structure of form III Tolbutamide.

Parabens are a group of alkyl esters of p-hydroxybenzoic acid and are widely used as preservatives in cosmetics, toiletries, pharmaceuticals, food, skin creams, shampoos and eye makeup to protect users from infections, rashes. Methyl paraben (MP) is particularly important because of its higher solubility (2.7 mg/mL in phosphate buffer) compared to higher esters in the series. Approximately 30,000 lbs of methyl paraben is consumed annually in the USA.

A second polymorph (form II) of methyl paraben was crystallized by sublimation technique concomitantly with form I crystals. Cell parameters, space groups, ($P2_1/n$, form II and Cc , form I), Z' value ($Z'=1$ for form II, $Z'=3$ for form I) and the calculated XRPD lines of the form II and the reported form I are entirely different. Crystal structure analysis revealed that form I has a 3D packing whereas the form II is a layered structure.

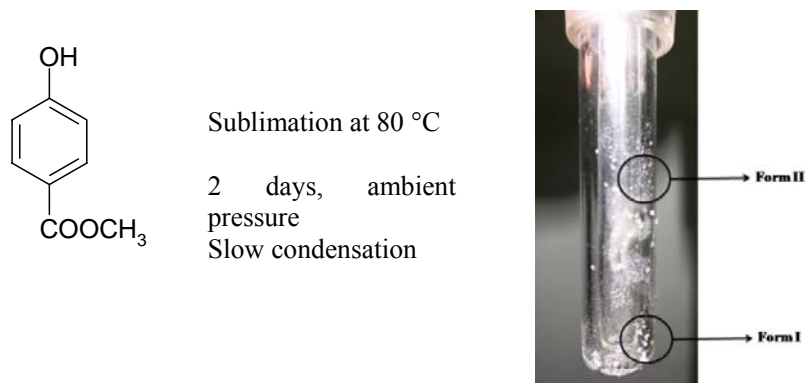


Figure 6.2 Slow sublimation at 80°C for 2 days gave a second polymorph of methyl paraben.

Zolpidem is a prescription medication used for the short-term treatment of insomnia, as well as some brain disorders. Because of the low solubility of Zolpidem free base in water various salt forms are reported in patents and is marketed in the form of Zolpidem tartarate. Zolpidem is conformational flexible around the p-tolyl group. Two conformational cocrystal polymorphs of Zolpidem with succinic in 1: 0.5 ratios were solved by X-ray diffraction (single crystal X-ray and powder XRD), spectroscopy (FT-IR, FT-Raman and ss-NMR) and by DSC. Form I crystallized in orthorhombic non-centrosymmetric polar space group $Iba2$ whereas form II crystallized in centrosymmetric $P2_1/c$ space group.

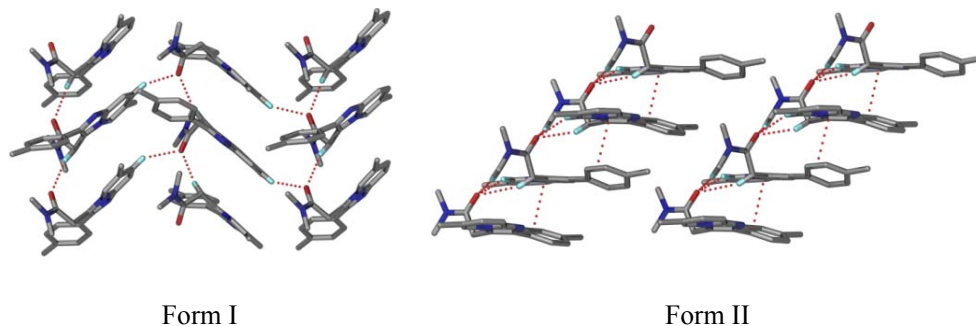


Figure 6.3 Two polymorphs of Zolpidem Succinic acid (1: 0.5) cocrystal.

CHAPTER SEVEN

Conclusion and Future Prospects

Polymorphism and isostructurality are the twin facets of materials chemistry and are important to our understanding of crystal nucleation and growth as well as crystal structure prediction. Extensive studies of polymorphism and isostructurality have been carried out on model organic compounds of triiodohydroxybenzenes, Fuchsones and Sulfonylhydrazones. Isostructurality among polymorphs of different compounds are rare in literature and presented in chapter 2 and 3. In the series of triiodohydroxybenzenes H→OH functional group exchange among the polymorphs was observed whereas in the Fuchsones and Sulfonylhydrazones polymorphism, halogen-Me and inter halogen exchange was studied. The effect of t-Butyl group in the crystallization of a conformationally flexible molecule in chiral space group along with concomitant crystallization of three other racemic polymorphs was serendipitously detected in t-Butylditolylfuchstone. A new polymorph (form V) of Tolbutamide, an antidiabetic drug, is isolated along with a modulated high Z' structure of reported form III, in presence of coformers. Another important compound in day to day life is methyl paraben. There has been a recent controversy regarding polymorphism of this important molecule. A second polymorph of methyl paraben was successfully crystallized. Conformational cocrystal polymorphs of zolpidem-succinic acid open up the possibility of finding new multi crystalline forms of the parent drug or its cocrystal/ salts.

CONTENTS

Certificate	v
Declaration	vii
Acknowledgement	ix-x
Synopsis	xi - xxi
 Chapter One	
Introduction	1-41
1.1 Chemistry of Solid State and Crystal Forms.....	2
1.2 Polymorphism: Definition and Background.....	4
1.3 Classification and Terminologies.....	6
1.4 Basis of Polymorphism – Kinetic Vs Thermodynamic Polymorph...	10
1.5 The Experimental Search for Polymorphs.....	13
1.6 Statistics on Polymorphs.....	15
1.7 Importance of Polymorphism.....	16
1.7.1 Polymorphism in pharmaceutical industry.....	17
1.7.2 Importance of polymorphism in other fields.....	19
1.8 Characterization of Polymorphs.....	20
1.9 Utility of Hirshfeld Surface Analysis in Polymorphism.....	21
1.10 Isomorphism and Isostructurality: Definitions and Background.....	23
1.11 When Isostructurality Occurs?.....	24
1.12 Isostructurality Among Polymorphs.....	27
1.13 Descriptors of Isostructurality.....	28
1.14 Solid Solution.....	29
1.15 Importance of Isostructurality.....	30
1.16 References.....	31

Chapter Two

Isostructural Polymorphs of Triiodoresorcinol and 42-68

Triiodophloroglucinol

2.1	Introduction	43
2.1.1	Hetero-seeding.....	45
2.2	Interactions Involving Halogens.....	45
2.2.1	Inter-halogen interactions.....	45
2.2.2	Halogen bonding.....	46
2.2.3	Halogens in hydrogen bonding.....	47
2.3	Results and Discussion.....	47
2.3.1	Polymorphism.....	48
2.3.2	Isostructurality and solid solution.....	53
2.3.3	Crystal structure of solid solutions.....	55
2.4	Discussion.....	56
2.5	Conclusions and Future Studies.....	62
2.6	Experimental Section.....	62
2.7	References.....	63

Chapter Three

Isostructurality and Polymorphism in Fuchsones and 69-113

Sulfonylhydrazones

3.1	Introduction.....	70
3.2	Chloro-Methyl Exchange and Polymorphism in Fuchsones.....	73
3.2.1	Crystallization and polymorphism.....	74
3.2.2	Crystal structure analysis.....	76
3.2.3	Chloro-methyl exchange and isostructurality.....	83
3.2.4	Solid solutions of TMF, CMF and MCF.....	84
3.3	Color Polymorphism in CMF.....	86
3.4	Polymorphism and Isostructurality in Sulfonylhydrazones.....	88
3.4.1	Crystal structure analysis, isostructurality and polymorphism.....	89
3.5	Comparison of Crystal Structures Using XPac Analysis.....	94

3.5.1	XPac analysis of Fuchsones.....	95
3.5.2	XPac analysis of Sulfonylhydrazones.....	99
3.6	Discussion.....	101
3.7	Conclusion.....	104
3.8	Experimental Section.....	105
3.9	References.....	110

Chapter Four

Chiral and Racemic Tetramorphs of t-Butylditolylfuchsone		114-142
4.1	Introduction.....	115
4.1.1	The spontaneous generation of chirality in achiral molecules.....	115
4.1.2	Spontaneous resolution or spontaneous symmetry breaking.....	117
4.2	Results and Discussion.....	119
4.2.1	The case of 2, 6-di-t-butylditolylfuchsone (2t-Bu).....	120
4.2.2	Conformational chirality of 2t-Bu.....	122
4.2.3	Crystal structure analysis.....	124
4.2.4	Why t-butyl group?.....	128
4.2.5	Resolution of the enantiomers.....	129
4.3	Phase Transition Study.....	130
4.3.1	Hot stage microscopy (HSM) and single crystal XRD unit cell determination.....	130
4.3.2	Differential scanning calorimetry (DSC).....	132
4.4	Stability of Four Polymorphs and Validity of Wallach’s rule.....	133
4.5	CSD Search on Tetramorphic and Higher Polymorph Clusters.....	135
4.6	Conformational Differences.....	136
4.7	Conclusion.....	137
4.8	Experimental Section.....	137
4.9	References.....	139

Chapter Five

Neutral and Zwitterionic Polymorphs of 2-(*p*-Tolylamino) Nicotinic 143-175

Acid (TNA)

5.1	Introduction.....	144
5.2	Results and Discussion.....	149
5.2.1	Crystal structure analysis.....	150
5.2.2	Similarities and differences in the crystal structures of TNA-I and TNA-III.....	155
5.2.3	XPac analysis of polymorphs I and III.....	157
5.2.4	Thermal and spectroscopic characterization.....	158
5.2.5	Conformational difference.....	162
5.2.6	CSD search.....	163
5.2.7	Hirshfeld 2D fingerprint plot.....	163
5.3	Discussion.....	165
5.3.1	Intramolecular proton transfer, ΔpK_a rule.....	165
5.3.2	What is the role of pyridine coformers to give a zwitterionic structure of TNA?.....	168
5.4	Conclusion.....	169
5.5	Experimental Section.....	170
5.6	References.....	171

Chapter Six

Polymorphism in Few Active Pharmaceutical Ingredients 176-220

6.1	Introduction.....	177
6.1.1	Modulated structure.....	178
6.2	Tolbutamide.....	179
6.2.1	Modulated high Z' structure of Tolbutamide.....	180
6.2.2	Novel form V of Tolbutamide.....	184
6.2.3	Characterization by FT-IR.....	188
6.2.4	Phase transformation of form V.....	189
6.2.5	Hirshfeld fingerprint plots.....	190

6.3	Crystal Structure of Methyl Paraben Polymorph II.....	191
6.3.1	Results and discussion.....	192
6.3.2	Hirshfeld fingerprint plots of MP form I and form II.....	199
6.4	Conformational Polymorphism in Zolpidem•Succinic Acid Cocrystal.....	200
6.4.1	Results and discussion.....	201
6.4.2	Zolpidem•succinic acid cocrystal polymorphs (ZM•Suc).....	202
6.4.3	Stability and phase transformation of form I and form II.....	205
6.4.4	Spectral analysis of ZM•Suc polymorphs.....	207
6.4.5	Conformational flexibility observed in crystal structures of ZM.....	209
6.5	Conclusion.....	212
6.6	Experimental Section.....	213
6.7	References.....	215

Chapter Seven

Conclusion	221-227
-------------------	---------

7.1	Polymorphism in Isostructural Molecules.....	222
7.2	Polymorphism in Two Special Cases: Chiral Vs Racemic and Neutral Vs Zwitterionic Polymorphs.....	224
7.3	Polymorphism in Active Pharmaceutical Ingredients.....	225

Appendix	228-241
-----------------	---------

Salient crystallographic details.....	228
DSCs of Fuchsones.....	236
DSC and TGA of molecular complexes of Zolpidem.....	238
Comparison of calculated and experimental XRPDs of molecular complexes Zolpidem.....	240

About the Author.....	242
List of Publications.....	244